



MACQUARIE
University
SYDNEY • AUSTRALIA

Nutraceutical properties of whole dried sugarcane extracts studied by proteomics

Daniel Bucio Noble

A thesis presented for the degree of

Doctor of Philosophy

Department of Molecular Sciences

Faculty of Science and Engineering

Macquarie University, NSW, Australia

November 2017

Table of Contents

List of figures	<i>v</i>
List of tables	<i>vi</i>
Declaration	<i>vii</i>
Acknowledgments.....	<i>ix</i>
Conference proceedings and Awards	<i>xi</i>
Abstract	<i>xiii</i>
Abbreviations	<i>xv</i>
CHAPTER 1 INTRODUCTION.....	<i>1</i>
1.1 Nutraceuticals	<i>3</i>
1.1.1 Polyphenols	<i>3</i>
1.1.2 Dietary fibre.....	<i>5</i>
1.2 Oxidative stress, immune response and inflammation.....	<i>5</i>
1.3 Inflammatory signalling pathways.....	<i>7</i>
1.3.1 Nuclear factor κ B (NF κ B)	<i>7</i>
1.3.2 Activator protein 1 (AP-1).....	<i>9</i>
1.3.3 Signal transducer and activator of transcription 3 (STAT3).....	<i>10</i>
1.3.4 Monitoring changes in signalling pathways using ‘omics approaches.....	<i>11</i>
1.4 Antioxidants and inflammation.....	<i>11</i>
1.4.1 Metabolism of phytochemicals.....	<i>17</i>
1.4.2 Selenium in antioxidant defence.....	<i>18</i>

1.4.3 <i>In vitro</i> models of intestinal inflammation.....	19
1.4.4 <i>In vivo</i> models of inflammation in response to HFD supplementation.....	19
1.5 Sugarcane.....	20
1.5.1 Sugarcane as a nutraceutical	21
1.6 Proteomics to investigate the therapeutic effects of nutraceuticals	22
1.6.1 SWATH-MS as a data-independent acquisition technique.....	24
1.6.2 The application of MS-based proteomics to assess dietary interventions.....	26
1.6.3 Phosphoproteomics analysis in food interventions	28
1.6.4 Multiplex bead-based ELISA.....	30
1.7 Aims and scope of the project	32
 CHAPTER 2 REGULATION OF INFLAMMATORY MEDIATORS BY DRIED SUGARCANE EXTRACTS IN AN <i>IN VITRO</i> COLON CANCER CELL MODEL OF LPS-INDUCED INFLAMMATION	 33
2.1 Abstract.....	39
2.2 Introduction.....	41
2.3 Methods.....	43
2.4 Results	49
2.5 Discussion.....	53
2.6 Conclusions.....	57
 CHAPTER 3 PHOSPHOPROTEOMICS ANALYSIS OF CELL SIGNALLING ASSOCIATED WITH DRIED SUGARCANE EXTRACTS IN AN <i>IN VITRO</i> COLON CANCER CELL MODEL OF LPS-INDUCED INFLAMMATION.....	 83

3.1 Abstract	89
3.2 Introduction	91
3.3 Methods	93
3.4 Results.....	97
3.5 Discussion	101
3.6 Conclusions	106
 CHAPTER 4 <i>IN VIVO</i> SUPPLEMENTATION OF WHOLE DRIED SUGARCANE IN A HFD MOUSE MODEL.....	 119
4.1 Introduction	123
4.2 Methods	124
4.2.1 Animal handling and sample collection	124
4.2.2 Intraperitoneal glucose tolerance test (IPGTT)	125
4.2.3 Expression of circulating markers of inflammation in plasma	125
4.2.4 Mass spectrometry based proteomics analysis	126
4.2.5 Ingenuity pathway analysis	126
4.3 Results.....	127
4.3.1 Concentration of circulating plasma marker proteins.....	130
4.3.2 Diet induced changes in liver protein expression in response to HFD, WDS and BF	132
4.3.3 Protein based predicted effect on liver functions and canonical pathways	143
4.4 Discussion	146
4.4.1 Dietary effect on body weight gain	146
4.4.2 Dietary changes on circulating inflammatory markers.....	146
4.4.3 Nutraceutical-dependent inhibition of cytokines.....	147

4.4.4 HFD effect on the liver proteome	148
4.4.5 WDS regulation of selenium-related proteins.....	149
4.4.6 WDS-dependent anti-inflammatory effect.....	151
4.4.7 Inhibition of AQP1 and T120A	152
4.4.8 Modulation of cellular events by BF.....	152
4.4.9 Sugarcane supplementation in animal models	154
4.5 Conclusions.....	154
 CHAPTER 5 GENERAL DISCUSSION AND FUTURE DIRECTIONS.....	157
 5.1 Main findings and contributions to new knowledge	159
 5.2 Limitations and future directions	163
 References.....	167
 Appendices.....	199
Appendix 1 Table 2A.1 Nutritional information of WDS	201
Appendix 2 Figure 2A.1 Cell viability in SW480 cells in response to LPS, WDS EE and RSV addition.....	203
Appendix 3 Table 2A.2 Significantly regulated proteins expressed as LPS/C ratio.....	205
Appendix 4 Table 3A.1 Kinase enrichment motif performed on WDS EE/LPS significant regulated phosphosites	207
Appendix 5 Figures 4A.1 and 4A.2 Plasma marker expression in response to dietary changes	209
Appendix 6 Figure 4A.3 Prediction of diseases and functions based on hepatic protein expression induced by WDS and BF supplementation.	211
Appendix 7 Tables 4A.1 4A.2 and 4A.3 Normal chow, high fat diet and Benefiber composition and nutritional parameters	213

Appendix 8 Table 4A.3 Significantly down-regulated proteins expressed as HFD/NC ratio	215
Appendix 9 Table 4A.4 Significantly up-regulated proteins expressed as HFD/NC ratio ...	219
Appendix 10 Examining cellular responses to kinase drug inhibition through phosphoproteome mapping of substrates	221
Biosafety and Animal Ethics approvals.....	239

List of figures

Figure 1.1 Chemical characterisation of the polyphenol family.....	4
Figure 1.2 NFκB activation pathway.....	8
Figure 1.3 AP-1 activation pathway	9
Figure 1.4 STAT3 activation pathway.....	10
Figure 1.5 SWATH-MS quantitation workflow	21
Figure 1.6 SILAC (red) and label-free (blue) quantitation strategies	30
Figure 1.7 (a) Multiplex bead-based principle detection. (b) IL-1β calibration curve and fluorescent intensity from samples and blank	31
Figure 2.1 (a) Total polyphenolic content and (b) Total flavonoid content of whole dried sugarcane extracts.....	59
Figure 2.2 (a) Hierarchical clustering and (b) principal component analysis of the protein expression in SW480-treated cells	61
Figure 2.3 Differential (a) up-regulation and (b) down-regulation proteins in response to WDS EE and RSV	63
Figure 2.4 Diseases and functions prediction based on protein expression induced by WDS EE and RSV introduction	61
Figure 2.5 WDS EE effect on the NFκB signalling pathway	63
Figure 2.6 RSV effect on the PI3K/AKT signalling pathway	69

Figure 3.1 Free-radical scavenging and antioxidant activity of WDS EE	103
Figure 3.2(a) Hierarchical clustering and (b) principal component analysis of the phosphoprotein expression of SW480-treated cells.....	105
Figure 3.3 Differential (a) down-regulated and (b) up-regulated phosphorylated peptides in response to WDS EE and RSV.	107
Figure 3.4 C-Raf inhibition on WDS EE-treated SW480 cells.....	113
Figure 4.1 Body weight gain and food intake in response to dietary changes	128
Figure 4.2 Intraperitoneal glucose tolerance test (IPGTT) and area-under-the-curve (AUC) in response to dietary changes.	129
Figure 4.3 Organ weight in response to dietary changes.	130
Figure 4.4 Plasma markers expression in response to dietary changes.....	131
Figure 4.5 MS-based hepatic protein expression in response to dietary changes.	133
Figure 4.6 Differential up-regulation (a) and down-regulation (b) of proteins in response to WDS and BF supplementation.....	135
Figure 4.7 Top 10 diseases and functions prediction based on hepatic protein expression induced by WDS and BF supplementation	144
Figure 4.8 Canonical pathway prediction in response to WDS and BF supplementation	145
Figure 5.1 WDS ethanol extracts (WDS EE) effects <i>in vitro</i> . Integration of main proteomics and phosphoproteomics findings	160

List of Tables

Table 1.1 Polyphenols research in the context of IBD models	14
Table 1.2 Proteomics research on nutraceutical interventions in the context of inflammation..	27
Table 2.1 Significantly regulated proteins expressed as WDS EE/LPS ratio.	71
Table 2.2 Significantly regulated proteins expressed as RSV/LPS ratio.	71
Table 2.3 Predicted upstream analysis based on protein expression induced by WDS EE and RSV.....	77

Table 3.1 Number of phosphorylated peptides detected by MS in SW480 cells after treatments	111
Table 3.2 Significant regulation of relevant phosphorylated peptides expressed as WDS EE/LPS and RSV/LPS ratios	113
Table 4.1 Significant regulated proteins expressed as WDS/HFD ratio	137
Table 4.2 Significant regulated proteins expressed as BF/HFD ratio	139

Declaration

I declare that the work presented in this thesis entitled “Nutraceutical properties of whole dried sugarcane extracts studied by proteomics” was conducted by me under the supervision of Assoc. Prof. Mark P. Molloy. The work presented here has not been submitted for the purpose of obtaining any other degree. The assistance and contribution of others have been appropriately acknowledged.

The research presented in this thesis was approved by the Biosafety Committee (Reference number MAM150115BHA) and the Animal Ethics Committee (Reference number 5201500129) from Macquarie University.

Daniel Bucio Noble

November 2017

Acknowledgements

I would like to express my sincere gratitude to my supervisor Assoc. Prof. Mark P. Molloy. I could not ask for a better mentor, your encouragement, sharp observations and guidance eased this journey.

The completion of this project could not be possible without the invaluable support of Dr. Liisa Kautto in coordinating the animal experimentation. I thank Dr. Christoph Krisp and his enormous help in assisting with the operation of the mass spectrometers. It is recognised the support and feedback provided by our industry partner Gratuk Pty. Ltd. and Dr. Malcolm S. Ball. I acknowledge Dr. Alamgir Khan, Dr. Edmond Breen, and Dr. Dana Pascovici from APAF for their assistance in the multiplex and bioinformatics analysis. Special mention to our collaborators in the University of Sydney and in particular to Assoc. Prof. Anandwardhan Hardikar and his team.

Friendship has made this process an incredible experience. To the friends that were present during this time: Erick, Shila, Hasinika, and Miriam, but also to the new friends I made inside and outside the lab: Karthik, Hannah, Crystal, Brad, Atul, Ian, Franziska, Emila and Dennis.

This thesis is dedicated to my loving family. My siblings: Jesús, Vivi, Mari, Dany and Monse; nunca se rindan. Most importantly to my parents Daniel and Viviana; éste logro es compartido, los amo. Abuelo Daniel y tío Jorge, esto también es por ustedes.

Conference proceedings

Oral presentations

- Bucio Noble D, Kautto L, Ball M, Molloy M. Anti-inflammatory properties of sugarcane dietary fibre. Food Allergen Management Symposium, May 2015, Sydney, Australia.
- Bucio Noble D, Molloy M. Understanding the anti-inflammatory properties of dried sugarcane extracts by proteomics. 22nd Annual Lorne Proteomics Symposium, February 2017, Lorne, Australia.

Posters

- Bucio Noble D, Kautto L, Ball M, Molloy M. Antioxidant properties of sugarcane dietary fibre. Islet Society & Australian Islet Group VII Annual Scientific Meeting, University of Sydney, July 2015, Sydney, Australia.
- Bucio Noble D, Kautto L, Ball M, and Molloy M. Antioxidants and anti-inflammatory properties of sugarcane dietary fibre. 12th Annual Conference US HUPO, March 2016, Boston, USA.

Awards

Awarded “SoAPS Presentation Award” at the 22nd Annual Lorne Proteomics Symposium, February 2017, Lorne, Australia.

Awarded the Postgraduate Research Fund (\$5,000 AUD) for conference travel from Macquarie University, Australia.

Awarded the Australian Research Council Industrial Transformation Training Centre Scholarship to undertake the Doctor of Philosophy degree.

Awarded the High Degree International CONACYT Scholarship to undertake the Doctor of Philosophy degree.

Abstract

Many chronic diseases are associated with the activation of inflammatory mediators. This can lead to excessive release of pro-inflammatory cytokines and the generation of reactive oxygen species (ROS). Some nutraceuticals are rich in polyphenols providing strong antioxidant attributes which have been reported to counteract some of the deleterious effects of ROS. However, cellular mechanisms underlying nutraceutical therapeutic properties are often not well elucidated. In this thesis, the anti-inflammatory properties of the nutraceutical, whole dried sugarcane (WDS), was investigated using proteomic techniques. Chemical assays of WDS ethanol extracts (WDS EE) showed the presence of polyphenols and flavonoids conferring potent antioxidant activity. In lipopolysaccharide (LPS)-stimulated SW480 colon cancer cells, WDS EE reversed the phosphorylation of NF κ B and inhibited the secretion of IL-8 in a mechanism shown to be dependent of C-Raf and AKT phosphorylation. Mass spectrometry (MS)-based proteomics using label-free SWATH-MS demonstrated WDS EE to alter the expression of oxidative stress mediators FOXRED1 and the selenoprotein SELH, amongst others. Based on protein expression, prediction analysis proposed the down-regulation of NF κ B pathway members TLR2, TLR4, NIK and I κ B. In the same model, phosphoproteomics studies indicated that WDS EE interferes in the phosphorylation of cell stress regulator proteins c-Jun, EGFR, PKA, PKC β and SIRT1, interpreted as regulating anti-inflammatory related signalling mechanisms.

As a feed supplement to mice on high-fat diet (HFD), WDS was shown to reduce the plasma concentration of the circulating markers of inflammation IL-1 β and GM-CSF. The proteomic analysis of liver tissue from WDS-feed, HFD mice showed changes to STAT3 and the selenium associated proteins SEP15 and SecS. Prediction analysis based on protein expression indicated the down-regulation of inflammatory-related hepatic functions. Taken

together, this thesis has revealed some of the mechanisms associated with the anti-inflammatory properties of WDS extracts in *in vitro* and *in vivo* models.

Abbreviations

2-DE	Two dimensional gel electrophoresis
AKT/PKB	Protein kinase B
AP-1	Activator protein 1
AQP1	Aquaporin 1
AUC	Area-under-the-curve
BF	Benefiber®
CD	Crohn's disease
CDK	Cyclin dependent kinase
CE	(+)-catechin equivalents
CYP	Cytochrome P450
DIA	Data independent acquisition
DPPH	2,2-diphenyl-1-picrylhydrazyl
EGCG	(-)-epigallocatechin-3-gallate
EGFR	Epidermal growth factor receptor
ELISA	Enzyme-linked immunosorbent assay
FC	Fold change
FOXRED1	FAD-dependent oxidoreductase domain containing 1 protein
FRAP	Ferric reducing ability potential
GAE	Gallic acid equivalents
GLP-1	Glucagon-like peptide-1
GM-CSF	Granulocyte macrophage colony stimulating factor
GST	Glutathione-S-transferase
HFD	High fat diet
IBD	Inflammatory bowel disease
ICAM-1	Intracellular adhesion molecule 1
IDA	Information dependent analysis
IFN γ	Interferon γ
IKK	I κ B kinase
IL	Interleukin
iNOS	Inducible nitric oxide synthase
IPGTT	Intraperitoneal glucose tolerance test
JNK	c-Jun N-terminal kinase
LC	Liquid chromatography
LPS	Lipopolysaccharides
MS	Mass spectrometry
NAFLD	Non-alcoholic fatty liver disease
NASH	Non-alcoholic fatty steatohepatitis

NC	Normal chow
NFκB	Nuclear factor κB
NIK	NFκB-inducing kinase
PAI-1	Plasminogen activator inhibitor 1
PKD2	Pyruvate dehydrogenase kinase 2
PKA	Protein kinase A
PKCβ	Protein kinase C β subunit
ROS	Reactive oxygen species
RSV	Resveratrol
SBP2	Selenium binding protein 2
SecS	Selenocysteine synthase
SELH	Selenoprotein H
SEP15	15kDa selenoprotein
SILAC	Stable isotope labelling of amino acids in cell culture
SIRT1	Sirtuin 1
STAT3	Signal transducer and activator of transcription 3
SWATH	Sequential window acquisition of all theoretical fragment-ion spectra
T120A	Transmembrane protein 120A
TFC	Total flavonoid content
TLR	Toll-like receptor
TNFα	Tumour necrosis α
TPC	Total polyphenol content
UC	Ulcerative colitis
WDS EE	Whole dried sugarcane ethanol extract

Chapter 1 Introduction

1.1 Nutraceuticals

Nutraceuticals can be defined as a food, or part of a food, that provides health benefits for disease treatment and/or prevention. This classification is relevant to isolated nutrients, dietary supplements and herbal products, among others [1]. Plant nutraceuticals take the form of phytochemicals such as terpenoids, polyphenols and alkaloids and other nitrogen containing constituents [2].

1.1.1 Polyphenols

Compelling evidence widely recognises polyphenols for their therapeutic utility. More than 8,000 polyphenols have been described and are characterised by an aromatic ring with one or more hydroxyl groups. The Phenol-Explorer database has catalogued 501 polyphenols from over 400 food sources [3]. Major subgroups of polyphenols consist of phenolic acids (C_6-C_1 or C_6-C_3), flavonoids ($C_6-C_3-C_6$), stilbenes ($C_6-C_2-C_6$) tannins and lignans. Examples of each family are gallic acid, quercetin, resveratrol, tannic acid and secoisolariciresinol, respectively. Flavonoids are the most complex group comprising two-thirds of the polyphenol families and can be further classified as flavonols, flavones, isoflavones, flavanones, flavan-3-ols and anthocyanins. (Figure 1.1). These phytochemicals are highly distributed in fruits, vegetables and grains. For instance, gallic acid is reported to be present in bananas and avocados [4]. Rice cultivars are rich sources of the phenolics ferulic acid and p-coumaric acid [5]. Quercetin can be detected in pomegranate among other fruits [6], luteolin can be present in broccoli and chillies [7]. Resveratrol (RSV) is an important constituent of grape skin and wine [8]. Despite the diversity of these phytochemicals, some polyphenols exhibit antioxidant attributes that confer protective functions against invading pathogens and other external challenges. Some of these mechanisms include the ability of polyphenols to chelate metal ions such as Fe and

Cu impeding the generation of reactive oxygen species (ROS). Polyphenols are also effective in neutralising and quenching and have been reported as excellent free-radical scavengers [9].

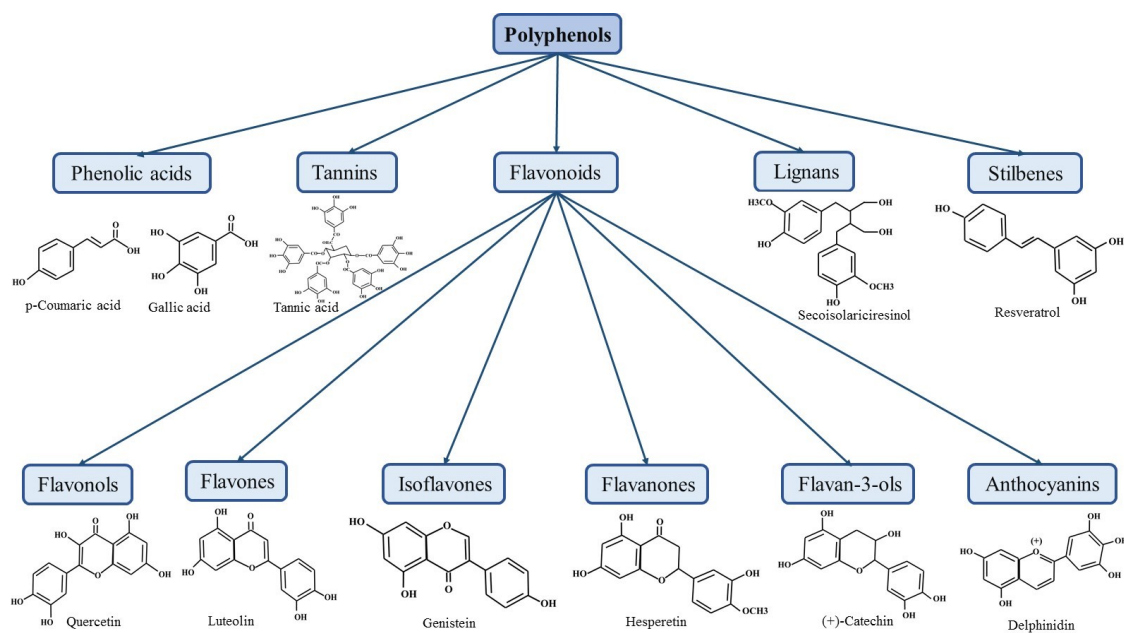


Figure 1.1 Chemical characterisation of the polyphenol family

There is overarching evidence that implicates polyphenols either in its pure form or derived from soluble food extracts in regulating anti-inflammatory mechanisms in several diseases. For instance, polyphenol extracts from various plant and food sources are reported to regulate several intracellular inflammatory mediators in *in vitro* and *in vivo* biological models of inflammatory bowel disease (IBD) [10]. Plant food polyphenols are also identified to yield improvement in glucose homeostasis, attenuation of oxidative stress, and inhibition of pro-inflammatory agents in cellular and animal models of type 2 diabetes [11]. Cardiovascular protective effects of polyphenols include the reduced digestion and absorption of dietary lipids, free radical scavenging activity, and improvement of endothelial function among others [12].

Multiple studies have assessed polyphenol interventions in human studies. Clinical trials show that food products rich in polyphenols such as cranberry juice reduced the levels of

fasting blood glucose and the cardiovascular risk marker apolipoprotein B in type 2 diabetes patients [13]. Consistently, consumption of red wine is shown to decrease plasma insulin and apolipoprotein A concentrations as well as insulin resistance in high cardiovascular risk patients [14]. Additional studies present evidence of the health benefit effects of dark chocolate and cocoa in the management of diabetes, intestinal inflammation and cardiovascular disease [15][16].

1.1.2 Dietary fibre

Dietary fibres are defined as non-digestible carbohydrates and lignins that are resistant to digestion in the upper gut. Recent definitions also comprehend oligosaccharides such as inulin and resistant starches [17]. Dietary fibre can be classified according to its solubility. The viscous or colon fermentable type is known as soluble fibre (i.e. pectin, inulin and β -glucans) whereas the partially fermented type is defined as insoluble fibre (i.e. starch and oligosaccharides). Although most of the natural food products contain both soluble and insoluble dietary fibre, soluble fibre is mainly found in fruits and vegetables whilst insoluble fibre can be found in whole grain and bran products [18].

Some of the beneficial effects attributed to soluble dietary fibre include reduction in postprandial glucose response and total and low-density lipoprotein (LDL) cholesterol and increase of colonic fermentation associated with short-chain fatty acids. In the case of insoluble fibre the benefits include reduced risk of type 2 diabetes and increased insulin sensitivity [19].

1.2 Oxidative stress, immune response and inflammation

Inflammation is a complex and essential process that regulates the immune response against stimuli including external substances or invading pathogens. In this regard, initiation of the immune response can be modulated by the pattern recognition receptors such as the toll-like

receptors (TLRs). These are crucial in coupling with specific bacterial products to release the inflammatory mechanisms [20]. The inflammatory mechanisms are characterised by the interconnection of inflammatory signalling pathways, and the expression of pro-inflammatory cytokine and chemokines consisting of interleukins (ILs), tumour necrosis alpha (TNF α), interferon gamma (IFN γ), monocyte chemotactic protein-1 (MCP-1), and transforming growth factor- β (TGF- β), among others. Cytokines and chemokines act by recruiting inflammatory cells leading to the activation of the immune response mediated by TLRs. Expression of pro-inflammatory genes and related signalling networks are also essential in the regulation of other functions such as the integrity of the intestinal epithelium and sustaining mucosal homeostasis [21]. In normal conditions, acute inflammation serves in removing the foreign agent, promoting repair and re-establishing original tissue functions [22].

Dysregulation of these mechanisms can result in a chronic inflammatory state characteristic of diseases such as IBD, arthritis, asthma, diabetes, obesity, and cancer. Intestinal inflammation observed in Crohn's disease (CD) and ulcerative colitis (UC) are two forms of IBD. In these conditions, unregulated response of the immune system to resident enteric microflora leads to chronic gut inflammation [23]. For example, CD and UC are characterised by aberrant activation of the mucosal lymphocytes T-helper (Th) 1 and 2. In this mechanism, inflammatory stimulation of Th1 promotes secretion of IL-2 and IFN γ that induces macrophage activation. This event further produces cytokines such as IL-1, IL-6, IL-12, IL-18, TNF α , and IFN γ leading to the amplification of inflammatory signals and thus prolonged activity of Th1 and related cells [22]. The interplay among the distinct signals is causative in the perpetuation of the inflammatory response.

Another fundamental component of chronic inflammation is the excessive release of ROS. ROS are free radicals that include hydroxyl, superoxide, and peroxy groups among others,

each with varied levels of reactivity [24]. ROS, produced under normal cellular metabolic reactions, are essential for the migration of immune cells in combating inflammation [23]. However, overproduction of free radicals promotes oxidative stress a condition characterised by the accumulation of non-enzymatic oxidative damage that threatens normal cell function. In conjunction with impaired antioxidant defence, oxidative stress results in damage to specific cellular proteins, membrane lipids and nucleic acids. In these conditions, instead of the initiation of the wound healing process observed in tissue damage, the immune system coordinates a dysregulated fibrosis response associated with persistent injury and altered tissue function [25]. Oxidative damage is therefore an imbalance between oxidant and antioxidant production that favours a state of chronic inflammation [26].

The liver has an important role in the systematic antioxidant defence mechanism. Some of the main functions of the liver include the metabolism of drugs, carcinogens, hormones, and fatty acids, and it is also where the metabolic processing of phytochemicals and polyphenols occur after absorption in the gastrointestinal tract [27]. Xenobiotic processing is mediated by a series of enzymatic-driven oxidative and reductive reactions that permit the absorption of metabolites and the excretion of toxic compounds [28]. Nonetheless, these oxidative related processes lead to generation of free-radicals that can damage the liver [29]. Conversely, phytochemical therapies can provide a potential protective mechanism against ROS challenge. For example, olive oil rich in polyphenols promoted the expression of the antioxidant endogenous system as a potential defence mechanism against fatty liver conditions promoted by palm oil [30].

1.3 Inflammatory signalling pathways

1.3.1 Nuclear factor κ B (NF κ B)

NF κ B is considered as a master regulator of the inflammatory response [31]. Initiation of this signalling pathway involves interaction of the TLRs (mainly TLR2 and TLR4) with their

respective ligands. Lipopolysaccharides (LPS), a glycolipid outer membrane component of Gram negative bacteria interact with TLR4 [32], whereas peptidoglycans from Gram positive bacteria strongly activate TLR2 [33]. In addition, activation can also occur by TNF α recognition by its receptors (TNFRs) [34].

Inflammatory signal dependent of TLR2 and TLR4 requires the recruitment of myeloid differentiation protein (MyD88) and IL-1 receptor associated kinase (IRAK). IRAK is then disassociated and phosphorylates tumour necrosis factor receptor-associated factor 6 (TRAF6), which in association with TGF- β -activated kinase 1 (TAK1) phosphorylates NF κ B-inducing kinase (NIK) [35]. Activation of NIK leads to the phosphorylation and activation of the I κ B kinase (IKK) complex that phosphorylates the NF κ B inhibitory adaptor, I κ B, producing proteasomal degradation. Released NF κ B (a heterodimer of p50 and p65 units) is then phosphorylated at serine 536 permitting migration into the nucleus (Figure 1.2) [36]. Once nuclear translocated, NF κ B activates transcription on genes containing the κ B binding site in their promoter regions. The majority of these transcription products are associated with inflammatory and immune events including cell adhesion molecules, growth factors, oxidative stress related enzymes, transcription factors, cytokines and chemokines [31]. Some of these include ILs, inducible nitric oxide synthase (iNOS), granulocyte macrophage colony stimulating factor (GM-CSF), and intracellular adhesion molecule 1 (ICAM-1), among others.

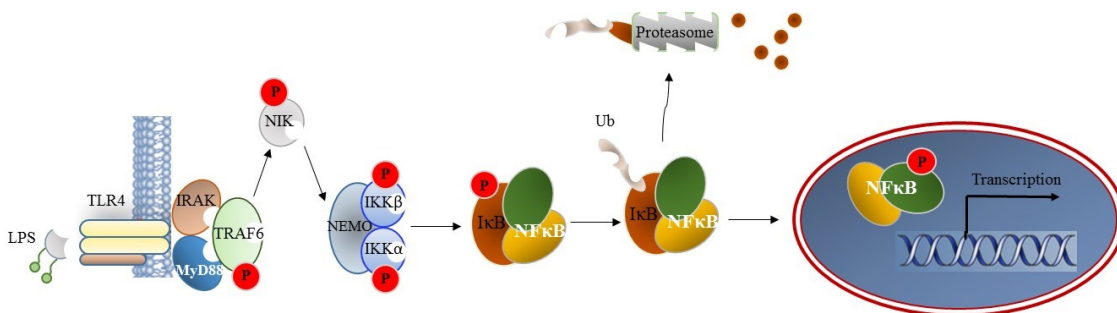


Figure 1.2 NF κ B activation pathway

Overall, aberrant activation of NF κ B is linked to its own constitutive phosphorylation operated by IKK activity and I κ B degradation. These events are identified as plausible targets for the development of anti-inflammatory therapies [23].

1.3.2 Activator protein 1 (AP-1)

AP-1 is a dimeric complex composed of the transcription factors Jun, Fos, Maf and ATF, from which c-Jun appears as the most important modulator of AP-1 transcriptional activity [37]. Similar to NF κ B pathway, activation and DNA binding activity of AP-1 is induced by inflammatory challenge produced by LPS [38] or cytokine stimulation [34]. Activation of AP-1 requires the participation of the MAPK signalling pathways c-Jun N-terminal kinase (JNK), extracellular-signal-regulated kinase (ERK1/2) and p38 as observed in intestinal epithelial cells [39]. However, JNK-dependent activation of AP-1 appears to have a more important role in the context of inflammatory insults. Inflammatory signals either from TNF α or LPS stimulation require recruitment of TRAF2 and TRAF6, respectively, leading to the activation of apoptosis regulating kinase 1 (ASK1). Activated ASK1 is responsible for the phosphorylation of JNK, event necessary for nuclear translocation and subsequent phosphorylation-induced activation of c-Jun on residues serine 63 and serine 73, critical events that precede AP-1 nuclear activation (Figure 1.3) [40]. Ultimately, nuclear localised AP-1 transcribes the expression of pro-inflammatory genes that are central in the immune response such as TNF α , and cyclooxygenase 2 (COX-2) [41].

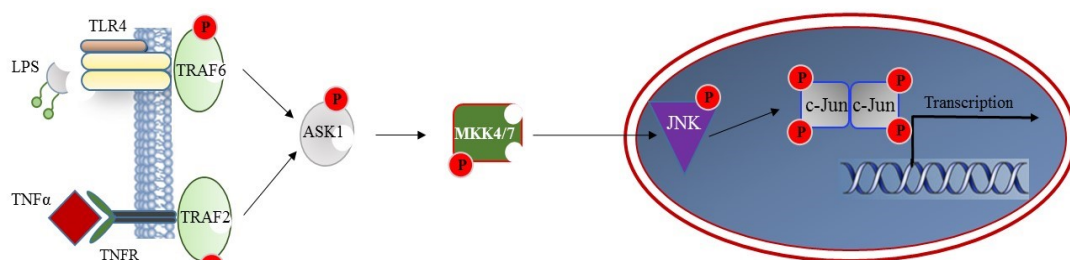


Figure 1.3 AP-1 activation pathway

1.3.3 Signal transducer and activator of transcription 3 (STAT3)

STAT3 is another important mediator of inflammatory signalling. Enhanced activity of STAT3 is associated with external stimulation with growth factors, bacterial products and cytokines. IL-6, a key transcriptional product of NF κ B, is characterised as a major effector in the STAT3 pathway [42]. Consistent with the role of phosphorylation in the transcriptional activity of NF κ B and AP-1, phosphorylation of tyrosine 705 by janus kinase 2 (JAK2) positively regulates STAT3 activity [43]. Phosphorylation-dependent activation of STAT3 is also dependent on the coupling of LPS with TLR4 [44]. Once phosphorylated, STAT3 forms a homo dimer complex that facilitates nuclear import which initiates the expression of inflammatory, stress response and immune function related genes (Figure 1.4). Some of these genes include ICAM-1, COX-2, IL-1 β , and IL-6 [45]. STAT3 activity is greatly influenced by dietary conditions. For instance, high fat diet (HFD) consumption drives a chronic inflammatory effect in the liver that is propagated by the IL-6/STAT3 pathway. Pathologies associated with the enhanced activity of this pathway range from non-alcoholic fatty liver disease (NAFLD) to non-alcoholic fatty steatohepatitis (NASH), cirrhosis and hepatocarcinoma [46].

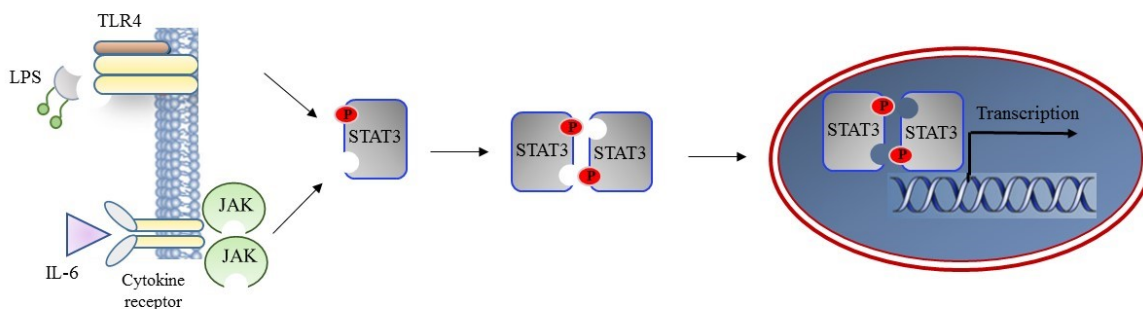


Figure 1.4 STAT3 activation pathway

1.3.4 Monitoring changes in signalling pathways using ‘omics approaches

As described in this section, signal transduction pathways present a great level of complexity that can be regulated at the protein and phosphoprotein levels. Dysregulated activity of these signalling pathways is considered as a hallmark of cancer and inflammatory diseases [47]. Cooperative signals is also determinant in the development of the inflammatory response; for instance, interaction between NF κ B and STAT3 signals is crucial for the expression of key cancer promoter genes and malignant progression [48].

In order to characterise the inherent intricacy of these signals, sophisticated approaches such as the ‘omics techniques are necessary. Transcriptomics studies identify changes in gene expression with the use of microarrays and quantitative reverse transcription polymerase chain reaction (RT-qPCR) data. However, mRNA expression levels often do not reflect the protein expression levels, limiting its application in providing signalling activity information [49]. Proteomics on the other hand, is described as a holistic and unbiased approach that reflects the activity of the molecular transducers and its associated mechanisms. Thus proteomics quantitative strategies are relevant in the assessment of the activity of these pathways, for instance by investigating the phosphorylation on a global proteome-wide scale or by dissecting the specific phosphorylation events instigated by specific kinases [50].

1.4 Antioxidants and inflammation

Generation of ROS is a key factor in the development of oxidative stress and inflammation [51]. It is well established that accumulation of oxidative species lead to oxidative damage when the antioxidant defence is unfavourable. Lipid hydro-peroxides derived from unsaturated fatty acids and metal ions are important sources of ROS in the diet [52]. Deleterious effect of pro-oxidative damage include up-regulation of signalling pathways such as NF κ B, AP-1 and sterol regulatory element-binding protein and its target genes in liver and small intestine [53].

In this regard, the mechanisms associated with antioxidant therapies involve hydrogen donation that is shown to have an effect in controlling redox sensitive transcription factors and enhancing the antioxidant endogenous system. The mechanisms by which antioxidants reduce oxidative damage involve free radical scavenging, metal ion chelation (i.e. Fe^{2+} and Cu^{2+}) and electron transport catalysis [9].

Maintenance of the cellular defence against pro-oxidant challenge involves the action of antioxidant enzymes such as glutathione peroxidase (GSH-Px), superoxide dismutase (SOD), catalase, thioredoxin and coenzyme Q. However, intake of nutrients including vitamins, carotenoids, ascorbic acid and polyphenols have a major role [52].

Multiple review articles have analysed the literature in regards to polyphenol research in inflammation [10], immunity [54], metabolic conditions [16] among others. Some of these studies condensed the existing knowledge of polyphenols effect in *in vitro* and *in vivo* IBD models [55][56]. They classified the studies in accordance to the polyphenol class and food tested: anthocyanins (present in grape juice and berries), green tea (EGCG and green tea extract), curcumin, cocoa, isoflavones and soy, flavonoids, RSV, purified phenolics etc. In some of these studies food extracts were investigated including cranberry, propolis, olive oil, apples, pomegranate, citrus, oat bran, and blueberry fibre. Although the dosage greatly depends on the study, authors stress the importance of employing relevant quantities that can be translatable to human consumption.

Table 1.1 summarises some of the literature exploring the outcome of polyphenols in the IBD context [55]. Many polyphenols are found to modulate the NF κ B pathway and induce the nuclear factor-erythroid 2-related factor-2 (Nrf2). Other actions include the reduction of inflammatory cytokines, inhibition of NO production, inhibition of COX2 activity and

improvement gut microbiota. Nevertheless, these effects vary as result of the great diversity and complexity of these molecules [55][56].

Even though there is great complexity among the polyphenol family, most of the research regarding their effect on inflammatory models is concentrated on only a few compounds. *In vitro* studies using the colon cancer cell lines SW480 and HT29 treated with RSV show reversal of the inflammatory state induced by LPS. Specifically, RSV reduced the phosphorylation of I κ B and the expression of TLR4 and iNOS [57]. In another cell culture study, luteolin reversed the effect induced by cytokines in the macrophage cell line RAW264.7 in terms of the expression of iNOS, IL-1 β , IL-6 and TNF α . These events are shown to be mediated by STAT3 since luteolin effectively inhibits its phosphorylation [58].

Studies on individual isolated compounds have shed light on the mechanistic principles of antioxidant therapies [59]. However, it is suggested that the therapeutic benefits relies on the combination of different antioxidants rather than the effects of purified molecules. Chemical complexity of the components present in fruits, vegetables, beverages and medicinal plants is hypothesised to prevent the onset of inflammatory related diseases [26][60]. In this regard, a red wine extract rich in polyphenols was shown to ameliorate the expression of inflammatory markers IL-8, COX2 and iNOS in cytokine challenged HT29 colon cells [61]. Similarly, *in vivo* supplementation with grapes and wine extracts on a mouse model of IBD was demonstrated to mitigate colon inflammation by reduced expression of phosphorylated I κ B and the secretion of IL-1 β , IL-6 and TNF α [62]. In line with the use of natural therapies, a polyphenol extract of the plant *Salvia miltiorrhizae* was proven to interfere in the progression of the NF κ B pathway by suppressing phosphorylated IKK and enhancing I κ B degradation on the rat intestinal cell line IEC-18 stimulated with LPS. Transcriptional activity of NF κ B measured by green fluorescent protein expression in primary cell culture shows further evidence of the extract-dependent inhibition of this pathway [63]. Therefore, the employment

of therapies rich in phytochemicals might carry extra health benefits compared to single-molecule interventions due to the additive and synergetic effect [64].

Table 1.1 Polyphenols research in the context of IBD models. Adapted from [55]

Polyphenol	Model	Significant regulation, altered functions	Reference
Apple polyphenol	LPS/IFN γ challenged human cells (DLD1, T84, MonoMac6, Jurkat)	TNF α \downarrow , IL-1 β \downarrow , MIG \downarrow , IP-10 \downarrow , COX-2 \downarrow , CYP3A4. STAT1 \downarrow , via NF κ B \downarrow , IP-10 \downarrow , IL-8 promoter \downarrow , STAT1 reporter gene activity.	[65]
	DSS and oxazolone-induced mice	Mortality rate \downarrow , weight loss via IL-8 \downarrow	[66]
	LPS-induced Caco2/15 cells	SOD \uparrow , glutathione reductase and peroxidase \uparrow , TNF α \downarrow , IL-1 β \downarrow , IL-6 \downarrow , COX-2 \downarrow , PGE2 \downarrow , NF κ B; via \uparrow Nrf2 and \uparrow PGC-1 α activity	[67]
	DSS induction in genetically immunodeficient mice	Weight loss \downarrow , colonic inflammation \downarrow , colonic shortening \downarrow , IL-1 β \downarrow , TNF- α \downarrow , IL-6 \downarrow , IL-17 \downarrow , IL-22 \downarrow , IP-10 \downarrow , I-TAC \downarrow , MIG \downarrow , IFN- γ \downarrow	[68]
	TNBS-induced rats	Colonic damage \downarrow , COX-2 \downarrow , TNF- α \downarrow , calpain \downarrow , recovery of wounded fibroblast tissue \uparrow , transglutaminase \uparrow	[69]
Bilberry anthocyanins	Cytokine-challenged T84 human colon cells	TNF- α \downarrow , IP-10 \downarrow , I-TAC \downarrow , ICAM-1 \downarrow , GRO- α \downarrow	[70]
	DSS -induced mice	Colonic damage \downarrow , histological scores \downarrow , disease severity \downarrow , inflammation \downarrow , TNF- α \downarrow , IFN- γ \downarrow	[71]
	Cytokine-induced HT-29 cells	NO \downarrow , PGE2 \downarrow , IL-8 \downarrow , iNOS \downarrow , COX-2 \downarrow at via activated STAT1 \downarrow accumulated in the cell nucleus	[72]
Curcumin	TNBS-induced rats	Colonic damage \downarrow , histological scores \downarrow , MPO \downarrow , TNF- α \downarrow , colonic levels of nitrites \downarrow , COX-2 \downarrow , iNOS expression \downarrow ; via p38-MAPK activation \downarrow	[73]
	<i>IL-10</i> ^{-/-} mice (model of chronic colitis)	Colonic damage \downarrow , histology injury scores \downarrow , weight-to-length ratios of colon \downarrow , MPO \downarrow , IFN- γ \downarrow , IL-17 \downarrow	[74]
	TNBS-induced mice	Colonic damage and histopathology \downarrow , IL-1 β \downarrow , MPO \downarrow ; via NF κ B activation \downarrow and p38-MAPK signalling \downarrow	[75]
EGCG and green tea polyphenols	IEC-6 rat intestinal cells	NF κ B \downarrow through IKK activation \downarrow , phosphorylation of I κ B α -GST \downarrow	[76]
	<i>IL-2</i> ^{-/-} mice	Colonic damage and histological scores \downarrow via IFN- γ \downarrow , TNF- α \downarrow	[77]
	LPS-induced peritoneal macrophages	NO production \downarrow , iNOS gene expression \downarrow via NF κ B \downarrow	[78]
Naringenin	DSS-induced mice	Colon shortening \downarrow , colitis severity \downarrow , histological scores \downarrow , iNOS \downarrow , ICAM-1 \downarrow , MCP-1 \downarrow , COX-2 \downarrow , TNF- α \downarrow , IL-6 \downarrow in colon mucosa via mucosal TLR4 mRNA and protein \downarrow , phospho-NF κ B p65 \downarrow , phospho-I κ B α \downarrow	[79]
Olive oil polyphenols	H ₂ O ₂ or xanthine oxidase stress in Caco-2 cells	LPO \downarrow with MDA \downarrow and paracellular inulin transport \downarrow , ROS \downarrow	[80]
	DSS-induced mice	DAI \downarrow , histological scores \downarrow , MCP-1 \downarrow , TNF- α \downarrow , iNOS \downarrow , COX-2 \downarrow via I κ B α \downarrow , PPAR γ \uparrow , phospho-p38 \downarrow , phospho-JNK-MAPKs \downarrow	[81]
Pomegranate polyphenols	DSS-induced rats	Colonic damage \downarrow , histological scores \downarrow , inflammatory cells infiltration \downarrow , PGE2 \downarrow , NO	[82]

and ellagic acid		production ↓, iNOS ↓, PGES ↓, improvement of microbiota condition oxidative stress (ROS and MDA) in plasma and colon mucosa ↓	
	DSS-induced mice	Colonic damage ↓, histological scores ↓, DAI ↓, MPO ↓, histamine (marker of mast cell degranulation) ↓, superoxide anion generation ↓, LPO ↓	[83]
	TNBS-induced rats	Colonic damage ↓, histological scores ↓, MPO ↓, TNF-α ↓, iNOS ↓, COX-2 ↓ via p38- MAPKs phosphorylation ↓, IKBa ↓, nuclear p65 [NFkB] activation ↓	[84]
Quercetin and glycosides	TNBS-induced rats	NOS ↓ and AP ↓ in colonic tissue, MDA ↓, electrolyte absorption ↑	[85]
	DSS-induced rats	Colonic damage ↓, DAI ↓, MPO ↓, IL-1β ↓, TNF-α ↓, iNOS ↓ via NFkB activity ↓ performed by quercetrin; quercetin had no preventive action	[86]
	DSS-induced mice	Weight loss ↓; colonic shortening ↓, histopathological score ↓, IL-1 β ↓, IL-6 ↓, GM-CSF ↓ and COX-2 mRNA ↓ performed by rutin; quercetin had no effect	[87]
	Acetic acid-induced mice	Colonic damage ↓, histological alterations ↓, neutrophil recruitment ↓, edema ↓, via IL-1β ↓ and IL-33 ↓ and IL-10 ↑	[88]
	LPS-induced Caco-2 and SW480 cells	iNOS mRNA and protein expression dose-dependently ↓, NO production ↓ via TLR4 ↓, phosphorylation of IκB ↓	[57]
Resveratrol and piceatannol	TNBS-induced rats	Colonic damage and histological scores ↓, weight loss ↓, MPO activity ↓ via ICAM-1 ↓ and VCAM-1 ↓ levels in the colon and serum, antioxidant function (LPO ↓, GSH ↑)	[89]
	DSS-induced mice	Weight loss ↓, diarrhoea and rectal bleeding ↓, colonic damage and histological scores ↓ via TNF-α ↓, IL-1β ↓, PGES-1 ↓, COX-2 ↓, iNOS ↓, and IL-10 ↑; p38-MAPK signalling ↑	[90]
	DSS-induced mice	Colonic damage and histological scores ↓, weight loss ↓, colon shortening ↓, amyloid A level in serum ↓, TNF-α ↓, IL-6 ↓, IL-1β ↓, percentage of CD4+ T cells and macrophages in mesenteric lymphnodes ↓; via SIRT1 ↑, IκB expression and NFkB activation ↓	[91]
Red wine extract	Cytokine-induced HT29 cells	IL-8 ↓, COX2 ↓, iNOS ↓	[61]
Grapes and wine extract	DSS-induced mice	IL-1β ↓, IL-6 ↓, TNFα ↓ via phosphorylated IκB ↓	[62]
<i>Salvia miltiorrhizae</i> polyphenol extract	LPS-induced IEC-18 rat cells	NFkB pathway ↓ via phosphorylated IKK ↓, IκB degradation ↑	[63]

↑ Increase, ↓ Decrease, COX-2: cyclooxygenase-2; DNBS: dinitrobenzene sulphonic acid; DSS: dextran sodium sulfate; EGCG: epigallocatechin-3-gallate; ERK: extracellular signal-regulated kinase; GM-CSF: granulocyte macrophage colony-stimulating factor; GPO: glutathione peroxidase; GRO-α: growth regulated oncogene-alpha; GSH: glutathione; GST: glutathione S-transferase; IBD: inflammatory bowel disease; ICAM-1: intercellular adhesion molecule 1; IκB: inhibitory κB; IKK: IκB kinase; IL: interleukin; INF: interferon; iNOS: inducible NO synthase; IP-10: Interferoninducible protein-10; IRF1: INF regular factor 1; I-TAC: Interferon-inducible T-cell alpha chemoattractant; JNK: c-Jun N-terminal kinase; LDH: lactate dehydrogenase; LPO: lipid peroxidation; LPS: lipopolysaccharide; MAPK: mitogen-activated protein kinases; MCP-1: monocyte chemoattractant protein-1; MDA: malondialdehyde; MIF: macrophage-migration inhibitory factor; MIG: monokine induced by gamma interferon; MPO: myeloperoxidase; NFkB: nuclear factor-κB; NO: nitric oxide; PGC-1α: peroxisome proliferator-activated receptor gamma coactivator-1 alpha; PGD2: prostaglandin D2; PGES: prostaglandin E synthase; PPAR: Peroxisome proliferator-activated receptor; ROS: reactive oxygen species; sICAM-1: soluble ICAM-1; SOD: superoxide dismutase; SIRT1: silent mating type information regulation-1; STAT: signal transducer and activator of transcription; TLR4: Toll-like receptor 4; TNBS: trinitrobenzene sulfonic acid; TNF: tumor necrosis factor; VCAM-1: vascular cell adhesion molecule-1.

1.4.1 Metabolism of phytochemicals

Based on food consumption studies, it is estimated that the daily human intake of polyphenols is around 1 g/day, being cereals and fruits the major food sources of phenolic acids, anthocyanins and flavonoids [92]. Bioavailability of polyphenols depends not only on their chemical structure but also on isomerism, polymerisation, solubility, hydrophobicity, and the presence of sugars [93][94].

Dietary studies evaluating the metabolism of phytochemicals has been tested in a number of *in vivo* models. Comalada *et al.* presented evidence in which quercetrin, the glycosylated form of quercetin exerts an anti-inflammatory effect in terms of NFκB selective inhibition over AP-1 signalling in a mouse model of IBD. Conversely, the aglycone quercetin only shows efficacy in the inhibition of iNOS and ILs expression when tested in macrophage cells LPS-stimulated *in vitro*. The role of glycoside cleavage in the gut was essential for effective delivery of quercetin into the colon where the therapeutic function is performed [86].

Once absorbed through the gut barrier, polyphenols are conjugated to form *O*-glucuronides, sulphate esters and *O*-methyl ethers. Physical-chemical properties of polyphenols (i.e. mass, charge, hydrophobicity) are known to be altered after conjugation. Changes in these properties impact the metabolites excretion via the kidneys or liver. More importantly, these modifications reduce the number of free hydroxyl groups impacting the antioxidant properties and the ability of polyphenols to interact with enzymes, receptors and transporters [95]. Glucuronide metabolites of EGCG present reduced radical scavenging activity compared to EGCG measured by 1,1-diphenyl-2-picrylhydryl (DPPH) assay. Similarly, tea metabolites present less effectivity in inhibiting cell growth in HT29 colon cancer cells than EGCG [96]. On the other hand, conjugation improves antioxidant activity in some metabolites of ellagic acid, EGCG, and chlorogenic acid compared to the intact polyphenols suggesting that these metabolites play an important antioxidative role after consumption [97]. Digestion of onion

dry skin rich in quercetin in pigs renders methylated, glucuronided and sulphated metabolites in blood with potent radical scavenging activities [98]. Colonic metabolism performed by the microflora is also important in the bioavailability of polyphenols [27]; for instance, proanthocyanidins from red wine can only be absorbed in the gut as low molecular weight phenolic acids [99]. The complexity in the chemistry of polyphenols and derived metabolites warrants further investigation in order to explain their physiological function and biological activities.

1.4.2 Selenium in antioxidant defence

In line with the beneficial effects of phytochemicals, consumption of minerals is identified to carry health benefits for a large array of diseases. In particular, supplementation of selenium in the diet has been consistently reported to produce benefits in the management of inflammatory related conditions. High supplementation of dietary selenium protects against the development of colon inflammation in rats according to tissue histology analysis [100]. In rats under HFD regimen, selenium incorporation reduced triglyceride and ROS levels in the liver and increased the enzyme activity of the oxidative stress protector paraoxonase 1 showing positive outcomes against hypercholesterolemia [101]. Incorporation of selenium into the protein structure as selenocysteine is observed to occur in a small group of proteins known as selenoproteins, however, the physiological role for the majority of these proteins is still lacking [102]. Some of the selenoproteins such as the glutathione peroxidases [103] and thioredoxin reductases [104] provide a protective mechanism against oxidative stress and intestinal inflammation as part of the endogenous antioxidant system. Other members of this family include selenoprotein H (SELH) and 15kDa selenoprotein (SEP15), both reported as potential regulators of cell defence mechanisms [105][106].

1.4.3 *In vitro* models of intestinal inflammation

Various transformed cell lines have been tested in intestinal models of inflammation. Commonly reported *in vitro* models include SW480, Caco-2, HCT116 and HT29 human cells where an inflammatory response can be induced by LPS or cytokine exposure [10]. The great differences in the morphology of these cells and their susceptibility to inflammatory stimulants is a fundamental factor in these type of studies. In the case of LPS challenge, sensitivity is suggested to depend on TLR4 expression. In particular, TLR4 induction with LPS *in vitro* might be considered a suitable model of IBD since patients suffering from UC and CD highly express TLR4 in intestinal epithelial cells [20]. Taking this into consideration, the intestinal epithelial cell line SW480 is an appropriate model of IBD given its high expression of TLR4 and its sensitivity to LPS in comparison to other cell lines such as HCT116 and HT29 [107]. SW480 is a cell line derived from primary adenocarcinoma arising in the colon [108]; it exhibits mutations in the *K-ras* (glycine to valine-12) [109] and *p53* (arginine to histidine-273 and proline to serine-309) [110] genes, and no mutations have been reported in the NF κ B signal pathway genes. Of crucial importance in *in vitro* models of intestinal inflammation, the concentration of tested polyphenol extracts ranges from 50-300 μ M as this reflects the reported physiological content in the gut [111].

1.4.4 *In vivo* models of inflammation in response to HFD supplementation

Metabolic syndromes such as obesity are linked to the expression of inflammatory and immune signals. Concordantly, obese animals are characterised with high levels of expression of pro-inflammatory mediators and stress-response genes such as ILs, leptin, macrophage migration inhibitory factor (MIF), MCP-1 and TGF- β [112]. Consumption of HFD is associated with the generation of ROS resulting in lipid oxidation and is linked to chronic inflammation. Thus, animal HFD supplementation has been used as a model to study the physiological response of excess lipid on the onset of inflammatory related conditions such

as obesity, diabetes type II and NAFLD [113][114]. In addition, HFD supplementation significantly modulates the secretion of obesity and diabetes markers such as insulin and glucagon-like peptide-1 (GLP-1) among others. For instance, GLP-1 is associated with the regulation of glucose levels through increasing insulin and glucagon secretion [115]. In these studies, the mouse strain C57BL/6J is often used as it displays features resembling obesity and diabetes in humans including body weight gain, increased plasma blood glucose and insulin resistance [116]. Deleterious effects of HFD and the potential beneficial effects from nutraceuticals including pure polyphenols [117], fruit and vegetable extracts [118] and fibre [119][120] have been studied. In these studies, the therapeutic efficacy was assessed by their ability to reverse the physiological conditions arising from HFD supplementation such as body weight gain and fasting plasma glucose levels. Further, starch supplementation is reported to elevate the levels of antioxidant enzymes and thus increased antioxidant capacity along with significant alteration in lipid and glucose metabolism genes [120]. These interventions also show effectiveness in inhibiting inflammatory mediators such as NF κ B, AP-1 and ILs in colon, liver and plasma samples [117][118][119].

1.5 Sugarcane

Sugarcane is a tropical grass belonging to the *Saccharum* genus. The crop can be classified into two main species: *Saccharum spontaneum* (wild type) and *Saccharum officinarum* (domesticated). The latter is known to produce thick juicy canes with higher sucrose content and lower fibre content than wild types. Other varieties of sugarcane are suggested as the result of interbreeding such as *Saccharum sinense* (grown in India and China) and *Saccharum barberi* (grown in India, poor sugar content) [121].

Sugarcane is of great economic importance since around 70% of the sugar consumed worldwide is extracted from the plant. Although Brazil and India are the largest producers of sugarcane in the world, Australia accounted for 36,500 thousand metric tons in 2016 [122].

In general terms, cane sugar is produced after sugarcane juice (obtained after mechanical crushing of the plant) is evaporated, crystallised and refined. Ethanol, another important product from this process, can be produced after sugarcane juice fermentation and when combined with petrol at different proportions can be used as a vehicle fuel [123]. The fibre component after juice extraction, known as bagasse, is the main by-product in the sugar production process. In the traditional industrial process, bagasse can be burnt for electricity generation or used as cattle stock feed, however inefficient utilisation of this fibre is a main inconvenient of this process [124].

1.5.1 Sugarcane as a nutraceutical

Sugarcane and its derivatives have long been known to exhibit therapeutic properties. For instance, sugarcane molasses are mixed with powdered leaves from the plant *Tinospora cordifolia* and given to diabetic patients in order to reduce glucose levels according to Bangladeshi traditional medicine [125]. Furthermore, the young stem of this cultivar is used in northeast India as a folk remedy against diabetes [126]. Indian medicine also regards sugarcane stems as useful in gastrointestinal pathologies, cardiac debility, bronchitis, anaemia, and related conditions [127]. Other therapeutic uses of sugarcane include the treatment of vaginal discharge, excessive uterine bleeding and endometriosis [128].

The health benefits associated with the sugarcane plant might be correlated with its chemical composition. Different types of phytochemicals are present in sugarcane and its derivatives, including triterpenoids, sterols, polyphenols and flavonoids found in the ethanol extracts of green and red varieties of sugarcane. The highest concentrations of these compounds were observed in the plant's rind, but also in other parts such as pith, node and tip [129]. Polyphenols, flavonoids and antioxidant activity from sugarcane juice and leaves, are responsible for the observed protective effect against free radical damage [130]. Some of the polyphenolic compounds detected in sugarcane juice and leaves include ferulic acid, p-

coumaric acid and quercetrin among others [131]. Related chemicals and antioxidant activity have been observed in brown sugar [132] and molasses [133]. Interestingly, high concentrations of coumaric acid are obtained after alkaline hydrolysis from bagasse [124].

The presence of these phytochemicals in sugarcane has been suggested to provide anti-inflammatory properties. Ledón *et al.* demonstrated that a mixture of fatty acids derived from sugarcane wax oil reduced the formation of granulomas after subcutaneous cotton pellet insertion in mice. This mixture significantly reduces vascular permeability after acetic acid induction of peritoneal inflammation [134]. In a mouse model of induced diarrhoea, treatment with methanol extracts of the whole plant showed an effective dose dependent reduction in defecation [135]. Aqueous extracts of sugarcane inhibit the nuclear activity of the pro-inflammatory mediator NF κ B and the secretion of IL-8 in Caco-2 colon cells stimulated with IL-1 β [136]. In *in vivo* studies, sugarcane fibre presented positive results in several physiological parameters in the control of obesity. Supplementation of sugarcane fibre in a mouse model of HFD reduced body weight gain, fat mass and fasting glucose and insulin levels compared to control. In addition, sugarcane fibre reversed the expression of ghrelin, leptin and GLP-1 promoted by HFD [119]. Bagasse has been shown to lowered fasting glucose and glucagon levels in streptozotocin-induced diabetic rats [137]. Even though sugarcane is suggested as an anti-inflammatory therapeutic agent, there is only limited information regarding the molecular mechanisms of action orchestrated by this plant.

1.6 Proteomics to investigate the therapeutic effects of nutraceuticals

The recent emergence of state-of-the-art technologies has facilitated the study of nutraceuticals impact at the molecular level. To this end, genomics, transcriptomics, proteomics and metabolomics have been used in the identification of the molecular routes and effectors responsible for the observed beneficial effects [138][49]. Among the ‘omics techniques, proteomics has demonstrated a prominent role in this regard. The field of

proteomics involves the study of proteins at a large scale. The versatility of proteomics permits its application in addressing biological questions related to proteins including identification, quantitation, interactions, post-translational modifications (phosphorylation, glycosylation, methylation etc.), and structure characterisation, among others [139]. Mass spectrometry (MS) is currently the most common approach for the identification and quantitation of proteins and is suitable for the analysis of a great variety of sample types. Known as the bottom-up workflow, proteins are digested with proteolytic enzymes into peptides prior to analysis. The enzyme trypsin produces peptides of an appropriate size and charge for MS applications by cleaving after frequently occurring amino acids, Arginine and Lysine. The complexity of the sample is resolved by the separation of peptides by liquid chromatography (LC) according to their hydrophobic affinity to octadecyl chains (C18) as stationary phase. Peptides are eluted by adjusting the organic solvent concentration, often using gradient elution. Ionisation of peptides through a capillary at high voltage permits nebulisation and delivery into the MS. Tandem MS/MS analysers enable ion separation in a MS1 survey, collision induced fragmentation of selected ions, and measurement of daughter ions in MS2 thus improving sensitivity of protein characterisation compared to previous technologies. The use of sequence database search engines, such as Mascot [131], is essential in the comparison and score-based matching of peptide patterns from the theoretical with empirical data. Introduction of novel MS instruments such as the hybrid quadrupole time-of-flight (TOF) technology affords higher resolution and accuracy in the identification and quantitation of low-abundant peptides in complex samples [140], sequential window acquisition of all theoretical fragment-ion spectra (SWATH)-MS being an important example currently.

1.6.1 SWATH-MS as a data-independent acquisition technique

Of fundamental importance for MS-based proteomics studies, conventional proteomics techniques make use of information dependent analysis (IDA) as a strategy for protein identification and quantitation. IDA methods are considered appropriate for the identification of the maximal number of proteins. However, acquisition for a precursor ion depends on predefined criteria such as selection of the most intense ions [141] which is detrimental for low abundant ions that are often missed during LC separation time scale and not quantitated. It is well known that IDA techniques lack reproducibility in terms of selection of precursor ions [142], making run-run quantitation difficult, needing to impute quantitative values.

SWATH is a data independent acquisition approach (DIA). As opposed to IDA strategies, all the precursor ions within predefined MS1 windows over the chromatographic elution range are sent for fragmentation and then analysed. This produces a complete recording of all analytes in the sample, reducing missing values and allowing accurate reproducibility in the quantitation of complex samples [143]. To enable identification from multiplexed MS2 spectra, a reference peptide spectral library is another element of vital importance for SWATH experiments. Generation of a local library by IDA with combined LC-retention time data is a suitable strategy, as in this case the same instrument and settings as the SWATH experiments are commonly applied. Other strategies consider the integration of local seed libraries with community data repositories [143]. Retention time information of each targeted peptide from the library is matched with the SWATH fragment ion data for a precise peptide identification (Figure 1.5) [144]

Taking these into consideration, SWATH exceeds classical IDA methods such as shotgun proteomics but also outperforms targeted techniques represented by selected reaction monitoring (SRM). Although reproducible and quantitatively accurate, SRM is only applicable to a limited number of precursor-ion mass transitions signals, reducing its employment in complex proteome quantitation [144]. In addition, Bourassa *et al.* compared SWATH-MS with the labelling technique known as isobaric tags for relative and absolute quantitation (iTRAQ) in the protein expression of duodenal tissue from insulin resistant and insulin sensitive patients. Both techniques demonstrated high correlation (Pearson, $r^2=0.72$) in the proteins commonly found and new insights were presented in terms of protein regulation in the context of insulin resistance. Interestingly, iTRAQ showed a higher number of identified proteins whereas SWATH revealed more proteins to be differentially expressed suggesting higher precision [145]. The results from this work illustrate the potential of

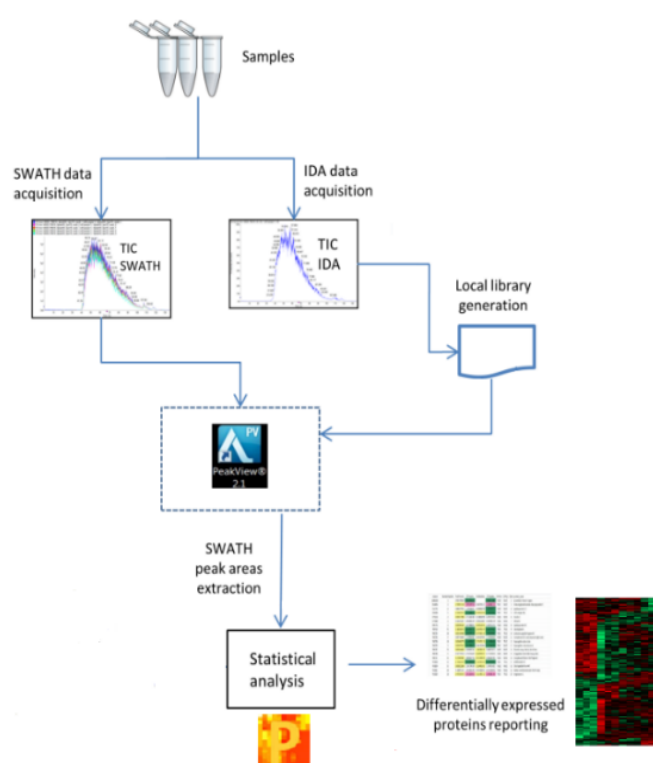


Figure 1.5 SWATH-MS quantitation workflow

Adapted from [143]

SWATH-MS in protein quantitation and its application to the under-explored field of dietary studies.

1.6.2 The application of MS-based proteomics to assess dietary interventions

MS-based proteomics analysis has emerged in recent years as an effective tool to investigate dietary constituents effects [146]. Representative proteomic studies in the context of nutraceuticals and inflammatory studies are summarised in Table 1.2.

Overall, these studies implicate nutraceuticals in causing changes to the proteome in functions linked to lipid and carbohydrate metabolism, fatty acid oxidation, redox signalling, and inflammatory and immune response.

Table 1.2 Proteomics research on nutraceutical interventions in the context of inflammation

Food extract	Model	Tissue analysed	Proteomics approach	Significant regulation, altered functions	Reference
Green tea polyphenols	<i>Mdr1a</i> ^{-/-} mice (model of human IBD)	Colon	2-DE, LC-MS/MS	Regulation of 33 proteins; several related with immune response and inflammation: PRDX1 ↑, SOD ↑, APOA1 ↓, MIF ↓ Predicted inhibition of NFκB (p65), STAT1, STAT3 among others	[147]
Rosemary polyphenols	HT29 colon cells	n/a	2-DE, LC-MS/MS	Regulation of 17 proteins; some related with antioxidant functions: PRDX4 ↑, SOD ↓, GST ↓	[49]
Curcumin	<i>Mdr1a</i> ^{-/-} mice	Colon	2-D DIGE, LC-MS/MS	Regulation of 35 proteins; several related with cellular stress and inflammation: PRDX1 ↑, TXN1 ↑, APOA1 ↓, HSPB1 ↓ Predicted inhibition of NFκB, STAT3, ERK, among others	[138]
Olive oil rich in polyphenols	<i>Apoe</i> ^{-/-} mice (model of atherosclerosis)	Liver	2-DE, LC-MS/MS	Modulation of proteins linked to antioxidant defence and carbohydrate metabolism: SOD ↑, glucokinase ↑, APOA1 ↓	[30]
Corn and wheat bran	Lactating goats	Liver	2-DE, LC-MS/MS	Modulation of 51 proteins associated with redox state and metabolic processes: α-enolase ↑, calreticulin ↑, CYT b5 ↑, GST ↓	[148]
Corn, soybean and wheat bran	Weaning rabbits	Caecum	2-DE, LC-MS/MS	Regulation of 29 proteins associated with stress response, energy metabolism: S100A8 ↓, coactosin 1 ↓, GAPDH ↓, SBP1 ↓	[149]
Polyunsaturated fatty acids	<i>Apoe</i> ^{-/-} mice + HepG2 cells	Liver	2-DE, LC-MS/MS	Alteration of proteins linked to metabolism and redox stress: pyruvate kinase M2 ↑, CYP2C70 ↑, PRDX4 ↑, HSP60 ↑, SOD ↑ Inhibition of NFκB and STAT3 phosphorylation <i>in vitro</i>	[150]
Root ginger extract	HFD fed mice	Liver	2-DE, LC-MS/MS	Regulation of 19 proteins, induction of oxidation of lipid related proteins: ACAA1 ↑, GST ↓, FABP1 ↑, CYT b5 ↑, ECHS1 ↑	[151]
Capsaicin	HFD fed mice	White adipose tissue	2-DE, LC-MS/MS	Regulation of 20 proteins associated with lipid oxidation and redox state: HSP27 ↓, GAPDH ↓, PRDX1 ↓, vimentin ↓, FABP4 ↓	[152]
Grape seed flavan-3-ols	HFD fed mice	Liver	iTRAQ, LC-MS/MS	Modulation of 75 proteins linked to fatty acid and glucose metabolism: pyruvate kinase ↑, FASN ↑, ACOX1 ↓, CYP2E1 ↑	[153]

↑ Increase, ↓ Decrease, Acyl-coenzyme A oxidase (ACOX1), Acetyl-coenzyme A acyltransferase 1 (ACAA1), Apolipoprotein A1 (APOA1), Cytochrome (CYT), Cytochrome P450 (CYP), Enoyl CoA hydratase (ECHS1), Fatty acid binding protein 1 (FABP1), Fatty acid synthase (FASN), Glyceraldehyde-3-phosphate dehydrogenase (GAPDH), Glutathione-S-transferase (GST), Heat shock protein (HSP), Peroxiredoxin (PRDX), Selenium binding protein 1 (SBP1), Superoxide dismutase (SOD), Thioredoxin (TXN), Two dimensional gel electrophoresis (2-DE).

1.6.3 Phosphoproteomics analysis in food interventions

The study of protein phosphorylation is of importance in recognising vital aspects of cellular mechanisms such as cell growth, differentiation and cell cycle. Phosphorylation plays a major role in modulating protein functions such as activation state, cellular localisation, interaction with other proteins and degradation [154]. Phosphorylation of serine, threonine and tyrosine residues mediated by protein kinases is considered as one of the most common post-translational modifications. This modification is studied with the use of proteomics techniques. In this regard, MS-based phosphoproteomics is an important tool that can be utilised in the characterisation of signalling networks and the putative mechanisms associated with diet interventions [146]. Reversible protein phosphorylation is central to the regulation/dysregulation of inflammatory mediators and is known to influence the development of chronic inflammatory pathologies [155].

One of the main challenges of phosphoproteome research is the low stoichiometry of phosphopeptides in the overall proteome. To overcome this, the use of enrichment strategies is of great relevance. Due to the negative charge of the phosphate group, phosphopeptides present affinity to metal oxides such as titanium dioxide (TiO₂) [156]. Quantitation of enriched phosphopeptides can be performed by either label or label-free methods. Stable isotope labelling of amino acids in cell culture (SILAC) is a common technique for labelling studies. In this technique, stable isotope ¹³C+¹⁵N-amino acids are incorporated in the growth media. After cell lysates are labelled with the heavy (¹³C+¹⁵N) or light (¹²C+¹⁴N) amino acids they can be mixed and two distinguishable versions of the same peptide can be detected by MS analysis. This technique affords high reproducibility between runs, high data quality and robustness [157].

SILAC is compatible with quantitative phosphoproteomics analysis. The combination of phosphopeptide enrichment with SILAC has been employed in the context of antioxidant

therapies. RSV treatment in human breast adenocarcinoma MCF7 cells under serum deprived conditions exhibited changes in the phosphorylation of members of the MTORC1/S6K pathway suggesting inhibition of the autophagy machinery in particular PRAS40 [158]. In another study, the soybean isoflavonoid genistein was identified to regulate apoptosis mediators in gastric cells as revealed by SILAC-phosphoproteomics. Some of these events included inhibition in the phosphorylation of several cell receptors, ERK1/2 and signalling products, suggesting MAPK and AKT cascades down-regulation [159].

One of the drawbacks of labelling techniques is the limited number of biological conditions that can be assessed [160]. Another limitation is the reduced applicability in cell culture given that only some cell lines can be grown in depleted media - as requirement of the SILAC approach. In addition, the need of a minimum passage number for complete isotope incorporation restricts SILAC use in primary cell lines [156].

In contrast, label-free quantitation of phosphopeptides is not limited in relation to the number of biological conditions to be assessed, and has no extra steps in terms of sample preparation. The label-free approach to the quantitation of phosphopeptides is applicable to most sample types, including clinical samples [160]. As observed in Figure 1.6, label-free performs relative quantitation to other samples. Label-free quantitation strategies are based on signal intensity of peptides or spectral counting. Although label-free quantitation techniques are broadly used in biomedical fields [161], to the best of our knowledge label-free phosphoproteomics is relatively under-explored in applications associated with food nutraceuticals.

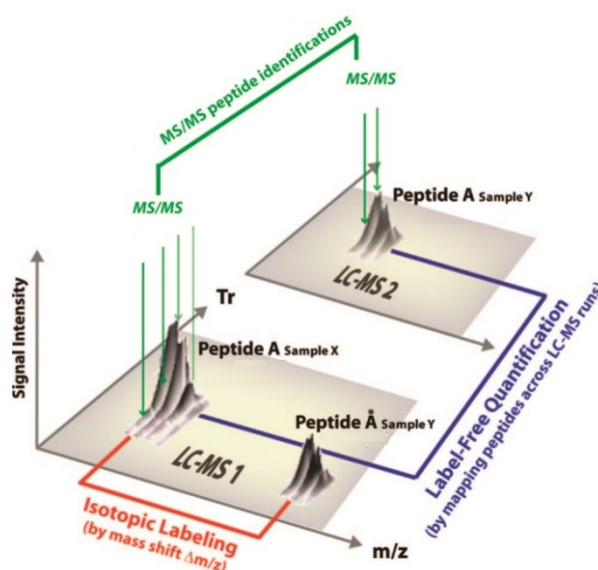


Figure 1.6 SILAC (red) and label-free (blue) quantitation strategies

Adapted from [160]

1.6.4 Multiplex bead-based ELISA

Even though MS-based techniques in proteomics have advanced significantly in recent years, the identification of low-abundant circulating markers such as cytokines remains a challenge. In this regard, levels of inflammatory markers in plasma are reported to occur at the femtomolar range [162] complicating their identification with conventional MS techniques. Alternative strategies for the quantitation of these analytes such as enzyme-linked immunosorbent assay (ELISA) although effective typically only detects one analyte per sample. Multiplex bead-based ELISA analysis is a more recent technology that combines ELISA's principle detection in immuno-linked fluorescent beads with flow cytometry making possible the detection of multiple analytes simultaneously. The principle consists of a capture antibody for each marker that is attached to a bead with a characteristic proportion of two fluorescent dyes. This feature permits pooling of multiple beads that can be later separated during data acquisition. Addition of a biotinylated antibody that contains a green fluorescent reporter dye serves for the quantitation of the markers in each subset of beads (Figure 1.7a).

Concentration is determined with the use of standards and the construction of a calibration curve in the same way as in ELISA methods [163] (Figure 1.7b).

Inflammatory circulating protein markers are biological molecules of major relevance in the development of disease state and particularly in nutritional studies [146], and multiplex bead-based quantitation has shown to be effective in this context. For instance, 0.8% quercetin supplementation in conjunction with HFD in C57BL/6J mice for 8 weeks showed reduction in the expression of IFN γ , IL-1 and IL-4 compared with the HFD group [164]. C57BL/6N mice suffering from chronic liver disease after chemical induction and HFD supplementation, showed decreased secretion of inflammatory mediators IL-3, IL-4, IL-6, TNF α , IFN γ among others after polyphenol extracts supplementation from *Lonicera caerulea* L. berry [165]. As exemplified with these studies, multiplex bead-based is a powerful tool to measure low abundant circulating proteins that would escape MS detection.

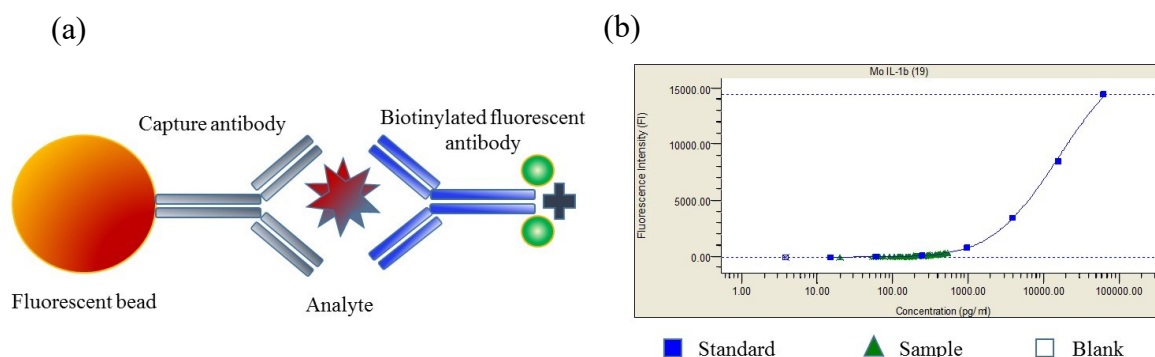


Figure 1.7 (a) Multiplex bead-based principle detection. **(b)** IL-1 β calibration curve and fluorescent intensity from samples and blank

1.7 Aims and scope of the project

This PhD project was conducted over 3.5 years in an industry partnership with Gratak Technologies Pty Ltd. to investigate the potential anti-inflammatory properties of whole dried sugarcane (WDS) as a nutraceutical. The first part of the thesis explored the mechanisms of WDS regulating inflammatory signalling in an *in vitro* colon cancer cell line model of LPS induced inflammation. This was followed by an *in vivo* study using a HFD mouse model to explore whether WDS dietary supplementation affects inflammatory modulator proteins. The specific aims were as follows:

- Determination of the polyphenol, flavonoid and antioxidant content of ethanol extracted WDS.
- Characterisation of the proteomic cellular response and impact on signalling pathways associated with WDS extracts in an *in vitro* gut inflammatory model.
- Characterisation of the effect on inflammation of WDS dietary supplementation in an *in vivo* HFD mouse model through measuring plasma inflammatory markers and the liver proteome.

Chapter 2 Regulation of inflammatory mediators by dried sugarcane extracts in an *in vitro* colon cancer cell model of LPS-induced inflammation

Chapter 2

Regulation of inflammatory mediators by dried sugarcane extracts in an *in vitro* colon cancer cell model of LPS-induced inflammation

Experimental work and data analysis from this chapter was performed by Daniel Bucio Noble. The mass spectrometer was run by Daniel Bucio Noble with the assistance from Dr. Christoph Krisp at the Australian Proteome Analysis Facility. Manuscript was written by Daniel Bucio Noble with contributions from Assoc. Prof. Mark P. Molloy, Dr. Liisa Kautto, Dr. Christoph Krisp, and Dr. Malcolm S. Ball.

Regulation of inflammatory mediators by dried sugarcane extracts in an *in vitro* colon cancer cell model of LPS-induced inflammation

Daniel Bucio-Noble¹, Liisa Kautto¹, Christoph Krisp^{1,2}, Malcolm S. Ball^{1,3}, Mark P. Molloy^{1,2*}

¹ Australian Research Council Industrial Transformation Training Centre for Molecular Technology in the Food Industry, Department of Chemistry and Biomolecular Sciences, Macquarie University, Sydney, Australia.

² Australian Proteome Analysis Facility, Macquarie University, Sydney, Australia.

³ Gratuk Technologies Pty Ltd., Sydney, Australia.

***Corresponding author:** Mark P. Molloy, Department of Chemistry and Biomolecular Sciences, Macquarie University, Level 3, Building E8C, Research Park Drive, Sydney 2109, Australia. Tel: +61 2 9850 6218. Fax+61 2 9850 6200. E-mail: mmolloy@proteome.org.au

Disclosures: MSB is an employee of Gratuk Technologies Pty Ltd who provided partial funding for this project under the Australian Research Council Industrial Transformation Training Centre scheme. All other authors have no disclosure to make.

2.1 Abstract

Sugarcane is an important commercial crop widely grown in tropical regions for sugar, associated food derivatives and for ethanol production. Sugarcane is also a rich source of phytochemicals but its nutraceutical potential has been under-explored. We show that ethanol extracts of whole dried sugarcane (WDS EE) recovers a rich source of polyphenols and flavonoids that act on inflammatory mediator proteins. To investigate the mechanisms of this activity we used a label-free SWATH-based mass spectrometry approach to profile the proteome of lipopolysaccharide-stimulated SW480 colon cancer cells after exposure to WDS EE and compared this response to that of the well-known polyphenol, resveratrol (RSV). We quantitated ~3,000 proteins and used pathway expression analysis, Western blot and ELISA to corroborate our findings. Proteomics results indicate that WDS EE significantly altered the expression of proteins related to oxidative stress regulation such as SELH and FOXRED1. Based on protein expression changes, WDS EE was predicted to down-regulate NFκB pathway members including TLR2, TLR4, NIK and IκB. We confirmed reduced levels of NFκB phosphorylation and IL-8 secretion. In contrast, RSV did not reduce IL-8 secretion and was predicted to act primarily through modulation of PI3K/AKT pathway in these cells. Our results present WSD EE as a potential functional food with utility for regulating key anti-inflammatory mediators.

Keywords: sugarcane; resveratrol; NFκB; polyphenols; inflammation; proteomics.

2.2 Introduction

Sugarcane is a cultivar of great economic importance grown in the tropics for sugar and ethanol production. Despite the major contributions of sugarcane in the economic development, this crop has a great under-explored potential as a nutraceutical. The presence of agents associated with health benefits such as polyphenols, flavonoids, phytosterols and triterpenoids have been documented [129]. Multiple studies have provided evidence of the potential benefits that can be attributed to sugarcane [119][136]. Sugarcane derivatives from the sugar production including juice, molasses and syrup are also important sources of phenolics with strong antioxidant activity [130][166]. Even though its potential therapeutic relevance, the molecular mechanisms involved in the treatments using sugarcane are poorly understood.

Nutraceuticals and functional foods have gained attraction in recent times thanks to its benefits in the prevention and treatment of inflammation and other conditions. For instance, dietary fibre is identified to reduce the expression of several molecular markers of inflammation due to the action of butyrate as its main fermentation product [167]. *In vitro* and *in vivo* studies have implicated polyphenols and flavonoids as important nutraceutical agents due to their strong antioxidant and anti-inflammatory properties [168]. The polyphenol resveratrol (RSV) is regarded as a potent anti-inflammatory and anti-carcinogenic molecule thanks to its ability to effectively modulate signalling cascades linked to inflammatory-related conditions [169].

Among the multiple signalling pathways that regulate the inflammatory response, NF κ B is identified to play a central role. Activation of the toll-like receptors (TLR) by inflammatory stimulants such as lipopolysaccharides (LPS) and cytokines triggers the mechanism that leads to phosphorylation and subsequent nuclear translocation of NF κ B [170]. Nuclear localised NF κ B initiates transcription of pro-inflammatory genes TNF α , IL-1, IL-8 among others [47].

Therefore, regulation of NF κ B translational activity is one therapeutic strategy to control induction of pro-inflammatory mediators [147].

Although widely used in biomedicine, the use of 'omics techniques such as genomics, transcriptomics, and proteomics is still emerging for investigations of functional foods. Mass spectrometry (MS)-based proteomics is a useful tool for the purpose of identifying the cellular response of dietary products [146]. For instance, *in vitro* experimentation on LPS-stimulated RAW264.7 cells treated with the *Lactobacillus acidophilus* product N-acetylmuramic acid (NAM), demonstrated an anti-inflammatory response based on the inhibition of NF κ B pathway members [171].

In this study, we characterised WDS EE for polyphenol and flavonoid concentrations, then investigated the proteome response in an *in vitro* gut inflammatory model of LPS-stimulated SW480 colon cells. We contrasted the response to that obtained the well-known polyphenol, RSV. Over 2900 proteins were quantitated by sequential window acquisition of all theoretical fragment-ion spectra (SWATH)-MS which revealed distinct responses of WDS EE and RSV to mediate anti-inflammatory activities. This study suggests that WDS EE has nutraceutical properties that could have utility for responding to cellular inflammation.

2.3 Methods

WDS extraction

WDS (provided by Gratuk Technologies Sydney, Australia) was obtained from whole sugarcane grown in Queensland, Australia. Briefly, fresh sugarcane was collected from a controlled field, cut into billets and transferred to cool ($<10\text{ }^{\circ}\text{C}$) storage for processing. Billets were processed within 24 hours of cutting. The billets underwent multiple size reduction steps using sheer force to disrupt the cell wall until particle size was approximately 10mm. The sugarcane was steeped using a proprietary technology to remove sucrose whilst maintaining the content of dietary fibre, minerals and other components. Water/sugar solution was removed by centrifugation and the particles dried using proprietary technology by exposing the sugarcane to super-dried air. The dried particles were milled using a gap mill until particle size was $<50\text{ }\mu\text{m}$. Nutritional information of WDS is presented in Appendix 1 Table 2A.1. Extraction of WDS and raisins (Coles, Sydney, Australia) was performed on 52% (v/v) ethanol in an ultra-sonic water bath at $60\text{ }^{\circ}\text{C}$ for 30 min following the protocol reported by Feng *et al* [129]. WDS suspended in ethanol was centrifuged at 5000 rpm for 5 min and the supernatant was collected and immediately analysed for polyphenol and flavonoid content. Full analysis of WDS extract is being conducted by PhD candidate Wei Chong, Macquarie University. It has been determined that WDS ethanol extract is composed of insoluble fibre (lignin, cellulose), soluble fibre (starch), protein and minerals (Wei Chong, personal communication). Cranberry juice (Ocean Spray Intl.) was used neat.

Total Polyphenol content (TPC)

TPC was determined as described by Singleton et al [172]. Briefly, WDS EE, raisins extract and cranberry juice ($20\text{ }\mu\text{L}$) was mixed with 1.58 mL of water and $100\text{ }\mu\text{L}$ of the Folin-Ciocalteu reagent (Sigma Aldrich). After 6 min of incubation, the solution was mixed with

300 μL of 7.5% (w/v) Na_2CO_3 and left to stand for 2 hours. Gallic acid was used as a standard over the concentration range of 25-500 mg/L. Optical density was read at 765 nm and results were reported in terms of mg gallic acid equivalents (GAE)/100g extract.

Total Flavonoid content (TFC)

TFC was determined by the aluminium chloride complex formation method [173]. Briefly, WDS EE, raisins extract and cranberry juice (250 μL) was mixed with 1.25 mL of water and 75 μL of 5% (w/v) NaNO_2 . After 6 min of incubation at room temperature, the solution was mixed with 150 μL of 10% (w/v) AlCl_3 . Final incubation of 5 min followed the addition of 0.5 mL 1M NaOH. (+)-catechin was used as a standard at over the concentration range of 50-500 mg/L. Optical density was read at 510nm and results were expressed as mg (+)-catechin equivalents (CE)/100 g extract.

Cell culture and protein extraction

The colon carcinoma cell line SW480 was cultured in RPMI 1640 medium supplemented with 1% (v/v) of L-glutamine (Thermo Fisher Scientific), 10% (v/v) of fetal bovine serum (Life Technologies), 1x GlutaMAX (Thermo Fisher Scientific), and 1% (v/v) antibiotic (penicillin, 100 $\mu\text{g}/\text{mL}$ and streptomycin, 100 $\mu\text{g}/\text{mL}$) and incubated at 37 °C and 5% CO_2 before lysis.

Concentration of polyphenols present in WDS EE was adjusted to 50 μM and dried before use for cell culture. Dried WDS EE was resuspended in RPMI 1640 medium before treatment. RSV (Sigma Aldrich) was dissolved in dimethyl sulfoxide (DMSO, Sigma Aldrich) to a concentration of 50 μM . Inflammatory response was induced by cells incubation with 5 $\mu\text{g}/\text{mL}$ of LPS from *Escherichia coli* (Sigma Aldrich) for 4 hours. After inflammatory stimulation, cells were exposed to WDS EE or RSV for 20 hours still in the presence of LPS.

For western blot determinations, LPS stimulation lasted for 2 hours followed by WDS EE and RSV exposure for 1 and 4 hours.

Cells were harvested by scraping them into ice cold phosphate buffered saline (PBS), and centrifuged at 3000 rpm for 3 min, supernatant was removed afterwards. Lysates were obtained by resuspending cell pellets in 250 μ L of 1% (w/v) of sodium deoxycholate, and boiled at 95 °C for 3 min. 0.1 μ L of benzonaze was added and incubated at room temperature for 30 min. Protein concentration was determined using the bicinchoninic acid assay (560 nm).

Western Blot

Protein (10-15 μ g) was reduced with 20 mM of dithiothreitol (DTT), and loaded on sodium dodecyl sulphate – polyacrylamide gel electrophoresis (SDS-PAGE, NuPAGE 4-12% Bis Tris gel, Thermo Fisher Scientific) followed by transfer onto a nitrocellulose membrane (Bio Rad). Membranes were blocked in 5% (w/v) skim milk tris buffered saline-Tween 20 (TBS-T, 100 mM NaCl/Tris pH 7.4, 0.1% (v/v) Tween-20) for 1 hour. Nitrocellulose membranes were blotted with primary antibodies anti-pNF κ B (Ser536), anti-NF κ B, anti-pAKT (Ser473), anti-AKT, anti-p p70S6K (Thr389) and anti-p70S6K (Cell Signalling) at 1:1000 dilution each, in a 5% (w/v) bovine serum albumin (BSA) TBS-T solution, and incubated overnight at 4°C. Membranes were washed three times with TBS-T and incubated with goat anti-rabbit secondary antibody (Li-COR) at 1:10,000 dilution in 5% (w/v) BSA TBS-T solution. Signals were visualised by exposure at 800 nm using the Odyssey Imaging System (Li-COR).

IL-8 quantitation by ELISA

Cell culture media was collected for control, LPS, WDS EE and RSV-treated cells, three biological replicates each. Supernatant was collected after centrifugation at 3,000 rpm for 10 min at 4 °C and stored at -80 °C until analysis. IL-8 concentration was measured on cell

culture by the human IL-8 ELISA kit (Elisakit) according to manufacturer's protocol. Concentration of IL-8 was determined in reference to a calibration curve made from standards provided in the kit. Each sample was analysed in two technical replicates. Briefly, 50 μ L of sample, standards and blank were incubated with 50 μ L of assay diluent for 2 hours at room temperature. After washing four times with washing buffer, 100 μ L of biotin labelled detection antibody was added and incubated for 2 hours at room temperature. Washing step was repeated and 100 μ L of streptavidin-HRP conjugate was added and incubated for 45 min at room temperature. Further washing was followed by the addition of 100 μ L of TMB substrate and incubated for 15 min at room temperature in the dark. Reaction was stopped with 50 μ L of stop solution. Optical density was determined at 480 nm.

Mass spectrometry (LC-MS/MS)

Protein (10 μ g) was reduced with 10 mM of DTT for 30 min at 60 °C and alkylated with 20 mM of iodoacetamide for 20 min at room temperature in the dark. Samples were digested with trypsin (Sigma Aldrich) in 1:50 ratio and incubated at 37 °C overnight. Impurities from digested peptides were removed in a C-18 column pre-conditioned with 100% (v/v) methanol and 2% (v/v) acetonitrile (ACN). Peptides were recovered in 70% (v/v) ACN, dried and resuspended in 1% (v/v) TFA for LC-MS/MS.

Library was generated by the fractionation of an untreated sample of SW480 cells in a high pH reverse phase high performance liquid chromatography (HPLC) using a C18 column 2.1 mm x 150 mm, 3.5 μ m (Zorbax). After sample injection, elution was performed in a buffer A of 5 mM of ammonia pH 10.4 – buffer B of 90% (v/v) acetonitrile, 5 mM of ammonia gradient. Library and SWATH-MS data were acquired in a 6600 Triple TOF mass spectrometer coupled with an Eksport 415 LC system (Sciex). For each sample 10 μ L (0.1 μ g/ μ L) was transferred onto a peptide trap using a 2% (v/v) ACN, 0.1% (v/v) formic acid isocratic flow at 5 μ L/min for 3 min. Sample was eluted with a gradient of 5-35% ACN using

a buffer B of 99.9% (v/v) ACN, 0.1% (v/v) formic acid. Library data was acquired in a data dependent acquisition mode by the selection of ion precursors of the 20 most intense ions in a 120 min run. SWATH data were acquired in a data independent mode with a mass range of 400-1250 m/z, 100 variable windows in a 60 min run per sample.

Data Analysis

Database searches utilised the ProteinPilot 5.0 (Sciex) software using the paragon search algorithm. Human SwissProt database (20,199 entries, February 2016) was used selecting the following parameters: trypsin as digestion enzyme, carbamidomethylation as fixed cysteine modification, biological modifications were allowed and the reversed database search was enabled to allow false discovery rate (FDR) calculation. We employed a protein global FDR of 1%. Information extracted from SWATH MS peak areas was performed using Peak View V2.1 with SWATH MicroApp 2.0 (Sciex) using the library search output file. Extraction of ion chromatograms (XICs) and determination of peak areas for the entire data set was performed using the following parameters: 6 transitions per peptide, exclusion of shared peptides, 100 as maximum number of peptides per protein, 99% confidence, <1% extraction FDR, 75ppm fragment accuracy, and 5 min extraction time window. Given that the abundance of shared peptides might be the result of the contributions from several proteins that are affected differently depending on the condition tested, shared peptides were excluded. Non-tryptic and semi-tryptic peptides were excluded focusing on fully tryptic peptides only. Other modifications rather than cysteine alkylation were excluded. It is described that the inclusion or exclusion of semi-tryptic peptides does not change the SWATH data analysis, as these will be extracted in the same manner as fully tryptic peptides [174]. The ion peak areas exported by Peak View for each sample were normalised by total area normalisation as described previously [143]. The total sum of all ion intensities for each sample was calculated and hence maximum total ion intensities determined. The total ion intensity of each sample

was then divided by the maximum totals, thus the normalised ion intensities sum up to the same amount for all samples. The normalised ion data was summed by peptide and protein. Quantitation was achieved based on XICs of MS/MS spectra. Computation of protein fold changes between groups takes into consideration all peptides showing up-regulation and down-regulation. Final fold change is calculated based on the direction that presents the maximum confidence (obtained from the reproducibility data from all peptides and the number of peptides showing the same direction) [175]. Significantly altered proteins is a reflection of both up and down-regulated peptides, and hence theoretically not all peptides agree with the final fold change at the protein level. However, from our experience most peptides from regulated proteins show the same trend in terms of fold change. Discrepancies in this relation could be due to an interference in one of the transition traces or an unknown modification present in one of the groups. Perseus 1.5.5 was employed for statistical analysis. Decoy peptides were removed prior to \log_2 transformation of peptide intensity. Statistical significant hits were identified by group comparison using the Student's t-test ($p\text{-value} < 0.05$) and a fold change greater than 1.5.

Ingenuity Pathway Analysis

IPA (Ingenuity Systems) was employed in order to obtain further information in regards to the protein expression promoted by the different treatments analysed in this study. Prediction of functions and diseases and upstream regulator analysis were performed considering the paired comparisons: WDS EE/LPS and RSV/LPS relative to the fold changes and p-values of the 2,944 proteins quantitated across all samples.

2.4 Results

WDS EE is a rich source of polyphenols and flavonoids

Using ethanol extraction as described by Feng et al [129], we determined the total polyphenol content (TPC) and total flavonoid content (TFC) of WDS EE. We referenced these values to gallic acid equivalents (GAE) and (+)-catechin equivalents (CE), respectively. Accordingly, WDS EE contains 330 mg of GAE/100g of TPC and 102 mg CE/100g of TFC (Figures 2.1a and 2.1b). TPC and TFC values reported for raisins and cranberry juice in the literature [176][177] are consistent with the values reported here, therefore these results should serve as a validation of the extraction methodology and the TPC/TFC quantitation employed in this study. Compared to other food products, WDS EE contains as much polyphenols and flavonoids as soluble extracts derived from apples, plums and black grapes [178][179].

WDS EE promotes proteome changes in an *in vitro* inflammatory cell model

To examine the potential anti-inflammatory utility of WDS EE we used a LPS-stimulated *in vitro* inflammatory model of colon epithelial cells using SW480 cancer cells. Following 4h LPS induction, cells were treated with either WDS EE or RSV for an additional 20 hours. Protein expression for three biological replicates of each group was analysed using the label-free mass spectrometry approach SWATH-MS [143]. We created a peptide spectral reference library composed of around 6,000 proteins and used it to extract peptide areas from SWATH acquisitions of all samples, enabling quantitative information on 2,944 proteins across all 12 samples.

Hierarchical clustering analysis of protein expression using ANOVA multiple sample tests and principal component analysis representing the overall changes among the four groups are illustrated in Figure 2.2. This demonstrates striking differences in the proteome response between WDS EE and RSV treatments. Using a criteria of >1.5-fold change in abundance

and $p\text{-value} < 0.05$, we identified 34 up-regulated and 18 down-regulated proteins in the LPS group compared to the control group (Appendix 3 Table 2A.2). WDS EE against LPS comparison showed 13 up-regulated and 21 down-regulated proteins (Table 2.1), whereas RSV against LPS comparison exhibited 47 up-regulated and 33 down-regulated proteins (Table 2.2). Focusing on the response to WDS EE, we noted up-regulation of Selenoprotein H (SEPH) and down-regulation of FAD-dependent oxidoreductase domain containing 1 protein (FOXRED1). From the up-regulated proteins only three were shared between the WDS EE and RSV groups, whereas only one down-regulated protein was common between the WDS EE and RSV groups (Figure 2.3), suggesting these agents work through differing mechanisms.

WDS EE and RSV show independent effects on protein expression

Ingenuity Pathway Analysis was used to examine the biological functions associated with WDS EE and RSV changes to the 2,944 quantitated proteins (Figure 2.4). Proteins from the WDS EE treatment showed down-regulation of biological functions annotated as fusion of cellular membrane, infection of tumour cells, internalisation by tumour cell lines, polymerization of filaments and tumorigenesis of tissue. Up-regulated functions from this treatment include growth of organism and formation of focal adhesions. Showing an opposite effect compared to WDS EE, RSV promotes the up-regulation of functions related to mitochondrial function such as length of mitochondria and transmembrane potential. Other up-regulated functions linked to RSV and down-regulated by WDS EE are growth of Golgi cisternae, translation of mRNA and translation of RNA. These results confirm that WDS EE and RSV promote different biological effects, which was not unexpected given the molecular complexity of the WDS EE compared to RSV.

WDS EE is predicted to act in a manner similar to some other polyphenols

To further investigate the molecular effects of WDS EE and RSV treatments, we utilised the upstream regulator analysis function of IPA [180]. This tool predicts the activation or deactivation of potential regulators based on the differentially regulated proteins detected by proteomic analysis. WDS EE is predicted to alter the proteome in a manner similarly to some polyphenols including quercetin (z-score 3), carnosol (z-score 2) and curcumin (z-score 1.7) (Table 2.3). These results are in accordance to the TPC and TFC determinations obtained from WDS EE (Figure 2.1). RSV on the other hand presents low similarities to the above mentioned polyphenols; carnosol (z-score 1) and curcumin (z-score -2.3) (Table 2.3).

WDS EE is predicted to down-regulate the NFκB signalling pathway

Upstream analysis identified that several members of the NFκB signalling pathway are inhibited after WDS EE treatment. As shown in Figure 2.5a, WDS EE is predicted to repress the expression of TLR2 (z-score -2), TLR4 (z-score -2), NIK (z-score -2.2), and IκB (z-score -2.4). WDS EE is also predicted to inhibit a pro-inflammatory target product of this pathway, TNFα (z-score -2.2). To corroborate these predictions, we measured NFκB activation by immunoblotting for phospho-Ser536 following WDS EE treatment. This phosphosite is associated with nuclear translocation and is known to be highly stimulated by LPS through TLR4 interaction [170]. As shown in Figure 2.5b, WDS EE and RSV significantly suppress phospho-NFκB after 4 hours, consistent with a role in regulating NFκB activity, as has been previously reported for RSV [181]. We also measured the concentration of the IL-8 pro-inflammatory cytokine in cell culture media. Secretion of IL-8, a transcription target of NFκB [47], was greatly stimulated in response to LPS, whereas subsequent WDS EE incubation significantly reduced the level of this cytokine by 30%, while RSV failed to alter IL-8 secretion after 20h (Figure 2.5c). Based on these observations, it is clear that WDS EE exerts

an anti-inflammatory response at least partly through the NF κ B pathway. Interestingly, despite reduction of phospho-Ser536 NF κ B after 4h with RSV, the absence of an effect to reduce the expression of the IL-8 target gene suggests other regulatory mechanisms are important in mediating RSV activity in colon cells.

RSV targets the PI3K/AKT/mTOR pathway

IPA up-stream regulator analysis suggested that RSV exerts its effects through the PI3K/AKT/mTOR pathway. This is seen with the predicted activation of PTEN (z-score 1.8) and AMPK (z-score 1.5). Additionally, RSV is predicted to inhibit MYC (z-score -2.7), mTOR (z-score -2.4), mTORC1 (z-score -1.3) and p70S6k (z-score -1.2) (Figure 2.6a). To confirm these predictions we used immunoblot to measure changes in phosphorylation of p70S6k and AKT. As opposed to WDS EE, RSV effectively reduced the phosphorylation of p70S6k Thr389 which is linked to kinase induction activity. Further, the phosphorylation of AKT Ser473, an event associated with the induction of AKT signalling was greatly reduced after 4h, whereas, WDS EE had no effect (Figure 2.6b). Overall, these results confirm that RSV exerts an anti-inflammatory effect through repressing the activity of the PI3K/AKT/mTOR pathway, and that signalling through this pathway is not affected by WDS EE.

2.5 Discussion

In this study we have shown that WDS EE contains a potent reservoir of phytochemicals that provide anti-inflammatory activity through regulation of NF κ B pathway activity in an LPS-induced colon cell inflammatory model. There is a consensus linking many phytochemicals with antioxidant properties effective in the treatment of chronic inflammatory conditions [182]. We showed that WDS EE contain high levels of polyphenols and flavonoids and hypothesised these to confer the measured anti-inflammatory effects.

The LPS model employed in this study was validated to promote inflammation given the augmented levels of phosphorylated NF κ B (Figure 2.5b), and increased secretion of IL8 (Figure 2.5c). Effective in countering these effects, WDS EE was assessed in its ability to reverse the inflammatory state induced by LPS, justifying the addition of the extract after the LPS challenge. In this study, the dosage employed (50 μ M) of WDS EE and RSV is appropriate and is considered within the range of the physiological content of polyphenols in the gut [111][136].

One caveat arising from this study refers to the use of DMSO as the vehicle to solubilise RSV in comparison to cell culture media used in WDS EE. Despite these differences, evidence suggests that DMSO is unlikely to produce any deleterious effect in cell functioning mechanisms at concentrations below 0.1% (v/v) [183]. The DMSO concentration employed in this study (0.06% (v/v)) is also below the maximum concentration suggested for *in vitro* experiments (0.5% (v/v)) [183]. Nonetheless, the main objective of this chapter was to study the effect of WDS EE on LPS-induced inflammation and thus RSV is not needed for this comparison.

For the statistical processing of the SWATH-MS generated data, we used a threshold consisting of p-values<0.05 and fold changes>1.5. Despite some studies consider the use of

a >1.2-fold change cut-off, selection of a higher cut-offs permits to focus on the most relevant changes in the proteome. Consequently, the robustness and accuracy of SWATH-based proteomics as the quantitation strategy permits the confident identification of significantly regulated proteins using higher fold change (>1.5) and p-value<0.05 cut-offs [143].

Our results indicate that applying stringent thresholds (i.e. FDR-corrected p-value<0.05 and fold change>1.5) is detrimental by reducing the number of significantly expressed proteins. In SWATH-based proteomics experiments, a conventional proteomics cut-off (i.e. p-value<0.05 and fold change>1.5) is more effective in augmenting the number of true positives and reducing the number of false positives compared to stringent thresholds (i.e. FDR-corrected p-value<0.05 and fold change>1.5), where almost no true positives are identified [143]. Although in this study the true and false positives are unknown, it is concluded that p-value FDR correction might be too stringent for pairwise comparisons [143].

The label-free SWATH-MS protein quantitation method that monitored expression of ~3,000 proteins in all samples indicated that WDS EE promoted some changes in the SW480 cell proteome. For instance, SELH belongs to the selenoprotein family that also includes the thioredoxin reductases and glutathione peroxidases. Selenoenzymes are considered part of the cell defence mechanism, acting against free radical oxidation. SELH in particular, confers an increase in antioxidant activity and expression of antioxidant enzymes such as glutamylcysteine synthetase under oxidative stress conditions in neuron cells *in vitro*. Further evidence implicates SELH as a DNA binding element that might control the response in changes in the redox status [184]. Recent evidence shows deficiency of SELH in zebrafish to induce inflammation, oxidative stress and DNA damage [185]. We hypothesise that up-regulation of SELH expression driven by WDS EE benefits the cell to manage oxidative stress.

FOXRED1 is an oxidoreductase enzyme member of the mitochondrial complex I which is essential for the ATP production by oxidative phosphorylation in the mitochondrial respiratory chain. Mutations in FOXRED1 partially affect the assembly and activity of the mitochondrial complex 1 [186]. Blocked activity of this complex is linked to oxidative stress and potential tumorigenesis based on the activation of AKT. These effects are in some degree reversed by antioxidant treatment with N-acetyl cysteine [187]. Although we have not tested it, it may be that the polyphenol and flavonoid content in WDS EE impacts the activity of FOXRED1, which would affect the function of mitochondrial complex 1 and oxidative stress. The observations of these altered proteins in response to WDS EE highlights the potential of discovery proteomics to shed new light on the mechanistic functions of functional food products.

Although none of the treatments produced any significant change in terms of cell viability (Appendix 2 Figure 2A.1), LPS and RSV promoted significant regulation of several proteins (Appendix 3 Table 2A.2) previously described in the literature which might confirm the reliability of our experiment. For example, increased expression of ICAM-1 is required for leukocyte recruitment in inflammatory conditions and is promoted by LPS and other bacterial products [188]. Similarly, inhibition of WNT5A, a member responsible for the activation of the WNT signalling is reported to occur in response to RSV in cell culture as a deactivating effect of this pathway [189]. Similar reduction in WNT5A following RSV was confirmed in this study.

Proteomic analysis revealed striking differences between the activities of WDS EE and RSV on protein abundances, suggesting different molecular mechanisms of action as illustrated on Figure 2.4. Consistent with the changes in the expression of FOXRED1 and the potential implications in the mitochondrial function, WDS EE is predicted to down-regulate elements associated with this organelle. RSV on the other hand, shows an opposite effect in these

functions and this is consistent with previous reports. For instance, RSV is known to up-regulate mitochondrial activity by activating the cell protector SIRT1, which induces resistance against diet induced obesity in mice [190]. Similarly, growth of the Golgi cisternae seems to be altered in opposite ways by WDS EE and RSV. Changes in the morphology of the Golgi cisternae has an effect in the trafficking of synthesised proteins. For example, increases in the area of the Golgi cisternae is observed after glucose stimulation in pancreatic cells, resulting in disturbed protein traffic [191]. Fusion of the cellular membrane is another function predicted to be altered in opposite ways by WDS EE and RSV. Metabolites from the polyphenol (-)-epigallocatechin-3-gallate (EGCG) for instance, produce changes in the fusion of the cellular membrane in what is interpreted as a possible mechanism of interaction with HT29 cells [192]. Given the limited knowledge in relation to polyphenols and their impact on the different organelles function, our results highlight new priority avenues of study.

In order to corroborate the effect of WDS EE on NF κ B pathway regulation, western blot analysis confirmed WDS EE suppression of the phosphorylation of NF κ B (phospho-Ser536). Inhibition of this phosphorylation event is consistent with the effect provided by other anti-inflammatory treatments. Piceatannol, a stilbene structurally related to RSV which is produced by fungal attack in infected sugarcane, inhibits the phosphorylation of I κ B and NF κ B and the nuclear translocation of NF κ B under multiple inflammatory insults including LPS [193]. We also demonstrated that WDS EE reduced the secretion of the pro-inflammatory cytokine IL-8, a gene regulated by the NF κ B transcription factor. Secretion of IL-8 is described as a marker of intestinal inflammation given its chemoattractant role in neutrophil activation and infiltration which leads to free radical release [194]. Consistent to our data, aqueous extracts of sugarcane showed inhibition of NF κ B activity and decreased IL-8 release in IL-1 β -treated Caco2 cells [136]. Interestingly, treatment of LPS-stimulated SW480 cells with RSV failed to modulate IL-8 secretion, despite reducing NF κ B

phosphorylation after 4h (Figure 2.5). However, it should be noted that the degree of NFκB phospho-Ser536 suppression was not as great as seen with the WDS EE that was particularly effective, even after 1h.

RSV is well documented for its therapeutic properties [195]. The analysis performed in this proteomics study using IPA suggested the inhibitory effect of RSV also acts via the PI3K/AKT/mTOR pathway, some of these events were confirmed by western blotting (Figure 2.6). It has been previously shown that RSV decreases the phosphorylation of AKT Ser473 through the activation of PTEN in colon HCT116 cells providing an anti-carcinogenic effect [196]. Further, and consistent with our data, RSV is proven to target PTEN [197], p70S6K [198] and AMPK [199].

2.6 Conclusions

The results presented in this study show that WDS EE contains a rich source of polyphenols and flavonoids. Protein quantitation by SWATH revealed that WDS EE activity is regulated through NFκB and that induces regulation of oxidative stress mediators SELH and FOXRED1. WDS EE was shown to suppress the phosphorylation of NFκB and inhibit secretion of the pro-inflammatory cytokine IL-8. In contrast, the polyphenol RSV appeared to regulate the PI3K/AKT/mTOR pathway, which was not seen with WDS EE. Future studies will more deeply probe the cell signalling pathways activated by WDS EE and test the nutraceutical properties of WDS EE in *in vivo* model systems.

The mass spectrometry proteomics data have been deposited to the ProteomeXchange Consortium via the PRIDE partner repository with the dataset identifier PXD005418.

Acknowledgements

MPM acknowledges funding support from the Australian Research Council ITTC program and Cancer Institute NSW Research Equipment grant. DBN is a recipient of an Australian Research Council ITTC PhD scholarship, Macquarie University MQRES partial scholarship and Conacyt International Scholarship. Aspects of this research were conducted at APAF supported by the Australian Government's National Collaborative Research Infrastructure Scheme.

Supplementary files (in CD)

Supplementary table 1. SWATH-based MS Normalised peak area. Supplementary table 2. Complete list of regulated proteins after two sample t-test analysis, LPS/C ratio. Supplementary table 3. Complete list of regulated proteins after two sample t-test analysis, WDS EE/LPS ratio. Supplementary table 4. Complete list of regulated proteins after two sample t-test analysis, RSV/LPS ratio.

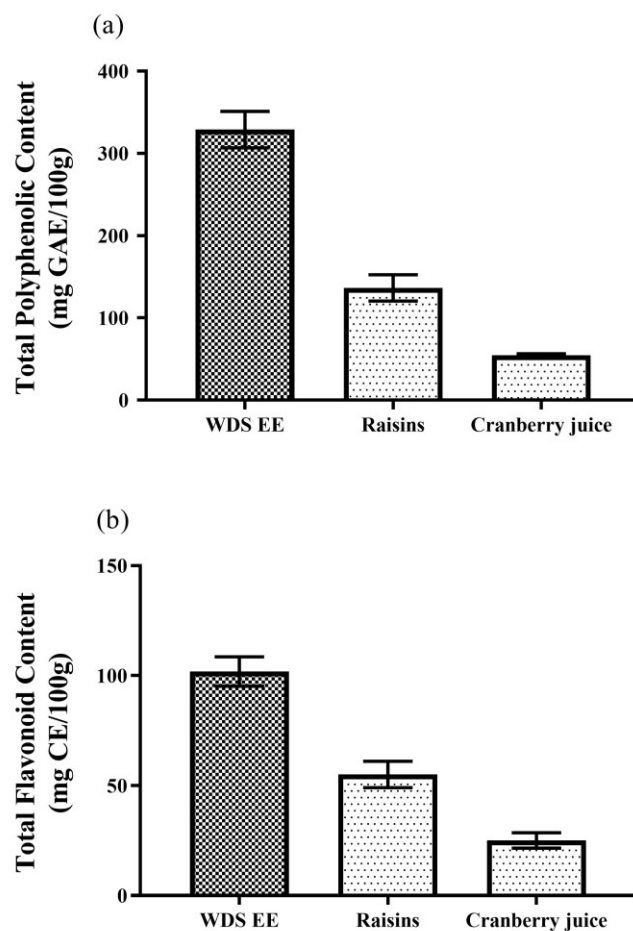


Figure 2.1 (a) Total polyphenolic content and **(b)** Total flavonoid content of whole dried sugarcane extracts

TPC (mg gallic acid equivalents/100g) and TFC (mg (+)-catechin equivalents/100g) were determined for whole dried sugarcane ethanol extract (WDS EE), raisins and cranberry juice. $n=3$, mean \pm SD.

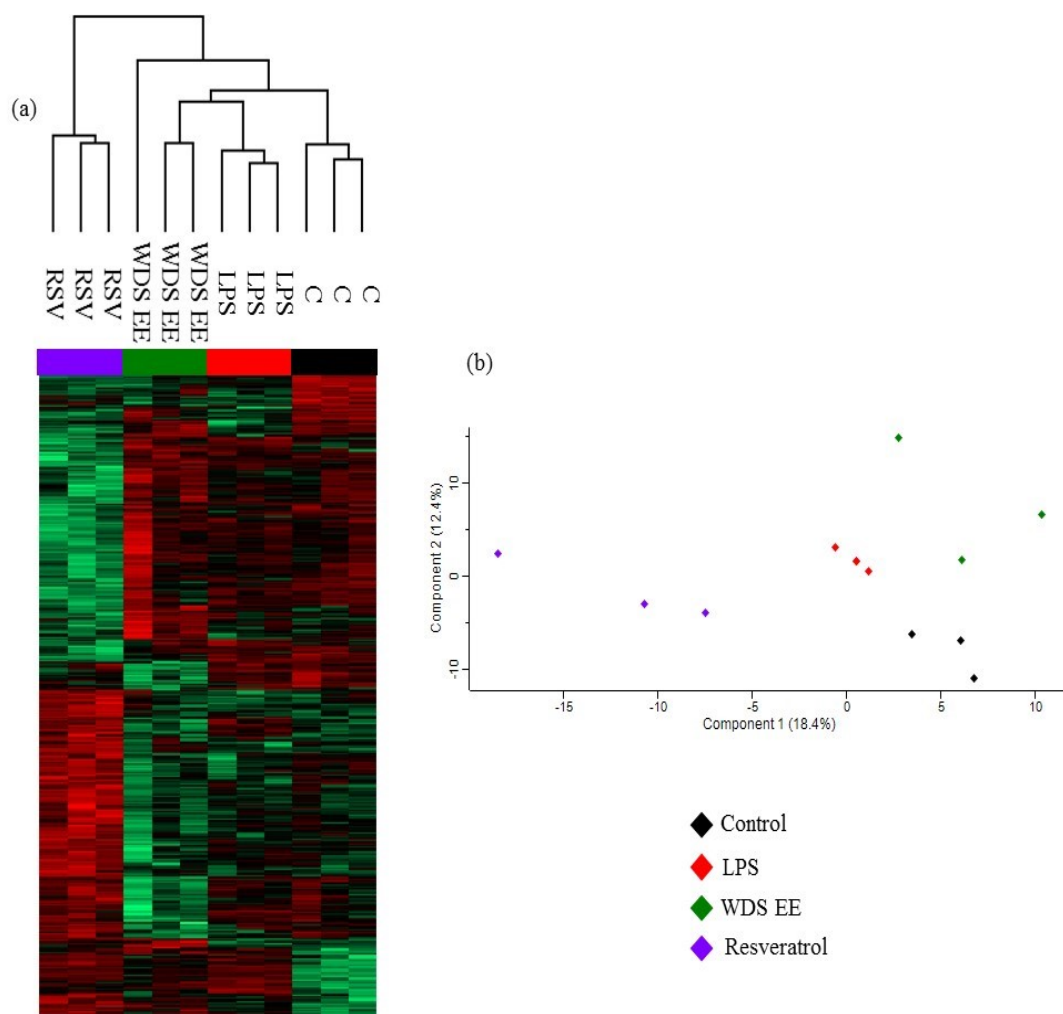


Figure 2.2 (a) Hierarchical clustering and **(b)** principal component analysis of the protein expression in SW480-treated cells

Protein expression of untreated cells (C), lipopolysaccharide (LPS)-stimulated with 5 μ g/ml, LPS-stimulated and co-incubated with 50 μ M of whole dried sugarcane ethanol extract (WDS EE), and LPS-stimulated and co-incubated with 50 μ M of resveratrol (RSV) for 24 hours. Up-regulation (z-score >0) is denoted by red whereas down-regulation (z-score <0) is represented by green. n=3, ANOVA multiple sample test, Permutation based FDR 0.05.

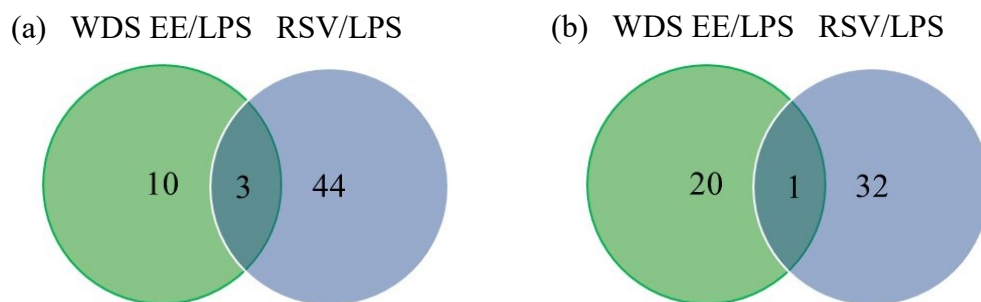


Figure 2.3 Differential (a) up-regulation and (b) down-regulation of proteins in response to WDS EE and RSV

Differential protein expression is based on the comparison of whole dried sugarcane ethanol extract (WDS EE) and resveratrol (RSV) against lipopolysaccharide (LPS)-challenged cells. Students t-test, $p\text{-value} < 0.05$, ± 1.5 fold change.

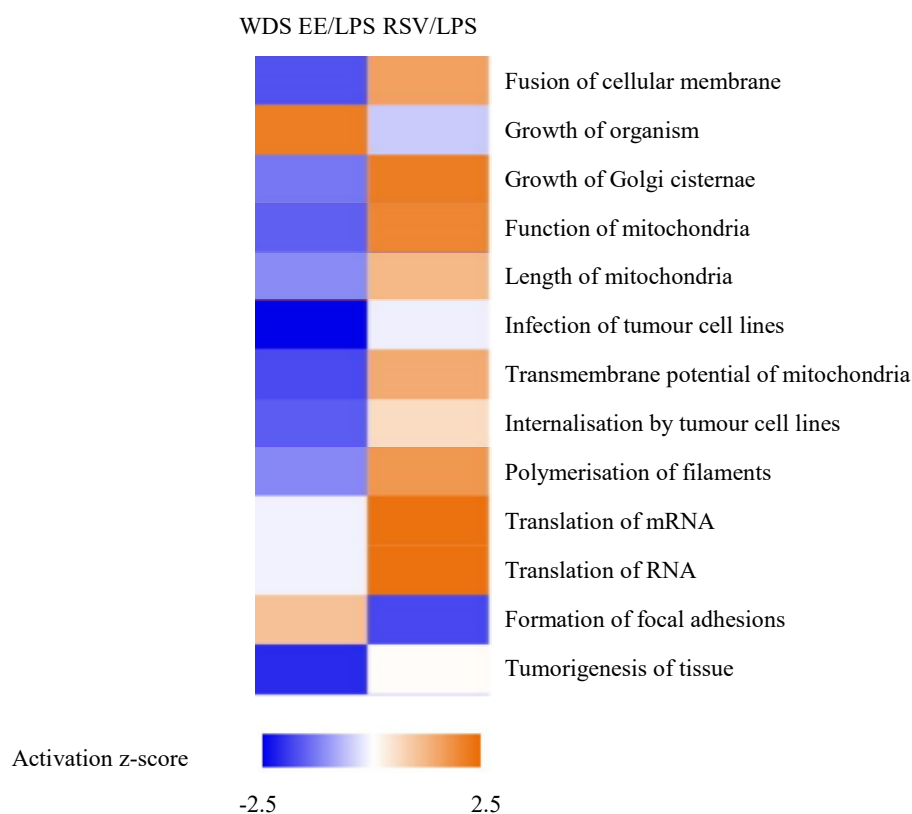


Figure 2.4 Diseases and functions prediction based on protein expression induced by WDS EE and RSV introduction

WDS EE/LPS and RSV/LPS fold changes and p-values were analysed for paired comparisons using IPA (Ingenuity Systems). Up-regulation (z-score >0) is denoted by orange whereas down-regulation (z-score <0) is represented by blue.

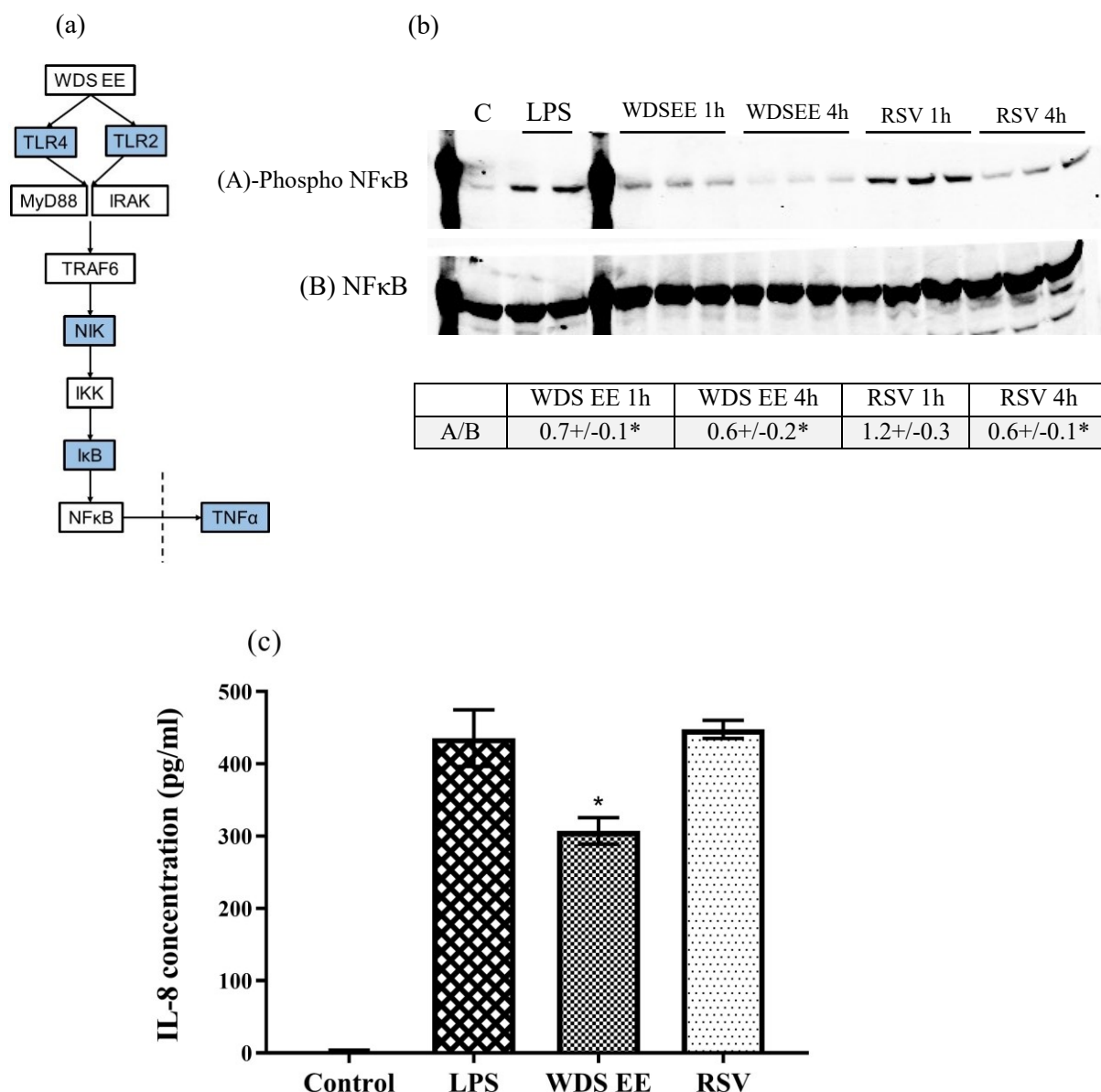


Figure 2.5 WDS EE effect on the NFκB signalling pathway

(a) WDS EE is predicted to inhibit (blue) members of the NFκB pathway as predicted by IPA (Ingenuity Systems). **(b)** Phosphorylation of NFκB (Ser536) normalised with the total expression of NFκB. Four conditions were tested: untreated cells (C), lipopolysaccharide (LPS) stimulated with 5μg/ml, LPS-stimulated and co-incubated with 50μM of WDS EE, and LPS-stimulated and co-incubated with 50μM of resveratrol (RSV). **(c)** Secreted IL-8 (pg/mL) in culture media in response to C, LPS, LPS followed by WDS EE, and LPS followed by RSV. n=3, mean +/- SD, * p-value <0.05 compared to LPS.

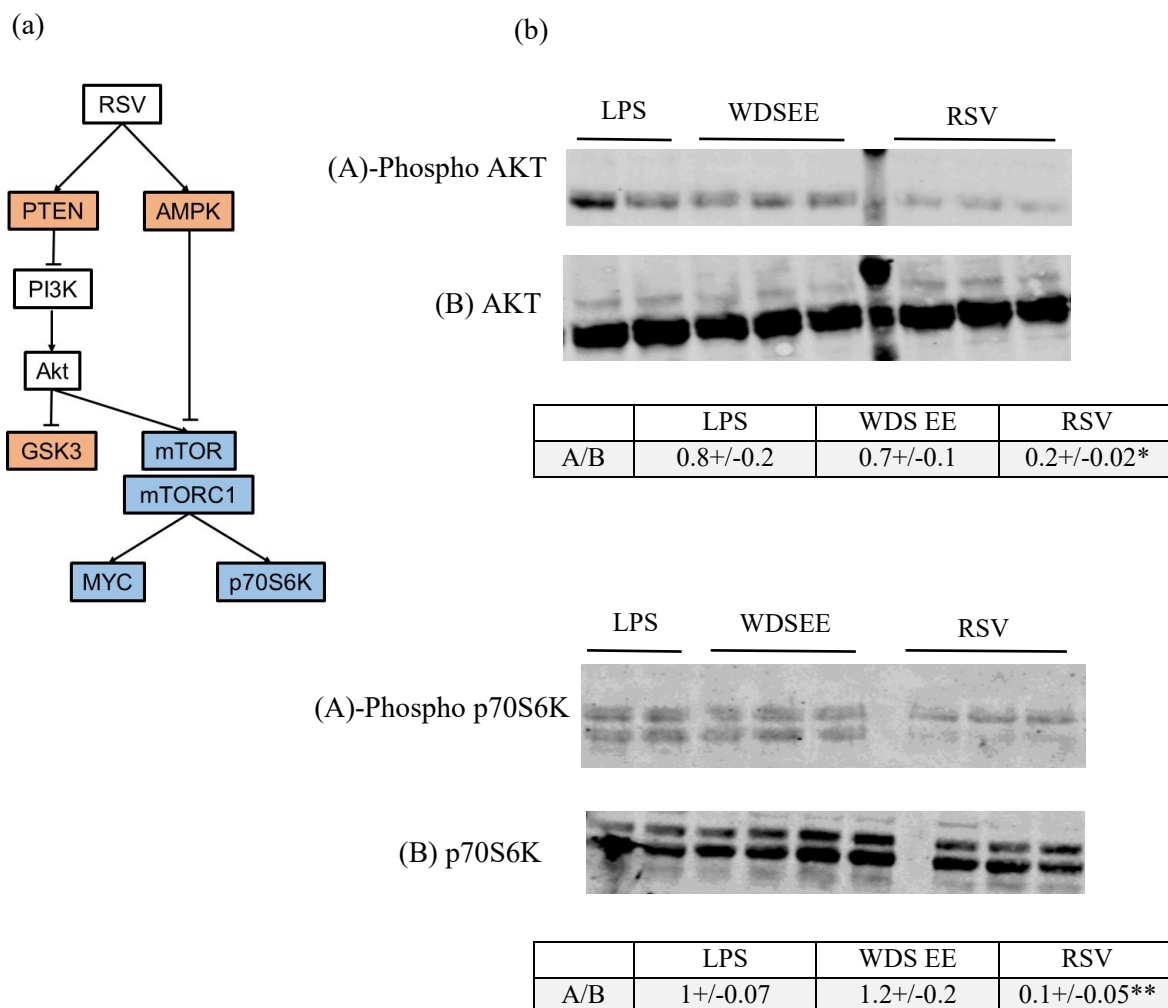


Figure 2.6 RSV effect on the PI3K/AKT signalling pathway

(a) RSV is predicted to inhibit (blue) and activate (red) members of the PI3K/AKT pathway as predicted by IPA (Ingenuity Systems). **(b)** Phosphorylation of AKT (Ser473) and p70S6K (Thr389) normalised with the total expression of the corresponding protein. Four conditions were tested: untreated cells (C), lipopolysaccharide (LPS) stimulated with 5µg/ml, LPS-stimulated and co-incubated with 50µM of whole dried sugarcane ethanol extract (WDS EE), LPS-stimulated and co-incubated with 50µM of RSV after 4h. n=3, mean +/- SD, * p-value <0.05, **p-value<0.01 compared to LPS.

Table 2.1 Significantly regulated proteins expressed as WDS EE/LPS ratio.

Two-sample t test (p-value <0.05), fold change >1.5.

Uniprot accession number	Gene	Protein name	Fold change WDS EE/LPS	P-value	Gene ontology, molecular function
Q96P11	<i>NSUN5</i>	Probable 28S rRNA (cytosine-C(5))-methyltransferase	27.3	2.6E-03	RNA binding ; RNA methyltransferase activity; S-adenosylmethionine-dependent methyltransferase activity
Q8IZQ5	<i>SELH</i>	Selenoprotein H	2.4	4.9E-02	RNA binding
Q16850	<i>CP51A</i>	Lanosterol 14-alpha demethylase	1.8	2.3E-03	Heme binding, iron ion binding, sterol 14-demethylase activity
O75376	<i>NCOR1</i>	Nuclear receptor corepressor 1	1.7	4.7E-02	Histone deacetylase binding; ligand-dependent nuclear receptor binding; nuclear hormone receptor binding; RNA polymerase II activating transcription factor binding; thyroid hormone receptor binding; transcription corepressor activity; transcription regulatory region DNA binding
Q02952	<i>AKA12</i>	A-kinase anchor protein 12	1.7	2.1E-03	Adenylate cyclase binding; protein kinase A binding
P53602	<i>MVD1</i>	Diphosphomevalonate decarboxylase	1.7	3.3E-02	ATP binding; diphosphomevalonate decarboxylase activity; Hsp70 protein binding; protein homodimerization activity
Q92597	<i>NDRG1</i>	Protein NDRG1	1.6	1.1E-02	Cadherin binding; gamma-tubulin binding; microtubule binding; Rab GTPase binding
P06703	<i>S10A6</i>	Protein S100-A6	1.6	3.4E-02	Calcium-dependent protein binding; calcium ion binding; ion transmembrane transporter activity; protein homodimerization activity; S100 protein binding; tropomyosin binding; zinc ion binding
P32929	<i>CGL</i>	Cystathionine gamma-lyase	1.6	1.2E-03	Calmodulin binding; carbon-sulfur lyase activity; cystathionine gamma-lyase activity; cystathionine gamma-synthase activity; homocysteine desulfhydrase activity; identical protein binding; L-cysteine desulfhydrase activity; L-cystine L-cysteine-lyase (deaminating); pyridoxal phosphate binding
P08758	<i>ANXA5</i>	Annexin A5	1.6	6.5E-03	Calcium-dependent phospholipid binding; calcium ion binding; phospholipase inhibitor activity; phospholipid binding
O00443	<i>P3C2A</i>	Phosphatidylinositol 4-phosphate 3-kinase C2 domain-containing subunit alpha	1.6	3.6E-02	1-phosphatidylinositol-3-kinase activity; 1-phosphatidylinositol-4-phosphate 3-kinase activity; ATP binding; phosphatidylinositol 3-kinase activity; phosphatidylinositol binding
Q13501	<i>SQSTM</i>	Sequestosome-1	1.5	7.5E-04	Enzyme binding; identical protein binding; ionotropic glutamate receptor binding; K63-linked polyubiquitin modification-dependent protein binding; protein homodimerization activity; protein kinase binding; protein kinase C binding; protein

Q92974	<i>ARHG2</i>	Rho guanine nucleotide exchange factor 2	1.5	2.5E-02	serine/threonine kinase activity; receptor tyrosine kinase binding; SH2 domain binding; ubiquitin binding; ubiquitin protein ligase binding; zinc ion binding
O15460	<i>P4HA2</i>	Prolyl 4-hydroxylase subunit alpha-2	-1.5	1.3E-02	Guanylnucleotide exchange factor activity; microtubule binding; Rac GTPase binding; Rac guanylnucleotide exchange factor activity; Rho GTPase binding; Rho guanylnucleotide exchange factor activity; transcription factor binding; zinc ion binding
Q6PL18	<i>ATAD2</i>	ATPase family AAA domain-containing protein 2	-1.5	1.3E-02	Electron carrier activity; iron ion binding; L-ascorbic acid binding; oxidoreductase activity, acting on single donors with incorporation of molecular oxygen, incorporation of two atoms of oxygen; procollagen-proline 4-dioxygenase activity
Q9BQ48	<i>RM34</i>	39S ribosomal protein L34, mitochondrial	-1.5	1.2E-03	ATPase activity; ATP binding; chromatin binding; histone binding
P36915	<i>GNL1</i>	Guanine nucleotide-binding protein-like 1	-1.6	2.5E-02	structural constituent of ribosome
Q6NUQ4	<i>TM214</i>	Transmembrane protein 214	-1.6	6.4E-03	GTPase activity; GTP binding; structural molecule activity
P80404	<i>GABT</i>	4-aminobutyrate aminotransferase, mitochondrial	-1.6	4.2E-02	(S)-3-amino-2-methylpropionate transaminase activity; 4-aminobutyrate:2-oxoglutarate transaminase activity; 4-aminobutyrate transaminase activity; iron-sulfur cluster binding; metal ion binding; protein homodimerization activity; pyridoxal phosphate binding; succinate-semialdehyde dehydrogenase binding
Q9BYC9	<i>RM20</i>	39S ribosomal protein L20, mitochondrial	-1.6	2.9E-02	RNA binding; rRNA binding; structural constituent of ribosome
P61457	<i>PHS</i>	Pterin-4-alpha-carbinolamine dehydratase	-1.7	1.0E-03	4-alpha-hydroxytetrahydrobiopterin dehydratase activity; identical protein binding; phenylalanine 4-monooxygenase activity; transcription coactivator activity
P09234	<i>RUIC</i>	U1 small nuclear ribonucleoprotein C	-1.7	1.8E-04	Pre-mRNA 5'-splice site binding; protein homodimerization activity; RNA binding; single-stranded RNA binding; U1 snRNP binding; zinc ion binding
P24752	<i>THIL</i>	Acetyl-CoA acetyltransferase, mitochondrial	-1.9	7.3E-04	Acetyl-CoA C-acetyltransferase activity; carbon-carbon lyase activity; coenzyme binding; enzyme binding; ligase activity, forming carbon-carbon bonds; metal ion binding; protein homodimerization activity
Q9NVV4	<i>PAPD1</i>	Poly(A) RNA polymerase, mitochondrial	-2.4	4.2E-03	ATP binding; identical protein binding; magnesium ion binding; manganese ion binding; polynucleotide adenylyltransferase activity; protein homodimerization activity; RNA binding; UTP binding
Q96CU9	<i>FXRD1</i>	FAD-dependent oxidoreductase domain-containing protein 1	-2.5	3.3E-02	Oxidoreductase activity
P49005	<i>DPOD2</i>	DNA polymerase delta subunit 2	-2.5	5.1E-03	DNA binding; DNA-directed DNA polymerase activity
Q9H9H4	<i>VP37B</i>	Vacuolar protein sorting-associated protein 37B	-2.6	1.5E-02	Calcium-dependent protein binding
Q15334	<i>L2GL1</i>	Lethal(2) giant larvae protein homolog 1	-3.0	1.7E-02	GTPase activator activity; protein kinase binding; Rab GTPase binding; structural molecule activity

P03928	<i>ATP8</i>	ATP synthase protein 8	-3.3	3.8E-02	Hydrogen ion transmembrane transporter activity; transmembrane transporter activity
P21926	<i>CD9</i>	CD9 antigen	-3.4	2.0E-03	Integrin binding
Q9Y5Y2	<i>NUBP2</i>	Cytosolic Fe-S cluster assembly factor NUBP2	-3.6	6.7E-04	4 iron, 4 sulfur cluster binding; ATP binding; metal ion binding; nucleotide binding
Q6ZU65	<i>UBN2</i>	Ubinuclein-2	-4.0	7.9E-03	
Q86YS6	<i>RAB43</i>	Ras-related protein Rab-43	-8.2	4.7E-02	GTPase activity; GTP binding
O43292	<i>GPAA1</i>	Glycosylphosphatidylinositol anchor attachment 1 protein	-11.9	1.3E-02	Tubulin binding

Table 2.2 Significantly regulated proteins expressed as RSV/LPS ratio.

Two-sample t test (p-value <0.05), fold change >1.5.

Uniprot accession number	Gene	Protein name	Fold change RSV/LPS	P-Value	Gene ontology, molecular function
Q9Y4C1	<i>KDM3A</i>	Lysine-specific demethylase 3A	11.5	3.1E-03	Androgen receptor binding; chromatin DNA binding; core promoter binding; dioxygenase activity; histone demethylase activity; histone demethylase activity (H3-K9 specific); iron ion binding; transcription factor activity, sequence-specific DNA binding; transcription regulatory region sequence-specific DNA binding
Q96T23	<i>RSF1</i>	Remodeling and spacing factor 1	6.7	8.9E-03	Histone binding; metal ion binding
Q9UMX5	<i>NENF</i>	Neudesin	4.7	4.3E-06	Growth factor activity; metal ion binding
Q8TAA5	<i>GRPE2</i>	GrpE protein homolog 2, mitochondrial	3.9	4.6E-03	Adenyl-nucleotide exchange factor activity; chaperone binding; protein homodimerization activity; unfolded protein binding
Q9NVT9	<i>ARMC1</i>	Armadillo repeat-containing protein 1	3.7	3.4E-02	Metal ion binding
P21926	<i>CD9</i>	CD9 antigen	3.4	9.0E-03	Integrin binding
O43169	<i>CYB5B</i>	Cytochrome b5 type B	3.1	1.4E-03	Heme binding; metal ion binding
O75376	<i>NCOR1</i>	Nuclear receptor corepressor 1	2.5	9.0E-04	Histone deacetylase binding; ligand-dependent nuclear receptor binding; nuclear hormone receptor binding; RNA polymerase II activating transcription factor binding; thyroid hormone receptor binding; transcription corepressor activity; transcription regulatory region DNA binding
Q6NUM9	<i>RETST</i>	All-trans-retinol 13,14-reductase	2.2	3.3E-04	All-trans-retinol 13,14-reductase activity; oxidoreductase activity
Q9H3M7	<i>TXNIP</i>	Thioredoxin-interacting protein	2.1	1.2E-02	Enzyme inhibitor activity; ubiquitin protein ligase binding
P05121	<i>PAII</i>	Plasminogen activator inhibitor 1	2.1	2.3E-03	Protease binding; receptor binding; serine-type endopeptidase inhibitor activity
Q9NRK6	<i>ABCBA</i>	ATP-binding cassette sub-family B member 10, mitochondrial	2.0	2.6E-02	ATPase activity, coupled to transmembrane movement of substances; ATP binding; protein homodimerization activity; transporter activity
P05362	<i>ICAM1</i>	Intercellular adhesion molecule 1	2.0	7.8E-06	Integrin binding; receptor activity; transmembrane signaling receptor activity; virus receptor activity
P10909	<i>CLUS</i>	Clusterin	1.9	4.7E-02	Amyloid-beta binding; chaperone binding; low-density lipoprotein particle receptor binding; misfolded protein binding; protein complex binding; ubiquitin protein ligase binding

Q9UHN6	<i>TMEM2</i>	Transmembrane protein 2	1.9	4.7E-02	Cadherin binding; calcium ion binding; hyaluronoglucosaminidase activity
Q13501	<i>SQSTM</i>	Sequestosome-1	1.9	1.7E-03	Enzyme binding; identical protein binding; ionotropic glutamate receptor binding; K63-linked polyubiquitin modification-dependent protein binding; protein homodimerization activity; protein kinase binding; protein kinase C binding; protein serine/threonine kinase activity; receptor tyrosine kinase binding; SH2 domain binding; ubiquitin binding; ubiquitin protein ligase binding; zinc ion binding
P51648	<i>AL3A2</i>	Fatty aldehyde dehydrogenase	1.8	7.4E-03	Aldehyde dehydrogenase (NAD) activity; aldehyde dehydrogenase [NAD(P)+] activity; long-chain-alcohol oxidase activity; long-chain-aldehyde dehydrogenase activity; medium-chain-aldehyde dehydrogenase activity
P17676	<i>CEBPB</i>	CCAAT/enhancer-binding protein beta	1.8	3.8E-04	Chromatin binding; DNA binding; glucocorticoid receptor binding; histone acetyltransferase binding; histone deacetylase binding; kinase binding
Q16822	<i>PCKGM</i>	Phosphoenolpyruvate carboxykinase [GTP], mitochondrial	1.8	8.9E-06	GTP binding; metal ion binding; phosphoenolpyruvate carboxykinase (GTP) activity; phosphoenolpyruvate carboxykinase activity
P49721	<i>PSB2</i>	Proteasome subunit beta type-2	1.7	1.3E-03	Threonine-type endopeptidase activity
Q96AB3	<i>ISOC2</i>	Isochorismatase domain-containing protein 2	1.7	5.0E-02	Catalytic activity
Q9UNP9	<i>PPIE</i>	Peptidyl-prolyl cis-trans isomerase E	1.7	3.8E-02	Cyclosporin A binding; peptidyl-prolyl cis-trans isomerase activity; RNA binding
Q8WV74	<i>NUDT8</i>	Nucleoside diphosphate-linked moiety X motif 8	1.6	6.9E-04	Hydrolase activity; metal ion binding
Q709F0	<i>ACD11</i>	Acyl-CoA dehydrogenase family member 11	1.6	7.7E-04	Acyl-CoA dehydrogenase activity; flavin adenine dinucleotide binding; long-chain-acyl-CoA dehydrogenase activity; medium-chain-acyl-CoA dehydrogenase activity; very-long-chain-acyl-CoA dehydrogenase activity
P05455	<i>LA</i>	Lupus La protein	1.6	6.0E-04	mRNA binding; poly(U) RNA binding; RNA binding; sequence-specific mRNA binding; tRNA binding
Q99570	<i>PI3R4</i>	Phosphoinositide 3-kinase regulatory subunit 4	1.6	2.9E-02	1-phosphatidylinositol-3-kinase activity; ATP binding; protein kinase activity; protein serine/threonine kinase activity
P32929	<i>CGL</i>	Cystathionine gamma-lyase	1.6	1.4E-02	Calmodulin binding; carbon-sulfur lyase activity; cystathionine gamma-lyase activity; cystathionine gamma-synthase activity; homocysteine desulfhydrase activity; identical protein binding; L-cysteine desulfhydrase activity; L-cystine L-cysteine-lyase (deaminating); pyridoxal phosphate binding
P31350	<i>RIR2</i>	Ribonucleoside-diphosphate reductase subunit M2	1.6	1.3E-03	Metal ion binding; ribonucleoside-diphosphate reductase activity, thioredoxin disulfide as acceptor
Q15334	<i>L2GL1</i>	Lethal(2) giant larvae protein homolog 1	1.6	4.6E-02	GTPase activator activity; protein kinase binding; Rab GTPase binding; structural molecule activity
Q9P289	<i>STK26</i>	Serine/threonine-protein kinase 26	1.6	1.0E-02	ATP binding; identical protein binding; magnesium ion binding; MAP kinase kinase kinase activity; protein homodimerization activity; protein kinase activity

P62308	<i>RUXG</i>	Small nuclear ribonucleoprotein G	1.6	2.7E-02	RNA binding
P78536	<i>ADA17</i>	Disintegrin and metalloproteinase domain-containing protein 17	1.6	9.4E-03	Integrin binding; interleukin-6 receptor binding; metal ion binding; metalloendopeptidase activity; metalloproteinase activity; Notch binding; PDZ domain binding; SH3 domain binding
P51784	<i>UBP11</i>	Ubiquitin carboxyl-terminal hydrolase 11	1.6	2.3E-03	Cysteine-type endopeptidase activity; thiol-dependent ubiquitin-specific protease activity; thiol-dependent ubiquitinyl hydrolase activity
P17535	<i>JUND</i>	Transcription factor jun-D	1.6	7.3E-03	Enzyme binding; ligand-dependent nuclear receptor binding; RNA polymerase II core promoter proximal region sequence-specific DNA binding; RNA polymerase II transcription factor activity, sequence-specific DNA binding; transcriptional activator activity, RNA polymerase II core promoter proximal region sequence-specific binding; transcription coactivator activity; transcription factor binding; transcription regulatory region DNA binding
Q9BX68	<i>HINT2</i>	Histidine triad nucleotide-binding protein 2, mitochondrial	1.6	1.5E-03	Hydrolase activity; nucleotide binding
Q4G176	<i>ACSF3</i>	Acyl-CoA synthetase family member 3, mitochondrial	1.6	8.5E-03	Acid-thiol ligase activity; ATP binding; malonyl-CoA synthetase activity; very long-chain fatty acid-CoA ligase activity
Q13263	<i>TIF1B</i>	Transcription intermediary factor 1-beta	1.6	2.9E-04	Chromatin binding; chromo shadow domain binding; DNA binding; Krueppel-associated box domain binding; promoter-specific chromatin binding; protein kinase activity
P04179	<i>SODM</i>	Superoxide dismutase [Mn], mitochondrial	1.5	2.1E-03	Identical protein binding; manganese ion binding; superoxide dismutase activity
O95777	<i>LSM8</i>	U6 snRNA-associated Sm-like protein LSM8	1.5	1.7E-02	RNA binding; U6 snRNA binding
Q13616	<i>CUL1</i>	Cullin-1	1.5	3.0E-02	Ubiquitin protein ligase binding; ubiquitin-protein transferase activity
Q86WB0	<i>NIPA</i>	Nuclear-interacting partner of ALK	1.5	2.0E-03	Protein kinase binding; zinc ion binding
Q9H9P8	<i>L2HDH</i>	L-2-hydroxyglutarate dehydrogenase, mitochondrial	1.5	1.3E-02	2-hydroxyglutarate dehydrogenase activity
P35244	<i>RFA3</i>	Replication protein A 14 kDa subunit	1.5	2.8E-02	Damaged DNA binding; single-stranded DNA binding
P25787	<i>PSA2</i>	Proteasome subunit alpha type-2	1.5	1.6E-02	Threonine-type endopeptidase activity
Q96HV5	<i>TM41A</i>	Transmembrane protein 41A	1.5	7.8E-05	
P08243	<i>ASNS</i>	Asparagine synthetase [glutamine-hydrolyzing]	1.5	1.8E-02	Asparagine synthase (glutamine-hydrolyzing) activity; ATP binding; cofactor binding; protein homodimerization activity
P09455	<i>RET1</i>	Retinol-binding protein 1	-1.5	2.0E-02	Retinal binding; retinoid binding; retinol binding; transporter activity
P51153	<i>RAB13</i>	Ras-related protein Rab-13	-1.5	2.5E-02	GTPase activity; GTP binding; protein kinase A catalytic subunit binding

O15460	<i>P4HA2</i>	Prolyl 4-hydroxylase subunit alpha-2	-1.5	3.7E-02	Electron carrier activity; iron ion binding; L-ascorbic acid binding; oxidoreductase activity, acting on single donors with incorporation of molecular oxygen, incorporation of two atoms of oxygen; procollagen-proline 4-dioxygenase activity
P46779	<i>RL28</i>	60S ribosomal protein L28	-1.5	4.3E-02	RNA binding; structural constituent of ribosome
P04818	<i>TYSY</i>	Thymidylate synthase	-1.6	5.4E-03	Cofactor binding; drug binding; folic acid binding; nucleotide binding; protein homodimerization activity; sequence-specific mRNA binding; thymidylate synthase activity; translation repressor activity, nucleic acid binding
Q96TA2	<i>YMEL1</i>	ATP-dependent zinc metalloprotease YME1L1	-1.6	2.4E-02	ATP binding; ATP-dependent peptidase activity; metal ion binding; metalloendopeptidase activity; metalloprotease activity
Q9HCU9	<i>BRMS1</i>	Breast cancer metastasis-suppressor 1	-1.6	3.7E-02	Histone deacetylase activity; histone deacetylase binding; NF-kappaB binding
Q15370	<i>ELOB</i>	Elongin-B	-1.6	8.3E-04	ubiquitin protein ligase binding
O15372	<i>EIF3H</i>	Eukaryotic translation initiation factor 3 subunit H	-1.6	2.1E-02	RNA binding; translation initiation factor activity
P61313	<i>RL15</i>	60S ribosomal protein L15	-1.6	5.4E-06	Cadherin binding; RNA binding; structural constituent of ribosome
P35221	<i>CTNA1</i>	Catenin alpha-1	-1.7	2.9E-02	Actin filament binding; beta-catenin binding; cadherin binding; gamma-catenin binding; identical protein binding; protein heterodimerization activity; RNA binding; structural molecule activity; vinculin binding
O00203	<i>AP3B1</i>	AP-3 complex subunit beta-1	-1.7	7.5E-03	GTP-dependent protein binding; protein phosphatase binding
Q16763	<i>UBE2S</i>	Ubiquitin-conjugating enzyme E2 S	-1.7	1.5E-03	ATP binding; ubiquitin conjugating enzyme activity; ubiquitin protein ligase activity; ubiquitin protein ligase binding; ubiquitin-protein transferase activity
O75534	<i>CSDE1</i>	Cold shock domain-containing protein E1	-1.7	4.3E-02	DNA binding; RNA binding
P29590	<i>PML</i>	Protein PML	-1.7	4.9E-06	Cobalt ion binding; DNA binding; protein heterodimerization activity; protein homodimerization activity; SMAD binding; SUMO binding; transcription coactivator activity; ubiquitin protein ligase binding; zinc ion binding
P52292	<i>IMA1</i>	Importin subunit alpha-1	-1.8	1.0E-02	Histone deacetylase binding; nuclear localization sequence binding; protein transporter activity; RNA binding
P25774	<i>CATS</i>	Cathepsin S	-1.8	1.1E-04	Collagen binding; cysteine-type endopeptidase activity; fibronectin binding; laminin binding; proteoglycan binding; serine-type endopeptidase activity
Q9BXJ9	<i>NAA15</i>	N-alpha-acetyltransferase 15, NatA auxiliary subunit	-1.8	2.8E-02	Ribosome binding; RNA binding
Q7Z460	<i>CLAP1</i>	CLIP-associating protein 1	-1.8	1.8E-03	Dystroglycan binding; kinetochore binding; microtubule binding; microtubule plus-end binding
P20290	<i>BTF3</i>	Transcription factor BTF3	-1.9	1.7E-02	RNA binding
Q99733	<i>NP1L4</i>	Nucleosome assembly protein 1-like 4	-1.9	3.5E-02	Nucleosome binding; RNA binding; unfolded protein binding

P62829	<i>RL23</i>	60S ribosomal protein L23	-1.9	1.1E-02	Large ribosomal subunit rRNA binding; RNA binding; structural constituent of ribosome; transcription coactivator binding; ubiquitin ligase inhibitor activity; ubiquitin protein ligase binding
Q01085	<i>TIAR</i>	Nucleolysin TIAR	-2.1	7.3E-03	AU-rich element binding; DNA binding; RNA binding
Q4V328	<i>GRAP1</i>	GRIP1-associated protein 1	-2.1	3.1E-02	
Q9HA92	<i>RSAD1</i>	Radical S-adenosyl methionine domain-containing protein 1, mitochondrial	-2.1	2.3E-02	4 iron, 4 sulfur cluster binding; coproporphyrinogen oxidase activity; metal ion binding
Q15382	<i>RHEB</i>	GTP-binding protein Rheb	-2.2	3.7E-02	GDP binding; GTPase activity; GTP binding; magnesium ion binding; protein kinase binding
Q9NQZ2	<i>SAS10</i>	Something about silencing protein 10	-2.4	8.5E-03	RNA binding
P61009	<i>SPCS3</i>	Signal peptidase complex subunit 3	-2.5	1.5E-02	Peptidase activity
P01037	<i>CYTN</i>	Cystatin-SN	-2.6	1.8E-04	Cysteine-type endopeptidase inhibitor activity; protease binding
P43003	<i>EAA1</i>	Excitatory amino acid transporter 1	-2.7	5.0E-02	Amino acid transmembrane transporter activity; glutamate:sodium symporter activity; glutamate binding; high-affinity glutamate transmembrane transporter activity; L-glutamate transmembrane transporter activity; metal ion binding
P41221	<i>WNT5A</i>	Protein Wnt-5a	-2.7	5.2E-03	Chemoattractant activity involved in axon guidance; cytokine activity; frizzled-2 binding; frizzled binding; protein domain specific binding; receptor agonist activity; receptor tyrosine kinase-like orphan receptor binding; transcription factor activity, sequence-specific DNA binding; transcription regulatory region DNA binding
Q9Y6H1	<i>CHCH2</i>	Coiled-coil-helix-coiled-coil-helix domain-containing protein 2	-3.3	9.3E-03	Sequence-specific DNA binding; transcription factor binding
P63313	<i>TYB10</i>	Thymosin beta-10	-3.8	2.0E-02	actin monomer binding

Table 2.3 Predicted upstream analysis based on protein expression induced by WDS EE and RSV

Z-scores predicting activation (>0) or deactivation (<0) based on WDS EE/LPS and RSV/LPS ratios. Non-significant (NS)

	WDS EE/LPS	RSV/LPS
Quercetin	3	NS
Carnosol	2	1
Curcumin	1.7	-2.3

**Chapter 3 Phosphoproteomics analysis of cell signalling
associated with dried sugarcane extracts in an *in vitro*
colon cancer cell model of LPS-induced inflammation**

Chapter 3

Phosphoproteomics analysis of cell signalling associated with dried sugarcane extracts in an *in vitro* colon cancer cell model of LPS-induced inflammation

Experimental work and data analysis from this chapter was performed by Daniel Bucio Noble. The mass spectrometer was run by Daniel Bucio Noble at the Australian Proteome Analysis Facility. Manuscript was written by Daniel Bucio Noble with contributions from Assoc. Prof. Mark P. Molloy, Dr. Liisa Kautto, and Dr. Malcolm S. Ball.

Phosphoproteomics analysis of cell signalling associated with dried sugarcane extracts in an *in vitro* colon cancer cell model of LPS-induced inflammation

Daniel Bucio-Noble¹, Liisa Kautto¹, Malcolm S. Ball^{1,2}, Mark P. Molloy^{1, 3*}

¹ ARC Training Centre for Molecular Technology in the Food Industry, Department of Chemistry and Biomolecular Sciences, Macquarie University, Sydney, Australia.

² Gratuk Technologies Pty Ltd., Level 9, Avaya House, 123 Epping Road, Sydney, Australia.

³ Australian Proteome Analysis Facility, Macquarie University, Sydney, Australia.

***Corresponding author:** Mark P. Molloy, Department of Chemistry and Biomolecular Sciences, Macquarie University, Level 3, Building E8C, Research Park Drive, Sydney 2109, Australia. Tel: +61 2 9850 6218. Fax+61 2 9850 6200. E-mail: mmolloy@proteome.org.au

Disclosures: MSB is an employee of Gratuk Technologies Pty Ltd who provided partial funding for this project under the Australian Research Council Industrial Transformation Training Centre scheme. All other authors have no disclosures to make.

3.1 Abstract

Chronic inflammation involves dysregulation in the synthesis of pro-inflammatory mediators which are associated with several diseases. Some natural plant products are known to possess anti-inflammatory properties based on their high content of antioxidants. In this study, we demonstrate that whole dried sugarcane ethanol extract (WDS EE) is a potent source of antioxidants with high free-radical scavenging activity. WDS EE effect *in vitro* was studied in a cellular model of intestinal inflammation using LPS-stimulated SW480 cells and compared with the well-known polyphenol resveratrol. Mass spectrometry based phosphoproteomic analysis demonstrates that each regulates some unique cellular responses. For WDS EE the responses included the regulation of inflammatory-modulators SIRT1, PKA, PKC β , EGFR and c-Jun. Kinase enrichment analysis and confirmatory western blot data point to the role of C-Raf kinase as a key regulator of WDS EE activity. Our findings suggest that WDS EE antioxidants have potential to impart health benefits associated with regulating inflammatory-related conditions.

Keywords sugarcane; antioxidants; phosphoproteome; NF κ B; inflammation; SW480 cells.

3.2 Introduction

Consumption of fruits and vegetables rich in antioxidant activity are inversely related with markers of inflammation and oxidative stress [200]. Further, plant-derived nutrients characterised as strong antioxidants provide a protective effect against free radical oxidative damage observed in inflammatory-related conditions [201].

Aberrant expression of pro-inflammatory regulators is a condition present in chronic inflammation and multiple diseases such as cancer and inflammatory bowel disease (IBD) [22]. These pro-inflammatory regulators include transcription factors such as NF κ B and activator protein 1 (AP-1) which are essential in the expression of pro-inflammatory genes that leads to the progression of the inflammatory state. In this regard, consumption of plant antioxidants might be an effective strategy in the inhibition of NF κ B and related inflammatory pathways as potential treatment of IBD [147].

Resveratrol (RSV) is a polyphenol mostly found in grapes and red wine that has shown positive outcomes in the treatment of cancer, inflammation, and heart disease [195]. Among these, antioxidant properties of RSV appear to take a central role in the management of these conditions. For instance, RSV improves oxidative colon injury in an *in vivo* model of IBD through the inhibition of pro-inflammatory mediators and the activation of protective enzymes [194].

Similarly to RSV, sugarcane (*Saccharum officinarum* L.) is a known source of antioxidant activity which potentially provides anti-inflammatory outcomes [129][134]. From previous work, WDS EE influenced significant changes at the protein level including the inhibition of the NF κ B signalling pathway. In this study, we investigated the antioxidant properties of WDS EE using antioxidant assays and phosphoproteomic techniques. Anti-inflammatory effects of WDS EE were tested in a cell model of inflammation where lipopolysaccharide

(LPS)-treated SW480 cells were incubated with WDS EE and compared with the effects seen with the well-known antioxidant RSV. Our results demonstrate that the antioxidant effects of WDS EE are mediated through the potential inhibition of a number of signalling network associated with protection from inflammatory responses.

3.3 Methods

Micronutrient extraction

Sucrose-depleted WDS, obtained from whole sugarcane was kindly provided by Gratuk Technologies Ltd Pty, Australia. Ethanol extraction was performed as indicated in Chapter 2, Methods section. Concentration of polyphenols present in WDS EE was adjusted to 50 μ M and dried before use for cell culture.

Antioxidant potential, ferric reducing ability potential (FRAP) assay

The determination was performed as previously reported [202]. Briefly, FRAP reagent was prepared by mixing 300 mM acetate buffer (pH 3.6), 10 mM 2,4,6-tripyridil-s-triazine (TPTZ) solution and 20 mM FeCl_3 at a 10:1:1 ratio. WDS EE (20 μ L) was mixed with 0.2 mL of water and 1.8 mL of FRAP reagent and incubated for 10 min at 37 °C. Ferrous sulphate served as a standard over the concentration range of 125-2500 μ M. Optical density was measured at 593 nm and results were expressed in mM FeSO_4/kg .

DPPH (2,2-diphenyl-1-picrylhydrazyl) free radical scavenging activity

The determination was performed as previously reported [203]. Briefly, 80 μ L of WDS EE was mixed with 3mL of 0.1 mM DPPH in 80% (v/v) methanol and incubated for 10min at room temperature. Ascorbic acid served as the standard over the concentration range of 10-100 mg/L. Optical density was determined at 517 nm and results were expressed in mg ascorbic acid equivalents (AAE) / 100 g extract.

Cell culture and protein extraction

The colon carcinoma cell line SW480 was cultured in RPMI 1640 medium supplemented with 1% (v/v) of L-glutamine (Life Technologies), 10% (v/v) of fetal bovine serum (Life Technologies), 1x GlutaMAX (Life Technologies), and 1% (v/v) antibiotic (penicillin, 100 μ g/mL and streptomycin, 100 μ g/mL) and incubated at 37 °C and 5% CO_2 before lysis.

An inflammatory response was induced by exposing cells to 5 $\mu\text{g/mL}$ of LPS from *Escherichia coli* (Sigma Aldrich) for 2 hours. Dried WDS EE was resuspended in RPMI 1640 medium before treatment. RSV (Sigma Aldrich) was dissolved in dimethyl sulfoxide (DMSO, Sigma Aldrich) to a concentration of 50 μM . After LPS stimulation, WDS EE and RSV were added to the cells for 1 and 4 hours before harvesting. When indicated, the specific C-Raf inhibitor GW5074 (Selleckchem) was co-incubated with the WDS EE at varied concentrations (0.5, 1 and 5 μM).

Cells were collected, lysed and protein concentration determined as described in Chapter 2, Methods section.

Western Blot

This procedure was performed as described in Chapter 2, Methods section. Nitrocellulose membranes were blotted with primary antibodies anti-pNF κ B (Ser536), anti-NF κ B, anti-pAKT (Ser473) and anti-AKT (Cell Signalling) at 1:1000 dilution each, in a 5% (w/v) bovine serum albumin (BSA) TBS-T solution, and incubated overnight at 4 °C.

Phosphopeptide enrichment

Protein (500 μg) was reduced with 10mM of DTT for 30 min at 60 °C and alkylated with 20 mM of iodoacetamide for 20 min at room temperature in the dark. Samples were digested with trypsin (Promega) in 1:50 ratio and incubated at 37 °C overnight. Deoxycholate salt was removed with pure formic acid at a 2% (v/v) of final concentration. Peptide solution was diluted ten times with 80% (v/v) acetonitrile (ACN), 5% (v/v) tri-fluoro acetic acid (TFA) and 76 mg/mL glycolic acid and incubated with 3 mg of TiO₂ beads (Titansphere, 5 μm) for 30 min with shaking. The peptide solution was transferred to a new batch of TiO₂ beads and incubated again for 30 min with shaking and the solution was discarded afterwards. TiO₂ beads from the two incubations were pooled and washed with 80% (v/v) ACN, 1% (v/v) TFA

and 10% (v/v) ACN and 0.1% (v/v) TFA. Phosphopeptides were eluted with 1% ammonia solution (v/v) for 10min with shaking, followed by a cleaning step in a C-18 column pre-conditioned with 100% (v/v) methanol and 2% (v/v) ACN. Phosphopeptides were recovered in 70% (v/v) ACN, dried and resuspended in 1% (v/v) TFA for LC-MS/MS.

Mass Spectrometry (LC-MS/MS)

MS analysis were performed on a Q-Exactive (Thermo Fisher Scientific) mass spectrometer. Phosphopeptide separation was achieved on a 75 μm x 100 mm C18 Halo, 2.7 μm bead size, 160 Å pore size column. Peptides were eluted with an A buffer B (100% (v/v) ACN, 0.1% (v/v) formic acid) gradient of 5-35% in 100 min run using electrospray ionisation. Data-dependent MS/MS acquisition mode consisted of a full MS resolution of 70,000 scan acquisition and 350 to 1800 m/z . Phosphopeptide fragmentation required 10 HCD and a MS² resolution of 17,500. MaxQuant 1.5.2 was used for the processing of the *.raw* files using a 1% peptide and protein FDR [204]. Label-free quantitation mode (LFQ) was employed for relative quantitation. Data base searches utilised the following parameters: two missed cleavages, peptide mass tolerance of 4.5ppm, carbamidomethylation (C) as fixed modification and oxidation (M), acetylation (Protein N-term), and phosphorylation (STY) as variable modifications, and match between runs. Perseus 1.5.2 was employed for statistical analysis [205]. Reverse and contaminant peptides were removed prior to log₂ transformation of peptide intensity. Only peptides with a localisation probability higher than 75% were considered in the analysis. Intensity data was considered valid only in peptides quantified in at least 9 out of the 12 samples analysed, missing values were replaced or imputed from a typical normal distribution region. Statistical significant hits were identified by group comparison using the Student's t-test FDR method (<20%). Fisher's exact test was performed on WDS EE significantly regulated phosphopeptides compared to LPS-treated

phosphopeptides in order to identify kinase motifs significantly regulated. Enrichment factors were calculated using the Benjamini-Hochberg FDR method ($\text{FDR} > 0.2$).

3.4 Results

WDS EE exhibits strong antioxidant and free-radical scavenging activities

Sucrose-depleted WDS EE has potential as a dietary supplement, but the bioactive components have not been characterised. Antioxidant and free-radical activities of WDS EE were performed by two methods, the DPPH assay which determines the free-radical scavenging potential measured by reduction of DPPH [203], and the FRAP method, which measures the reduction of a ferric-tripyridyltriazine complex to its coloured ferrous form [202].

We determined that WDS EE contains 119 ± 11.1 mg AA/100g in terms of DPPH reduction and 26.1 ± 0.7 mmol FeSO₄/kg in terms of FRAP reduction (Figure 3.1). Our results are consistent with the values described for green sugarcane cultivars for the two methods tested [129][206]. The antioxidant activity of cranberry juice and raisins was also measured and our values fall within the range of previously reported data for different brands [207] and varieties [208], respectively. These results compared to other studies where a large cohort of food products were analysed indicate that WDS EE is as rich in antioxidant and free-radical scavenging activities as other nutritious foods such as olives and strawberries which have shown to have health benefits in some studies [209].

WDS EE and resveratrol mediate different phosphoproteomes indicative of independent mechanisms of action

To further explore the cellular responses to WDS EE we monitored changes in phospho-signaling networks using mass spectrometry. TiO₂-based phosphopeptide enrichment was employed and label-free quantitation determined using MaxQuant [204]. Three biological replicates were measured for each of the following four groups: control, LPS, LPS + 4h WDS EE (WDS EE) and LPS + 4h RSV (RSV). The number of phosphorylated peptides quantitated

in each replicate range between 1500-2400, by averaging the respective replicates we found in control 2241, LPS 2197, WDS EE 1709 and RSV 1606 phosphopeptides (Table 3.1). Hierarchical clustering and principal component analysis (PCA) (Figure 3.2) clearly illustrated unique phosphoproteome differences associated with WDS EE or RSV treatment in LPS induced cells. Given that phosphoproteome reflects cell signalling activities it is evident that WDS EE and RSV mediate numerous independent pathways.

Figure 3.3 shows the number of phosphopeptides that were differentially regulated by a minimum of 1.5-fold change (FC) between WDS EE and RSV, compared to LPS-stimulated phosphopeptides. Our results show 411 down-regulated and 463 up-regulated phosphopeptides compared to the LPS-induced state. Interestingly, almost all down-regulated phosphopeptides following WDS EE were also reduced with RSV, although ~12% (53 phosphopeptides) were uniquely repressed by WDS EE. Quite strikingly, we detected an additional 179 phosphopeptides that were only down-regulated by RSV. Similarly, WDS EE treatment induced up-regulation of 100 phosphorylated peptides compared to 193 phosphorylated peptides induced by RSV, with only ~36% of phosphopeptides commonly found with both treatments. These observations reinforce that the antioxidant extracts from WDS EE generate different biological responses to RSV.

Analysis of the phosphorylation events revealed changes in the levels of phosphopeptides with links to the inflammatory response (Table 3.2). Function and biological implications for each phosphosite were collected from previous studies and data reported in repositories such as PhosphoSitePlus. Some of these phosphosites belong to proteins associated with cell stress response (sirtuin 1, SIRT1), inflammatory regulators (protein kinase A, PKA, protein kinase C β , PKC β , epidermal growth factor receptor, EGFR and c-Jun) and cell cycle regulation (cyclin dependent kinase 1, CDK1).

C-Raf is a potential regulator of the antioxidant effect of WDS EE

In order to further elucidate the molecular mechanisms associated with the WDS EE treatment, we used the Fisher's exact test to calculate the most represented kinase motifs in the WDS EE -linked phosphorylation sites (Appendix 4 Table 3A.1). In this statistical test, significantly regulated phosphorylation sites were compared with all phosphorylation sites in the search of common kinase motifs using Perseus. From this analysis the substrate motif associated with C-Raf kinase presented the highest enrichment factor (+2). The statistical significance observed in this approach led us to question the role of C-Raf in the WDS EE biological response. To further question the role of C-Raf, SW480 cells were treated with LPS and WDS EE and co-incubated with the selective C-Raf inhibitor GW5074. As observed in Figure 3.4a, addition of GW5074 in conjunction with WDS EE permitted increased phosphorylation of NF κ B Ser536 compared to WDS EE treatment alone after 4 hours. Similarly, Figure 3.4b illustrates that WDS EE induced phosphorylation levels of AKT Ser473 were significantly reduced upon c-Raf inhibition. This demonstrates a role for C-Raf-dependent signalling in mediating the phosphorylation of NF κ B and AKT.

3.5 Discussion

In this study, we characterised the antioxidant and free-radical scavenging potential of WDS EE and investigated the mechanisms of action of these extracts by studying the phosphoproteome. Antioxidant characterisation performed here demonstrates WDS EE as a strong source of these agents. High antioxidant content has been linked to anti-inflammatory health benefits [200].

Phosphoproteomic analysis of WDS EE and RSV-treated cells enabled an unbiased view of downstream signalling activities measured through changes in protein phosphorylation. In particular, we identified the occurrence of the phosphorylation of SIRT1 as an event associated with protection from cell stress. Phosphorylation of Ser27 in SIRT1 was up-regulated following both treatments, WDS EE (+2 FC) and RSV (+2.8 FC). Phosphorylation is an important mediator of SIRT1 enzymatic activity [210]; in particular, phosphorylated Ser27 appears to increase not only deacetylase activity but nuclear localisation mediated by c-Jun N-terminal kinase (JNK) [211]. Further evidence implicates RSV to control the activation of NF κ B and other markers of intestinal inflammation by the up-regulation of SIRT1 in colitis-induced mice [91]. Anti-proliferative properties of RSV in SW480 and HCT116 cells require the participation of SIRT1. For instance, knock-down of SIRT1 reverses the inactivation, dephosphorylation and deacetylation of NF κ B provided by RSV [212]. Our results might implicate the phosphorylation of SIRT1 as a target of RSV and WDS EE as a modulatory mechanism of inflammation.

In regards to the modulation of the inflammatory response, we identified several phosphorylation sites linked to NF κ B regulation. For instance, Thr198 from PKA and Thr500 from PKC β were both down-regulated (-6.5 and -2.2 FC, respectively), events only found after WDS EE treatment. Both located in the activation loop, phosphorylation of these two

residues regulates kinase activity [213]. For instance, PKA phosphorylation in Thr198 is required for full biological activity and it is necessary in the synthesis of IL-4 under inflammatory stimulation [214]. Relevant to this work, PKA is identified to form an inhibitory cytosolic complex with NF κ B and I κ B α , LPS stimulation activates PKA which phosphorylates NF κ B leading to nuclear translocation and I κ B α proteasome degradation [215]. Similarly as Thr 198 in PKA, Thr500 phosphorylation is a prerequisite for full catalytic activity of PKC β [216].

Interestingly, PKA and PKC are identified to promote NF κ B DNA-binding activity and nuclear translocation [217]. Additionally, the antioxidant EGCG mainly present in green tea induces an anti-inflammatory action in human umbilical vein endothelial cells (HUVEC) through a mechanism that involves the inhibition of PKC, and NF κ B nuclear translocation [218]. Thus we consider that down-regulation of these important activating phosphosites found only with WDS EE is central to maintaining low NF κ B phosphorylation levels (as shown in Chapter 2, Results section).

Another phosphorylation event only observed in response to WDS EE treatment was the up-regulation of EGFR Thr693 (+1.6 FC). Although tyrosine phosphorylation is required for kinase activity, Thr693 phosphorylation is reported to down-regulate the activity of EGFR-associated signalling pathways. According to site mutagenesis studies, this modification along with Thr678 phosphorylation prevents JNK activation upon EGF stimulation resulting in inhibition of cell transformation [219]. EGFR is also studied given its effect on the activation of other signalling pathways in human malignancies. The polyphenol therapy using EGCG is reported to inhibit cell proliferation, induce apoptosis, suppress the phosphorylation of tyrosine EGFR, ERK, AKT, and reduces the transcriptional activity of AP-1 and NF κ B in HT29 colon cancer [220]. Although our study did not present any evidence in the inhibition of tyrosine phosphorylation of EGFR, our data might implicate Thr693 phosphorylation as

another inflammatory marker target by the WDS EE treatment with a potential inhibitory effect upon JNK signalling.

Consistently, WDS EE is also observed to down-regulate Ser63 in c-Jun (-1.9 FC), a subunit of the AP-1 transcription factor. AP-1 is composed of homo or heterodimeric units of c-Jun and others which presents high activity in response to inflammatory stimulation [221]. AP-1 inhibition is also predicted to occur as a result of green tea polyphenols supplementation to an animal model of IBD using a transcriptomics/proteomics approach [147]. Interestingly, inflammatory stimulation with LPS activates JNK signalling resulting in phosphorylation of Ser63 [222]. Additionally, anti-inflammatory polyphenols from tea are known to inhibit the DNA binding activity of AP-1 and c-Jun phosphorylation through a JNK-dependent mechanism [223]. In line with the proposed inhibitory effect on the EGFR-JNK signalling, our data further suggests WDS EE regulates JNK activity through the under-expression of c-Jun phosphorylation.

Similarly, we discovered that WDS EE and RSV promoted modifications in other proteins known to interact with NF κ B. WDS EE and RSV up-regulated the phosphorylation of nuclear factor related to κ B binding protein (NFR κ B, Ser228); whereas the WDS EE treatment alone reduced NF κ B activating protein (NKAP, Ser149) and protein LYRIC (Ser308 and Ser568). NKAP is known to localise and interact with NF κ B in the nucleus and overexpression of NKAP promotes NF κ B transcriptional activity [224]. Inflammatory insults enhance nuclear compartmentalisation and binding of LYRIC and NF κ B, and the ability of NF κ B to bind DNA is enhanced upon overexpression of LYRIC [225]. There is a dearth of information regarding the biological function of these sites, however given their response to WDS EE and RSV determined in this study, we can clearly report their involvement in mediating the inflammatory cascade associated with NF κ B activation.

RSV is a member of the stilbene polyphenol family with well documented therapeutic properties [195]. There have been limited number of phosphoproteomic studies examining activity of RSV. In Alayev *et al.* they used SILAC-based MS quantitation on MCF7 cells to show that RSV inhibited AKT/mTORC1 signalling during serum-deprived conditions [158]. Although our experimental conditions differ to this study, both Alayev *et al.* and our study observed that RSV reduced the phosphorylation of CDK12 Ser681 (-2.5 FC). We also found RSV induced phosphorylation of Ser1083 on CDK12 (+2.2 FC), while down-regulating CDK7 Ser164 (-6 FC). The role of these phosphosites are not understood, and the changes were not seen with WDS EE treatments. RSV also induced phosphorylation of CDK1 Thr14/Tyr15 (+2.9 FC), an important activating site of the CDK1-Cyclin complex. In agreement with this observation, RSV promotes the same effect in SW480 cells leading to kinase inhibition and cell cycle arrest [226]. This evidence may indicate that RSV as opposed to WDS EE, can promote cell cycle arrest, partly through the inhibition of CDK1 activity.

C-Raf is a kinase member of the signalling pathway required for the activation of ERK and the subsequent transcription of genes involved in cell survival, among other functions. WDS EE -driven inhibition of phospho-NF κ B was reversed in the presence of GW5074, the specific inhibitor of C-Raf. Similar to this observation, inhibition of C-Raf shows the involvement of this kinase in the control of NF κ B activity as a protective effect in neuron cells [227]. Indeed, C-Raf is reported to modulate the activity of NF κ B even when MEK activity is abrogated suggesting an independent mechanism from the MEK-ERK canonical pathway [228], we therefore explored the involvement of other kinase pathways.

Protein kinase B or AKT, activated by phosphorylation on Ser473, is known to participate in the inflammatory response upon NF κ B activation [229]. Acting as a negative regulator, AKT through the phosphatidylinositol 3-kinase (PI3K) pathway suppresses pro-inflammatory inducers and limits the inflammatory response [230]. The phosphorylation levels of AKT are

significantly inhibited in the presence of GW5074, suggesting the involvement of AKT and C-Raf in the WDS EE treatment. Previously discussed (Chapter 2, Discussion section), the sugarcane-derived stilbene piceatannol is described to alter the phosphorylation levels of AKT and C-Raf as a mechanism that controls the down-regulation of NF κ B activity [231]. Taken together our data, we demonstrate that involvement of C-Raf and AKT activities in the WDS EE-driven changes in the phosphoproteome. This observation warrants further investigation.

Our results indicate the participation of important regulators of cell mechanisms in response to the WDS EE therapy. Apart from the effects of C-Raf on mediating NF κ B and AKT phosphorylation, C-Raf is reported in the literature to interact with other potential targets of the WDS EE driven response. PKA attenuates C-Raf activity in a mechanism that involves phosphorylation [232]. Moreover, C-Raf inhibition through the induction of NF κ B nuclear translocation limits the phosphorylation of c-Jun as a neuroprotective mechanism [227]. The complexity in the relationship of these modulators will need to be addressed in future studies to more fully unveil the signalling mechanisms of WDS EE treatment. Conjectures between these phosphorylation events and the results presented in Chapter 2 are further addressed in Chapter 5.

3.6 Conclusions

It is becoming increasingly accepted that the consumption of nutraceuticals provides health benefits in the management of inflammatory diseases such as IBD. In this study we showed that WDS EE is a strong source of antioxidants and regulates the activity of important signalling proteins (PKA, PKC β , c-Jun and EGFR). While we noted some overlap in signalling pathways regulated by both WDS EE and RSV, RSV appeared to interfere in the activity of CDKs, linking this molecule to modulation of the cell cycle. In conclusion, we have demonstrated that WDS EE antioxidants show potential health benefits towards controlling NF κ B-driven inflammatory pathways in a human gut model.

Acknowledgements

MPM acknowledges funding support from the Australian Research Council ITTC program and Cancer Institute NSW Research Equipment grant. DBN is a recipient of an Australian Research Council ITTC PhD scholarship, Macquarie University MQRES partial scholarship and Conacyt International Scholarship. Aspects of this research were conducted at APAF supported by the Australian Government's National Collaborative Research Infrastructure Scheme.

Supplementary files (in CD)

Supplementary table 1. Phosphopeptide intensity data. Supplementary table 2. Complete list of regulated phosphopeptides, WDS EE/LPS ratio. Supplementary table 3. Complete list of regulated phosphopeptides, RSV/LPS ratio.

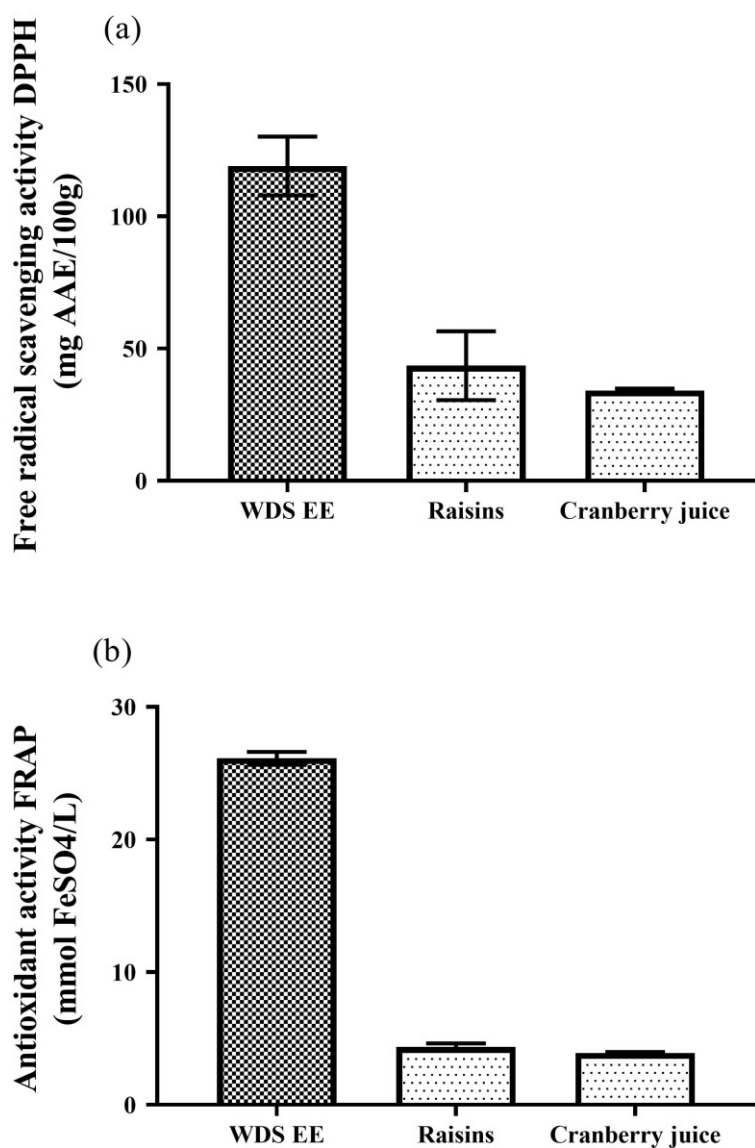


Figure 3.1 Free-radical scavenging and antioxidant activity of WDS EE

(a) Free-radical scavenging activity measured by the DPPH method (mg ascorbic acid equivalents/100g) and (b) antioxidant activity measured by the FRAP method (mmol FeSO₄/kg) of whole dried sugarcane ethanol extracts (WDS EE), raisins and cranberry juice. n=3, mean +/- SD.

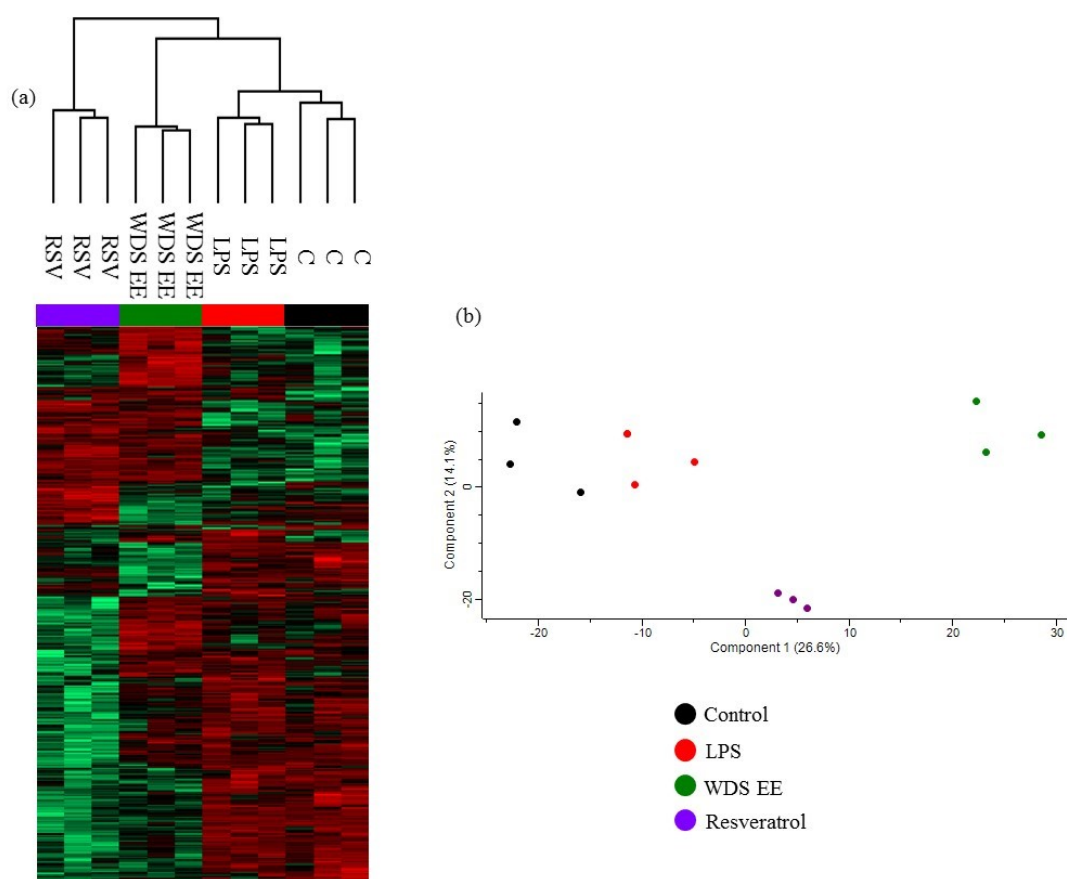


Figure 3.2(a) Hierarchical clustering and **(b)** principal component analysis of the phosphoprotein expression of SW480-treated cells

Phosphoprotein expression of untreated cells (C), lipopolysaccharide (LPS)-stimulated with 5 μ g/ml, LPS-stimulated and co-incubated with 50 μ M of whole dried sugarcane ethanol extract (WDS EE), and LPS-stimulated and co-incubated with 50 μ M of resveratrol (RSV) for 4 hours. Up-regulation (z-score > 0) is denoted by red whereas down-regulation (z-score < 0) is represented by green. n=3, ANOVA multiple sample test, Permutation based FDR 0.05.

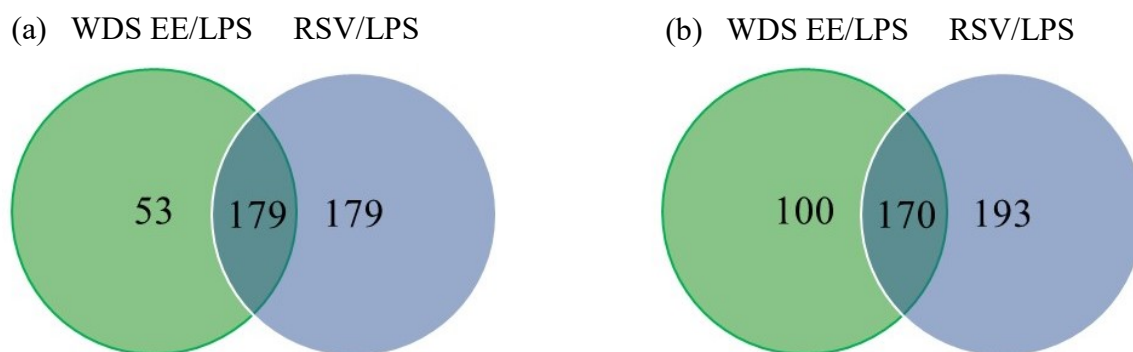


Figure 3.4 Differential **(a)** down-regulated and **(b)** up-regulated phosphorylated peptides in response to WDS EE and RSV

Differential phosphopeptide expression is based on the comparison of whole dried sugarcane ethanol extract (WDS EE) and resveratrol (RSV) against lipopolysaccharide (LPS)-challenged cells. Students t-test, permutation based FDR<0.2, +/- 1.5 fold change.

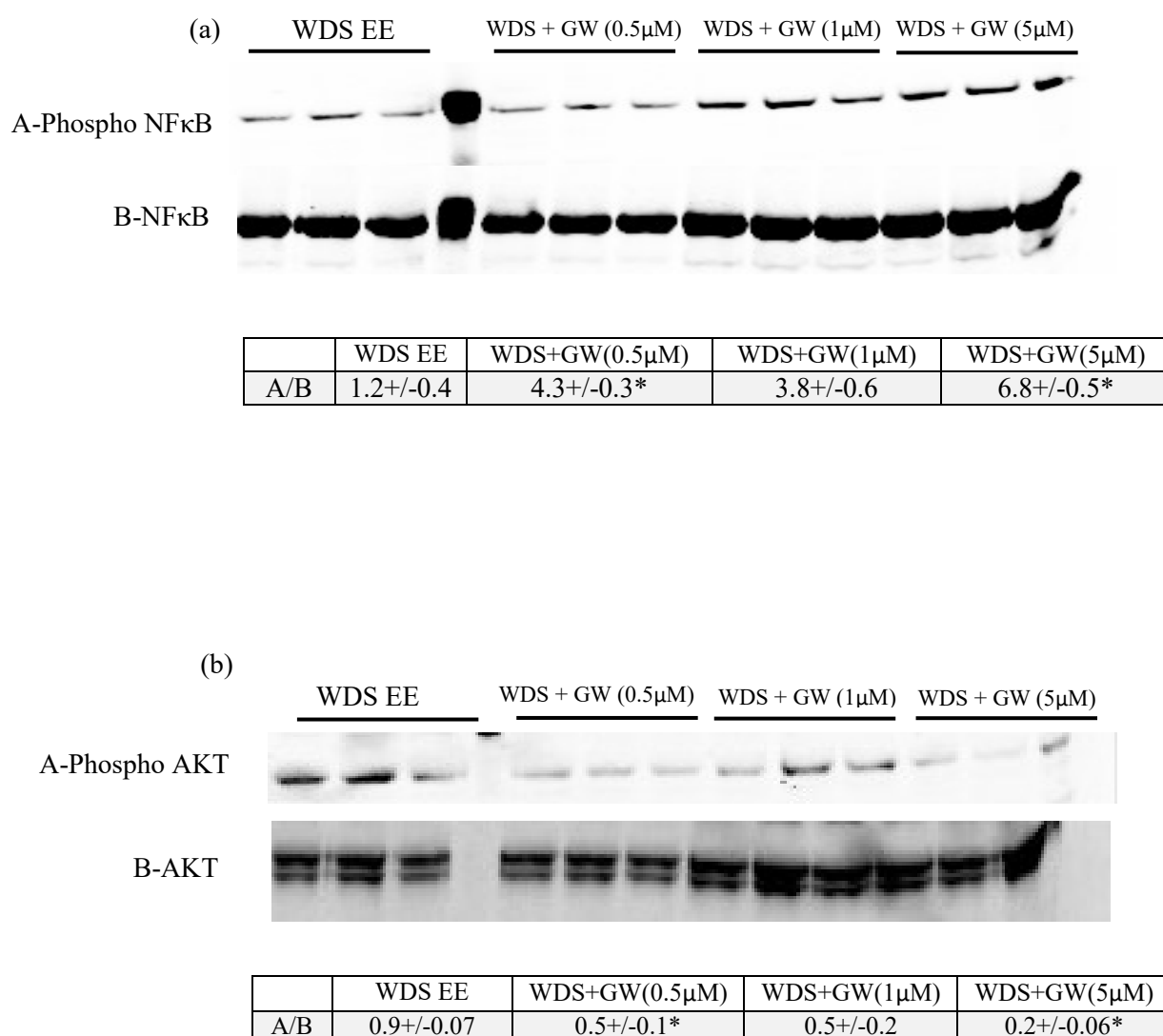


Figure 3.4 C-Raf inhibition on WDS EE-treated SW480 cells

(a) Phosphorylation of NFκB (serine 536) and **(b)** AKT (serine 473) normalised with the total expression of the corresponding protein. Cells were administered with LPS for 2h followed by incubation with whole sugarcane dried ethanol extract for 4h (WDS EE) and the C-Raf inhibitor GW5074 (WDS+GW) at three concentrations (0.5, 1 and 5 μM). n=3, mean+/-SD, * p-value<0.05.

Table 3.1 Number of phosphorylated peptides detected by MS in SW480 cells after treatments

Number of phosphorylated peptides		Average
C1	2248	2241
C2	2295	
C3	2180	
LPS1	1749	2197
LPS2	2469	
LPS3	2374	
WDS EE1	1652	1709
WDS EE2	1893	
WDS EE3	1583	
RSV1	1482	1606
RSV2	1608	
RSV3	1728	

Table 3.2 Significant regulation of relevant phosphorylated peptides expressed as WDS EE/LPS and RSV/LPS ratios

Students t-test, permutation based FDR<0.2. NS-not significant.

Uniprot accession number	Gene	Protein name	Phosphorylated residues	Fold change	
				WDS EE/LPS	RSV /LPS
Q96EB6	<i>SIRT1</i>	Sirtuin-1	S27	2	2.8
P00533	<i>EGFR</i>	Epidermal growth factor receptor (EGFR)	T693	1.6	NS
P22694	<i>PRKACB</i>	cAMP-dependent protein kinase catalytic subunit beta (PKA)	T198	-6.5	NS
P05771	<i>PRKCB</i>	Protein kinase C beta type (PKC)	T500	-2.2	NS
P05412	<i>JUN</i>	Activator protein 1, c-Jun subunit (c-Jun)	S63	-1.9	NS
P06493	<i>CDK1</i>	Cyclin-dependent kinase 1	T14/Y15	NS	2.9
Q9NYV4	<i>CDK12</i>	Cyclin-dependent kinase 12	S1083	NS	2.2
P50613	<i>CDK7</i>	Cyclin-dependent kinase 7	S164	NS	-6
Q6P4R8	<i>NFRKB</i>	Nuclear factor related to kB-binding protein	S228 S351	6.7 1.5	4.6 1.7
Q8N5F7	<i>NKAP</i>	NF-kappa-B-activating protein	S149	-5.6	NS
Q86UE4	<i>MTDH</i>	Protein Lyric	S308 S568	3.7 1.9	NS 4.7

Chapter 4 *In vivo* supplementation of whole dried sugarcane in a HFD mouse model

Chapter 4

***In vivo* supplementation of whole dried sugarcane in a HFD mouse model**

This chapter describes the experiments performed on a HFD mouse model supplemented with WDS. Physiological data, such as body weight and intraperitoneal glucose tolerance test (IPGTT), were gathered throughout the time course of the experiment. Inflammatory protein marker expression in plasma determined by multiplex bead-based ELISA and hepatic proteome characterisation by SWATH-MS, revealed significant regulation of proteins associated with inflammation and antioxidant defence. Further, bioinformatics analyses predicted the alteration of specific molecular functions and canonical pathways as a result of this dietary supplementation.

Animal experimentation was conducted in collaboration with Assoc. Prof. Anandwardhan Hardikar at the University of Sydney. IPGTTs were conducted with the guidance of Mr. Mamdouh Nessiem at the University of Sydney. Multiplex analysis was performed under the supervision of Dr. Alamgir Khan and bioinformatics analyses from these results were carried out by Dr. Edmond Breen and Dr. Dana Pascovici from the Australian Proteome Analysis Facility.

4.1 Introduction

High fat consumption is highly associated with the onset of multiple pathological conditions that include obesity, type 2 diabetes, and non-alcoholic fatty liver disease (NAFLD), among others [113][114]. It is established that fat deposition in the liver triggers a chronic inflammatory response that is observed to be causative of these pathologies [233]. Metabolic reactions in the liver are mediated by the two phases of the xenobiotic process which are fundamental for the biotransformation of drugs, fats, sugars and many micronutrients. Xenobiotic metabolism phase I involves oxidation reactions and is predominantly regulated by the cytochrome P450 (CYP) proteins. In phase II, reactions such as sulphation, glucuronidation and glutathione conjugation are essential for solubilisation and excretion of toxic metabolites [28]. Due to the generation of ROS in response to these metabolic functions, the liver is sensitive to oxidative stress and inflammatory challenge [234].

Multiple studies have employed MS-based proteomics techniques in diet studies. For instance, HFD administration in animal models instigated protein expression in the liver associated with carbohydrate and lipid metabolism and antioxidant defence [235]; thus providing evidence of the molecular processes leading to NAFLD [236]. Conversely, proteomics may be used as a tool to decipher the mechanisms of action of nutraceuticals. For example, olive oil rich in polyphenol content and polyunsaturated fatty acids administered in *Apoe*^{-/-} mice showed alterations in proteins that act on inflammation and redox stress functions in the liver [30][150].

In the previous chapters, we determined WDS ethanol extracts to modulate the phosphorylation of inflammatory regulators such as NFκB, SIRT1, c-Jun, EGFR, PKA, and PKCβ in SW480 cells. For this study, the C57BL/6J mouse strain was subject to a HFD regimen and the impact of WDS supplementation determined. We contrasted the response to the commercially available wheat dextrin-based supplement Benefiber® (BF,

GlaxoSmithKline). Wheat dextrin is reported to promote health by increasing the population of health associated bacteria and inducing the production of beneficial short-chain fatty acids, among other properties [237]. Short-chain fatty acids are the main products of colonic fermentation of dietary fibre and multiple studies link their action with anti-inflammatory attributes [19][238]. The effect of WDS and BF as nutraceuticals was measured on circulating markers of inflammation by multiplex bead-based ELISA. Additionally, liver protein expression was characterised by SWATH-MS.

4.2 Methods

4.2.1 Animal handling and sample collection

Eleven week old C57BL/6J mice were provided with food and water *ad libitum*. Normal chow (NC, Specialty Feeds Australia) was initially given to all the mice (n=50) for two weeks before the beginning of the experiment. High fat diet (HFD, 60% fat, Specialty Feeds Australia) was introduced at baseline to a group of mice (n=41) (composition and nutritional parameters of these diets are shown in Appendix 7 Tables 4A.1, 4A.2 and 4A.3). At 17 weeks, WDS (5% (w/w) incorporated in HFD, Specialty Feeds Australia) and BF (5% (w/w) incorporated in HFD, Specialty Feeds Australia) were introduced to a set of the HFD group (HFD n=14, WDS n=14 and BF n=13). NC group (n=9) were maintained without any dietary change throughout the experiment. Animals were kept on a 12h/12h light/dark schedule in a temperature and humidity controlled room. Cages were changed every week and fresh feed and water were provided weekly. Weight gain and food intake were recorded every week. The procedures involved animal handling were approved by the Animal Ethics Committee Macquarie University. Mice were sacrificed at week 33 by cervical dislocation. Prior to liver excision, mice were perfused with ice cold PBS to remove blood content. Right atria vein was cut and PBS was pumped through the heart's left ventricle. Livers were removed after a few minutes once they turned pale, immediately snap frozen in dry ice and stored at -80°C before

analysis. Blood (100 μ L approx.) was collected after mandibular vein piercing at 0, 17 and 33 weeks and gently mixed with EDTA at a final concentration of 4mM pH 7.0. Blood was centrifuged at 1000xg for 10 min at 4 °C, plasma samples were collected, aliquoted and stored at -80 °C before analysis.

4.2.2 Intraperitoneal glucose tolerance test (IPGTT)

IPGTT (2 g/kg) was performed in conscious 6 hour-fasted mice at weeks 17 and 23. Blood glucose concentrations were measured at baseline, 15, 30, 45, 60, 90 and 120 min after injection. Area-under-the-curve (AUC) was calculated per mouse and averaged per group.

4.2.3 Expression of circulating markers of inflammation in plasma

Cytokine marker (8-plex: GM-CSF, IFN γ , IL-1 β , IL-2, IL-4, IL-5, IL-10 and TNF α , catalogue number: M60000007A) and diabetes marker (8-plex: ghrelin, GIP, GLP-1, glucagon, insulin, leptin, PAI-1 and resistin, catalogue number: 171F7001M) (Bio-rad) quantitation was determined according to the manufacturer's protocol. Briefly, plasma samples were diluted (1:4) in sample diluent. Plasma samples, standards and blank were incubated with coupled magnetic beads for 1 hour at room temperature with shaking at 850 rpm. After washing three times with washing buffer in a magnetic station, detection antibody was added and incubated in the dark for 30 min at room temperature with shaking. After washing, streptavidin conjugate was added and incubated in the dark for 10min with shaking. Wells were further washed and coupled beads were resuspended in assay buffer before reading. Samples were analysed using the Bio-Plex 200 instrument (Bio-rad). The fluorescence values were log2 normalised using the random effects model which corrects for subject, time and plate to plate variation [239]. Differences between groups were analysed by Student's t test and ANOVA (Wald Chi square test). P-value correction was performed according to the Holm's method [240].

4.2.4 Mass spectrometry based proteomics analysis

Approximately 10 mg of liver was prepared for proteomics analysis from 40 samples: NC n=9, HFD n=10, WDS n=11 and BF=10. Briefly, tissue was resuspended in 500 μ L of 1% (w/v) sodium deoxycholate, 0.1 M triethylammonium bicarbonate (Sigma Aldrich) supplemented with protease inhibitor cocktail (Roche). Lysis was performed using a probe sonicator for 2 min. Lysates were boiled at 95 °C for 2 min. After centrifugation at 5000 rpm for 10 min, supernatants were collected and protein concentration was determined by the bicinchoninic acid assay. Protein (15 μ g) was reduced with 10 mM DTT for 30 min at 60 °C, alkylated with 20mM iodoacetamide for 20 min in the dark, trypsin digested (Sigma Aldrich) in 1:50 ratio and incubated at 37 °C overnight. Peptides were purified using a C-18 mini column, recovered in 70% acetonitrile (ACN), dried, and resuspended in 1% TFA for LC-MS/MS.

The SWATH reference spectral library was generated out of a pooled liver lysate made from representative samples of the four different diets. Library and samples were acquired on a 6600 Triple TOF using the same conditions described previously for SWATH quantitation (Chapter 2, Methods section). Database searches utilised the murine SwissProt database. Search modifications, peak extractions, and parameters were the same as indicated previously (Chapter 2, Methods section). Statistical significant proteins were determined using a threshold of p-value<0.05 and fold change greater than 1.5.

4.2.5 Ingenuity pathway analysis

Prediction of functions and diseases based on protein expression was performed as previously indicated (Chapter 2, Methods section) for the 2,388 proteins quantitated across all 40 samples considering the paired comparisons: NC/HFD, WDS/HFD and BF/HFD.

4.3 Results

In this work, we sought to determine the impact of WDS as a dietary supplement in a HFD mouse model. We contrasted their response against use of BF as a dietary supplement. Chemical characterisation shows both WDS and BF as sources of dietary fibre (Wei Chong, Macquarie University. Personal communication), being BF a commercially available product. Throughout the experiment several physiological parameters were monitored including body weight gain, food intake and glucose tolerance. As observed in Figure 4.1a and b, there are mean differences among groups in respect to body weight gain however not statistical significant. However, in the case of food intake values there is a strong significance of HFD, WDS and BF compared to NC (Figure 4.1c and d). Interestingly, during IPGTT in week 17 HFD individuals showed significantly higher glucose levels and thus higher AUC compared to the NC group. IPGTT performed on week 23 indicates that supplementation of HFD with either WDS or BF produced no significant change in glucose tolerance (Figure 4.2). Plasma samples were collected at weeks 0, 17 and 33 for quantitation of circulating markers of inflammation. Mice were euthanized at week 33 and livers were collected after perfusion with saline solution for proteomics analysis. Measurement of fat pad, liver, and kidney mass was also determined, however, no statistical significance was produced among groups (Figure 4.3).

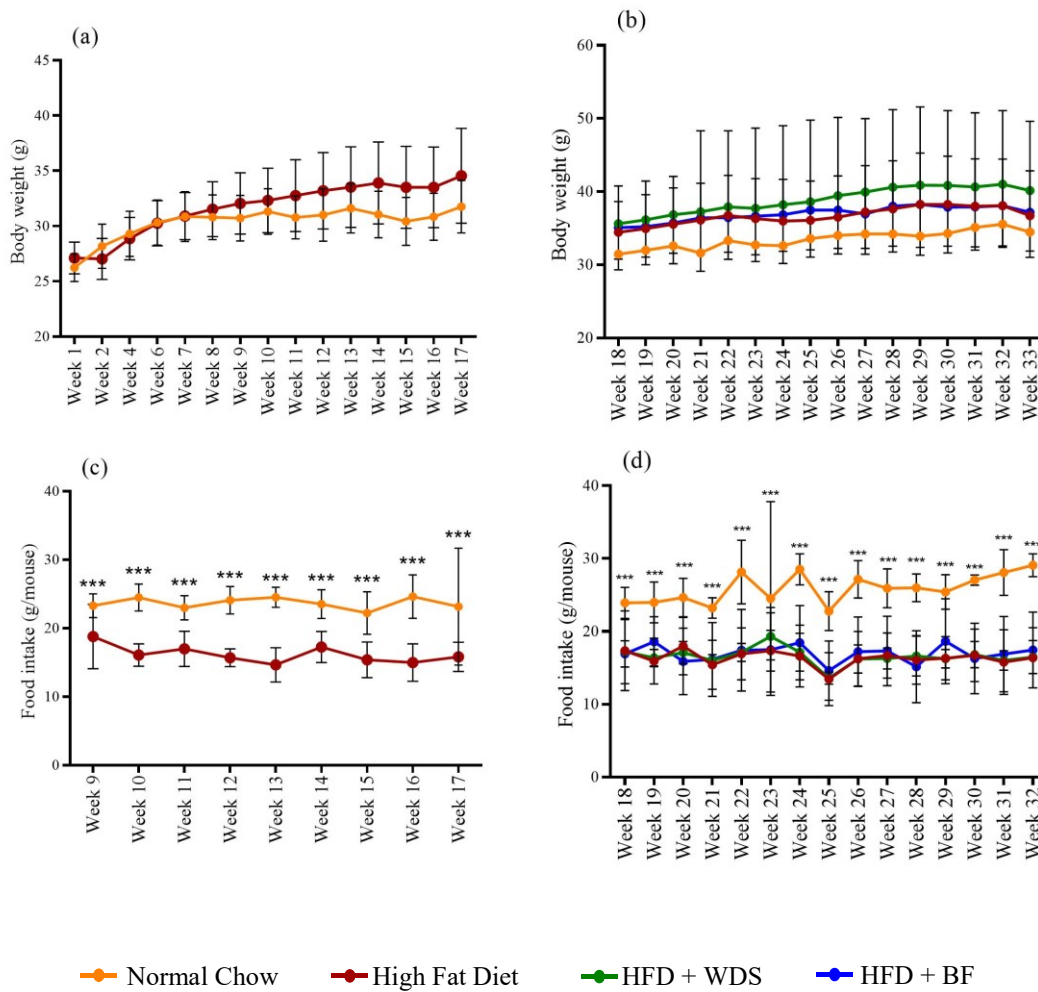


Figure 4.1 Body weight gain and food intake in response to dietary changes

Normal chow and high fat diet (HFD) effect on **(a)** body weight and **(c)** food intake were monitored until week 17, NC n=9 and HFD n=41. Whole dried sugarcane (WDS) and Benefiber (BF) were introduced in week 18 and these variables were monitored until the end of the study **(b)** and **(d)**, NC n=9, HFD n=14, WDS n=14 and BF=13. Mean \pm SD, *** p-value < 0.001.

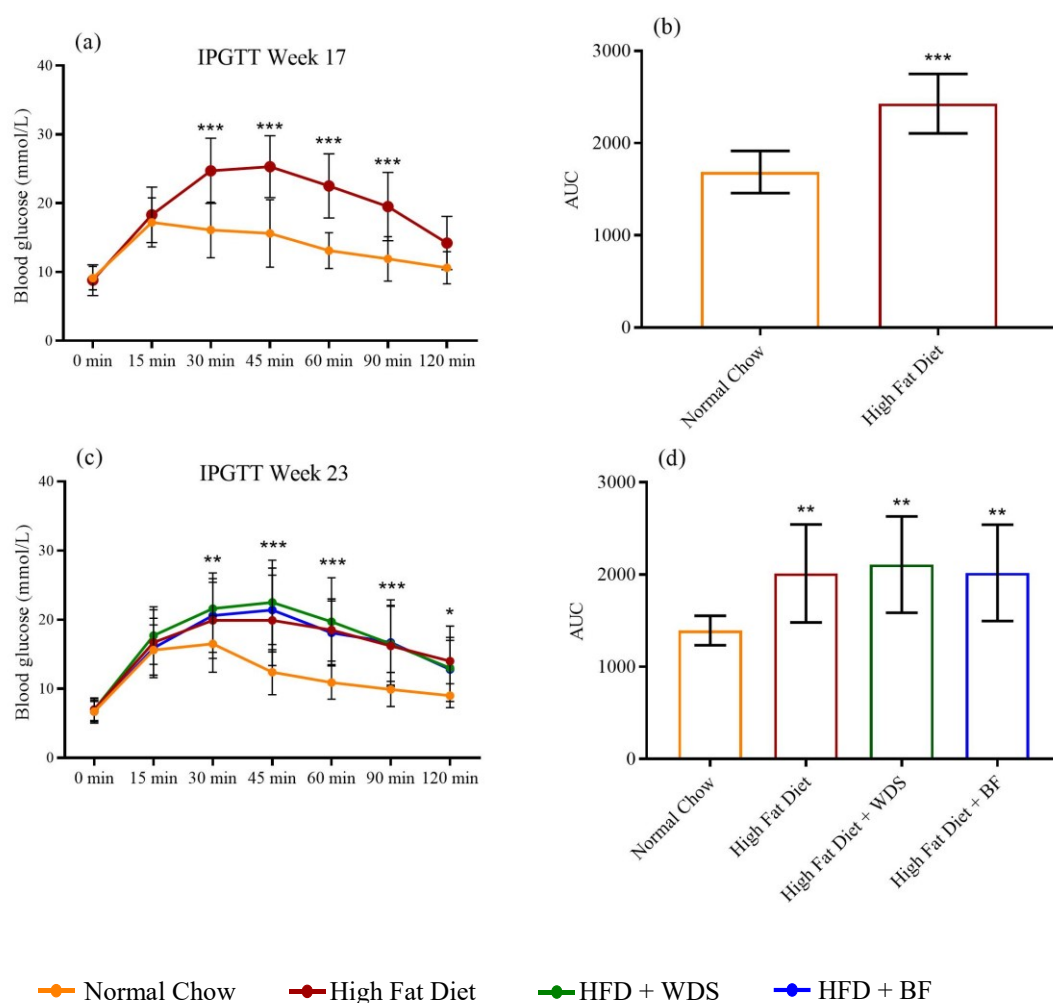


Figure 4.2 Intraperitoneal glucose tolerance test (IPGTT) and area-under-the-curve (AUC) in response to dietary changes.

(a) IPGTT was performed in week 17 on normal chow and high fat diet (HFD) fed mice. **(b)** Calculated AUC, NC n=9 and HFD n=41. **(c)** IPGTT was again performed in week 23 after whole dried sugarcane (WDS) and Benefiber (BF) introduction. **(d)** Calculated AUC, NC n=9, HFD n=14, WDS n=14 and BF=13. Mean \pm SD, * p-value <0.05, ** p-value <0.01, *** p-value <0.001.

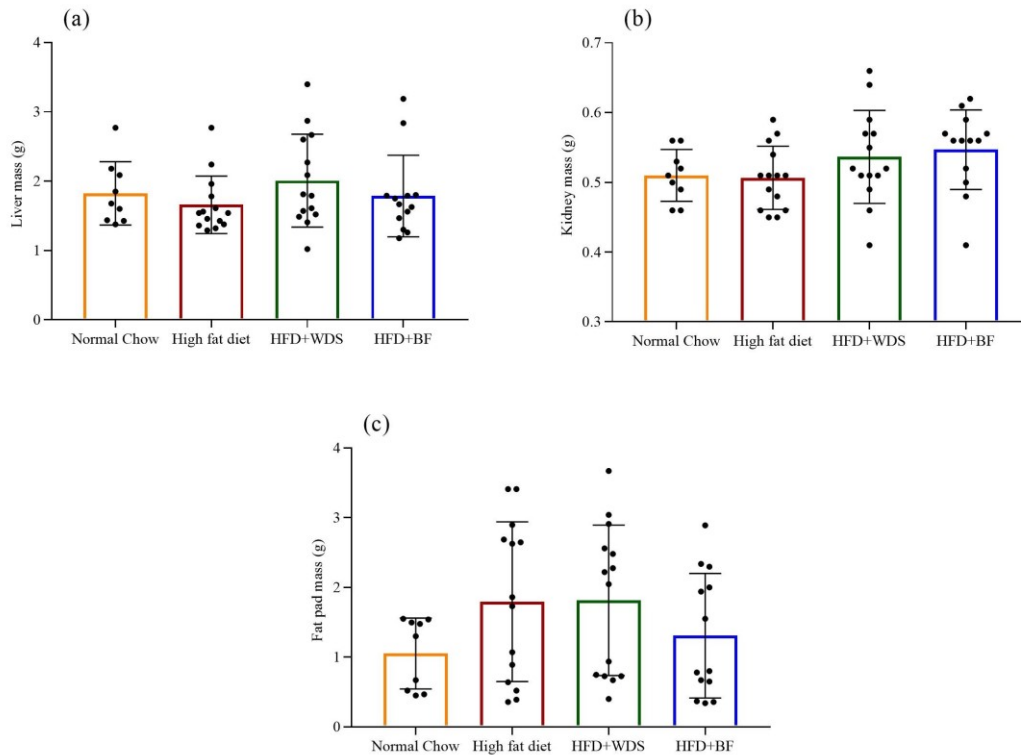


Figure 4.3 Organ weight in response to dietary changes.

(a) Liver, (b) kidney, and (c) fat pad weight values. NC n=9, HFD n=14, WDS n=14, and BF n=13. Mean \pm SD.

4.3.1 Concentration of circulating plasma marker proteins

To understand the potential effects of the different diets in the promotion of pathologies, we quantified the expression of inflammatory markers from plasma samples using the multiplex bead-based ELISA technology. Although there was not any statistical change among the HFD, WDS, and BF supplemented animals in the markers tested (Appendix 5 Figures 4.A1 and 4A.2); in mice fed with HFD, WDS and BF the levels of GLP-1, insulin and plasminogen activator inhibitor 1 (PAI-1) were significantly increased compared to NC fed mice (Figure 4.4a, b, and c). Interestingly, the pro-inflammatory cytokines GM-CSF and IL-1 β significantly decreased in plasma from animals fed with WDS and BF compared to NC (Figure 4.4d and e).

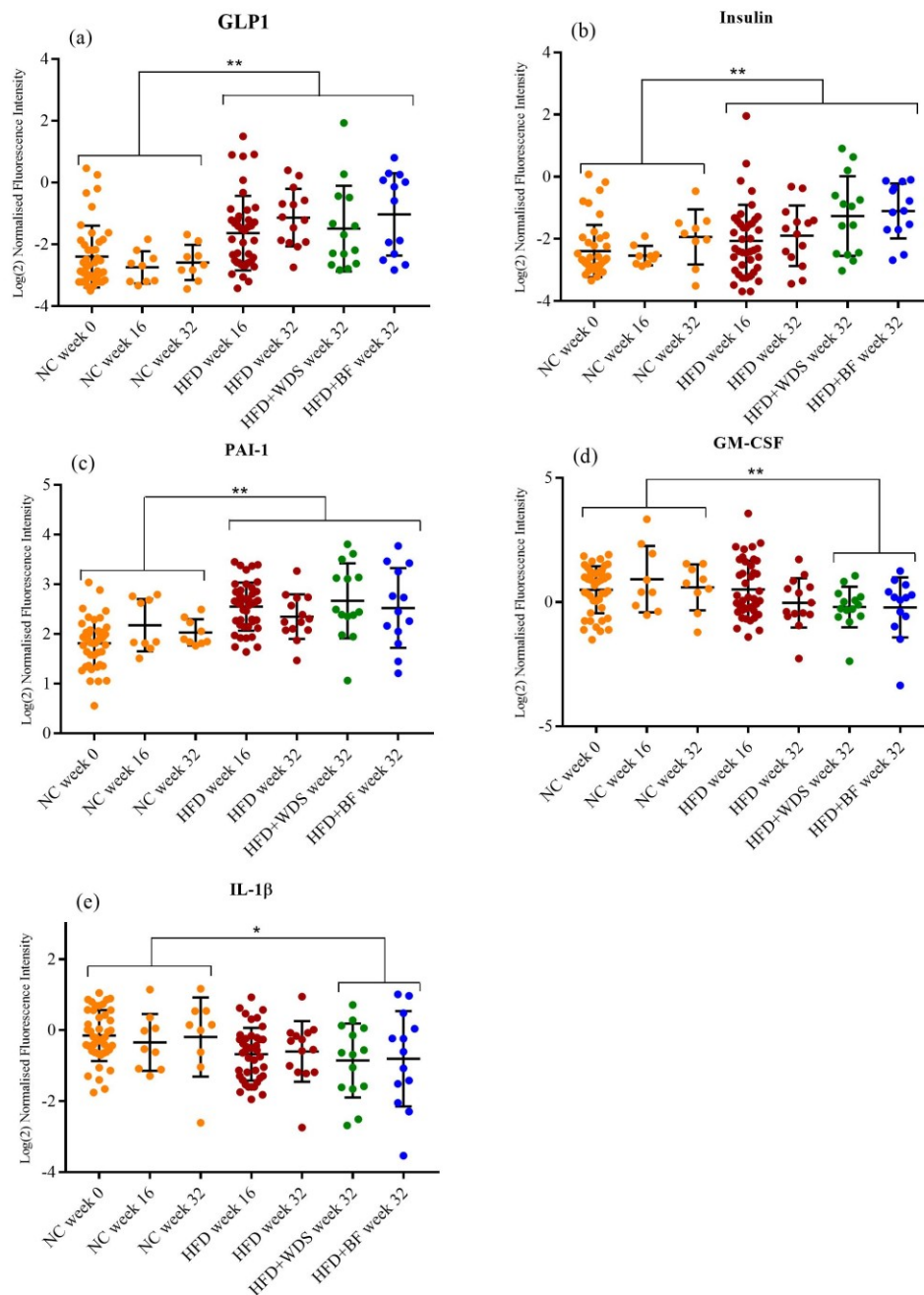


Figure 4.4 Plasma marker expression in response to dietary changes.

Plasma samples were obtained at baseline (week 0, NC n=50), week 16 (NC n=9 and HFD n=41), and week 32 (NC n=9, HFD n=14, WDS n=14 and BF=13). Values expressed as log(2) normalised fluorescence intensity. (a) GLP-1, (b) Insulin, (c) PAI-1, (d) GM-CSF and (e) IL-1 β . * p-value <0.05, ** p-value <0.01.

4.3.2 Diet induced changes in liver protein expression in response to HFD, WDS and BF

Given that these diets produced changes in the expression of some plasma markers, it was studied their effect on the protein expression in liver tissue by employing a label-free SWATH-MS proteomics approach [143]. A spectral library was created by fractionating a pooled liver lysate from each diet under basic reverse phase conditions prior to LC-MS/MS identification. The library was composed of 4,064 proteins which was used to extract information from the 40 samples (NC n=9, HFD n=10, WDS n=11 and BF=10) analysed by SWATH-MS. From these, quantitative information was obtained for 2,388 proteins across all 40 samples. Hierarchical clustering and principal component analysis represents the overall changes induced by the four diets as presented in Figure 4.5. As observed, hepatic protein expression from NC fed mice form a discernible cluster. Contrastingly, there is no clear separation among the protein expression from HFD, WDS and BF supplemented individuals, an observation that is consistent with the findings reported in the quantitation of inflammatory markers (Figure 4.4).

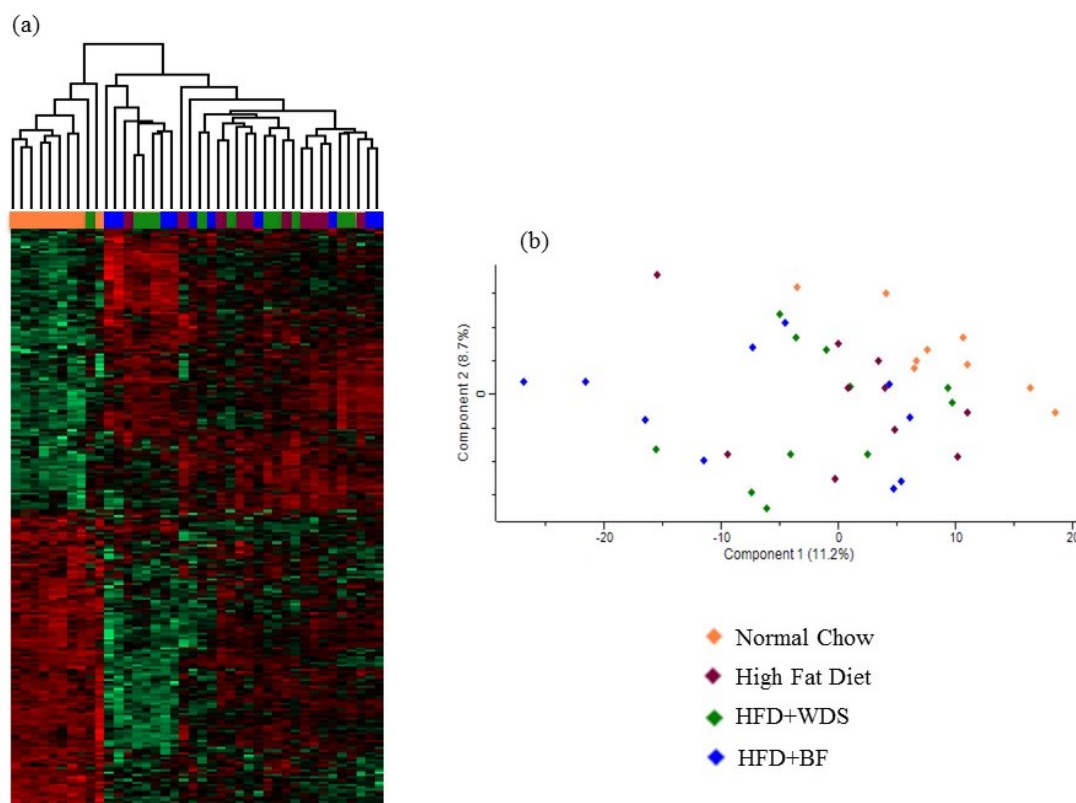


Figure 4.5 MS-based hepatic protein expression in response to dietary changes.

(a) Hierarchical clustering and **(b)** principal component analysis, NC n=9, HFD n=10, WDS n=11 and BF=10. Up-regulation (z-score >0) is denoted by red whereas down-regulation (z-score <0) is represented by green. ANOVA multiple sample test, Permutation based FDR 0.05.

Two-sample t-test performed on the HFD (n=10) compared to the NC (n=9)-driven liver protein expression shows striking differences in these two groups. For instance, 75 proteins were observed as statistical significantly up-regulated ($p\text{-value} < 0.05$, fold change $> \pm 1.5$) and 80 proteins down-regulated as a consequence of HFD. Among the down-regulated proteins, we identified the major urinary protein 1 (MUP1), selenium binding protein 2 (SBP2), glutathione S-transferase P1 (GSTP1), histidine ammonia-lyase (HUTH), ornithine aminotransferase mitochondrial (OAT), persulfide dioxigenase ETHE1 (ETHE1), argininosuccinate synthase (ASSY), carbamoyl phosphate synthase (CPSM), 10-formyltetrahydrofolate dehydrogenase (AL1L1) and betaine-homocysteine S-

methyltransferase 1 (BHMT1). Protein up-regulation in response to HFD include acyl-coenzyme A thioesterase 2 (ACOT2), apolipoprotein A-IV (APOA4), peroxisomal bifunctional enzyme (ECHP), hydroxymethylglutaryl-CoA synthase 1 and 2 (HMGCS1 and HMGCS2). According to previous proteomic studies, HFD supplementation in mice is proven to promote changes in the expression of these proteins in the liver [153][235][236][241] which confirm our results.

HFD also led to significant up-regulation of other proteins linked to fatty acid oxidation and inflammatory response functions such as pantetheinase, CD36, carnitine O-acetyltransferase (CRAT), heat shock protein beta 1 (HSPB1), cathepsin S, and pyruvate dehydrogenase kinase 1 and 2 (PDK1 and PDK2). Complete list of proteins significantly regulated by HFD is shown in appendices section (Appendices 8 and 9 Tables 4A.3 and A.4).

In contrast, WDS supplementation compared to HFD produced significant changes in the down-regulation of 10 proteins and the up-regulation of 14 proteins (Table 4.1). Of interest to this study, we identified STAT3, transmembrane protein 120A (T120A), aquaporin 1 (AQP1) and 15kDa selenoprotein (SEP15) from the down-regulated group. From the up-regulated proteins, selenocysteine synthase (SecS) was observed in this group. Liver protein expression from animals fed with BF showed the down-regulation of 17 proteins and the up-regulation of 26 proteins (Table 4.2). This includes PDK2 from the decreased group and UDP-glucuronosyltransferase 1-9 (UGT1A9) from the increased group. Only two proteins were common to WDS and BF treatments, T120A and guanidinoacetate N-methyltransferase (GAMT) found down and up-regulated, respectively (Figure 4.6).

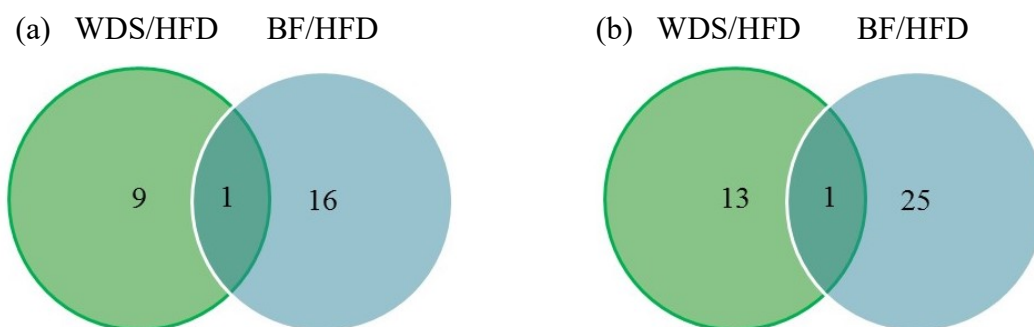


Figure 4.6 Differential **(a)** up-regulation and **(b)** down-regulation of proteins in response to WDS and BF supplementation.

Differential protein expression is based on the comparison of WDS and BF against HFD fed mice. Students t-test, p -value <0.05 , fold change ± 1.5 .

Table 4.4 Significant regulated proteins expressed as WDS/HFD ratio

Two-sample t-test (p-value<0.05), fold change>1.5

Uniprot accession number	Gene	Protein name	Fold change WDS/HFD	P-values	Gene ontology, molecular functions
A2AGT5	<i>CKAP5</i>	Cytoskeleton-associated protein 5	2.2	3.70E-03	Cadherin binding; microtubule binding; microtubule plus-end binding; ribonucleoprotein complex binding
Q6P6M7	<i>SPCS</i>	Selenocysteine synthase	2.2	4.37E-02	Transferase activity, transferring selenium-containing groups; tRNA binding
P16110	<i>LEG3</i>	Galectin-3	2.1	2.24E-02	Carbohydrate binding; chemoattractant activity; IgE binding; laminin binding; RNA binding
Q8R1F1	<i>NIBL1</i>	Niban-like protein 1	2	2.46E-02	Cadherin binding; transcription coactivator activity
P00375	<i>DYR</i>	Dihydrofolate reductase	1.8	2.21E-02	Dihydrofolate reductase activity; dihydrofolic acid binding; drug binding; folic acid binding; methotrexate binding; mRNA binding ; NADPH binding; sequence-specific mRNA binding; translation repressor activity, nucleic acid binding
Q6URW6	<i>MYH14</i>	Myosin-14	1.6	3.48E-02	Actin-dependent ATPase activity; actin filament binding; ATPase activity; ATP binding; calmodulin binding; microfilament motor activity
Q4VAA2	<i>CDV3</i>	Protein CDV3	1.6	2.32E-02	
Q9CQ01	<i>RNT2</i>	Ribonuclease T2	1.6	1.30E-02	Ribonuclease activity; ribonuclease T2 activity; RNA binding
Q8K2Q9	<i>SHOT1</i>	Shootin-1	1.6	4.52E-02	Actin filament binding; cadherin binding; kinesin binding
Q9R060	<i>NUBP1</i>	Cytosolic Fe-S cluster assembly factor NUBP1	1.6	4.47E-02	4 iron, 4 sulfur cluster binding; ATP binding; iron-sulfur cluster binding; metal ion binding
Q9Z0G0	<i>GIPC1</i>	PDZ domain-containing protein GIPC1	1.6	2.24E-02	Actin binding; cadherin binding; GTPase activator activity; myosin binding; PDZ domain binding; protein homodimerization activity; receptor binding
O35969	<i>GAMT</i>	Guanidinoacetate N-methyltransferase	1.6	1.65E-02	Guanidinoacetate N-methyltransferase activity
P97372	<i>PSME2</i>	Proteasome activator complex subunit 2	1.5	3.60E-02	Endopeptidase activator activity; identical protein binding
Q6PER3	<i>MARE3</i>	Microtubule-associated protein RP/EB family member 3	1.5	2.93E-02	Identical protein binding; microtubule binding
Q9ERR7	<i>SEP15</i>	15 kDa selenoprotein	-1.5	4.86E-02	
Q9ER88	<i>RT29</i>	28S ribosomal protein S29, mitochondrial	-1.6	7.27E-03	RNA binding; structural constituent of ribosome
Q9D273	<i>MMAB</i>	Cob(I)yrinic acid a,c-diamide adenosyltransferase, mitochondrial	-1.6	1.62E-02	ATP binding; cob(I)yrinic acid a,c-diamide adenosyltransferase activity

Q8C878	<i>UBA3</i>	NEDD8-activating enzyme E1 catalytic subunit	-1.7	2.80E-02	Acid-amino acid ligase activity; ATP binding; identical protein binding; ligand-dependent nuclear receptor binding; NEDD8 activating enzyme activity; protein heterodimerization activity
Q3UFK8	<i>FRMD8</i>	FERM domain-containing protein 8	-1.7	1.59E-02	
Q8BH59	<i>CMC1</i>	Calcium-binding mitochondrial carrier protein Aralar1	-1.7	3.32E-02	Calcium ion binding; L-aspartate transmembrane transporter activity; L-glutamate transmembrane transporter activity
Q02013	<i>AQP1</i>	Aquaporin-1	-1.7	3.49E-02	Ammonium transmembrane transporter activity; carbon dioxide transmembrane transporter activity; ephrin receptor binding; glycerol transmembrane transporter activity; identical protein binding; intracellular cGMP activated cation channel activity; nitric oxide transmembrane transporter activity; potassium channel activity; potassium ion transmembrane transporter activity; transmembrane transporter activity; water channel activity; water transmembrane transporter activity
Q8C1E7	<i>TI20A</i>	Transmembrane protein 120A	-1.9	2.04E-02	
P42227	<i>STAT3</i>	Signal transducer and activator of transcription 3	-2.0	1.85E-03	CCR5 chemokine receptor binding; chromatin DNA binding; DNA binding; glucocorticoid receptor binding; identical protein binding; nuclear receptor activity; protein dimerization activity; protein homodimerization activity; protein kinase binding; protein phosphatase binding; RNA polymerase II core promoter proximal region sequence-specific DNA binding; RNA polymerase II repressing transcription factor binding; RNA polymerase II transcription factor activity, sequence-specific DNA binding; sequence-specific DNA binding; transcriptional activator activity, RNA polymerase II core promoter proximal region sequence-specific binding; transcriptional activator activity, RNA polymerase II transcription regulatory region sequence-specific binding; transcription factor activity, sequence-specific DNA binding; transcription factor binding; transcription regulatory region DNA binding
Q6PHN9	<i>RAB35</i>	Ras-related protein Rab-35	-2.6	3.96E-03	GDP binding; GTPase activity; GTP binding; phosphatidylinositol-4,5-bisphosphate binding

Table 4.2 Significant regulated proteins expressed as BF/HFD ratio

Two-sample t-test (p-value<0.05), fold change>1.5

Uniprot accession number	Gene	Protein name	Fold change BF/HFD	P-values	Gene ontology, molecular functions
Q8R409	<i>HEX11</i>	Protein HEXIM1	2.5	3.41E-02	7SK snRNA binding; cyclin-dependent protein serine/threonine kinase inhibitor activity; snRNA binding
P97315	<i>CSRP1</i>	Cysteine and glycine-rich protein 1	2.2	2.91E-03	Metal ion binding; RNA binding
Q3UVK0	<i>ERMP1</i>	Endoplasmic reticulum metalloproteinase 1	2	2.71E-02	Metal ion binding; metalloproteinase activity
P14901	<i>HMOX1</i>	Heme oxygenase 1	2	1.78E-02	Enzyme binding; heme binding; heme oxygenase (decyclizing) activity; metal ion binding; phospholipase D activity; protein homodimerization activity; signal transducer activity
Q62452	<i>UD19</i>	UDP-glucuronosyltransferase 1-9	2	2.37E-02	Drug binding; enzyme binding; enzyme inhibitor activity; fatty acid binding; glucuronosyltransferase activity; protein heterodimerization activity; protein homodimerization activity; protein kinase C binding; steroid binding
Q9D0W5	<i>PPIL1</i>	Peptidyl-prolyl cis-trans isomerase-like 1	1.9	7.67E-03	Disordered domain specific binding; peptidyl-prolyl cis-trans isomerase activity
Q9EP71	<i>RAI14</i>	Ankycorbin	1.9	1.89E-02	
Q99L45	<i>IF2B</i>	Eukaryotic translation initiation factor 2 subunit 2	1.8	2.86E-02	Metal ion binding; RNA binding; translation initiation factor activity
O08808	<i>DIAP1</i>	Protein diaphanous homolog 1	1.8	2.64E-02	Actin binding; identical protein binding; ion channel binding; profilin binding; Rho GTPase binding; RNA binding
Q925N0	<i>SFXN5</i>	Sideroflexin-5	1.8	4.83E-02	Citrate transmembrane transporter activity
P51885	<i>LUM</i>	Lumican	1.8	2.41E-02	Collagen binding
Q9CWI3	<i>BCCIP</i>	BRCA2 and CDKN1A-interacting protein	1.7	1.20E-02	Kinase regulator activity; RNA binding; tubulin binding
Q00915	<i>RET1</i>	Retinol-binding protein 1	1.7	4.28E-02	Retinal binding; retinoid binding; retinol binding; transporter activity
Q9JLQ0	<i>CD2AP</i>	CD2-associated protein	1.7	2.87E-02	Beta-catenin binding; cadherin binding; protein complex binding; protein C-terminus binding; SH3 domain binding; vascular endothelial growth factor receptor binding
P32261	<i>ANT3</i>	Antithrombin-III	1.7	2.12E-04	Heparin binding; identical protein binding; protease binding; serine-type endopeptidase inhibitor activity
Q99MZ3	<i>MLXPL</i>	Carbohydrate-responsive element-binding protein	1.6	4.23E-02	Carbohydrate response element binding; protein heterodimerization activity; RNA polymerase II core promoter proximal region sequence-specific DNA binding;

					transcriptional repressor activity, RNA polymerase II core promoter proximal region sequence-specific binding; transcription factor binding
Q6IRU2	<i>TPM4</i>	Tropomyosin alpha-4 chain	1.6	2.66E-02	Actin filament binding; identical protein binding; metal ion binding; protein heterodimerization activity; protein homodimerization activity; structural constituent of muscle
P08905	<i>LYZ2</i>	Lysozyme C-2	1.6	4.21E-02	Identical protein binding; lysozyme activity
P15379	<i>CD44</i>	CD44 antigen	1.6	4.77E-02	Hyaluronic acid binding; type II transforming growth factor beta receptor binding
Q8BGS2	<i>BOLA2</i>	BolA-like protein 2	1.6	5.78E-03	
Q8BFW7	<i>LPP</i>	Lipoma-preferred partner homolog	1.6	1.20E-02	Metal ion binding
P47941	<i>CRKL</i>	Crk-like protein	1.5	5.56E-03	Cadherin binding; identical protein binding; phosphotyrosine residue binding; RNA binding
P56389	<i>CDD</i>	Cytidine deaminase	1.5	2.94E-02	Cytidine deaminase activity; identical protein binding; nucleoside binding; protein homodimerization activity; zinc ion binding
Q04447	<i>KCRB</i>	Creatine kinase B-type	1.5	7.50E-03	ATP binding; creatine kinase activity; ubiquitin protein ligase binding
Q62159	<i>RHOC</i>	Rho-related GTP-binding protein RhoC	1.5	3.89E-02	GTPase activity; GTP binding; signal transducer activity
O35969	<i>GAMT</i>	Guanidinoacetate N-methyltransferase	1.5	4.77E-02	Guanidinoacetate N-methyltransferase activity
Q64458	<i>CP2CT</i>	Cytochrome P450 2C29	-1.5	1.16E-02	Arachidonic acid epoxygenase activity; aromatase activity; caffeine oxidase activity; estrogen 16-alpha-hydroxylase activity; heme binding; iron ion binding; monooxygenase activity; steroid hydroxylase activity
P70195	<i>PSB7</i>	Proteasome subunit beta type-7	-1.5	4.09E-02	Threonine-type endopeptidase activity
Q9DCP2	<i>S38A3</i>	Sodium-coupled neutral amino acid transporter 3	-1.5	1.27E-02	Antiporter activity; L-alanine transmembrane transporter activity; L-asparagine transmembrane transporter activity; L-glutamine transmembrane transporter activity; L-histidine transmembrane transporter activity; symporter activity
Q8R0Y8	<i>S2542</i>	Mitochondrial coenzyme A transporter SLC25A42	-1.5	4.75E-02	Adenosine-diphosphatase activity; ADP transmembrane transporter activity; AMP transmembrane transporter activity; ATP transmembrane transporter activity; coenzyme A transmembrane transporter activity
Q8JZS0	<i>LIN7A</i>	Protein lin-7 homolog A	-1.6	4.03E-02	L27 domain binding
P04945	<i>KV6AB</i>	Ig kappa chain V-VI region NQ2-6.1	-1.6	5.67E-03	Antigen binding
Q6WKZ7	<i>NOSTN</i>	Nostrin	-1.6	2.67E-02	DNA binding
Q6XVG2	<i>CP254</i>	Cytochrome P450 2C54	-1.6	8.33E-03	Arachidonic acid epoxygenase activity; aromatase activity; heme binding; iron ion binding; linoleic acid epoxygenase activity; steroid hydroxylase activity
Q8C1E7	<i>T120A</i>	Transmembrane protein 120A	-1.7	4.87E-02	

P21126	<i>UBL4A</i>	Ubiquitin-like protein 4A	-1.7	1.57E-02	Chaperone binding
A2AN08	<i>UBR4</i>	E3 ubiquitin-protein ligase UBR4	-1.7	1.44E-02	Calmodulin binding; ubiquitin-protein transferase activity; zinc ion binding
Q9JK42	<i>PKD2</i>	Pyruvate dehydrogenase kinase isozyme 2, mitochondrial	-1.7	1.35E-02	ATP binding; protein homodimerization activity; pyruvate dehydrogenase (acetyl- transferring) kinase activity
Q9CQL5	<i>RM18</i>	39S ribosomal protein L18, mitochondrial	-1.7	2.10E-02	5S rRNA binding; structural constituent of ribosome
Q9R013	<i>CATF</i>	Cathepsin F	-1.7	4.77E-02	Cysteine-type endopeptidase activity; cysteine-type peptidase activity
Q8BTW3	<i>EXOS6</i>	Exosome complex component MTR3	-1.7	1.16E-02	RNA binding
Q9WVQ5	<i>MTNB</i>	Methylthioribulose-1- phosphate dehydratase	-1.8	4.09E-02	Identical protein binding; methylthioribulose 1-phosphate dehydratase activity; zinc ion binding
P56382	<i>ATP5E</i>	ATP synthase subunit epsilon, mitochondrial	-2.1	1.27E-02	Hydrogen-exporting ATPase activity, phosphorylative mechanism; proton-transporting ATP synthase activity, rotational mechanism

4.3.3 Protein based predicted effect on liver functions and canonical pathways

Based on the protein expression induced by the different supplements, prediction of diseases and functions was performed using IPA. The top 10 diseases and functions representing the predicted effects driven by NC, WDS and BF compared to HFD are shown in Figure 4.7 (complete analysis is presented in Appendix 6 Figure 4A.3). Accordingly, WDS is predicted to provide a protective effect by the down-regulation of IPA annotated pathways associated with incidence of liver tumour, incidence of hepatocellular carcinoma, liver adenoma, fibrosis of liver, benign neoplasm of liver, liver metastasis, cell death of liver cells, and damage of liver. Although BF is also predicted to down-regulate these functions (except for cell death of liver cells, shown as up-regulated), the activation z-score is not as strong as presented for WDS suggesting a milder effect. Both nutraceuticals are predicted to up-regulate hepatic steatosis and conjugation of glutathione. Analysis of predicted canonical pathways illustrates several differences among the treatments (Figure 4.8). Eukaryotic initiation factor 2 (eIF2), a transduction pathway linked to the progression of stress conditions, is presented with a positive z-score in NC fed animals. Conversely, eIF2 signalling was repressed in response to WDS and BF supplementation. As additional effects, the regulation of eIF4 and p70S6K signalling is augmented by BF, but not with NC and WDS, whilst mTOR signalling is predicted to be up-regulated by WDS and BF with a stronger effect in the latter in contrast to the predicted inhibition by NC.

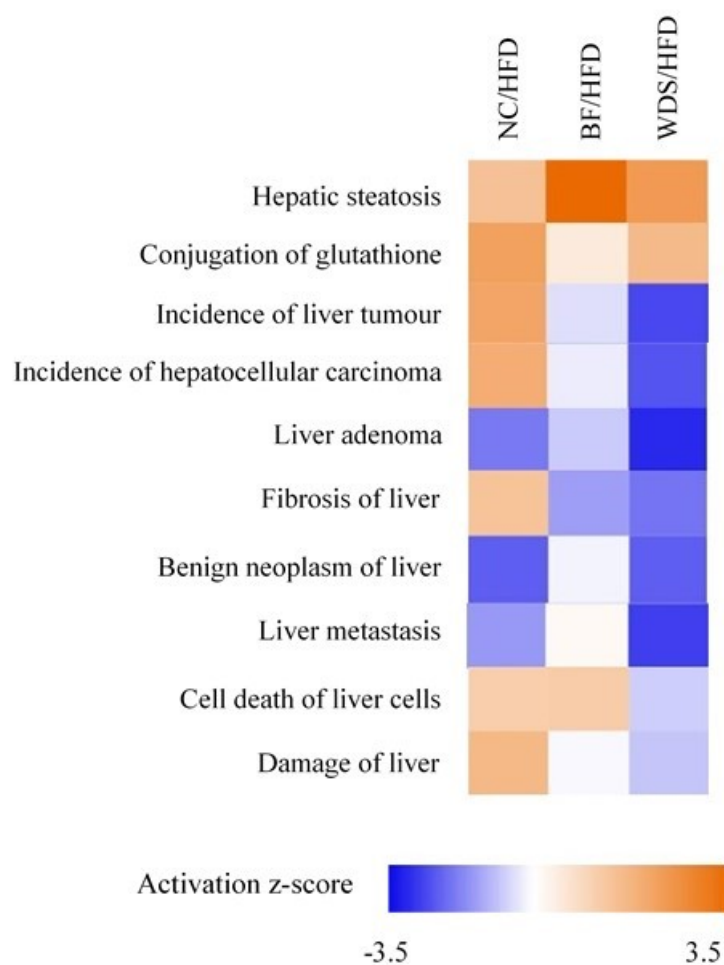


Figure 4.7 Top 10 diseases and functions prediction based on hepatic protein expression induced by WDS and BF supplementation

NC/HFD, WDS/HFD and BF/HFD fold changes and p-values were analysed for paired comparisons using IPA (Ingenuity Systems). Up-regulation (z-score >0) is denoted by orange whereas down-regulation (z-score <0) is represented by blue.

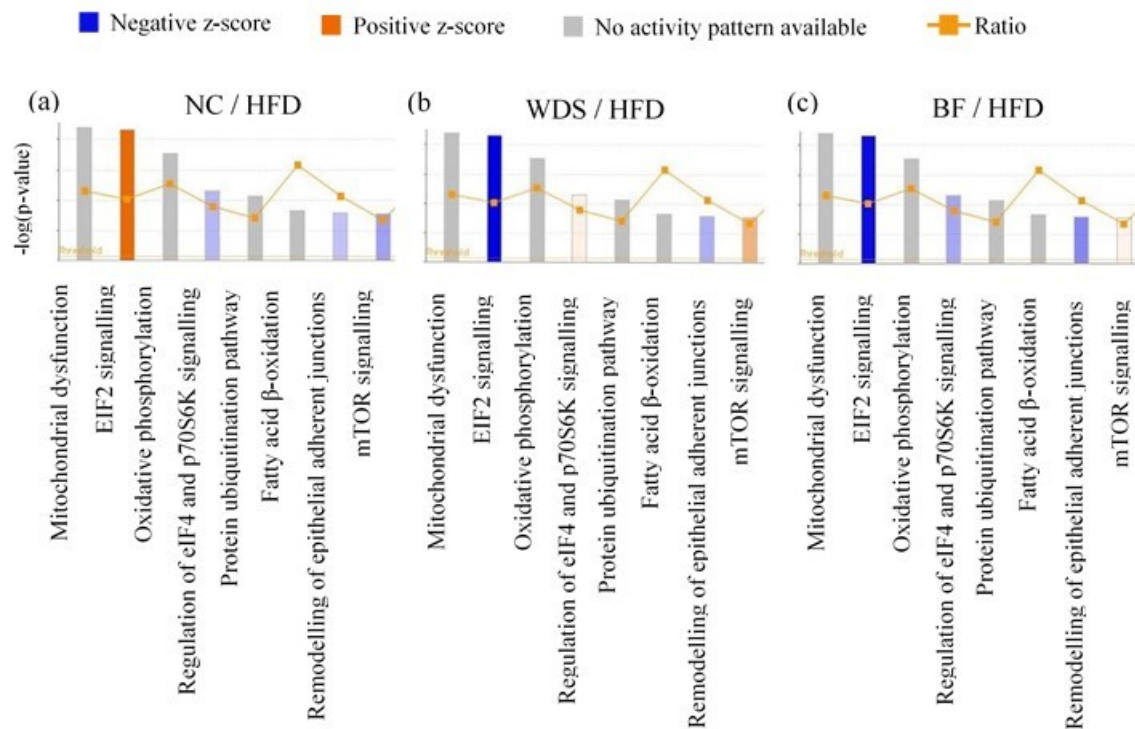


Figure 4.8 Canonical pathway prediction in response to WDS and BF supplementation

(a) NC/HFD, (b) WDS/HFD and (c) BF/HFD fold changes and p-values were analysed using IPA (Ingenuity Systems). The ratio line represents the number of proteins altered by the dietary change divided by the total number of proteins from the canonical pathway. Up-regulation (z-score >0) is denoted by orange whereas down-regulation (z-score <0) is represented by blue.

4.4 Discussion

4.4.1 Dietary effect on body weight gain

In the experiments reported here, we determined the effect of the nutraceuticals WDS and BF in a HFD mouse model. Our results show that HFD, WDS or BF does not induce any significant change in body weight gain compared to NC. Although HFD is used to model obesity and chronic inflammatory conditions in animals [113][114], in some studies high fat supplementation has been observed to produce no statistical significant change in body weight gain and fasting glucose levels compared to NC diet [236][242]. It is also suggested that HFD challenge on the mouse strain employed in this study, C57BL/6J and some sub-strains, are protected from weight gain and therefore do not respond to diet induced obesity [243]. Similarly, some nutraceutical interventions on animal models are reported to produce no change in these parameters. For example, the polyphenol curcumin, effective in the treatment of inflammation, although modulates important inflammatory pathways does not lead to weight loss in a mouse IBD model [138]. In another study, quercetin supplementation in a HFD mouse model reduced the secretion of IFN γ , IL-1 and IL-4 although it did not produce any change in terms of weight gain compared to the HFD group [164]. We therefore investigated the relation of these nutraceuticals with inflammatory-related molecular mechanisms.

4.4.2 Dietary changes on circulating inflammatory markers

In regards to the inflammatory marker concentration in plasma samples, our results showed a significant up-regulation of GLP-1, insulin and PAI-1 from HFD, WDS and BF compared to NC fed individuals (Figure 4.4a, b and c), all indicators of reduced tolerance to glucose likely associated with HFD consumption. GLP-1 is a potent stimulator of insulin secretion in response to glucose presence [244]. It is established that nutrient ingestion promotes GLP-1 release in the gastrointestinal tract. According to previous studies, GLP-1 administration is

correlated with reduction in the food intake which appears to be in accordance to our results [245]. As observed in the food intake values (Figure 4.1c and d), HFD, WDS and BF promoted lower food intake compared to NC fed mice suggesting a satiety effect presumably due to the high fat content. Consistently with the literature, sugarcane fibre is reported to induce GLP-1 expression in plasma and it is also speculated that appetite signals are involved [119]. However, the significance of these results are not clear since this effect appears to be mediated by HFD and not by the nutraceuticals introduction.

On the other hand, PAI-1 levels in plasma are positively correlated with abdominal subcutaneous fat, obesity, and insulin secretion [246]. Further, PAI-1 was associated in the development of obesity and augmented insulin levels in response to HFD fed animals [247]. In line with this role, increased insulin levels is associated with initiation of the inflammatory cascade in the liver coordinated by ROS generation and oxidative stress [113]. The data presented here shows elevated levels of PAI-1 and insulin and are consistent with the effects provided by HFD supplementation. Impaired glucose tolerance (Figure 4.2), another sign of metabolic disorder progression due to prolonged HFD consumption in mice [113], is corroborated in this study. However, the subsequent addition of the two nutraceuticals does not present any significant change in this context.

4.4.3 Nutraceutical-dependent inhibition of cytokines

Interestingly, HFD does not produce any significant shift in cytokine secretion in plasma even though their release is linked to the development of chronic inflammation conditions such as obesity in HFD fed mice [248]. Nevertheless, this null effect of HFD has been reported in the case of TNF α and IL-6 and authors speculated the cytokine mediated pathway to be independent of the molecular mechanisms associated with HFD supplementation [249]. Contrastingly, the introduction of the two nutraceuticals significantly lowered the expression of GM-CSF and IL-1 β compared to NC fed animals. Although the impact of dietary fibre in

the expression of pro-inflammatory cytokines is unknown, β -glucans from barley and oat repressed IL-12 and induced IL-10 secretion in LPS-stimulated dendritic cells. The immune modulatory effect is dependent on the molecular structure of the β -glucans suggesting the physico-chemical properties of fibre to influence the inflammatory response [250]. Inhibition of GM-CSF is reported to produce a therapeutic effect in multiple models of inflammatory conditions [251]. However, GM-CSF^{-/-} mutant mice present increased levels of cytokine secretion and atherosclerosis induction under HFD supplementation [252]. In another study, HFD does not promote any change in GM-CSF levels [253]. This inconsistency in the role of GM-CSF permit to speculate that this regulator has no implication in the mechanism associated with WDS or BF.

High fat and cholesterol diet is shown to elevate the gene expression of IL-1 β and other cytokines in mice in the context of fatty liver disease [253]. Administration of fish oil or vegetable oil rich in polyunsaturated fatty acids to healthy volunteers reduced the secretion of IL-1 β [254]. Further, IL-1 β depletion has been shown to protect mice from the progression of chronic liver diseases and therefore considered as a therapeutic target against liver inflammation [255]. Therefore WDS and BF appears to confer an anti-inflammatory effect by reducing IL-1 β secretion; this observation will require additional investigation.

4.4.4 HFD effect on the liver proteome

For SWATH-MS proteomics analysis performed in this chapter, we included in the experimental design 40 biological replicates that were quantified and statistically analysed employing the same strategy as in Chapter 2. Given the complexity of *in vivo* systems, it was found appropriate to utilise this large number of biological replicates that combined with the cut-offs mentioned for the previous experiments (fold change >1.5 and p-value<0.05) ensures a high level of confidence in the identification of statistical significant regulated proteins.

The proteomics analysis on liver tissue from HFD fed mice compared to NC fed mice reported here, is consistent with previous studies in the expression of several proteins [153][235][236][241]. In particular, under-expression of MUP1 in response to HFD might be considered as a therapeutic target against glucose insensitivity and metabolic dysregulation [256]. SBP2, responsible for selenocysteine incorporation [257] and down-regulated in this study, appears to combat oxidative stress at the cell level [102]. In accordance to our study, it has been reported the up-regulation of pantetheinase [258], CD36 [259], CRAT [260], HSPB1 [259][261], and cathepsin S [262] promoted by HFD regimen at the gene level. Overexpression of the isoenzymes PDK1 and PDK2, observed herein, is associated with augmented fasting plasma glucose and insulin levels and body fat accumulation [263][264]. Overall, the protein expression instigated by HFD in this experiment is suspected to induce functions related to fatty acid and carbohydrate metabolism, inflammatory promotion and antioxidant regulation.

4.4.5 WDS regulation of selenium-related proteins

Proteomics studies in animal interventions using fibre food products has been performed in only a limited number of studies [148][149]. In this chapter, Proteomics analysis revealed WDS to significantly change the abundance of relevant proteins to antioxidant defence and inflammation. Recently, it has been reported that oxidative stress-driven HFD consumption is linked to repressed levels of the selenoproteins thioredoxin and thioredoxin reductase in liver [265]. In line with the inhibition of SBP2 expression in response to HFD, WDS is observed to significantly alter the selenocysteine synthesis enzyme SecS and the selenoprotein SEP15. SecS, up-regulated by WDS, mediates the last step in the synthesis of selenocysteine which is then inserted in the protein sequence by SBP2 and other proteins [257]. SecS function in selenium incorporation appears to be fundamental in health and disease, gene mutations present in certain populations are linked to deprive enzyme activity

and neuronal dysfunction [266]. Hence this finding might indicate a positive role of WDS in promoting SecS function and selenoprotein biosynthesis.

Down-regulated SEP15, exclusively found in WDS and not BF supplemented animals, is associated with folding assistance of glycoproteins and tumour development. Different studies point out to a role of SEP15 in tumour progression, however there is not a clear consensus since it is implicated in preventing liver and prostate cancer [267] but more recently linked in colon cancer promotion [268]. Tsuji *et al.* employing SEP15 knockout mice observed increased levels of IFN γ in plasma and higher incidence of colon cancer compared to wild type mice, suggesting a protective role of SEP15 inhibition [268]. Overall, selenium proteins are considered as important promoters of health. The potential role of WDS in regulating selenoprotein expression is of great relevance since we identified in our *in vitro* model an increased expression of Selenoprotein H in response to WDS (Chapter 2, Discussion section). These new observations provide additional levels of evidence of the role of WDS in selenium regulation *in vivo* and might be linked to the anti-inflammatory response described *in vitro*.

We also paid special attention to the predicted up-regulation of the conjugation of glutathione function in WDS supplemented mice (Figure 4.7). The conjugation phase II, another step of the xenobiotic metabolism process, is mediated by glutathione-S-transferases. Elevated glutathione activity is clearly associated with improved antioxidant defence against ROS-derived oxidative stress pathologies. For instance, green tea polyphenols presented health benefits in chemical-induced diabetic mice by improving glutathione levels in the liver [269]. In a different animal study, chitosan-starch supplementation under HFD regimen increased antioxidant capacity by improving the activity of glutathione peroxidase and superoxide dismutase in liver tissue compared to control group [120]. While it was not explored the

reason for the link between WDS and glutathione induction, the outcome would favour improved ability to metabolise toxic compounds.

4.4.6 WDS-dependent anti-inflammatory effect

Our proteomics data also presents evidence related to the potential anti-inflammatory functions of WDS. STAT3, a transcription factor with a prominent position in the regulatory mechanisms of cancer, immune response, and inflammation in the liver, was significantly down-regulated in WDS-supplemented mice whilst BF produced no significant effect. In Chapter 2, we learnt WDS ethanol extracts inhibit the activation of the NFκB signalling pathway *in vitro*. Interestingly, it is established that STAT3 collaborates with NFκB in the progression of the inflammatory response in the liver [45]. In mouse models of chronic inflammation, NFκB takes a prominent role in orchestrating the expression of cytokines in liver tissue. HFD administration induces tumour formation in a mechanism involving TNFα, IL-1β and IL-6 release and STAT3 activation in hepatic tissue from mouse [248]. There is evidence linking dietary changes to influence the expression of STAT3. The phenolic chlorogenic acid reverses the deleterious effects carried by chemical promoted cholestasis and liver injury partially by the suppression of STAT3, NFκB and cytokine release [270]. In a different study, a model of induced liver fibrosis in mice revealed plumbagin, a bioactive extracted from the medicinal plant *Plumbago zeylanica* L., to significantly alleviate liver injury and this was partially explained through the down-regulation of STAT3 which was also confirmed *in vitro* [271]. Apart from the reduced inflammation in colon tissue promoted by curcumin and green tea polyphenols in IBD-induced mice, these two therapies produced gene and protein expression predicted to inhibit STAT3 [138][147].

The inhibitory effect promoted by WDS and BF in the secretion of IL-1β appears to be linked to repression of inflammatory-related functions as observed in the function prediction analysis (Figure 4.7). However, the suppression of the inflammatory inducer STAT3 only

observed after WDS and not BF supplementation, might suggest an independent mechanism between STAT3 and IL-1 β inhibition.

4.4.7 Inhibition of AQP1 and T120A

Another protein exclusively down-regulated by WDS is AQP1. Important for water transportation to the bile, AQP1 is a membrane associated protein expressed in the liver [272]. AQP1 is relevant in obesity and metabolic disorders. HFD supplementation on AQP1^{-/-} mice provokes less body weight gain as opposed to wild type mice on HFD diet. Thus, AQP1 is suggested to confer a protective function against obesity although deleterious effects such as fat malabsorption were also observed [273]. Even though our HFD model did not produce weight loss in response to WDS incorporation, AQP1-dependent regulation might be of interest for future studies.

Special attention was also given to T120A given its induction by HFD and subsequent repression by WDS and BF. T120A is expressed in white adipose tissue in the inner nuclear membrane and there is evidence of its function in inducing adipogenesis *in vitro* [274]. In the liver, gene expression of T120A is interpreted to play a role in fatty acid metabolism [275]. Significant up-regulation of T120A in liver from HFD administered mice as opposed to its down-regulation in WDS and BF mice might link these two nutraceuticals in altering fat production related cellular activities.

4.4.8 Modulation of cellular events by BF

Predicted modulation of canonical pathways might reveal novel mechanisms associated with WDS and BF, such as the inhibition of eIF2 signalling promoted by the two nutraceuticals (Figure 4.8). Induction of this signalling is promoted by bacterial infection and associated with NF κ B activity and cytokine expression [276]. Conversely, phosphorylation-dependent inhibition of eIF2 α is described as an effective therapy against the inflammatory related

Alzheimer's disease-driven memory loss and synaptic failure [277]. Although this mechanism requires further investigation in the liver and diet context it anticipates new avenues of study.

Restricted to BF and not to WDS supplementation, it was observed the up-regulation of UGT1A9 as an opposite effect to the down-regulation provided by HFD. UGT19A mRNA levels are known to be differentially affected in patients suffering from non-alcoholic fatty steatohepatitis (NASH) [278]. Despite the importance of UGT19A as part of the phase II of the xenobiotic metabolism, its implications in the liver in response to HFD are not clear. In contrast to the HFD-driven up-regulation of PDK2, BF down-regulated this kinase, event not associated with WDS supplementation. These results might show BF to induce a reversal effect in the progression of some metabolic functions promoted by HFD that will require further study.

Surprisingly, based on protein expression BF was predicted to stimulate the mTOR and eIF4-p70S6K signalling pathways as a mechanism not completely shared by WDS (Figure 4.8). Although more studies are needed on this subject, it is understood that mTOR signalling is fundamental in the metabolism of fatty acids in the liver [279] and its activation at the gene level in HFD fed mice is demonstrated [261]. Conversely, S6K^{-/-} mice are protected from HFD in terms of insulin sensitivity and weight gain. This effect might potentially implicate high oxidation rates of lipids in contrast to obese wild type mice that presents augmented levels of S6K activity [280]. The relevance of these pathways is emphasised in nutraceutical interventions; for example, the clove oil-derived eugenol administered to C57BL6/J mice challenged with HFD showed reduced liver inflammation with decreased protein phosphorylation levels of mTOR and p70S6K thereby preventing the transcription of lipogenic genes [281].

4.4.9 Sugarcane supplementation in animal models

Previous studies have evaluated the effect of sugarcane derivatives in HFD animal models. For example, Wang *et al.* compared sugarcane fibre with cellulose and psyllium husk and demonstrated the former to reduce body weight, fat mass, and to improve insulin sensitivity and glucose tolerance. Sugarcane fibre was also shown to inhibit ghrelin and leptin secretion and to improve GLP-1 levels [119]. This fibre was also proved to modulate the insulin transduction pathway by induced phosphorylation of the insulin receptor substrate 1, insulin receptor, AKT, AMPK and PI3K activity [282]. These differences compared to the results reported in this thesis are discussed in Chapter 5.

4.5 Conclusions

In this work, we characterised the effect of WDS and BF supplemented on a HFD *in vivo* model by the quantitation of circulating inflammatory markers in plasma and proteomics analysis on liver tissue. Based on the IPGTTs, HFD promoted glucose intolerance. Even though WDS or BF administration did not alter this effect, both fibre supplements revealed changes in plasma markers and hepatic protein expression suggestive of an anti-inflammatory response. For instance, WDS inhibited the inflammatory mediators IL-1 β and STAT3 and promoted significant changes in selenium-related proteins indicative of antioxidant defence and inflammatory suppression. In line with these results, protein expression-based prediction analyses suggests WDS-dependent alterations on functions and canonical pathways associated with inflammatory events.

Supplementary files (in CD)

Supplementary table 1. Multiplex Log2 fluorescent intensity normalised data. Supplementary table 2. SWATH-based MS Normalised peak area. Supplementary table 3. Complete list of

regulated proteins, HFD/NC ratio. Supplementary table 4. Complete list of regulated proteins, WDS/HFD ratio. Supplementary table 5. Complete list of regulated proteins, BF/HFD ratio.

Chapter 5 General discussion and future directions

The usage of dietary supplements rich in antioxidant content can often be effective in counteracting the progression of some chronic diseases. In this regard, functional understanding of the molecular events associated with improved health benefits of nutraceuticals is fundamental for their acceptance and widespread use. This thesis set out to apply proteomics technologies to investigate how whole dried sugarcane (WDS) could exert anti-inflammatory properties.

5.1 Main findings and contributions to new knowledge

Nutraceutical research has grown rapidly in recent years. Although much of the effort involving bioactive studies has focused on purified natural products, there is also interest in the combinatorial effects gained from food product extracts. The first aim of this thesis was to undertake a broad chemical characterisation of ethanol extracts of WDS. WDS was of interest to examine since one of its components, bagasse, is usually a waste product despite being a source of antioxidants [124]. Characterisation of WDS extracts revealed the presence of polyphenols and flavonoids with strong antioxidant activity (Chapters 2 and 3). This represents the first characterisation of WDS. From the literature, it is expected that polyphenols, flavonoids and other antioxidants have anti-inflammatory properties. Thus it is likely this is the source of the anti-inflammatory properties exerted by proteomic/phosphoproteomic profiling (Chapters 2 and 3). It is not discarded that other components present in WDS extracts such as dietary fibre and minerals have a role or an additive effect in these results. Overall, the results reported in this thesis provide further evidence of the therapeutic properties of nutraceuticals.

The second and third aims of this thesis were to apply proteomics to characterise the molecular mechanisms regulated by WDS an *in vitro* inflammatory model and an *in vivo* mouse HFD model. In the *in vitro* model, SWATH-based proteomics (Chapter 2) and phosphoproteomics (Chapter 3) analysis yielded evidence of anti-inflammatory signalling

events. These findings are integrated in Figure 5.1, where WDS extracts regulate the phosphorylation of the master inflammatory controller NF κ B, leading to reduced secretion of IL-8 (Chapter 2) at least partly through the activation of C-Raf and AKT as demonstrated in Chapter 3. Additionally, PKA and PKC β phosphorylation is inhibited by WDS extracts, further preventing the activation of NF κ B. Concomitantly, other inflammatory mediators shown to be altered included the transcription factor c-Jun, EGFR and the histone deacetylase SIRT1 (Chapter 3) which allow us to hypothesise the involvement of their respective signalling pathways in mediating the action of WDS extracts. Phosphorylation of Ser27 on SIRT1, which was positively regulated by WDS extracts, is regarded as a crucial effector in cell defence mechanisms, specifically in SIRT1 enzymatic activity and nuclear localisation orchestrated by the JNK pathway [211].

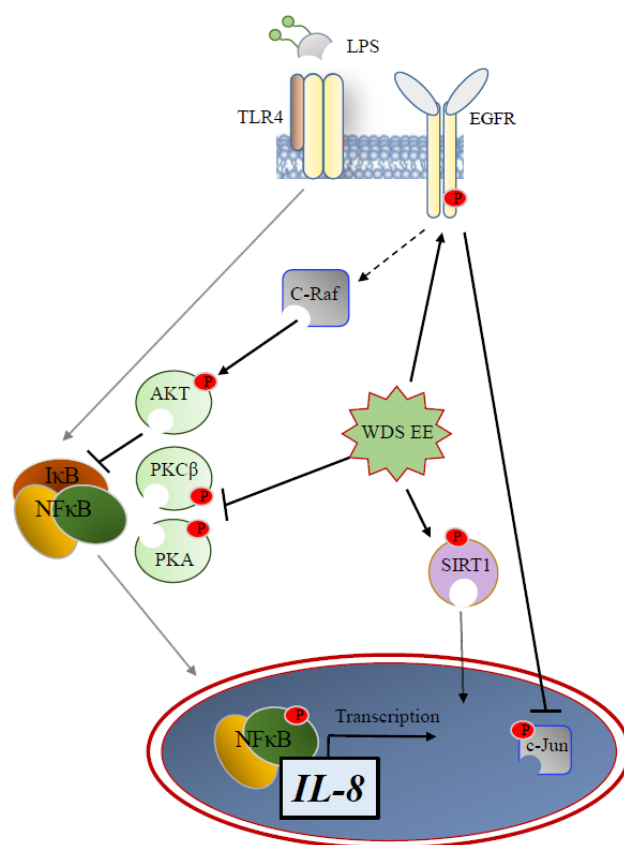


Figure 5.1 WDS ethanol extracts (WDS EE) effects *in vitro*. Integration of major proteomics and phosphoproteomics findings

Based on these findings, it is interesting to speculate further associations. Although not tested, it is conjectured that the activation of C-Raf and AKT is potentially mediated by the EGFR signalling cascade. Phosphorylation of Thr693, driven by WDS extracts (Chapter 3), is described as a critical event in the inhibition of the JNK signalling pathway [219]. Conversely, nutraceuticals are reported to control EGFR phosphorylation with a subsequent effect in other MAP kinase pathways. Curcumin is shown to inhibit NFκB nuclear activity through the modulation of AKT and EGFR tyrosine phosphorylation in prostate cells [283]. Although the implication of the phosphorylation of EGFR on Thr693 involves activation of MAPK signals [284], the high level complexity in the relation of these transduction signals will require further examination.

Chapter 4 explored *in vivo* supplementation of WDS in a HFD mouse model. SWATH was used as protein quantitation strategy as well as multiplex bead-based ELISA analysis for the analysis of inflammatory markers that are found at much lower circulating concentration levels. From the SWATH approach, around 2,400 proteins were quantified across 40 samples of mouse liver tissue. The results showed WDS to counteract some specific inflammatory events initially triggered by HFD such as the suppression of STAT3. Interestingly, there was no direct overlapping with the proteins described in the *in vitro* experiment. Cooperative signals between STAT3 and NFκB have been determined as a plausible explanation, since IL-6 as an inducer of STAT3 is a transcription product of NFκB [42]. However, our MS data analysis of mouse liver did not reveal any significant regulation of the NFκB transduction signals. It is difficult to extrapolate and compare the two models since human colon cells were employed for *in vitro* analysis and mouse liver tissue was used for *in vivo* experiments. It is speculated that rather than the absence of NFκB *in vivo* or STAT3 *in vitro*, the characteristics of each model determined the orchestrating signalling pathway. For instance, LPS rendered SW480 cells to an inflammatory state by NFκB activation whilst HFD resulted in acute

inflammation in mice due to STAT3 activity. Therefore, it is proposed that the levels of expression of the transcription factors when not participating remained constantly depressed and thus not detected as changing protein levels. Nevertheless, the evidence presented shows WDS as an effective agent to selectively repress the inflammatory machinery in two different models.

Another possible explanation to the selectivity of the pathways regulated by WDS might involve the mechanisms by which it is delivered to the cells. In the *in vitro* experiments, WDS was extracted in 52% ethanol, dried and then delivered directly to the colon cells. On the other hand, in the *in vivo* experimentation, WDS was integrated into HFD chow, was digested and went through more complex processes that included the modification by commensal bacteria, absorption in the colon epithelium and metabolism in the liver. These striking differences might impact on the chemical nature of the WDS metabolites and therefore the proteome response. For example, it is documented that the antioxidant activity of quercetin varies depending on its multiple metabolites [98], but also quercetin's anti-inflammatory effect is dependent on the chemical modification and whether *in vitro* or *in vivo* models are tested [86].

It is established that selenium incorporation in the diet carries important health benefits. Despite the complexity of the biological systems tested in this work, we observed a striking parallelism linking selenium associated proteins with WDS. In human colon cells, WDS extracts are shown to induce expression of SELH (Chapter 2), whilst in HFD mice supplemented with WDS, hepatic tissue was observed to have reduced levels of SEP15 and increased SecS levels compared to animals on HFD only (Chapter 4). SecS plays a fundamental role in the incorporation of the selenocysteine residue in the polypeptide chain. Selenoproteins are regarded as important promoters of health such as the glutathione peroxidases due to their antioxidant defence functions. Moreover, recent studies implicate

some of these proteins in functions associated with a dual role in cancer development and inhibition as in the case of SEP15. Selenium intake has been identified to positively control the mRNA abundance and translational activity of certain selenoproteins including SELH in liver tissue *in vivo* [285]. While we have not resolved the mechanism associated with selenoprotein regulation, it appears that WDS achieve this outcome. To the best of our knowledge, this is the first connection between sugarcane based nutraceutical and the selenoproteome in the context of inflammation.

This thesis showcased the application of proteomics techniques for the analysis of WDS nutraceutical properties. As shown in Table 1.2, protein differential expression by 2DE has been selected as the method of choice in most nutraceutical investigations. SWATH, as a state-of-the-art quantitation strategy, has been determinant in the elucidation of the proteome response in various studies. This thesis demonstrated the use of SWATH as a label-free quantitation technique in the context of nutraceutical research. Further, phosphoproteomics research in the context of nutritional studies is an under-explored territory. Some of the conclusions drawn from this work allow us to support the study of the phosphoproteome as another powerful tool in this discipline. From this work, investigation of the proteome and its global modification at the phosphorylation level provided an integral view of WDS mechanistic regulation *in vitro*. In the same way, phosphoproteomics characterisation *in vivo* will reveal further insights worth of consideration.

5.2 Limitations and future directions

One of the limitations of this thesis is the use of a cancer cell line for testing the proteomic impacts of WDS extracts. As justified in the introduction (Chapter 1, Section 4.2), SW480 cells are a suitable model for studying inflammation due to the cells sensitivity to LPS, triggering a classical inflammatory response. However, the architecture, growth, and response to external stimuli among other features between malignant and non-malignant cells suggest

differences may occur compared to primary cells. Therefore it would be of interest to contrast the findings here with the response of WDS extracts in non-cancerous cell lines such as the intestinal rat cell line IEC-18 or the human cell line HEK293.

The use of other inflammatory agents will complement the understanding of WDS interactions with the biological systems tested here. For example, TNF α or cytokine dependent stimulation of alternative signalling cascades will be valuable in this regard. Despite our SWATH proteomics data suggested the onset of metabolic disorders on animals supplemented with HFD, it is noted that we anticipated greater physiological differences between HFD and NC animals such as weight gain. Therefore, mice with genetic predisposition to obesity or chemical induced inflammation might be considered as alternative models to HFD supplementation. For instance, genetic deletion of the leptin gene produces different response in the induction of inflammatory signalling mediators as opposed to HFD feed wild type mice [46]. Overall, the selection of other models will expand the knowledge of nutraceuticals applicability in various models of disease.

Interestingly, the effects promoted by WDS *in vivo* differ from the studies published by Wang *et al.* using HFD mice supplemented with sugarcane fibre feed. As determined in those studies, sugarcane fibre reduced body weight gain, reversed the expression of GLP-1 and insulin, and modulated the insulin/AMPK signalling pathway, among other effects in contrast to the control group [119][282]. It is rationalised that the higher levels of incorporation in the sugarcane fibre studies (10% (w/w), as opposed to 5% (w/w) incorporation in this thesis) play a significant role in weight loss not observed in our study. It is also possible that the differences in phytochemical composition intrinsic to each sugarcane crop might be responsible for these variations. In addition, the distinctive signalling pathways regulated in each study (Chapter 4, Section 4.9) might be the result of the diversity regarding the chemical

content of the strains employed. Future experiments should pursue higher WDS addition into the diets in order to test this hypothesis.

The ultimate goal of nutritional research is validation in clinical trials. In this regard, additional elements to consider involving digestion, absorption, and secretion of nutrients complicate the study of nutraceuticals in humans. Nevertheless, the evaluation of nutraceutical's effect on protein markers has been assessed by MS-based proteomics in human studies [286]. The findings reported in this thesis provide the foundation and will inform any future clinical study on the health effects of WDS.

In conclusion, it has been demonstrated WDS has anti-inflammatory properties when tested in *in vitro* and *in vivo* systems. Future experiments may endeavour testing additional models of inflammation in various biological systems. Further, phosphoproteomics analysis in liver tissue from mice supplemented with nutraceuticals may contribute to the proteomics characterisation performed in this work. Validation of WDS as a novel supplement with anti-inflammatory properties provide evidence to support the alternative use of sugarcane.

References

- [1] DeFelice SL. The nutraceutical revolution: its impact on food industry R&D. *Trends Food Sci Technol* 1995;6:59–61. doi:10.1016/S0924-2244(00)88944-X.
- [2] Möller NP, Scholz-Ahrens KE, Roos N, Schrezenmeir J. Bioactive peptides and proteins from foods: Indication for health effects. *Eur J Nutr* 2008;47:171–82. doi:10.1007/s00394-008-0710-2.
- [3] Neveu V, Perez-Jimenez J, Vos F, Crespy V, du Chaffaut L, Mennen L, et al. Phenol-Explorer: an online comprehensive database on polyphenol contents in foods. *Database* 2010;2010:bap024-bap024. doi:10.1093/database/bap024.
- [4] Fu L, Xu BT, Xu XR, Gan RY, Zhang Y, Xia EQ, et al. Antioxidant capacities and total phenolic contents of 62 fruits. *Food Chem* 2011;129:345–50. doi:10.1016/j.foodchem.2011.04.079.
- [5] Zhou Z, Robards K, Helliwell S, Blanchard C. The distribution of phenolic acids in rice. *Food Chem* 2004;87:401–6. doi:10.1016/j.foodchem.2003.12.015.
- [6] Poyrazoğlu E, Gökmen V, Artık N. Organic Acids and Phenolic Compounds in Pomegranates (*Punica granatum* L.) Grown in Turkey. *J Food Compos Anal* 2002;15:567–75. doi:10.1006/jfca.2002.1071.
- [7] Miean KH, Mohamed S. Flavonoid (myricetin, quercetin, kaempferol, luteolin, and apigenin) content of edible tropical plants. *J Agric Food Chem* 2001;49:3106–12. doi:10.1021/jf000892m.
- [8] Atanacković M, Petrović A, Jović S, Bukarica LG, Bursać M, Cvejić J. Influence of winemaking techniques on the resveratrol content, total phenolic content and antioxidant potential of red wines. *Food Chem* 2012;131:513–8. doi:10.1016/j.foodchem.2011.09.015.
- [9] Al-Azzawie HF, Alhamdani MSS. Hypoglycemic and antioxidant effect of oleuropein in alloxan-diabetic rabbits. *Life Sci* 2006;78:1371–7. doi:10.1016/j.lfs.2005.07.029.
- [10] Romier B, Schneider YJ, Larondelle Y, During A. Dietary polyphenols can modulate the intestinal inflammatory response. *Nutr Rev* 2009;67:363–78. doi:10.1111/j.1753-4887.2009.00210.x.
- [11] Bahadoran Z, Mirmiran P, Azizi F. Dietary polyphenols as potential nutraceuticals in management of diabetes: a review. *J Diabetes Metab Disord* 2013;12:43. doi:10.1186/2251-6581-12-43.
- [12] Quiñones M, Miguel M, Aleixandre A. Beneficial effects of polyphenols on cardiovascular disease. *Pharmacol Res* 2013;68:125–31. doi:10.1016/j.phrs.2012.10.018.

- [13] Shidfar F, Heydari I, Hajimiresmaiel SJ, Hosseini S, Shidfar S, Amiri F. The effects of cranberry juice on serum glucose, apoB, apoA-I, Lp(a), and paraoxonase-1 activity in type 2 diabetic male patients. *J Res Med Sci* 2012;17:355–60.
- [14] Chiva-Blanch G, Urpi-Sarda M, Ros E, Valderas-Martinez P, Casas R, Arranz S, et al. Effects of red wine polyphenols and alcohol on glucose metabolism and the lipid profile: A randomized clinical trial. *Clin Nutr* 2013;32:200–6. doi:10.1016/j.clnu.2012.08.022.
- [15] Magrone T, Russo MA, Jirillo E. Cocoa and dark chocolate polyphenols: From biology to clinical applications. *Front Immunol* 2017;8. doi:10.3389/fimmu.2017.00677.
- [16] Amiot MJ, Riva C, Vinet A. Effects of dietary polyphenols on metabolic syndrome features in humans: A systematic review. *Obes Rev* 2016;17:573–86. doi:10.1111/obr.12409.
- [17] Anderson JW, Baird P, Davis RH, Ferreri S, Knudtson M, Koraym A, et al. Health benefits of dietary fiber. *Nutr Rev* 2009;67:188–205. doi:10.1111/j.1753-4887.2009.00189.x.
- [18] McKee LH, Latner TA. Underutilized sources of dietary fiber: A review. *Plant Foods Hum Nutr* 2000;55:285–304. doi:10.1023/A:1008144310986.
- [19] Weickert MO, Pfeiffer AFH. Metabolic effects of dietary fiber consumption and prevention of diabetes. *J Nutr* 2008;138:439–42. doi:10.3390/nu2121266.
- [20] Cario E, Podolsky DK. Differential alteration in intestinal epithelial cell expression of Toll-like receptor 3 (TLR3) and TLR4 in inflammatory bowel disease. *Infect Immun* 2000;68:7010–7. doi:10.1128/IAI.68.12.7010-7017.2000.
- [21] Zaph C, Troy AE, Taylor BC, Berman-Booty LD, Guild KJ, Du Y, et al. Epithelial-cell-intrinsic IKK-beta expression regulates intestinal immune homeostasis. *Nature* 2007;446:552–6. doi:10.1038/nature05590.
- [22] Podolsky DK. The current future understanding of inflammatory bowel disease. *Best Pract Res Clin Gastroenterol* 2002;16:933–43. doi:10.1053/bega.2002.0354.
- [23] Xavier RJ, Podolsky DK. Unravelling the pathogenesis of inflammatory bowel disease. *Nature* 2007;448:427–34. doi:10.1038/nature06005.
- [24] Buettner GR. The Pecking Order of Free Radicals and Antioxidants: Lipid Peroxidation, α -

- Tocopherol, and Ascorbate. *Arch Biochem Biophys* 1993;300:535–43. doi:10.1006/abbi.1993.1074.
- [25] Pellicoro A, Ramachandran P, Iredale JP, Fallowfield JA. Liver fibrosis and repair: immune regulation of wound healing in a solid organ. *Nat Rev Immunol* 2014;14:181–94. doi:10.1038/nri3623.
- [26] Blomhoff R. Dietary antioxidants and cardiovascular disease. *Curr Opin Lipidol* 2005;16:47–54. doi:10.1097/00041433-200502000-00009.
- [27] Scalbert A, Williamson G. Dietary intake and bioavailability of polyphenols. *J Nutr* 2000;130:2073S–85S. doi:10.1089/109662000416311.
- [28] Zamek-Gliszczyński MJ, Hoffmaster KA, Nezasa KI, Tallman MN, Brouwer KLR. Integration of hepatic drug transporters and phase II metabolizing enzymes: Mechanisms of hepatic excretion of sulfate, glucuronide, and glutathione metabolites. *Eur J Pharm Sci* 2006;27:447–86. doi:10.1016/j.ejps.2005.12.007.
- [29] Stadler K, Jenei V, Von Bölcsházy G, Somogyi A, Jakus J. Increased nitric oxide levels as an early sign of premature aging in diabetes. *Free Radic Biol Med* 2003;35:1240–51. doi:10.1016/S0891-5849(03)00499-4.
- [30] Arbones-Mainar JM, Ross K, Rucklidge GJ, Reid M, Duncan G, Arthur JR, et al. Extra virgin olive oils increase hepatic fat accumulation and hepatic antioxidant protein levels in APOE^{-/-} mice. *J Proteome Res* 2007;6:4041–54. doi:10.1021/pr070321a.
- [31] Hayden MS, Ghosh S. Shared principles in NF-kappaB signaling. *Cell* 2008;132:344–62. doi:10.1016/j.cell.2008.01.020.
- [32] Chow JC, Young DW, Golenbock DT, Christ WJ, Gusovsky F. Toll-like receptor-4 mediates lipopolysaccharide-induced signal transduction. *J Biol Chem* 1999;274:10689–92. doi:10.1074/jbc.274.16.10689.
- [33] Schwandner R, Dziarski R, Wesche H, Rothe M, Kirschning CJ. Peptidoglycan- and lipoteichoic acid-induced cell activation is mediated by Toll-like receptor 2. *J Biol Chem* 1999;274:17406–9. doi:10.1074/jbc.274.25.17406.
- [34] Baud V, Karin M. Signal transduction by tumor necrosis factor and its relatives. *Trends Cell Biol* 2001;11:372–7. doi:10.1016/S0962-8924(01)02064-5.

- [35] Ninomiya-Tsuji J, Kishimoto K, Hiyama A, Inoue J, Cao Z, Matsumoto K. The kinase TAK1 can activate the NIK-I κ B as well as the MAP kinase cascade in the IL-1 signalling pathway. *Nature* 1999;398:252–6. doi:10.1038/18465.
- [36] Sakurai H, Chiba H, Miyoshi H, Sugita T, Toriumi W. I κ B kinases phosphorylate NF- κ B p65 subunit on serine 536 in the transactivation domain. *J Biol Chem* 1999;274:30353–6. doi:10.1074/jbc.274.43.30353.
- [37] Mauviel A, Chung KY, Agarwal A, Tamait K, Uitto J. Cell-specific induction of distinct oncogenes of the jun family is responsible for differential regulation of collagenase gene expression by transforming growth factor-beta in fibroblasts and keratinocytes. *J Biol Chem* 1996;271:10917–23.
- [38] Hambleton J, Weinstein SL, Lem L, DeFranco AL. Activation of c-Jun N-terminal kinase in bacterial lipopolysaccharide-stimulated macrophages. *Proc Natl Acad Sci U S A* 1996;93:2774–8. doi:10.1073/pnas.93.7.2774.
- [39] Bamba S, Andoh A, Yasui H, Makino J, Kim S, Fujiyama Y. Regulation of IL-11 expression in intestinal myofibroblasts: role of c-Jun AP-1- and MAPK-dependent pathways. *Am J Physiol Gastrointest Liver Physiol* 2003;285:G529–38. doi:10.1152/ajpgi.00050.2003.
- [40] Minden A, Lin A, Smeal T, Dérjard B, Cobb M, Davis RJ, et al. c-Jun N-terminal phosphorylation correlates with activation of the JNK subgroup but not the ERK subgroup of mitogen-activated protein kinases. *Mol Cell Biol* 1994;14:6683–8. doi:10.1128/MCB.14.10.6683.Updated.
- [41] Wang D, Dubois RN. The role of COX-2 in intestinal inflammation and colorectal cancer. *Oncogene* 2010;29:781–8. doi:10.1038/onc.2009.421.
- [42] Grivennikov S, Karin E, Terzic J, Mucida D, Yu G-Y, Vallabhapurapu S, et al. IL-6 and Stat3 Are Required for Survival of Intestinal Epithelial Cells and Development of Colitis-Associated Cancer. *Cancer Cell* 2009;15:103–13. doi:10.1016/j.ccr.2009.01.001.
- [43] Catlett-Falcone R, Landowski TH, Oshiro MM, Turkson J, Levitzki A, Savino R, et al. Constitutive activation of Stat3 signaling confers resistance to apoptosis in human U266 myeloma cells. *Immunity* 1999;10:105–15. doi:10.1016/s1074-7613(00)80011-4.
- [44] Samavati L, Rastogi R, Du W, Hüttemann M, Fite A, Franchi L. STAT3 tyrosine phosphorylation is

- critical for interleukin 1 beta and interleukin-6 production in response to lipopolysaccharide and live bacteria. vol. 46. 2009. doi:10.1016/j.molimm.2009.02.018.
- [45] He G, Karin M. NF-kappaB and STAT3 - key players in liver inflammation and cancer. *Cell Res* 2011;21:159–68. doi:10.1038/cr.2010.183 [doi].
- [46] Park EJ, Lee JH, Yu GY, He G, Ali SR, Holzer RG, et al. Dietary and Genetic Obesity Promote Liver Inflammation and Tumorigenesis by Enhancing IL-6 and TNF Expression. *Cell* 2010;140:197–208. doi:10.1016/j.cell.2009.12.052.
- [47] Viatour P, Merville M-P, Bours V, Chariot A. Phosphorylation of NF-kappaB and IkappaB proteins: implications in cancer and inflammation. *Trends Biochem Sci* 2005;30:43–52. doi:10.1016/j.tibs.2004.11.009.
- [48] Yu H, Pardoll D, Jove R. STATs in cancer inflammation and immunity: a leading role for STAT3. *Nat Rev Cancer* 2009;9:798–809. doi:10.1038/nrc2734.
- [49] Ibáñez C, Valdés A, García-Cañas V, Simó C, Celebier M, Rocamora-Reverte L, et al. Global Foodomics strategy to investigate the health benefits of dietary constituents. *J Chromatogr A* 2012;1248:139–53. doi:10.1016/j.chroma.2012.06.008.
- [50] Alex P, Gucek M, Li X. Applications of proteomics in the study of inflammatory bowel diseases: Current status and future directions with available technologies. *Inflamm Bowel Dis* 2009;15:616–29. doi:10.1002/ibd.20652.
- [51] Bhattacharyya A, Chattopadhyay R, Mitra S, Crowe SE. Oxidative stress: an essential factor in the pathogenesis of gastrointestinal mucosal diseases. *Physiol Rev* 2014;94:329–54. doi:10.1152/physrev.00040.2012.
- [52] Surai PF and FVI. Antioxidant-Prooxidant Balance in the Intestine : Applications in Chick Placement and Pig Weaning. *J Veter Sci Med* 2015;3:1–16. doi:10.13188/2325-4645.1000011.
- [53] Roebuck KA. Oxidant stress regulation of IL-8 and ICAM-1 gene expression: differential activation and binding of the transcription factors AP-1 and NF-kappaB (Review). *Int J Mol Med* 1999;4:223–30. doi:10.3892/ijmm.4.3.223.
- [54] González-Gallego J, García-Mediavilla MV, Sánchez-Campos S, Tuñón MJ. Fruit polyphenols,

- immunity and inflammation. *Br J Nutr* 2010;104:S15–27. doi:10.1017/S0007114510003910.
- [55] Farzaei MH, Rahimi R, Abdollahi M. The Role of Dietary Polyphenols in the Management of Inflammatory Bowel Disease. *Curr Pharm Biotechnol* 2015;16:196–210. doi:10.2174/1389201016666150118131704.
- [56] Martin DA, Bolling BW. A review of the efficacy of dietary polyphenols in experimental models of inflammatory bowel diseases. *Food Funct* 2015;6:1773–86. doi:10.1039/c5fo00202h.
- [57] Panaro MA, Carofiglio V, Acquafredda A, Cavallo P, Cianciulli A. Anti-inflammatory effects of resveratrol occur via inhibition of lipopolysaccharide-induced NF-kappa B activation in Caco-2 and SW480 human colon cancer cells. *Br J Nutr* 2012;108:1623–32. doi:10.1017/s0007114511007227.
- [58] Wang S, Cao M, Xu S, Zhang J, Wang Z, Mao X, et al. Effect of luteolin on inflammatory responses in RAW264.7 macrophages activated with LPS and IFN- γ . *J Funct Foods* 2017;32:123–30. doi:10.1016/j.jff.2017.02.018.
- [59] Romier B, Van De Walle, Jacqueline During A, Larondelle Y, Schneider Y-J. Modulation of signalling nuclear factor-kB activation pathway by polyphenols in human intestinal Caco-2 cells. *Br J Nutr* 2008;100:542–51. doi:doi:10.1017/S0007114508966666.
- [60] Halliwell B. The antioxidant paradox: Less paradoxical now? *Br J Clin Pharmacol* 2013;75:637–44. doi:10.1111/j.1365-2125.2012.04272.x.
- [61] Nunes C, Ferreira E, Freitas V, Almeida L, Barbosa RM, Laranjinha J. Intestinal anti-inflammatory activity of red wine extract: unveiling the mechanisms in colonic epithelial cells. *Food Funct* 2013;4:373–83. doi:10.1039/c2fo30233k.
- [62] Li R, Kim M-H, Sandhu AK, Gao C, Gu L. Muscadine Grape (*Vitis rotundifolia*) or Wine Phytochemicals Reduce Intestinal Inflammation in Mice with Dextran Sulfate Sodium-Induced Colitis. *J Agric Food Chem* 2017;4:769–76. doi:10.1021/acs.jafc.6b03806.
- [63] Kim JS, Narula AS, Jobin C. *Salvia miltiorrhiza* water-soluble extract, but not its constituent salvianolic acid B, abrogates LPS-induced NF-kB signalling in intestinal epithelial cells. *Clin Exp Immunol* 2005;141:288–97. doi:10.1111/j.1365-2249.2005.02844.x.
- [64] Seymour EM, Lewis SK, Urcuyo-Llanes DE, Tanone II, Kirakosyan A, Kaufman PB, et al. Regular

- tart cherry intake alters abdominal adiposity, adipose gene transcription, and inflammation in obesity-prone rats fed a high fat diet. *J Med Food* 2009;12:935–42. doi:10.1089/jmf.2008.0270.
- [65] Jung M, Triebel S, Anke T, Richling E, Erkel G. Influence of apple polyphenols on inflammatory gene expression. *Mol Nutr Food Res* 2009;53:1263–80. doi:10.1002/mnfr.200800575.
- [66] Yoshioka Y, Akiyama H, Nakano M, Shoji T, Kanda T, Ohtake Y, et al. Orally administered apple procyanidins protect against experimental inflammatory bowel disease in mice. *Int Immunopharmacol* 2008;8:1802–7. doi:10.1016/j.intimp.2008.08.021.
- [67] Denis MC, Furtos A, Dudonné S, Montoudis A, Garofalo C, Desjardins Y, et al. Apple Peel Polyphenols and Their Beneficial Actions on Oxidative Stress and Inflammation. *PLoS One* 2013;8. doi:10.1371/journal.pone.0053725.
- [68] Skyberg JA, Robison A, Golden S, Rollins MF, Callis G, Huarte E, et al. Apple polyphenols require T cells to ameliorate dextran sulfate sodium-induced colitis and dampen proinflammatory cytokine expression. *J Leukoc Biol* 2011;90:1043–54. doi:10.1189/jlb.0311168.
- [69] D'Argenio G, Mazzone G, Tuccillo C, Ribecco MT, Graziani G, Gravina AG, et al. Apple polyphenols extract (APE) improves colon damage in a rat model of colitis. *Dig Liver Dis* 2012;44:555–62. doi:10.1016/j.dld.2012.01.009.
- [70] Triebel S, Trieu HL, Richling E. Modulation of inflammatory gene expression by a bilberry (*Vaccinium myrtillus* L.) extract and single anthocyanins considering their limited stability under cell culture conditions. *J. Agric. Food Chem.*, vol. 60, 2012, p. 8902–10. doi:10.1021/jf3028842.
- [71] Piberger H, Oehme A, Hofmann C, Dreiseitel A, Sand PG, Obermeier F, et al. Bilberries and their anthocyanins ameliorate experimental colitis. *Mol Nutr Food Res* 2011;55:1724–9. doi:10.1002/mnfr.201100380.
- [72] Serra D, Paixão J, Nunes C, Dinis TCP, Almeida LM. Cyanidin-3-Glucoside Suppresses Cytokine-Induced Inflammatory Response in Human Intestinal Cells: Comparison with 5-Aminosalicylic Acid. *PLoS One* 2013;8. doi:10.1371/journal.pone.0073001.
- [73] Camacho-Barquero L, Villegas I, Sánchez-Calvo JM, Talero E, Sánchez-Fidalgo S, Motilva V, et al. Curcumin, a *Curcuma longa* constituent, acts on MAPK p38 pathway modulating COX-2 and iNOS

expression in chronic experimental colitis. *Int Immunopharmacol* 2007;7:333–42.

doi:10.1016/j.intimp.2006.11.006.

- [74] Ung VYL, Foshaug RR, MacFarlane SM, Churchill TA, Doyle JSG, Sydora BC, et al. Oral administration of curcumin emulsified in carboxymethyl cellulose has a potent anti-inflammatory effect in the IL-10 gene-deficient mouse model of IBD. *Dig Dis Sci* 2010;55:1272–7.
doi:10.1007/s10620-009-0843-z.
- [75] Salh B, Assi K, Templeman V, Parhar K, Owen D, Gómez-Muñoz A, et al. Curcumin attenuates DNB-induced murine colitis. *Am J Physiol - Gastrointest Liver Physiol* 2003;285:G235–43.
doi:10.1152/ajpgi.00449.2002.
- [76] Yang F, Oz HS, Barve S, de Villiers WJ, McClain CJ, Varilek GW. The green tea polyphenol (-)-epigallocatechin-3-gallate blocks nuclear factor-kappa B activation by inhibiting I kappa B kinase activity in the intestinal epithelial cell line IEC-6. *Mol Pharmacol* 2001;60:528–33.
- [77] Varilek GW, Yang F, Lee EY, deVilliers WJ, Zhong J, Oz HS, et al. Green tea polyphenol extract attenuates inflammation in interleukin-2-deficient mice, a model of autoimmunity. *J Nutr* 2001;131:2034–9.
- [78] Lin YL, Lin JK. (-)-Epigallocatechin-3-gallate blocks the induction of nitric oxide synthase by down-regulating lipopolysaccharide-induced activity of transcription factor nuclear factor-kappaB. *Mol Pharmacol* 1997;52:465–72.
- [79] Dou W, Zhang J, Sun A, Zhang E, Ding L, Mukherjee S, et al. Protective effect of naringenin against experimental colitis via suppression of Toll-like receptor 4/NF-κB signalling. *Br J Nutr* 2013;110:599–608. doi:10.1017/S0007114512005594.
- [80] Manna C, Galletti P, Cucciolla V, Molledo O, Leone a, Zappia V. The protective effect of the olive oil polyphenol (3,4-dihydroxyphenyl)-ethanol counteracts reactive oxygen metabolite-induced cytotoxicity in Caco-2 cells. *J Nutr* 1997;127:286–92.
- [81] Sánchez-Fidalgo S, Cárdeno A, Sánchez-Hidalgo M, Aparicio-Soto M, De la Lastra CA. Dietary extra virgin olive oil polyphenols supplementation modulates DSS-induced chronic colitis in mice. *J Nutr Biochem* 2013;24:1401–13. doi:10.1016/j.jnutbio.2012.11.008.

- [82] Larrosa M, González-Sarriás A, Yáñez-Gascón MJ, Selma M V., Azorín-Ortuño M, Toti S, et al. Anti-inflammatory properties of a pomegranate extract and its metabolite urolithin-A in a colitis rat model and the effect of colon inflammation on phenolic metabolism. *J Nutr Biochem* 2010;21:717–25. doi:10.1016/j.jnutbio.2009.04.012.
- [83] Singh K, Jaggi AS, Singh N. Exploring the ameliorative potential of *Punica granatum* in dextran sulfate sodium induced ulcerative colitis in mice. *Phyther Res* 2009;23:1565–74. doi:10.1002/ptr.2822.
- [84] Rosillo MA, Sánchez-Hidalgo M, Cárdeno A, Aparicio-Soto M, Sánchez-Fidalgo S, Villegas I, et al. Dietary supplementation of an ellagic acid-enriched pomegranate extract attenuates chronic colonic inflammation in rats. *Pharmacol Res* 2012;66:235–42. doi:10.1016/j.phrs.2012.05.006.
- [85] Sánchez De Medina F, Vera B, Gálvez J, Zarzuelo A. Effect of quercitrin on the early stages of hapten induced colonic inflammation in the rat. *Life Sci* 2002;70:3097–108. doi:10.1016/S0024-3205(02)01568-0.
- [86] Comalada M, Camuesco D, Sierra S, Ballester I, Xaus J, Galvez J, et al. In vivo quercitrin anti-inflammatory effect involves release of quercetin, which inhibits inflammation through down-regulation of the NF-kB pathway. *Eur J Immunol* 2005;35:584–92. doi:10.1002/eji.200425778.
- [87] Kwon KH, Murakami A, Tanaka T, Ohigashi H. Dietary rutin, but not its aglycone quercetin, ameliorates dextran sulfate sodium-induced experimental colitis in mice: Attenuation of pro-inflammatory gene expression. *Biochem Pharmacol* 2005;69:395–406. doi:10.1016/j.bcp.2004.10.015.
- [88] Guazelli CFS, Fattori V, Colombo BB, Georgetti SR, Vicentini FTMC, Casagrande R, et al. Quercetin-loaded microcapsules ameliorate experimental colitis in mice by anti-inflammatory and antioxidant mechanisms. *J Nat Prod* 2013;76:200–8. doi:10.1021/np300670w.
- [89] Kim YH, Kwon HS, Kim DH, Cho HJ, Lee HS, Jun JG, et al. Piceatannol, a stilbene present in grapes, attenuates dextran sulfate sodium-induced colitis. *Int Immunopharmacol* 2008;8:1695–702. doi:10.1016/j.intimp.2008.08.003.
- [90] Sánchez-Fidalgo S, Cárdeno A, Villegas I, Talero E, de la Lastra CA. Dietary supplementation of resveratrol attenuates chronic colonic inflammation in mice. *Eur J Pharmacol* 2010;633:78–84. doi:10.1016/j.ejphar.2010.01.025.

- [91] Singh UP, Singh NP, Singh B, Hofseth LJ, Price RL, Nagarkatti M, et al. Resveratrol (trans-3,5,4'-trihydroxystilbene) induces silent mating type information regulation-1 and down-regulates nuclear transcription factor-kappaB activation to abrogate dextran sulfate sodium-induced colitis. *J Pharmacol Exp Ther* 2010;332:829–39. doi:10.1124/jpet.109.160838.
- [92] Ovaskainen M-L, Törrönen R, Koponen JM, Sinkko H, Hellström J, Reinivuo H, et al. Dietary intake and major food sources of polyphenols in Finnish adults. *J Nutr* 2008;138:562–6.
- [93] Bermúdez-Soto MJ, Tomás-Barberán FA, García-Conesa MT. Stability of polyphenols in chokeberry (*Aronia melanocarpa*) subjected to in vitro gastric and pancreatic digestion. *Food Chem* 2007;102:865–74. doi:10.1016/j.foodchem.2006.06.025.
- [94] Bravo L. Polyphenols: Chemistry, Dietary Sources, Metabolism, and Nutritional Significance. *Nutr Rev* 2009;56:317–33. doi:10.1111/j.1753-4887.1998.tb01670.x.
- [95] Donovan JL, Manach C, Faulks RM, Kroon PA. Absorption and metabolism of dietary secondary metabolites. *Plant Second. Metab. Occur. Struct. Role Hum. Diet*, 2006, p. 303–51.
- [96] Lambert JD, Sang S, Yang CS. Biotransformation of green tea polyphenols and the biological activities of those metabolites. *Mol Pharm* 2007;4:819–25. doi:10.1021/mp700075m.
- [97] Ishimoto H, Tai A, Yoshimura M, Amakura Y, Yoshida T, Hatano T, et al. Antioxidative Properties of Functional Polyphenols and Their Metabolites Assessed by an ORAC Assay. *Biosci Biotechnol Biochem* 2012;76:395–9. doi:10.1271/bbb.110717.
- [98] Wiczkowski W, Szawara-Nowak D, Topolska J, Olejarz K, Zielinski H, Piskula MK. Metabolites of dietary quercetin: Profile, isolation, identification, and antioxidant capacity. *J Funct Foods* 2014;11:121–9. doi:10.1016/j.jff.2014.09.013.
- [99] Déprez S, Brezillon C, Rabot S, Philippe C, Mila I, Lapierre C, et al. Polymeric proanthocyanidins are catabolized by human colonic microflora into low-molecular-weight phenolic acids. *J Nutr* 2000;130:2733–8.
- [100] Tirosh O, Levy E, Reifen R. High selenium diet protects against TNBS-induced acute inflammation, mitochondrial dysfunction, and secondary necrosis in rat colon. *Nutrition* 2007;23:878–86. doi:10.1016/j.nut.2007.08.019.

- [101] Kaur HD, Bansal MP. Studies on HDL associated enzymes under experimental hypercholesterolemia: possible modulation on selenium supplementation. *Lipids Health Dis* 2009;8:55. doi:10.1186/1476-511X-8-55.
- [102] Papp LV, Lu J, Holmgren A, Khanna KK. From selenium to selenoproteins: synthesis, identity, and their role in human health. *Antioxid Redox Signal* 2007;9:775–806. doi:10.1089/ars.2007.1528.
- [103] Esworthy RS, Yang L, Frankel PH, Chu F-F. Epithelium-Specific Glutathione Peroxidase, Gpx2, Is Involved in the Prevention of Intestinal Inflammation in Selenium-Deficient Mice. *J Nutr* 2005;135:740–5.
- [104] Tamaki H, Nakamura H, Nishio A, Nakase H, Ueno S, Uza N, et al. Human Thioredoxin-1 Ameliorates Experimental Murine Colitis in Association With Suppressed Macrophage Inhibitory Factor Production. *Gastroenterology* 2006;131:1110–21. doi:10.1053/j.gastro.2006.08.023.
- [105] Novoselov S V., Kryukov G V., Xu XM, Carlson BA, Hatfield DL, Gladyshev VN. Selenoprotein H is a nucleolar thioredoxin-like protein with a unique expression pattern. *J Biol Chem* 2007;282:11960–8. doi:10.1074/jbc.M701605200.
- [106] Kasaikina M V., Fomenko DE, Labunskyy VM, Lachke SA, Qiu W, Moncaster JA, et al. Roles of the 15-kDa selenoprotein (Sep15) in redox homeostasis and cataract development revealed by the analysis of Sep 15 knockout mice. *J Biol Chem* 2011;286:33203–12. doi:10.1074/jbc.M111.259218.
- [107] Suzuki M, Hisamatsu T, Podolsky DK. Gamma interferon augments the intracellular pathway for lipopolysaccharide (LPS) recognition in human intestinal epithelial cells through coordinated up-regulation of LPS uptake and expression of the intracellular Toll-like receptor 4-MD-2 complex. *Infect Immun* 2003;71:3503–11. doi:10.1128/IAI.71.6.3503-3511.2003.
- [108] Leibovitz A, Stinson JC, Iii WBM, Leibovltz A, Stlnson JC, Mccombs WB, et al. Classification of Human Colorectal Adenocarcinoma Cell Lines Classification of Human Colorectal Adenocarcinoma Cell Lines. *Cancer Res* 1976;36:4562–9.
- [109] Ikehara N, Semba S, Sakashita M, Aoyama N, Kasuga M, Yokozaki H. BRAF mutation associated with dysregulation of apoptosis in human colorectal neoplasms. *Int J Cancer* 2005;115:943–50. doi:10.1002/ijc.20957.

- [110] Haapajarvi T, Kivinen L, Pitkanen K, Laiho M. Cell cycle dependent effects of uv radiation on p53 expression and retinoblastoma protein phosphorylation. *Oncogene* 1995;11:151–9.
- [111] Németh K, Plumb GW, Berrin JG, Juge N, Jacob R, Naim HY, et al. Deglycosylation by small intestinal epithelial cell β -glucosidases is a critical step in the absorption and metabolism of dietary flavonoid glycosides in humans. *Eur J Nutr* 2003;42:29–42. doi:10.1007/s00394-003-0397-3.
- [112] Wellen KE, Hotamisligil GS. Inflammation, stress, and diabetes. *J Clin Invest* 2005;115:1111–9. doi:10.1172/JCI200525102.
- [113] Matsuzawa-Nagata N, Takamura T, Ando H, Nakamura S, Kurita S, Misu H, et al. Increased oxidative stress precedes the onset of high-fat diet-induced insulin resistance and obesity. *Metabolism* 2008;57:1071–7. doi:S0026-0495(08)00114-5 [pii]r10.1016/j.metabol.2008.03.010.
- [114] Carmiel-Haggai M, Cederbaum AI, Nieto N. A high-fat diet leads to the progression of non-alcoholic fatty liver disease in obese rats. *FASEB J* 2005;19:136–8. doi:10.1096/fj.04-2291fje.
- [115] Larsson H, Holst JJ, Ahrén B. Glucagon-like peptide-1 reduces hepatic glucose production indirectly through insulin and glucagon in humans. *Acta Physiol Scand* 1997;160:413–22. doi:10.1046/j.1365-201X.1997.00161.x.
- [116] Collins S, Martin TL, Surwit RS, Robidoux J. Genetic vulnerability to diet-induced obesity in the C57BL/6J mouse: physiological and molecular characteristics. *Physiol Behav* 2004;81:243–8. doi:10.1016/j.physbeh.2004.02.006.
- [117] Bose M, Lambert JD, Ju J, Reuhl KR, Shapses SA, Yang CS. The major green tea polyphenol, (-)-epigallocatechin-3-gallate, inhibits obesity, metabolic syndrome, and fatty liver disease in high-fat-fed mice. *J Nutr* 2008;138:1677–83. doi:10.1016/j.bbi.2008.05.010.
- [118] Neyrinck AM, Van Hée VF, Bindels LB, De Backer F, Cani PD, Delzenne NM. Polyphenol-rich extract of pomegranate peel alleviates tissue inflammation and hypercholesterolaemia in high-fat diet-induced obese mice: potential implication of the gut microbiota. *Br J Nutr* 2013;109:802–9. doi:10.1017/S0007114512002206.
- [119] Wang ZQ, Zuberi AR, Zhang XH, Macgowan J, Qin J, Ye X, et al. Effects of dietary fibers on weight gain, carbohydrate metabolism, and gastric ghrelin gene expression in mice fed a high-fat diet.

- Metabolism 2007;56:1635–42. doi:10.1016/j.metabol.2007.07.004.
- [120] Si X, Strappe P, Blanchard C, Zhou Z. Enhanced anti-obesity effects of complex of resistant starch and chitosan in high fat diet fed rats. *Carbohydr Polym* 2017;157:834–41. doi:10.1016/j.carbpol.2016.10.042.
- [121] D'Hont A, Paulet F, Glaszmann JC. Oligoclonal interspecific origin of “North Indian” and “Chinese” sugarcane. *Chromosom Res* 2002;10:253–62. doi:10.1023/A:1015204424287.
- [122] ASMC. Australian Sugar Milling Council. Brisbane, Australia: 2016.
- [123] Goldemberg J, Coelho ST, Guardabassi P. The sustainability of ethanol production from sugarcane. *Energy Policy* 2008;36:2086–97. doi:10.1016/j.enpol.2008.02.028.
- [124] Ou SY, Luo YL, Huang CH, Jackson M. Production of coumaric acid from sugarcane bagasse. *Innov Food Sci Emerg Technol* 2009;10:253–9. doi:10.1016/j.ifset.2008.10.008.
- [125] Rahmatullah M, Ferdousi D, Mollik MAH, Jahan R, Chowdhury MH, Haque WM. A survey of medicinal plants used by Kavirajes of Chalna area, Khulna district, Bangladesh. *African J Tradit Complement Altern Med* 2010;7:91–7. doi:10.4314/ajtcam.v7i2.50859.
- [126] Tag H, Kalita P, Dwivedi P, Das A, Namsa N. Herbal medicines used in the treatment of diabetes mellitus in Arunachal Himalaya, northeast, India. *J Ethnopharmacol* 2012;141:786–95.
- [127] Varier vaidhyarathnam PS. Indian Medicinal plants a compendium of 500 species. *Indian Med. plants a Compend. 500 species*, 1996, p. 357.
- [128] Balick MJ, Kronenberg F, Ososki AL, Reiff M, Fugh-Berman A, Bonnie O, et al. Medicinal plants used by latino healers for women’s health conditions in New York City. *Econ Bot* 2000;54:344–57. doi:10.1007/BF02864786.
- [129] Feng S, Luo Z, Zhang Y, Zhong Z, Lu B. Phytochemical contents and antioxidant capacities of different parts of two sugarcane (*Saccharum officinarum* L.) cultivars. *Food Chem* 2014;151:452–8. doi:10.1016/j.foodchem.2013.11.057.
- [130] Kadam US, Ghosh SB, De S, Suprasanna P, Devasagayam TPA, Bapat VA. Antioxidant activity in sugarcane juice and its protective role against radiation induced DNA damage. *Food Chem* 2008;106:1154–60. doi:10.1016/j.foodchem.2007.07.066.

- [131] Abbas SR, Sabir SM, Ahmad SD, Boligon AA, Athayde ML. Phenolic profile, antioxidant potential and DNA damage protecting activity of sugarcane (*Saccharum officinarum*). *Food Chem* 2014;147:10–6. doi:10.1016/j.foodchem.2013.09.113.
- [132] Payet B, Sing ASC, Smadja J. Assessment of antioxidant activity of cane brown sugars by ABTS and DPPH radical scavenging assays: Determination of their polyphenolic and volatile constituents. *J Agric Food Chem* 2005;53:10074–9. doi:10.1021/jf0517703.
- [133] Takara K, Otsuka K, Wada K, Iwasaki H, Yamashita M. 1,1-diphenyl-2-picrylhydrazyl radical scavenging activity and tyrosinase inhibitory effects of constituents of sugarcane molasses. *Biosci Biotechnol Biochem* 2007;71:183–91. doi:10.1271/bbb.60432.
- [134] Ledón N, Casacó A, Rodriguez V, Cruz J, Gonzalez R, Tolon Z, et al. Anti-inflammatory and analgesic effects of a mixture of fatty acids isolated and purified from sugar cane wax oil. *Planta Med* 2003;69:367–9. doi:10.1055/s-2003-38880.
- [135] Vhuiyan MMI, Biva IJ, Saha MR, Islam MS. Anti-diarrhoeal and CNS Depressant Activity of Methanolic Extract of *Saccharum spontaneum* Linn. *Stamford J Pharm Sci* 2008;1:63–8.
- [136] Romier-Crouzet B, Walle J van de, During A, Joly A, Rousseau C, Henry O, et al. Inhibition of inflammatory mediators by polyphenolic plant extracts in human intestinal Caco-2 cells. *Food Chem Toxicol* 2009;47:1221–30. doi:10.1016/j.fct.2009.02.015.
- [137] Yamashita S, Yamashita K, Yasuda H, Ogata E. High-fiber diet in the control of diabetes in rats. *Endocrinol Jpn* 1980;27:169–73. doi:10.1507/endocrj1954.27.169.
- [138] Cooney JM, Barnett MPG, Dommels YEM, Brewster D, Butts CA, McNabb WC, et al. A combined omics approach to evaluate the effects of dietary curcumin on colon inflammation in the *Mdr1a*^{-/-} mouse model of inflammatory bowel disease. *J Nutr Biochem* 2016;27. doi:10.1016/j.jnutbio.2015.08.030.
- [139] Kussman M, Panchaud A, Affolter M. Proteomics in Nutrition: Status Quo and Outlook for Biomarkers and Bioactives. *J Proteome Res* 2010;9:4876–87. doi:10.1021/pr1004339.
- [140] Andrews GL, Simons BL, Young JB, Hawkridge AM, Muddiman DC. Performance Characteristics of a New Hybrid Triple Quadrupole Time-of-Flight Tandem Mass Spectrometer. *Anal Chem*

- 2011;83:5442–6. doi:10.1021/ac200812d.
- [141] Kapp E, Schütz F. Overview of tandem mass spectrometry (MS/MS) database search algorithms. *Curr Protoc Protein Sci* 2007;Chapter 25:Unit25.2. doi:10.1002/0471140864.ps2502s49.
- [142] Liu H, Sadygov RG, Yates JR. A Model for Random Sampling and Estimation of Relative Protein Abundance in Shotgun Proteomics. *Anal Chem* 2004;76:4193–201. doi:10.1021/ac0498563.
- [143] Wu JX, Song X, Pascovici D, Zaw T, Care N, Krisp C, et al. SWATH Mass Spectrometry Performance Using Extended Peptide MS/MS Assay Libraries. *Mol Cell Proteomics* 2016;15:2501–14. doi:10.1074/MCP.M115.055558.
- [144] Gillet LC, Navarro P, Tate S, Rost H, Selevsek N, Reiter L, et al. Targeted Data Extraction of the MS/MS Spectra Generated by Data-independent Acquisition: A New Concept for Consistent and Accurate Proteome Analysis. *Mol Cell Proteomics* 2012;11:O111.016717-O111.016717. doi:10.1074/mcp.O111.016717.
- [145] Bourassa S, Fournier F, Nehmé B, Kelly I, Tremblay A, Lemelin V, et al. Evaluation of iTRAQ and SWATH-MS for the quantification of proteins associated with insulin resistance in human duodenal biopsy samples. *PLoS One* 2015;10. doi:10.1371/journal.pone.0125934.
- [146] de Roos B, McArdle HJ. Proteomics as a tool for the modelling of biological processes and biomarker development in nutrition research. *Br J Nutr* 2008;99 Suppl 3:S66-71. doi:10.1017/S0007114508006909.
- [147] Barnett MPG, Cooney JM, Dommels YEM, Nones K, Brewster DT, Park Z, et al. Modulation of colonic inflammation in *Mdr1a*^{-/-} mice by green tea polyphenols and their effects on the colon transcriptome and proteome. *J Nutr Biochem* 2013;24:1678–90. doi:10.1016/j.jnutbio.2013.02.007.
- [148] Jiang X, Zeng T, Zhang S, Zhang Y. Comparative Proteomic and Bioinformatic Analysis of the Effects of a High-Grain Diet on the Hepatic Metabolism in Lactating Dairy Goats. *PLoS One* 2013;8:e80698. doi:10.1371/journal.pone.0080698.
- [149] Zhu Y, Wang C, Wang X, Li B, Li F. Effect of dietary fiber/starch balance on the cecal proteome of growing rabbits. *J Proteomics* 2014;103:23–34. doi:10.1016/j.jprot.2014.03.019.
- [150] Huang C-Y, Chen W-M, Tsay Y-G, Hsieh S-C, Lin Y, Lee W-J, et al. Differential regulation of

- protein expression in response to polyunsaturated fatty acids in the liver of apoE-knockout mice and in HepG2 cells. *J Biomed Sci* 2015;22:1–14. doi:10.1186/s12929-015-0118-2.
- [151] Beattie JH, Nicol F, Gordon M-J, Reid MD, Cantlay L, Horgan GW, et al. Ginger phytochemicals mitigate the obesogenic effects of a high-fat diet in mice: A proteomic and biomarker network analysis. *Mol Nutr Food Res* 2011;55:S203–13. doi:10.1002/mnfr.201100193.
- [152] Joo JI, Kim DH, Choi J-W, Yun JW. Proteomic analysis for antiobesity potential of capsaicin on white adipose tissue in rats fed with a high fat diet. *J Proteome Res* 2010;9:2977–87. doi:10.1021/pr901175w.
- [153] Baiges I, Palmfeldt J, Bladé C, Gregersen N, Arola L. Lipogenesis is decreased by grape seed proanthocyanidins according to liver proteomics of rats fed a high fat diet. *Mol Cell Proteomics* 2010;9:1499–513. doi:10.1074/mcp.M000055-MCP201.
- [154] Hunter T. Signaling--2000 and beyond. *Cell* 2000;100:113–27. doi:10.1016/j.surg.2006.06.009.
- [155] Ehrentauf SF, Colgan SP. Implications of protein post-translational modifications in IBD. *Inflamm Bowel Dis* 2012;18:1378–88. doi:10.1002/ibd.22859.
- [156] Eyrich B, Sickmann A, Zahedi RP. Catch me if you can: Mass spectrometry-based phosphoproteomics and quantification strategies. *Proteomics* 2011;11:554–70. doi:10.1002/pmic.201000489.
- [157] Ong SE, Mann M. Stable isotope labeling by amino acids in cell culture for quantitative proteomics. *Methods Mol Biol* 2007;359:37–52. doi:10.1007/978-1-59745-255-7_3.
- [158] Alayev A, Doubleday PF, Berger SM, Ballif BA, Holz MK. Phosphoproteomics reveals resveratrol-dependent inhibition of Akt/mTORC1/S6K1 signaling. *J Proteome Res* 2014;13:5734–42. doi:10.1021/pr500714a.
- [159] Yan GR, Yin XF, Xiao C Le, Tan ZL, Xu SH, He QY. Identification of novel signaling components in genistein-regulated signaling pathways by quantitative phosphoproteomics. *J Proteomics* 2011;75:695–707. doi:10.1016/j.jprot.2011.09.008.
- [160] Mueller LN, Brusniak M-Y, Mani DR, Aebersold R. An assessment of software solutions for the analysis of mass spectrometry based quantitative proteomics data. *J Proteome Res* 2008;7:51–61. doi:10.1021/pr700758r.

- [161] Parker R, Vella LJ, Xavier D, Amirkhani A, Parker J, Cebon J, et al. Phosphoproteomic Analysis of Cell-Based Resistance to BRAF Inhibitor Therapy in Melanoma. *Front Oncol* 2015;5:95. doi:10.3389/fonc.2015.00095.
- [162] Kenyon GL, DeMarini DM, Fuchs E, Galas DJ, Kirsch JF, Leyh TS, et al. Defining the mandate of proteomics in the post-genomics era: workshop report. vol. 1. 2002.
- [163] Vignali DAA. Multiplexed particle-based flow cytometric assays. *J Immunol Methods* 2000;243:243–55.
- [164] Stewart LK, Soileau JL, Ribnicky D, Wang ZQ, Raskin I, Poulev A, et al. Quercetin transiently increases energy expenditure but persistently decreases circulating markers of inflammation in C57BL/6J mice fed a high-fat diet. *Metabolism* 2008;57. doi:10.1016/j.metabol.2008.03.003.
- [165] Wu S, Yano S, Hisanaga A, He X, He J, Sakao K, et al. Polyphenols from *Lonicera caerulea* L. berry attenuate experimental nonalcoholic steatohepatitis by inhibiting proinflammatory cytokines productions and lipid peroxidation. *Mol Nutr Food Res* 2017;61:1600858. doi:10.1002/mnfr.201600858.
- [166] Duarte-Almeida JM., Salatino A., Genovese MI., Lajolo FM. Phenolic composition and antioxidant activity of culms and sugarcane (*Saccharum officinarum* L.) products. *Food Chem* 2011;125:660–4. doi:10.1016/j.foodchem.2010.09.059.
- [167] Galisteo M, Duarte J, Zarzuelo A. Effects of dietary fibers on disturbances clustered in the metabolic syndrome. *J Nutr Biochem* 2008;19:71–84. doi:10.1016/j.jnutbio.2007.02.009.
- [168] Bahadoran Z, Mirmiran P, Azizi F. Dietary polyphenols as potential nutraceuticals in management of diabetes: a review. *J Diabetes Metab Disord* 2013;12:43. doi:10.1186/2251-6581-12-43.
- [169] Bishayee A. Cancer prevention and treatment with resveratrol: from rodent studies to clinical trials. *Cancer Prev Res (Phila)* 2009;2:409–18. doi:10.1158/1940-6207.CAPR-08-0160.
- [170] Yang F, Tang E, Guan K, Wang C-Y. IKK beta plays an essential role in the phosphorylation of RelA/p65 on serine 536 induced by lipopolysaccharide. *J Immunol* 2003;170:5630–5. doi:10.4049/jimmunol.170.11.5630.
- [171] Wu Z, Pan D, Guo Y, Zeng X. N-acetylmuramic acid triggers anti-inflammatory capacity in LPS-

- induced RAW 264.7 cells and mice. *J Funct Foods* 2015;13:108–16. doi:10.1016/j.jff.2014.12.048.
- [172] Singleton VL, Rossi Jr. JA, Rossi J A Jr. Colorimetry of Total Phenolics with Phosphomolybdic-Phosphotungstic Acid Reagents. *Am J Enol Vitic* 1965;16:144–58. doi:10.12691/ijebb-2-1-5.
- [173] Zhishen J, Mengcheng T, Jianming W. The determination of flavonoid contents in mulberry and their scavenging effects on superoxide radicals. *Food Chem* 1999;64:555–9. doi:10.1016/S0308-8146(98)00102-2.
- [174] Schubert OT, Gillet LC, Collins BC, Navarro P, Rosenberger G, Wolski WE, et al. Building high-quality assay libraries for targeted analysis of SWATH MS data. *Nat Protoc* 2015;10:426–41. doi:10.1038/nprot.2015.015.
- [175] Lambert JP, Ivosev G, Couzens AL, Larsen B, Taipale M, Lin ZY, et al. Mapping differential interactomes by affinity purification coupled with data-independent mass spectrometry acquisition. *Nat Methods* 2013;10:1239–45. doi:10.1038/nmeth.2702.
- [176] Meng J, Fang Y, Zhang A, Chen S, Xu T, Ren Z, et al. Phenolic content and antioxidant capacity of Chinese raisins produced in Xinjiang Province. *Food Res Int* 2011;44:2830–6. doi:10.1016/j.foodres.2011.06.032.
- [177] Mullen W, Marks SC, Crozier A. Evaluation of Phenolic Compounds in Commercial Fruit Juices and Fruit Drinks. *J Agric Food Chem* 2007;55:3148–57. doi:10.1021/jf062970x.
- [178] Balasundram N, Sundram K, Samman S. Phenolic compounds in plants and agri-industrial by-products: Antioxidant activity, occurrence, and potential uses. *Food Chem* 2006;99:191–203. doi:10.1016/j.foodchem.2005.07.042.
- [179] Marinova D, Ribarova F, Atanassova M. Total phenolics and total flavonoids in bulgarian fruits and vegetables. *J Univ Chem Technol Metall* 2005;40:255–60.
- [180] Krämer A, Green J, Pollard J, Tugendreich S. Causal analysis approaches in Ingenuity Pathway Analysis. *Bioinformatics* 2014;30:523–30. doi:10.1093/bioinformatics/btt703.
- [181] Kundu JK, Shin YK, Kim SH, Surh Y-J. Resveratrol inhibits phorbol ester-induced expression of COX-2 and activation of NF-kappaB in mouse skin by blocking IkappaB kinase activity. *Carcinogenesis* 2006;27:1465–74. doi:10.1093/carcin/bgi349.

- [182] García-Lafuente A, Guillamón E, Villares A, Rostagno MA, Martínez JA. Flavonoids as anti-inflammatory agents: Implications in cancer and cardiovascular disease. *Inflamm Res* 2009;58:537–52. doi:10.1007/s00011-009-0037-3.
- [183] Chen X, Thibeault S. Effect of DMSO concentration, cell density and needle gauge on the viability of cryopreserved cells in three dimensional hyaluronan hydrogel. *Conf Proc . Annu Int Conf IEEE Eng Med Biol Soc IEEE Eng Med Biol Soc Annu Conf* 2013;2013:6228–31. doi:10.1109/EMBC.2013.6610976.
- [184] Panee J, Stoytcheva ZR, Liu W, Berry MJ. Selenoprotein H is a redox-sensing high mobility group family DNA-binding protein that up-regulates genes involved in glutathione synthesis and phase II detoxification. *J Biol Chem* 2007;282:23759–65. doi:10.1074/jbc.M702267200.
- [185] Cox AG, Tsomides A, Kim AJ, Saunders D, Hwang KL, Evason KJ, et al. Selenoprotein H is an essential regulator of redox homeostasis that cooperates with p53 in development and tumorigenesis. *Proc Natl Acad Sci U S A* 2016;113:E5562–71. doi:10.1073/pnas.1600204113.
- [186] Formosa LE, Mimaki M, Frazier AE, McKenzie M, Stait TL, Thorburn DR, et al. Characterization of mitochondrial FOXRED1 in the assembly of respiratory chain complex I. *Hum Mol Genet* 2015;24:2952–65. doi:10.1093/hmg/ddv058.
- [187] Sharma LK, Fang H, Liu J, Vartak R, Deng J, Bai Y. Mitochondrial respiratory complex I dysfunction promotes tumorigenesis through ROS alteration and AKT activation. *Hum Mol Genet* 2011;20:4605–16. doi:10.1093/hmg/ddr395.
- [188] Huang GTJ, Eckmann L, Savidge TC, Kagnoff MF. Infection of human intestinal epithelial cells with invasive bacteria upregulates apical intercellular adhesion molecule-1 (ICAM-1) expression and neutrophil adhesion. *J Clin Invest* 1996;98:572–83. doi:10.1172/JCI118825.
- [189] Zhang P, Li H, Yang B, Yang F, Zhang L-L, Kong Q-Y, et al. Biological significance and therapeutic implication of resveratrol-inhibited Wnt, Notch and STAT3 signaling in cervical cancer cells. *Genes Cancer* 2014;5:154–64.
- [190] Lagouge M, Argmann C, Gerhart-Hines Z, Meziane H, Lerin C, Daussin F, et al. Resveratrol Improves Mitochondrial Function and Protects against Metabolic Disease by Activating SIRT1 and PGC-1alpha. *Cell* 2006;127:1109–22. doi:10.1016/j.cell.2006.11.013.

- [191] Noske AB, Costin AJ, Morgan GP, Marsh BJ. Expedited approaches to whole cell electron tomography and organelle mark-up in situ in high-pressure frozen pancreatic islets. *J Struct Biol* 2008;161:298–313. doi:10.1016/j.jsb.2007.09.015.
- [192] Hong J, Lu H, Meng X, Ryu JH, Hara Y, Yang CS. Stability, cellular uptake, biotransformation, and efflux of tea polyphenol (-)-epigallocatechin-3-gallate in HT-29 human colon adenocarcinoma cells. *Cancer Res* 2002;62:7241–6. doi:10.1146/annurev.pharmtox.42.082101.154309.
- [193] Ashikawa K, Ashikawa K, Majumdar S, Majumdar S, Banerjee S, Banerjee S, et al. Piceatannol inhibits TNF-induced NF- κ B activation and NF- κ B-mediated gene expression through suppression of I κ B α kinase and p65 phosphorylation. *J Immunol* 2002;169:6490–7. doi:10.4049/jimmunol.169.11.6490.
- [194] Yao J, Wang JY, Liu L, Li YX, Xun AY, Zeng W Sen, et al. Anti-oxidant Effects of Resveratrol on Mice with DSS-induced Ulcerative Colitis. *Arch Med Res* 2010;41:288–94. doi:10.1016/j.arcmed.2010.05.002.
- [195] Baur JA, Sinclair DA. Therapeutic potential of resveratrol: the in vivo evidence. *Nat Rev Drug Discov* 2006;5:493–506. doi:10.1038/nrd2060.
- [196] Liu YZ, Wu K, Huang J, Liu Y, Wang X, Meng ZJ, et al. The PTEN/PI3K/Akt and Wnt/beta-catenin signaling pathways are involved in the inhibitory effect of resveratrol on human colon cancer cell proliferation. *Int J Oncol* 2014;45:104–12. doi:10.3892/ijo.2014.2392.
- [197] Roy S, Yu Y, Padhye SB, Sarkar FH, Majumdar APN. Difluorinated-Curcumin (CDF) Restores PTEN Expression in Colon Cancer Cells by Down-Regulating miR-21. *PLoS One* 2013;8. doi:10.1371/journal.pone.0068543.
- [198] Liu M, Wilk SA, Wang A, Zhou L, Wang RH, Ogawa W, et al. Resveratrol inhibits mTOR signaling by promoting the interaction between mTOR and DEPTOR. *J Biol Chem* 2010;285:36387–94. doi:10.1074/jbc.M110.169284.
- [199] Puissant A, Auberger P. AMPK- and p62/SQSTM1-dependent autophagy mediate resveratrol-induced cell death in chronic myelogenous leukemia. *Autophagy* 2010;6:655–7. doi:10.4161/auto.6.5.12126.
- [200] Holt EM, Steffen LM, Moran A, Basu S, Steinberger J, Ross JA, et al. Fruit and vegetable

- consumption and its relation to markers of inflammation and oxidative stress in adolescents. *J Am Diet Assoc* 2010;109:414–21. doi:10.1016/j.jada.2008.11.036.Fruit.
- [201] Rice-Evans CA, Miller NJ, Paganga G. Antioxidant properties of phenolic compounds. *Trends Plant Sci* 1997;2:152–9. doi:10.1016/S1360-1385(97)01018-2.
- [202] Benzie IF, Strain J. The ferric reducing ability of plasma (FRAP) as a measure of “antioxidant power”: the FRAP assay. *Anal Biochem* 1996;239:70–6.
- [203] Brand-Williams W, Cuvelier ME, Berset C. Use of a free radical method to evaluate antioxidant activity. *LWT - Food Sci Technol* 1995;28:25–30. doi:10.1016/S0023-6438(95)80008-5.
- [204] Cox J, Mann M. MaxQuant enables high peptide identification rates, individualized p.p.b.-range mass accuracies and proteome-wide protein quantification. *Nat Biotechnol* 2008;26:1367–72. doi:10.1038/nbt.1511.
- [205] Tyanova S, Temu T, Sinitcyn P, Carlson A, Hein MY, Geiger T, et al. The Perseus computational platform for comprehensive analysis of (prote)omics data. *Nat Methods* 2016;13:731–40. doi:10.1038/nmeth.3901.
- [206] Chen G-L, Chen S-G, Zhao Y-Y, Luo C-X, Li J, Gao Y-Q. Total phenolic contents of 33 fruits and their antioxidant capacities before and after in vitro digestion. *Ind Crops Prod* 2014;57:150–7. doi:10.1016/j.indcrop.2014.03.018.
- [207] Seeram NP, Aviram M, Zhang Y, Henning SM, Feng L, Dreher M, et al. Comparison of antioxidant potency of commonly consumed polyphenol-rich beverages in the United States. *J Agric Food Chem* 2008;56:1415–22.
- [208] Kelebek H, Jourdes M, Selli S, Teissedre P-L. Comparative evaluation of the phenolic content and antioxidant capacity of sun-dried raisins. *J Sci Food Agric* 2013;93:2963–72. doi:10.1002/jsfa.6125.
- [209] Pellegrini N, Serafini M, Salvatore S, Del Rio D, Bianchi M, Brighenti F. Total antioxidant capacity of spices, dried fruits, nuts, pulses, cereals and sweets consumed in Italy assessed by three different in vitro assays. *Mol Nutr Food Res* 2006;50:1030–8. doi:10.1002/mnfr.200600067.
- [210] Sasaki T, Maier B, Koclega KD, Chruszcz M, Gluba W, Stukenberg PT, et al. Phosphorylation regulates SIRT1 function. *PLoS One* 2008;3. doi:10.1371/journal.pone.0004020.

- [211] Nasrin N, Kaushik VK, Fortier E, Wall D, Pearson KJ, de Cabo R, et al. JNK1 phosphorylates SIRT1 and promotes its enzymatic activity. *PLoS One* 2009;4. doi:10.1371/journal.pone.0008414.
- [212] Buhrmann C, Shayan P, Popper B, Goel A, Shakibaei M. Sirt1 is required for resveratrol-mediated chemopreventive effects in colorectal cancer cells. *Nutrients* 2016;8. doi:10.3390/nu8030145.
- [213] Belham C, Shilan W, Avruch J. Intracellular signalling: PDK1 - A kinase at the hub of things. *Curr Biol* 1999;9. doi:10.1016/S0960-9822(99)80058-X.
- [214] Nirula A, Ho M, Phee H, Roose J, Weiss A. Phosphoinositide-dependent kinase 1 targets protein kinase A in a pathway that regulates interleukin 4. *J Exp Med* 2006;203:1733–44. doi:10.1084/jem.20051715.
- [215] Zhong H, SuYang H, Erdjument-Bromage H, Tempst P, Ghosh S. The Transcriptional Activity of NF- κ B Is Regulated by the I κ B-Associated PKAc Subunit through a Cyclic AMP–Independent Mechanism. *Cell* 1997;89:413–24. doi:10.1016/S0092-8674(00)80222-6.
- [216] Dutil EM, Toker A, Newton AC. Regulation of conventional protein kinase C isozymes by phosphoinositide-dependent kinase 1 (PDK-1). *Curr Biol* 1998;8:1366–75. doi:10.1016/S0960-9822(98)00017-7.
- [217] Shirakawa F, Mizel SB. In vitro activation and nuclear translocation of NF-kappa B catalyzed by cyclic AMP-dependent protein kinase and protein kinase C. *Mol Cell Biol* 1989;9:2424–30.
- [218] Yang J, Han Y, Chen C, Sun H, He D, Guo J, et al. EGCG attenuates high glucose-induced endothelial cell inflammation by suppression of PKC and NF- κ B signaling in human umbilical vein endothelial cells. *Life Sci* 2013;92:589–97. doi:10.1016/j.lfs.2013.01.025.
- [219] Bagowski CP, Stein-Gerlach M, Choidas A, Ullrich A. Cell-type specific phosphorylation of threonines T654 and T669 by PKD defines the signal capacity of the EGF receptor. *EMBO J* 1999;18:5567–76. doi:10.1093/emboj/18.20.5567.
- [220] Shimizu M, Deguchi A, Lim JTE, Moriwaki H, Kopelovich L, Weinstein IB. (–)-Epigallocatechin Gallate and Polyphenon E Inhibit Growth and Activation of the Epidermal Growth Factor Receptor and Human Epidermal Growth Factor Receptor-2 Signaling Pathways in Human Colon Cancer Cells. *Clin Cancer Res* 2005;11:2735–46. doi:10.1158/1078-0432.CCR-04-2014.

- [221] Shaulian E, Karin M. AP-1 as a regulator of cell life and death. *Nat Cell Biol* 2002;4:E131–6. doi:10.1038/ncb0502-e131.
- [222] Wadleigh DJ, Reddy ST, Kopp E, Ghosh S, Herschman HR. Transcriptional activation of the cyclooxygenase-2 gene in endotoxin-treated RAW 264.7 macrophages. *J Biol Chem* 2000;275:6259–66. doi:10.1074/jbc.275.9.6259.
- [223] Dong Z, Ma W, Huang C, Yang CS. Inhibition of tumor promoter-induced activator protein 1 activation and cell transformation by tea polyphenols, (-)-epigallocatechin gallate, and theaflavins. *Cancer Res* 1997;57:4414–9.
- [224] Chen D, Li Z, Yang Q, Zhang J, Zhai Z, Shu HB. Identification of a nuclear protein that promotes NF- κ B activation. *Biochem Biophys Res Commun* 2003;310:720–4. doi:10.1016/j.bbrc.2003.09.074.
- [225] Emdad L, Sarkar D, Su Z, Randolph A, Boukerche H, Valerie K, et al. Activation of the nuclear factor kappaB pathway by astrocyte elevated gene-1: implications for tumor progression and metastasis. *Cancer Res* 2006;66:1509–16. doi:10.1158/0008-5472.CAN-05-3029.
- [226] Delmas D, Lancon A, Colin D, Jannin B, Latruffe N. Resveratrol as a Chemopreventive Agent: A Promising Molecule for Fighting Cancer. *Curr Drug Targets* 2006;7:423–42. doi:10.2174/138945006776359331.
- [227] Chin PC, Liu L, Morrison BE, Siddiq A, Ratan RR, Bottiglieri, Teodoro D'mello SR. The c-Raf inhibitor GW5074 provides neuroprotection in vitro and in an animal model of neurodegeneration through a MEK-ERK and Akt-independent mechanism. *J Neurochem* 2004;90:595–608. doi:10.1111/j.1471-4159.2004.02530.x.
- [228] Baumann B, Weber CK, Troppmair J, Whiteside S, Israel A, Rapp UR, et al. Raf induces NF-kappaB by membrane shuttle kinase MEKK1, a signaling pathway critical for transformation. *Proc Natl Acad Sci U S A* 2000;97:4615–20. doi:10.1073/pnas.080583397.
- [229] Romashkova JA, Makarov SS. NF-kappaB is a target of AKT in anti-apoptotic PDGF signalling. *Nature* 1999;401:86–90. doi:10.1038/43474.
- [230] Guha M, Mackman N. The phosphatidylinositol 3-kinase-Akt pathway limits lipopolysaccharide activation of signaling pathways and expression of inflammatory mediators in human monocytic cells.

- J Biol Chem 2002;277:32124–32. doi:10.1074/jbc.M203298200.
- [231] Islam S, Hassan F, Mu MM, Ito H, Koide N, Mori I, et al. Piceatannol prevents lipopolysaccharide (LPS)-induced nitric oxide (NO) production and nuclear factor (NF)-kappaB activation by inhibiting IkappaB kinase (IKK). *Microbiol Immunol* 2004;48:729–36. doi:10.1111/j.1348-0421.2004.tb03598.x.
- [232] Hafner S, Adler HS, Mischak H, Janosch P, Heidecker G, Wolfman A, et al. Mechanism of Inhibition of Raf-1 by Protein-Kinase-A. *Mol Cell Biol* 1994;14:6696–703.
- [233] Chitturi S, Farrell GC. Etiopathogenesis of Nonalcoholic Steatohepatitis. *Semin Liver Dis* 2001;21:27–41. doi:10.1055/s-2001-12927.
- [234] Szabo G, Csak T. Inflammasomes in liver diseases. *J Hepatol* 2012;57:642–54. doi:10.1016/j.jhep.2012.03.035.
- [235] Kirpich IA, Gobejishvili LN, Bon Homme M, Waigel S, Cave M, Arteel G, et al. Integrated hepatic transcriptome and proteome analysis of mice with high-fat diet-induced nonalcoholic fatty liver disease. *J Nutr Biochem* 2011;22:38–45. doi:10.1016/j.jnutbio.2009.11.009.
- [236] Zhang X, Yang J, Guo Y, Ye H, Yu C, Xu C, et al. Functional proteomic analysis of nonalcoholic fatty liver disease in rat models: Enoyl-coenzyme a hydratase down-regulation exacerbates hepatic steatosis. *Hepatology* 2010;51:1190–9. doi:10.1002/hep.23486.
- [237] Slavin JL, Savarino V, Paredes-Diaz, A. Fotopoulos G. A Review of the Role of Soluble Fiber in Health with Specific Reference to Wheat Dextrin. *J Int Med Res* 2009;37:1–17.
- [238] Tedelind S, Westberg F, Kjerrulf M, Vidal A. Anti-inflammatory properties of the short-chain fatty acids acetate and propionate: A study with relevance to inflammatory bowel disease. *World J Gastroenterol* 2007;13:2826–32. doi:10.3748/wjg.v13.i20.2826.
- [239] Breen EJ, Polaskova V, Khan A. Bead-based multiplex immuno-assays for cytokines, chemokines, growth factors and other analytes: Median fluorescence intensities versus their derived absolute concentration values for statistical analysis. *Cytokine* 2015;71:188–98. doi:10.1016/j.cyto.2014.10.030.
- [240] Holm S. A simple sequential rejective multiple test procedure. *Scand J Stat* 1979;6:65–70.

- doi:10.2307/4615733.
- [241] Huang C-Y, Chen W-M, Tsay Y-G, Hsieh S-C, Lin Y, Lee W-J, et al. Differential regulation of protein expression in response to polyunsaturated fatty acids in the liver of apoE-knockout mice and in HepG2 cells. *J Biomed Sci* 2015;22:12. doi:10.1186/s12929-015-0118-2.
 - [242] Safwat GM, Pisanò S, D'Amore E, Borioni G, Napolitano M, Kamal AA, et al. Induction of non-alcoholic fatty liver disease and insulin resistance by feeding a high-fat diet in rats: does coenzyme Q monomethyl ether have a modulatory effect? *Nutrition* 2009;25:1157–68. doi:10.1016/j.nut.2009.02.009.
 - [243] Kern M, Knigge A, Heiker JT, Kosacka J, Stumvoll M, Kovacs P, et al. C57BL/6JRj mice are protected against diet induced obesity (DIO). *Biochem Biophys Res Commun* 2012;417:717–20. doi:10.1016/j.bbrc.2011.12.008.
 - [244] Kolligs F, Fehmann HC, Goke R, Goke B. Reduction of the incretin effect in rats by the glucagon-like peptide 1 receptor antagonist exendin (9-39) amide. *Diabetes* 1995;44:16–9. doi:10.2337/diab.44.1.16.
 - [245] Flint A, Raben A, Ersbøll AK, Holst JJ, Astrup A. The effect of physiological levels of glucagon-like peptide-1 on appetite, gastric emptying, energy and substrate metabolism in obesity. *Int J Obes* 2001;25:781–92. doi:10.1038/sj.ijo.0801627.
 - [246] Alessi MC, Bastelica D, Mavri A, Morange P, Berthet B, Grino M, et al. Plasma PAI-1 levels are more strongly related to liver steatosis than to adipose tissue accumulation. *Arterioscler Thromb Vasc Biol* 2003;23:1262–8. doi:10.1161/01.ATV.0000077401.36885.BB.
 - [247] Ma LJ, Mao SL, Taylor KL, Kanjanabuch T, Guan Y, Zhang Y, et al. Prevention of obesity and insulin resistance in mice lacking plasminogen activator inhibitor 1. *Diabetes* 2004;53:336–46.
 - [248] Ej P, Jh L, Yu G-Y, He G, Sr A, Holzer RG. Dietary and Genetic Obesity Promote Liver Inflammation and Tumorigenesis by Enhancing IL-6 and TNF Expression. *Cell* 2010;140:197–208.
 - [249] Yoshinari K, Takagi S, Yoshimasa T, Sugatani J, Miwa M. Hepatic CYP3A expression is attenuated in obese mice fed a high-fat diet. *Pharm Res* 2006;23:1188–200. doi:10.1007/s11095-006-0071-6.
 - [250] Mikkelsen MS, Jespersen BM, Mehlsen A, Engelsen SB, Frøkiær H. Cereal β -glucan immune modulating activity depends on the polymer fine structure. *Food Res Int* 2014;62:829–36.

doi:10.1016/j.foodres.2014.04.021.

- [251] Hamilton JA. Colony-stimulating factors in inflammation and autoimmunity. *Nat Rev Immunol* 2008;8:533–45. doi:10.1016/S1471-4906(02)02260-3.
- [252] Ditiatkovski M, Toh BH, Bobik A. GM-CSF deficiency reduces macrophage PPAR-gamma expression and aggravates atherosclerosis in ApoE-deficient mice. *Arterioscler Thromb Vasc Biol* 2006;26:2337–44. doi:10.1161/01.ATV.0000238357.60338.90.
- [253] Stanton MC, Chen S-C, Jackson J V, Rojas-Triana A, Kinsley D, Cui L, et al. Inflammatory Signals shift from adipose to liver during high fat feeding and influence the development of steatohepatitis in mice. *J Inflamm* 2011;8:8–22. doi:10.1186/1476-9255-8-8.
- [254] Caughey GE, Mantzioris E, Gibson RA, Cleland LG, James MJ. The effect on human tumor necrosis factor alpha and interleukin 1 beta production of diets enriched in n-3 fatty acids from vegetable oil or fish oil. *Am J Clin Nutr* 1996;63:116–22.
- [255] Kamari Y, Shaish A, Vax E, Shemesh S, Kandel-Kfir M, Arbel Y, et al. Lack of interleukin-1 α or interleukin-1 β inhibits transformation of steatosis to steatohepatitis and liver fibrosis in hypercholesterolemic mice. *J Hepatol* 2011;55:1086–94. doi:10.1016/j.jhep.2011.01.048.
- [256] Hui X, Zhu W, Wang Y, Lam KSL, Zhang J, Wu D, et al. Major urinary protein-1 increases energy expenditure and improves glucose intolerance through enhancing mitochondrial function in skeletal muscle of diabetic mice. *J Biol Chem* 2009;284:14050–7. doi:10.1074/jbc.M109.001107.
- [257] Labunskyy VM, Hatfield DL, Gladyshev VN. Selenoproteins: molecular pathways and physiological roles. *Physiol Rev* 2014;94:739–77. doi:10.1152/physrev.00039.2013.
- [258] Motomura W, Yoshizaki T, Takahashi N, Kumei S, Mizukami Y, Jang S, et al. Analysis of vaninn1 upregulation and lipid accumulation in hepatocytes in response to a high fat diet and free fatty acids. *J Clin Biochem Nutr* 2012;51:163–9. doi:10.3164/jcbrn.12206.
- [259] Kim S, Sohn I, Ahn J-I, Lee K-H, Lee YS, Lee YS. Hepatic gene expression profiles in a long-term high-fat diet-induced obesity mouse model. *Gene* 2004;340:99–109. doi:10.1016/j.gene.2004.06.015.
- [260] Seiler SE, Martin OJ, Noland RC, Slentz DH, DeBalsi KL, Ilkayeva OR, et al. Obesity and lipid stress inhibit carnitine acetyltransferase activity. *J Lipid Res* 2014;55:635–44. doi:10.1194/jlr.M043448.

- [261] Balwierz A, Polus A, Razny U, Wator L, Dyduch G, Tomaszewska R, et al. Angiogenesis in the New Zealand obese mouse model fed with high fat diet. *Lipids Health Dis* 2009;8:13. doi:10.1186/1476-511X-8-13.
- [262] Huber J, Loeffler M, Bilban M, Reimers M, Kadl A, Todoric J, et al. Prevention of high-fat diet-induced adipose tissue remodeling in obese diabetic mice by n-3 polyunsaturated fatty acids. *Int J Obes* 2007;31:1004–13. doi:10.1038/sj.ijo.0803511.
- [263] Majer M, Popov KM, Harris R a, Bogardus C, Prochazka M. Insulin downregulates pyruvate dehydrogenase kinase (PDK) mRNA: potential mechanism contributing to increased lipid oxidation in insulin-resistant subjects. *Mol Genet Metab* 1998;65:181–6. doi:10.1006/mgme.1998.2748.
- [264] Jeoung NH, Rahimi Y, Wu P, Lee WNP, Harris RA. Fasting induces ketoacidosis and hypothermia in PDHK2/PDHK4-double-knockout mice. *Biochem J* 2012;443:829–39. doi:10.1042/BJ20112197.
- [265] Qin H, Zhang X, Ye F, Zhong L. High-fat diet-induced changes in liver thioredoxin and thioredoxin reductase as a novel feature of insulin resistance. *FEBS Open Bio* 2014;4:928–35. doi:10.1016/j.fob.2014.10.015.
- [266] Agamy O, Ben Zeev B, Lev D, Marcus B, Fine D, Su D, et al. Mutations disrupting selenocysteine formation cause progressive cerebello-cerebral atrophy. *Am J Hum Genet* 2010;87:538–44. doi:10.1016/j.ajhg.2010.09.007.
- [267] Kumaraswamy E, Malykh A, Korotkov K V., Kozyavkin S, Hu Y, Kwon SY, et al. Structure-expression relationships of the 15-kDa selenoprotein gene: Possible role of the protein in cancer etiology. *J Biol Chem* 2000;275:35540–7. doi:10.1074/jbc.M004014200.
- [268] Tsuji PA, Carlson BA, Naranjo-Suarez S, Yoo MH, Xu XM, Fomenko DE, et al. Knockout of the 15 kDa Selenoprotein Protects against Chemically-Induced Aberrant Crypt Formation in Mice. *PLoS One* 2012;7. doi:10.1371/journal.pone.0050574.
- [269] Sabu MC, Smitha K, Kuttan R. Anti-diabetic activity of green tea polyphenols and their role in reducing oxidative stress in experimental diabetes. *J Ethnopharmacol* 2002;83:109–16. doi:10.1016/S0378-8741(02)00217-9.
- [270] Tan Z, Luo M, Yang J, Cheng Y, Huang J, Lu C, et al. Chlorogenic acid inhibits cholestatic liver

- injury induced by α -naphthylisothiocyanate: involvement of STAT3 and NF κ B signalling regulation. *J Pharm Pharmacol* 2016;68:1203–13. doi:10.1111/jphp.12592.
- [271] Chen S, Chen Y, Chen B, Cai YJ, Zou ZL, Wang JG, et al. Plumbagin Ameliorates CCl₄ -Induced Hepatic Fibrosis in Rats via the Epidermal Growth Factor Receptor Signaling Pathway. *Evid Based Complement Altern Med* 2015;2015:645727. doi:10.1155/2015/645727.
- [272] Marinelli RA, Tietz PS, Pham LD, Rueckert L, Agre P, LaRusso NF. Secretin induces the apical insertion of aquaporin-1 water channels in rat cholangiocytes. *Am J Physiol* 1999;276:280–6.
- [273] Ma T, Jayaraman S, Wang KS, Song Y, Yang B, Li J, et al. Defective dietary fat processing in transgenic mice lacking aquaporin-1 water channels. *Am J Physiol Cell Physiol* 2001;280:C126–34.
- [274] Batrakou DG, De Las Heras JI, Czapiewski R, Mouras R, Schirmer EC. TMEM120A and B: Nuclear envelope transmembrane proteins important for adipocyte differentiation. *PLoS One* 2015;10. doi:10.1371/journal.pone.0127712.
- [275] Liu W, Ye H. Co-expression network analysis identifies transcriptional modules in the mouse liver. *Mol Genet Genomics* 2014;289:847–53. doi:10.1007/s00438-014-0859-8.
- [276] Shrestha N, Bahnan W, Wiley DJ, Barber G, Fields KA, Schesser K. Eukaryotic Initiation Factor 2 (eIF2) signaling regulates proinflammatory cytokine expression and bacterial invasion. *J Biol Chem* 2012;287:28738–44. doi:10.1074/jbc.M112.375915.
- [277] Ma T, Trinh MA, Wexler AJ, Bourbon C, Gatti E, Pierre P, et al. Suppression of eIF2 α kinases alleviates Alzheimer's disease-related plasticity and memory deficits. *Nat Neurosci* 2013;16:1299–305. doi:10.1038/nn.3486.
- [278] Hardwick RN, Ferreira DW, More VR, Lake AD, Lu Z, Manautou JE, et al. Altered UDP-glucuronosyltransferase and sulfotransferase expression and function during progressive stages of human nonalcoholic fatty liver diseases. *Drug Metab Dispos* 2013;41:554–61. doi:10.1124/dmd.112.048439.
- [279] Yecies JL, Zhang HH, Menon S, Liu S, Yecies D, Lipovsky AI, et al. Akt stimulates hepatic SREBP1c and lipogenesis through parallel mTORC1-dependent and independent pathways. *Cell Metab* 2011;14:21–32. doi:10.1016/j.cmet.2011.06.002.

- [280] Um SH, Frigerio F, Watanabe M, Picard F, Joaquin M, Sticker M, et al. Absence of S6K1 protects against age- and diet-induced obesity while enhancing insulin sensitivity. *Nature* 2004;431:200–5. doi:10.1038/nature02979.
- [281] Jo HK, Kim GW, Jeong KJ, Kim DY, Chung SH. Eugenol ameliorates hepatic steatosis and fibrosis by down-regulating SREBP1 gene expression via AMPK-mTOR-p70S6K signaling pathway. *Biol Pharm Bull* 2014;37:1341–51. doi:10.1248/bpb.b14-00281.
- [282] Wang ZQ, Yu Y, Zhang XH, Floyd ZE, Boudreau A, Lian K, et al. Comparing the effects of nano-sized sugarcane fiber with cellulose and psyllium on hepatic cellular signaling in mice. *Int J Nanomedicine* 2012;1:2999–3012. doi:10.2147/IJN.S30887.
- [283] Kim J-H, Xu C, Keum Y-S, Reddy B, Conney A, Kong A-NT. Inhibition of EGFR signaling in human prostate cancer PC-3 cells by combination treatment with beta-phenylethyl isothiocyanate and curcumin. *Carcinogenesis* 2006;27:475–82. doi:10.1093/carcin/bgi272.
- [284] Winograd-Katz SE, Levitzki A. Cisplatin induces PKB/Akt activation and p38(MAPK) phosphorylation of the EGF receptor. *Oncogene* 2006;25:7381–90. doi:10.1038/sj.onc.1209737.
- [285] Howard MT, Carlson BA, Anderson CB, Hatfield DL. Translational redefinition of UGA codons is regulated by selenium availability. *J Biol Chem* 2013;288:19401–13. doi:10.1074/jbc.M113.481051.
- [286] Mullen W, Gonzalez J, Siwy J, Franke J, Sattar N, Mullan A, et al. A Pilot Study on the Effect of Short-Term Consumption of a Polyphenol Rich Drink on Biomarkers of Coronary Artery Disease Defined by Urinary Proteomics. *J Agric Food Chem* 2011;59:12850–7. doi:10.1021/jf203369r.

Appendices

Appendix 1 Table 2A.1 Nutritional information of WDS (Supplied by Gratuk Ltd. Pty.)

Nutritional Information		
Serving size: 7.6g		
	Ave Qty Per serve	Ave Qty Per 100g
Energy	74 kJ	973 kJ
Protein	0.3g	3.9g
Fat, Total	0.1g	1.2g
-saturated	0.0g	0.2g
Carbohydrates	1.7g	22.2g
-sugars	0.1g	1.2g
Dietary Fibre	3.4g	44.7g
Sodium	1mg	17mg
Gluten	Not detected	Not detected
Chromium	26.6µg	350µg
Potassium	293µg	3.8g
Selenium	8.4µg	110µg
Iron	0.76µg	9.9µg
Molybdenum	1.4µg	18.2µg
Zinc	0.02mg	0.26mg
Magnesium	2.17mg	28.31mg

Appendix 2 Figure 2A.1 Cell viability in SW480 cells in response to LPS, WDS EE and RSV addition

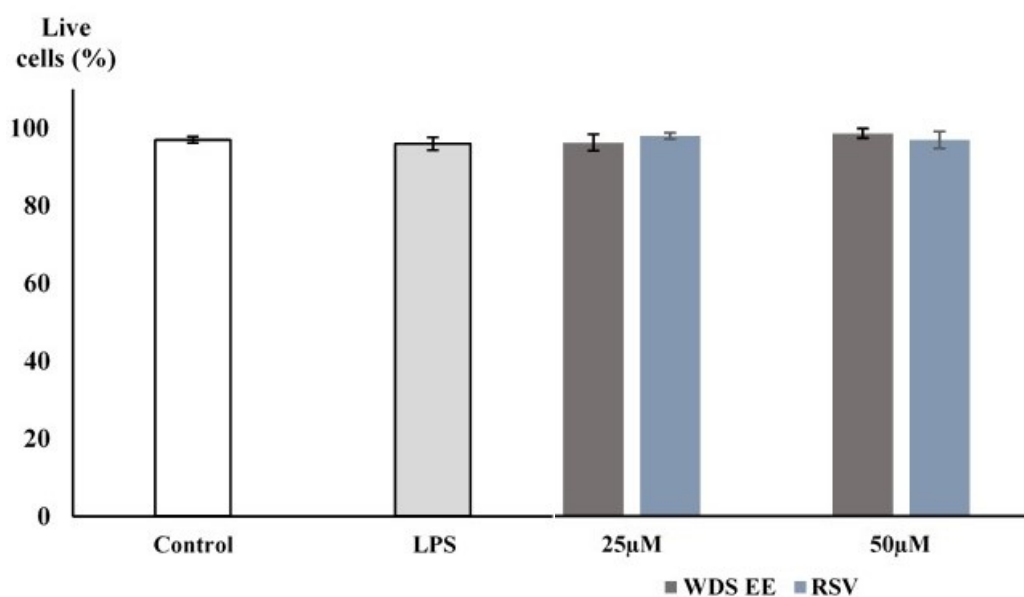


Figure 2A.1 Cell viability in SW480 cells in response to LPS, WDS EE and RSV addition. Cell viability expressed as % of live cells was determined in untreated SW480 cells (control), LPS-stimulated cells (5µg/ml), LPS-stimulated and co-incubated with WDS EE, and LPS-stimulated and co-incubated with RSV at 25µM and 50µM after 48 hours. n=3, mean +/- SD.

Appendix 3 Table 2A.2 Significantly regulated proteins expressed as LPS/C ratio.

Two-sample t test (p-value <0.05), fold change >1.5.

Uniprot accession number	Gene	Protein name	Fold change LPS/C
P05362	<i>ICAM1</i>	Intercellular adhesion molecule 1	13.0
Q96GM8	<i>TOE1</i>	Target of EGR1 protein 1	10.6
P0DJI8	<i>SAA1</i>	Serum amyloid A-1 protein	8.0
P01037	<i>CYTN</i>	Cystatin-SN	4.9
P30495	<i>IB56</i>	HLA class I histocompatibility antigen, B-56 alpha chain	4.6
Q7Z3B4	<i>NUP54</i>	Nucleoporin p54	4.5
P80404	<i>GABT</i>	4-aminobutyrate aminotransferase, mitochondrial	4.4
Q15678	<i>PTN14</i>	Tyrosine-protein phosphatase non-receptor type 14	4.3
P25774	<i>CATS</i>	Cathepsin S	3.6
Q03169	<i>TNAP2</i>	Tumor necrosis factor alpha-induced protein 2	3.1
O43924	<i>PDE6D</i>	Retinal rod rhodopsin-sensitive cGMP 3',5'-cyclic phosphodiesterase subunit delta	2.5
Q01831	<i>XPC</i>	DNA repair protein complementing XP-C cells	2.3
P01892	<i>IA02</i>	HLA class I histocompatibility antigen, A-2 alpha chain	2.2
P41221	<i>WNT5A</i>	Protein Wnt-5a	2.1
P01889	<i>IB07</i>	HLA class I histocompatibility antigen, B-7 alpha chain	2.1
Q13501	<i>SQSTM</i>	Sequestosome-1	2.0
P15170	<i>ERF3A</i>	Eukaryotic peptide chain release factor GTP-binding subunit ERF3A	2.0
Q9NVI1	<i>FANCI</i>	Fanconi anemia group I protein	1.9
P50479	<i>PDLI4</i>	PDZ and LIM domain protein 4	1.8
P05534	<i>IA24</i>	HLA class I histocompatibility antigen, A-24 alpha chain	1.7
Q9UH17	<i>ABC3B</i>	DNA dC->dU-editing enzyme APOBEC-3B	1.7
P30405	<i>PPIF</i>	Peptidyl-prolyl cis-trans isomerase F, mitochondrial	1.7
P04179	<i>SODM</i>	Superoxide dismutase [Mn], mitochondrial	1.6
O00754	<i>MA2B1</i>	Lysosomal alpha-mannosidase	1.6
P49589	<i>SYCC</i>	Cysteine--tRNA ligase, cytoplasmic	1.6
P62699	<i>YPEL5</i>	Protein yippee-like 5	1.6
Q6NUQ4	<i>TM214</i>	Transmembrane protein 214	1.6
P51153	<i>RAB13</i>	Ras-related protein Rab-13	1.6
Q9H147	<i>TDIF1</i>	Deoxynucleotidyltransferase terminal-interacting protein 1	1.5
Q9H4M9	<i>EHD1</i>	EH domain-containing protein 1	1.5
Q9Y4C8	<i>RBM19</i>	Probable RNA-binding protein 19	1.5
O95470	<i>SGPL1</i>	Sphingosine-1-phosphate lyase 1	1.5
Q9UPW6	<i>SATB2</i>	DNA-binding protein SATB2	1.5
Q6IAN0	<i>DRS7B</i>	Dehydrogenase/reductase SDR family member 7B	1.5
Q7L5N7	<i>PCAT2</i>	Lysophosphatidylcholine acyltransferase 2	-1.5
P32929	<i>CGL</i>	Cystathionine gamma-lyase	-1.5

Q53EL6	<i>PDCD4</i>	Programmed cell death protein 4	-1.5
Q9UHN6	<i>TMEM2</i>	Transmembrane protein 2	-1.5
P51648	<i>AL3A2</i>	Fatty aldehyde dehydrogenase	-1.5
Q9UHG3	<i>PCYOX</i>	Preylcysteine oxidase 1	-1.6
Q9H3M7	<i>TXNIP</i>	Thioredoxin-interacting protein	-1.6
Q15758	<i>AAAT</i>	Neutral amino acid transporter B(0)	-1.6
O14639	<i>ABLM1</i>	Actin-binding LIM protein 1	-1.7
P15529	<i>MCP</i>	Membrane cofactor protein	-1.8
Q92597	<i>NDRG1</i>	Protein NDRG1	-2.0
O75376	<i>NCOR1</i>	Nuclear receptor corepressor 1	-2.0
O76024	<i>WFS1</i>	Wolframin	-2.1
Q8TAA5	<i>GRPE2</i>	GrpE protein homolog 2, mitochondrial	-2.3
P53794	<i>SC5A3</i>	Sodium/myo-inositol cotransporter	-2.4
Q7Z2K6	<i>ERMP1</i>	Endoplasmic reticulum metalloproteinase 1	-2.4
Q14671	<i>PUM1</i>	Pumilio homolog 1	-3.6
Q9UMX5	<i>NENF</i>	Neudesin	-4.7

Appendix 4 Table 3A.1 Kinase enrichment motif performed on WDS EE/LPS significant regulated phosphosites

Benjamini Hochberg (FDR <0.2)

Substrate motif	Enrichment factor	p-value	Benj. Hoch. FDR
C-RAF kinase substrate motif	2.0	4.04E-03	1.56E-02
GSK3, Erk1, Erk2 and CDK5 kinase motif	1.9	2.17E-04	1.67E-03
HMGCoA Reductase kinase substrate motif	1.7	5.51E-02	1.03E-01
CDK5 kinase substrate motif	1.6	5.05E-02	1.05E-01
Phosphorylase kinase substrate motif	1.6	2.17E-03	9.78E-03
p70 Ribosomal S6 kinase substrate motif	1.5	8.24E-02	1.39E-01
Calmodulin-dependent protein kinase II alpha substrate motif	1.5	8.24E-02	1.44E-01
Plk1 PBD domain binding motif	1.5	5.23E-06	9.42E-05
MDC1 BRCT domain binding motif	1.5	5.23E-06	1.41E-04
AMP-activated protein kinase substrate motif	1.5	1.75E-02	4.98E-02

Appendix 5 Figures 4A.1 and 4A.2 Plasma marker expression in response to dietary changes

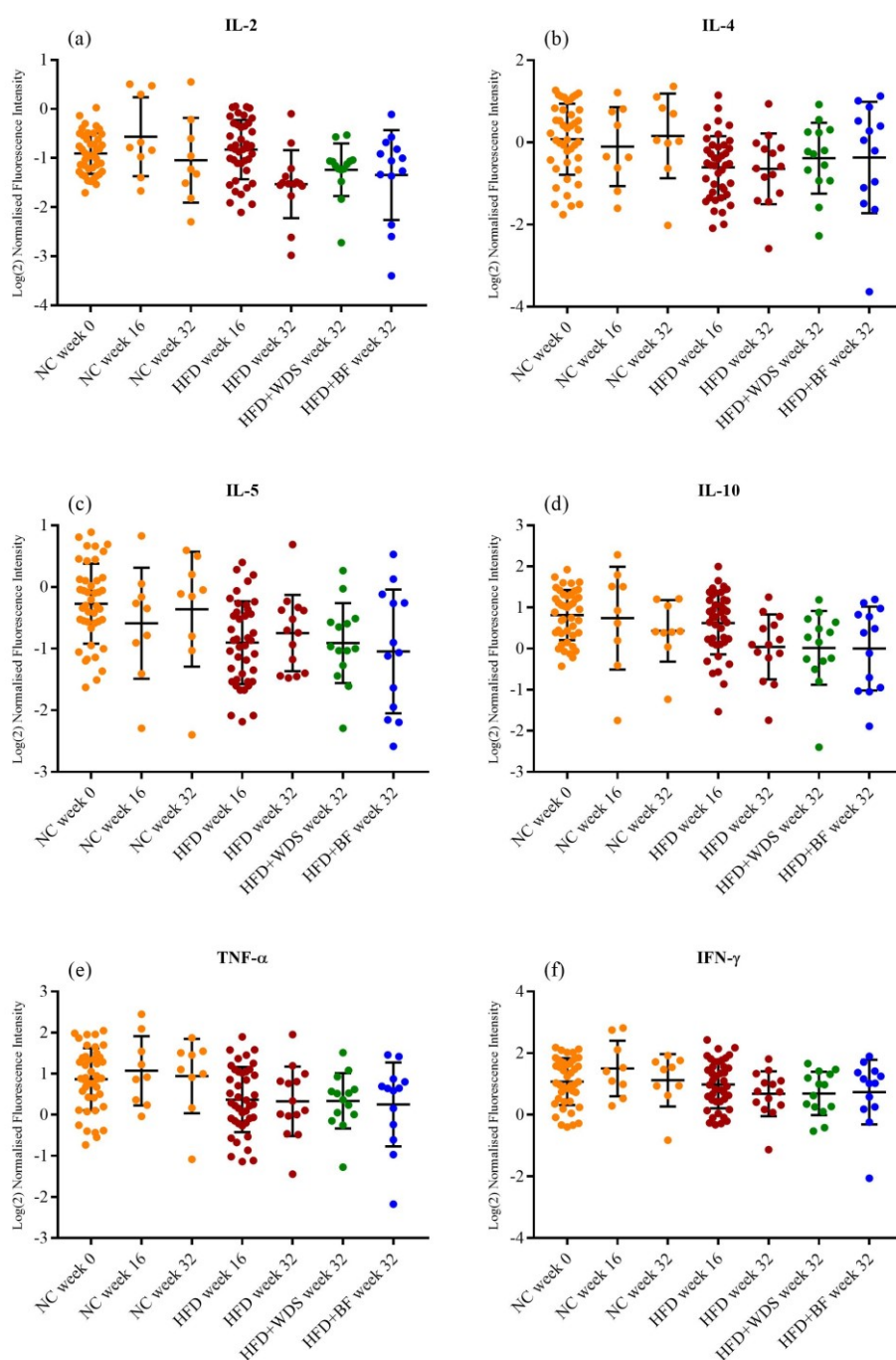


Figure 4A.1 Plasma marker expression in response to dietary changes. Plasma samples were obtained at baseline (week 0, NC n=50), week 16 (NC n=9 and HFD n=41), and week 32 (NC n=9, HFD n=14, WDS n=14 and BF=13). Values expressed as log(2) normalised fluorescence intensity. **(a)** IL-2, **(b)** IL-4, **(c)** IL-5, **(d)** IL-10 and **(e)** TNF- α , **(f)** IFN- γ .

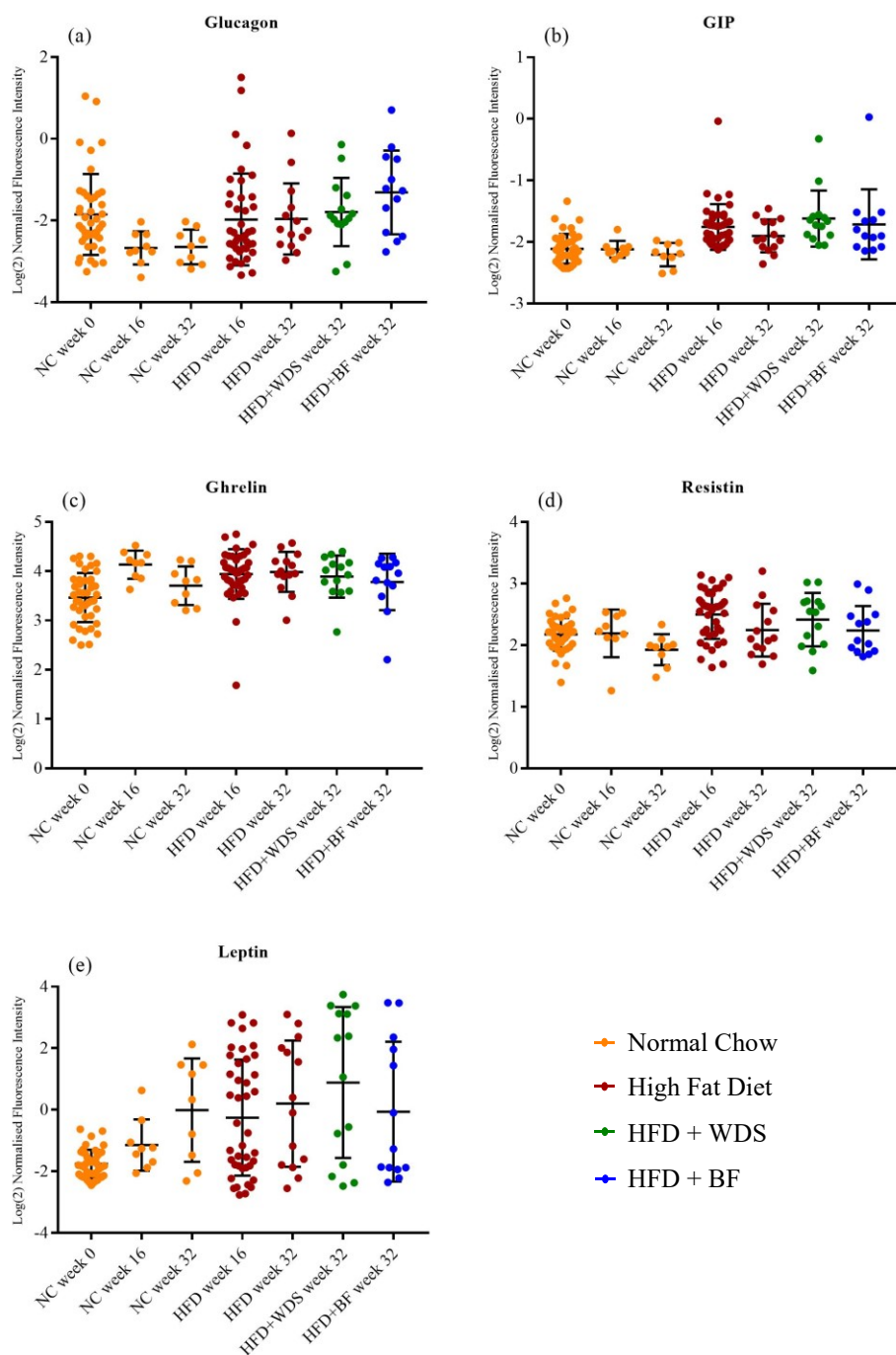


Figure 4A.2 Plasma marker expression in response to dietary changes. Plasma samples were obtained at baseline (week 0, NC n=50), week 16 (NC n=9 and HFD n=41), and week 32 (NC n=9, HFD n=14, WDS n=14 and BF=13). Values expressed as log(2) normalised fluorescence intensity. **(a)** Glucagon, **(b)** GIP, **(c)** ghrelin, **(d)** resistin and **(e)** leptin.

Appendix 6 Figure 4A.3 Prediction of diseases and functions based on hepatic protein expression induced by WDS and BF supplementation.

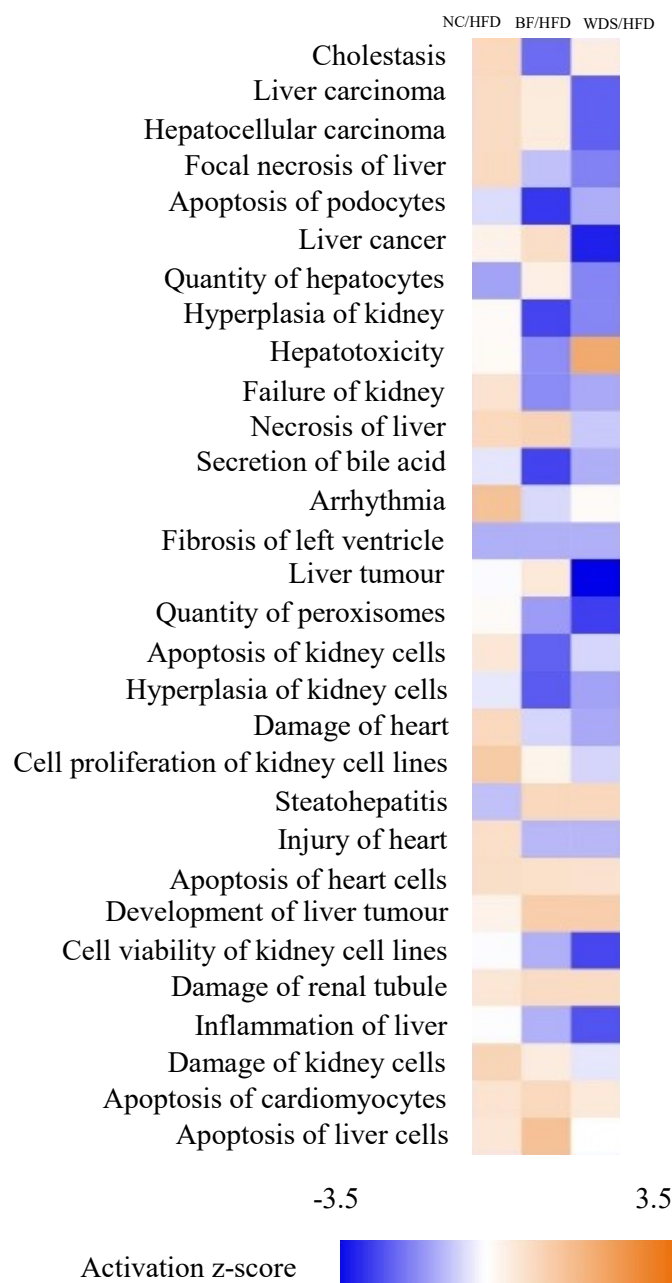


Figure 4A.3 Prediction of diseases and functions based on hepatic protein expression induced by WDS and BF supplementation. NC/HFD, WDS/HFD and BF/HFD fold changes and p-values were analysed for paired comparisons using IPA (Ingenuity Systems). Up-regulation (z-score >0) is denoted by orange whereas down-regulation (z-score <0) is represented by blue.

Appendix 7 Tables 4A.1 4A.2 and 4A.3 Normal chow, high fat diet and Benefiber
composition and nutritional parameters

Normal Chow is a fixed formula ratio using the following ingredients: wheat, barley, lupins, soya meal, fish meal, mixed vegetable oils, canola oil, salt, calcium carbonate, dicalcium phosphate, magnesium oxide, and a vitamin and trace mineral premix.

Protein	20%
Total fat	4.8%
Crude fibre	4.8%
Acid detergent fibre	7.6%
Neutral detergent fibre	16.4%
Total carbohydrate	59.4%
Digestible energy	14 MJ/kg
% Total calculated digestible energy from lipids	23%
% Total calculated digestible energy from protein	12%

Table 4A.2 High fat diet composition and nutritional parameters

Protein	19.4%
Total fat	60%
Crude fibre	4.7%
Acid detergent fibre	4.7%
Digestible fibre	24 MJ/kg
% Total calculated digestible energy from lipids	81%

Ingredients	Addition rate (g/kg)
Sucrose	106
Casein (acid)	200
Canola oil	100
Cocoa butter	400
Clarified butter	100
Cellulose	50
dI Methionine	3
AIN93 Trace minerals	1.4
Calcium carbonate	13.1
Sodium chloride	2.6
Potassium dihydrogen phosphate	6.9
Potassium sulphate	1.6
Potassium citrate	2.5
AIN_93 Vitamins	10
Choline Chloride 75% w/w	2.5

Table 4A.3 Benefiber composition and nutritional parameters

Ingredients: Wheat dextrin. Serving size: 4g.

Calories	15
Sodium	0g
Total carbohydrates	4g
Soluble dietary fibre	3g
Sugar	0g

Appendix 8 Table 4A.3 Significantly down-regulated proteins expressed as HFD/NC ratio

Two-sample t-test (p-value<0.05), fold change>1.5

Uniprot Accession number	Gene	Protein name	Fold change (HFD/NC)
B5X0G2	<i>MUP17</i>	Major urinary protein 17	-6.0
Q8K4G5	<i>ABLM1</i>	Actin-binding LIM protein 1	-3.9
Q8BFY9	<i>TNPO1</i>	Transportin-1	-3.2
P11588	<i>MUP1</i>	Major urinary protein 1	-3.2
Q8R409	<i>HEX11</i>	Protein HEXIM	-3.0
Q64459	<i>CP3AB</i>	Cytochrome P450 3A11	-2.9
Q68FF9	<i>S5A1</i>	3-oxo-5- α -steroid 4-dehydrogenase 1	-2.9
Q9QVP9	<i>FAK2</i>	Protein-tyrosine kinase 2-beta	-2.9
A6X935	<i>ITIH4</i>	Inter alpha-trypsin inhibitor, heavy chain 4	-2.6
Q99MZ3	<i>MLXPL</i>	Carbohydrate-responsive element-binding protein	-2.6
Q8R3V5	<i>SHLB2</i>	Endophilin-B2	-2.6
Q91WG0	<i>EST2C</i>	Acylcarnitine hydrolase	-2.6
P28230	<i>CXB1</i>	Gap junction beta-1 protein	-2.5
Q62264	<i>THRSP</i>	Thyroid hormone-inducible hepatic protein	-2.5
Q62452	<i>UD19</i>	UDP-glucuronosyltransferase 1-9	-2.5
Q6PDQ2	<i>CHD4</i>	Chromodomain-helicase-DNA-binding protein 4	-2.4
P04939	<i>MUP3</i>	Major urinary protein 3	-2.3
Q63836	<i>SBP2</i>	Selenium-binding protein 2	-2.3
Q9CZS1	<i>AL1B1</i>	Aldehyde dehydrogenase X	-2.2
P19157	<i>GSTP1</i>	Glutathione S-transferase P 1	-2.2
Q8BYL4	<i>SYYM</i>	Tyrosine--tRNA ligase, mitochondrial	-2.2
Q61694	<i>3BHS5</i>	3 beta-hydroxysteroid dehydrogenase type 5	-2.2
Q91XB0	<i>TREX1</i>	Three-prime repair exonuclease 1	-2.2
P63037	<i>DNJA1</i>	DnaJ homolog subfamily A member 1	-2.1
Q9JIY7	<i>NAT8</i>	N-acetyltransferase 8	-2.1
Q91W64	<i>CP270</i>	Cytochrome P450 2C70	-2.1
A7MCT6	<i>EKI2</i>	Ethanolamine kinase 2	-2.1
Q9D880	<i>TIM50</i>	Mitochondrial import inner membrane translocase subunit TIM50	-2.1
Q64458	<i>CP2CT</i>	Cytochrome P450 2C29	-2.1
Q9DBJ3	<i>BI2L1</i>	Brain-specific angiogenesis inhibitor 1-associated protein 2-like protein 1	-2.0
Q8VE95	<i>CH082</i>	UPF0598 protein C8orf82 homolog	-2.0
Q80YD1	<i>SUV3</i>	ATP-dependent RNA helicase SUPV3L1, mitochondrial	-2.0
Q8QZR3	<i>EST2A</i>	Pyrethroid hydrolase Ces2a	-2.0
Q283N4	<i>URAD</i>	2-oxo-4-hydroxy-4-carboxy-5-ureidoimidazoline decarboxylase	-2.0
Q8C196	<i>CPSM</i>	Carbamoyl-phosphate synthase [ammonia], mitochondrial	-2.0
P62849	<i>RS24</i>	40S ribosomal protein S24	-2.0

P20852	<i>CP2A5</i>	Cytochrome P450 2A5	-1.9
Q60991	<i>CP7B1</i>	25-hydroxycholesterol 7-alpha-hydroxyase	-1.9
Q8BGB8	<i>COQ4</i>	Ubiquinone biosynthesis protein COQ4 homolog, mitochondrial	-1.9
Q571F8	<i>GLSL</i>	Glutaminase liver isoform, mitochondrial	-1.9
Q00898	<i>AIAT5</i>	Alpha-1-antitrypsin 1-5	-1.9
Q9DBL1	<i>ACDSB</i>	Short/branched chain specific acyl-CoA dehydrogenase, mitochondrial	-1.9
P33267	<i>CP2F2</i>	Cytochrome P450 2F2	-1.9
Q91WL5	<i>CP4CA</i>	Cytochrome P450 4A12A	-1.9
Q8JZV9	<i>BDH2</i>	3-hydroxybutyrate dehydrogenase type 2	-1.8
Q9JL8	<i>SYSM</i>	Serine-tRNA ligase, mitochondrial	-1.8
Q3TIU4	<i>PDE12</i>	2',5'-phosphodiesterase 12	-1.8
Q99K51	<i>PLST</i>	Plastin-3	-1.7
P35492	<i>HUTH</i>	Histidine ammonia-lyase	-1.7
Q9DB60	<i>PGFS</i>	Prostamide/prostaglandin F synthase	-1.7
Q5SWU9	<i>ACACA</i>	Acetyl-CoA carboxylase 1	-1.7
P29758	<i>OAT</i>	Ornithine aminotransferase, mitochondrial	-1.7
Q9DCM0	<i>ETHE1</i>	Persulfide dioxygenase ETHE1, mitochondrial	-1.7
Q9DBW0	<i>CP4V2</i>	Cytochrome P450 4V2	-1.7
P16460	<i>ASSY</i>	Argininosuccinate synthase	-1.7
P15532	<i>NDKA</i>	Nucleoside diphosphate kinase A	-1.7
Q9CYW4	<i>HDHD3</i>	Haloacid dehalogenase-like hydrolase domain-containing protein 3	-1.6
O88533	<i>DDC</i>	Aromatic-L-amino-acid decarboxylase	-1.6
Q99P30	<i>NUDT7</i>	Peroxisomal coenzyme A diphosphatase NUDT7	-1.6
Q9QXF8	<i>GNMT</i>	Glycine N-methyltransferase	-1.6
Q8VE09	<i>TT39C</i>	Tetratricopeptide repeat protein 39C	-1.6
Q64435	<i>UD16</i>	UDP-glucuronosyltransferase 1-6	-1.6
O35490	<i>BHMT1</i>	Betaine--homocysteine S-methyltransferase 1	-1.6
Q9WU79	<i>PROD</i>	Proline dehydrogenase 1, mitochondrial	-1.6
Q9CPR5	<i>RM15</i>	39S ribosomal protein L15, mitochondrial	-1.6
P53657	<i>KPYR</i>	Pyruvate kinase PKLR	-1.6
Q04519	<i>ASM</i>	Sphingomyelin phosphodiesterase	-1.5
P50172	<i>DH11</i>	Corticosteroid 11-beta-dehydrogenase isozyme 1	-1.5
Q3UPH1	<i>PRRC1</i>	Protein PRRC1	-1.5
O88986	<i>KBL</i>	2-amino-3-ketobutyrate coenzyme A ligase, mitochondrial	-1.5
Q8VBT2	<i>SDHL</i>	L-serine dehydratase/L-threonine deaminase	-1.5
Q9JIL4	<i>NHRF3</i>	Na(+)/H(+) exchange regulatory cofactor NHE-RF3	-1.5
Q8VCN5	<i>CGL</i>	Cystathionine gamma-lyase	-1.5
Q9CR24	<i>NUDT8</i>	Nucleoside diphosphate-linked moiety X motif 8	-1.5
Q9CQV8	<i>1433B</i>	14-3-3 protein beta/alpha	-1.5

Q8VC12	<i>HUTU</i>	Urocanate hydratase	-1.5
P61922	<i>GABT</i>	4-aminobutyrate aminotransferase, mitochondrial	-1.5
Q6AW69	<i>CGNLI</i>	Cingulin-like protein 1	-1.5
Q8R0Y6	<i>ALILI</i>	Cytosolic 10-formyltetrahydrofolate dehydrogenase	-1.5
Q3UE37	<i>UBE2Z</i>	Ubiquitin-conjugating enzyme E2 Z	-1.5

Appendix 9 Table 4A.4 Significantly up-regulated proteins expressed as HFD/NC ratio

Two-sample t-test (p-value<0.05), fold change>1.5

Uniprot Accession number	Gene	Protein name	Fold change
O35728	<i>CP4AE</i>	Cytochrome P450 4A14	6.4
P14602	<i>HSPB1</i>	Heat shock protein beta 1	3.4
Q9QYR9	<i>ACOT2</i>	Acyl-coenzyme A thioesterase 2, mitochondrial	2.9
P62313	<i>LSM6</i>	U6 snRNA-associated Sm-like protein LSM6	2.7
Q9Z0K8	<i>VNN1</i>	Pantetheinase	2.6
P06728	<i>APOA4</i>	Apolipoprotein A-IV	2.5
Q3TCH7	<i>CUL4A</i>	Cullin-4A	2.4
Q9DBM2	<i>ECHP</i>	Peroxisomal bifunctional enzyme	2.4
P55050	<i>FABPI</i>	Fatty acid-binding protein, intestinal	2.3
P51885	<i>LUM</i>	Lumican	2.3
Q6TCG2	<i>PAQR9</i>	Progestin and adipoQ receptor family member 9	2.3
O55137	<i>ACOT1</i>	Acyl-coenzyme A thioesterase 1	2.3
P47740	<i>AL3A2</i>	Fatty aldehyde dehydrogenase	2.3
Q8C1E7	<i>TI20A</i>	Transmembrane protein 120A	2.2
P23249	<i>MOV10</i>	Putative helicase MOV-10	2.2
P47934	<i>CRAT</i>	Carnitine O-acetyltransferase	2.2
Q62433	<i>NDRG1</i>	Protein NDRG1	2.2
Q99LJ6	<i>GPX7</i>	Glutathione peroxidase 7	2.1
Q3UFF7	<i>LYPL1</i>	Lysophospholipase-like protein 1	2.1
P53798	<i>FDFT</i>	Squalene synthase	2.0
O70370	<i>CATS</i>	Cathepsin S	2.0
P57784	<i>RU2A</i>	U2 small nuclear ribonucleoprotein A'	2.0
Q8BWN8	<i>ACOT4</i>	Acyl-coenzyme A thioesterase 4	2.0
Q08857	<i>CD36</i>	CD36 Antigen Platelet glycoprotein 4	2.0
Q8N7N5	<i>DCAF8</i>	DDB1- and CUL4-associated factor 8	1.9
Q9QYI5	<i>DNJB2</i>	DnaJ homolog subfamily B member 2	1.9
Q9QYJ0	<i>DNJA2</i>	DnaJ homolog subfamily A member 2	1.9
Q8BH59	<i>CMC1</i>	Calcium-binding mitochondrial carrier protein Aralar1	1.9
O35459	<i>ECH1</i>	Delta(3,5)-Delta(2,4)-difbpyl-CoA isomerase	1.8
Q80XN0	<i>BDH</i>	D-beta-hydroxybutyrate dehydrogenase	1.8
Q9JK42	<i>PDK2</i>	[Pyruvate dehydrogenase (acetyl- transferring)] kinase isozyme 2	1.8
Q9ERI6	<i>RDH14</i>	Retinol dehydrogenase 14	1.8
Q9WV68	<i>DECR2</i>	Peroxisomal 2,4-dienoyl-CoA reductase	1.8
O88736	<i>DHB7</i>	3-keto-steroid reductase	1.8
Q9WUR2	<i>ECI2</i>	Enoyl-CoA delta isomerase 2	1.7
Q8BX70	<i>VP13C</i>	Vacuolar protein sorting-associated protein 13C	1.7
Q6PB44	<i>PTN23</i>	Tyrosine-protein phosphatase non-receptor type 23	1.7
Q8K0C4	<i>CP51A</i>	Lanosterol 14-alpha demethylase	1.7
Q64516	<i>GLPK</i>	Glycerol kinase	1.7
P54869	<i>HMCS2</i>	Hydroxymethylglutaryl-CoA synthase	1.7

Q9Z211	<i>PXI1A</i>	Peroxisomal membrane protein 11A	1.7
P06151	<i>LDHA</i>	L-lactate dehydrogenase A chain	1.7
Q9CQY5	<i>MAGT1</i>	Magnesium transporter protein 1	1.7
P28063	<i>PSB8</i>	Proteasome subunit beta type-8	1.7
P43883	<i>PLIN2</i>	Perilipin-2	1.7
Q8BFP9	<i>PDK1</i>	[Pyruvate dehydrogenase (acetyl-transferring)] kinase isozyme 1	1.6
Q61207	<i>SAP</i>	Prosaposin	1.6
Q02013	<i>AQP1</i>	Aquaporin-1	1.6
Q9JK53	<i>PRELP</i>	Prolargin	1.6
P07356	<i>ANXA2</i>	Annexin A2	1.6
O88455	<i>DHCR7</i>	7-dehydrocholesterol reductase	1.6
Q8VCC1	<i>PGDH</i>	15-hydroxyprostaglandin dehydrogenase [NAD(+)]	1.6
P51660	<i>DHB4</i>	Peroxisomal multifunctional enzyme type 2	1.6
P29416	<i>HEXA</i>	Beta-hexosaminidase subunit alpha	1.6
P11438	<i>LAMP1</i>	Lysosome-associated membrane glycoprotein 1	1.6
Q921H8	<i>THIKA</i>	3-ketoacyl-CoA thiolase A, peroxisomal	1.6
Q8JZK9	<i>HMCS1</i>	Hydroxymethylglutaryl-CoA synthase, cytoplasmic	1.6
Q04857	<i>CO6A1</i>	Collagen alpha-1(VI) chain	1.6
Q9CYV5	<i>TM135</i>	Transmembrane protein 135	1.6
Q80X19	<i>COE1</i>	Collagen alpha-1(XIV) chain	1.6
Q921M4	<i>GOGA2</i>	Golgin subfamily A member 2	1.6
Q5U5V2	<i>HYKK</i>	Hydroxylysine kinase	1.6
Q80XL6	<i>ACD11</i>	Acyl-CoA dehydrogenase family member 11	1.6
Q9CYR6	<i>AGM1</i>	Phosphoacetylglucosamine mutase	1.5
Q922E4	<i>PCY2</i>	Ethanolamine-phosphate cytidylyltransferase	1.5
O08547	<i>SC22B</i>	Vesicle-trafficking protein SEC22b	1.5
Q8QZT1	<i>THIL</i>	Acetyl-CoA acetyltransferase, mitochondrial	1.5
O88833	<i>CP4AA</i>	Cytochrome P450 4A10	1.5
Q8VCH0	<i>THIKB</i>	3-ketoacyl-CoA thiolase B, peroxisomal	1.5
Q2TPA8	<i>HSDL2</i>	Hydroxysteroid dehydrogenase-like protein 2	1.5
Q9CX80	<i>CYGB</i>	Cytoglobin	1.5
P36552	<i>HEM6</i>	Oxygen-dependent coproporphyrinogen-III oxidase, mitochondrial	1.5
P18572	<i>BASI</i>	Basigin	1.5
Q8CC88	<i>VWA8</i>	von Willebrand factor A domain-containing protein 8	1.5
Q5FW57	<i>GLYAL</i>	Glycine N-acyltransferase-like protein	1.5

Appendix 10 Examining cellular responses to kinase drug inhibition through phosphoproteome mapping of substrates

This protocol was prepared during the course of my PhD. It is an invited submission to be published in *Methods in Molecular Biology*. Manuscript was written by Daniel Bucio Noble with contributions from Assoc. Prof. Mark P. Molloy, and Dr. Crystal Semaan. This manuscript was accepted for publication on 29/9/2017.

Examining cellular responses to kinase drug inhibition through phosphoproteome mapping of substrates

Daniel Bucio-Noble¹, Crystal Semaan¹, Mark P. Molloy^{1, 2*}

¹ ARC Training Centre for Molecular Technology in the Food Industry, Department of Chemistry and Biomolecular Sciences, Macquarie University, Sydney, Australia.

² Australian Proteome Analysis Facility, Macquarie University, Sydney, Australia.

***Corresponding author:** Mark P. Molloy, Department of Chemistry and Biomolecular Sciences, Macquarie University, Level 3, Building E8C, Research Park Drive, Sydney 2109, Australia. Tel: +61 2 9850 6218. Fax+61 2 9850 6200. E-mail: mmolloy@proteome.org.au

1. Introduction

The study of protein phosphorylation is of importance in understanding many vital aspects of cell biology such as cell growth, differentiation and cell death. Chemical modification of proteins through reversible phosphorylation plays a major role in modulating protein functions including activation state, cellular localisation, degradation, and interactions with proteins and other biomolecules (1). Phosphorylation of serine, threonine and tyrosine amino acids is considered as one of the most common post-translational modifications (PTM) that involves sequence-specific kinases and phosphatases. This modification has been evidenced as central to cancer biology due to its roles in cell proliferation, oncogenic kinase signalling (2) and transcriptional regulation (3). The fact that phosphorylation sites are often altered in cancers by gene mutations, or structurally mimicked through amino acid conversion to provide oncogenes with structural similarity to activated kinases (4), has made this area highly relevant to cancer researchers.

A study investigating somatic cancer mutation datasets found that there was significant enrichment for mutations which resulted in gain/loss of phosphorylation when compared to other mutations (e.g. random amino acid substitutions) (5). Mutations in kinase genes in particular represented the highest number of mutations that disrupted phosphorylation, suggesting that phosphorylation target site mutations are associated with aberrant phosphorylation (5). Phosphorylation has also been shown to be pivotal in treatment, as it is a pharmacologically targetable mechanism (6, 7). For instance, Chapman *et al.* (2011) found that BRAF kinase inhibitor vemurafenib (PLX4032) showed promise for patients with metastatic melanoma carrying the BRAF V600E mutation (6). β -catenin, a protein associated with several cancers is phosphorylated on its tyrosine residues, which is thought to be associated with tumour invasiveness (8). Furthermore, a link has been found between its phosphorylation status and intestinal tumorigenesis in mice (8).

Mass spectrometry (MS) has emerged as a powerful tool in proteomics over the past decade, useful for both peptide identification and quantitation. (9-11). Quantitative MS allows for comparisons between biological samples to determine molecular changes at the expressed protein level. Addition of a phosphate group to the protein sequence is an event that often occurs at low stoichiometry and is also a reversible and dynamic mechanism. These elements complicate identification of phosphopeptides by MS.

In order to address these challenges, phosphopeptide enrichment prior to MS-based analysis is necessary. Phosphopeptide enrichment using metal oxides beads, such as titanium dioxide (TiO₂) enables the efficient capture of these modified peptides from the high background of non-phosphorylated peptides. There are different MS-based strategies for the quantitation of phosphorylated peptides. Labelling techniques such as stable isotope labelling by amino acids in cell culture (SILAC) have proven successful for quantitation of phosphopeptides. SILAC is a reliable strategy for simultaneous identification and quantitation of two or more samples of complex protein mixtures, such as cell lysates (12). On the other hand, SILAC can only assess a limited number of biological conditions and its usage is restricted to cell lines grown in depleted media –as requirement for metabolic labelling incorporation (13). In addition, the need of a minimum passage number for complete isotope incorporation restricts SILAC use in primary cell lines (14).

Label-free quantitation is a simple and cost effective strategy compatible with a wide range of sample types. It is also applicable to a larger number of samples compared to the limited number of samples afforded by labelling techniques (15). Label-free quantitation of the phosphoproteome has provided discoveries in the elucidation of cellular mechanisms. This approach showed the potential role of casein kinase 2 (CK2) in the modulation of the AKT signalling pathway in mutated BRAFV600E drug sensitive SW1736 cell line (16). Further, phosphoproteomics analysis can be employed in the characterisation of cell signalling in

response to treatment with kinase inhibitors in the context of cancer research and other pathologies (17). Deeper understanding of the phosphoproteome will provide more information in regards to the integrated system of cell signalling, particularly in pharmacological intervention. In this protocol we present a straight forward methodology that we use for phosphopeptide enrichment, data acquisition and informatic analysis. Special consideration is taken particularly in the technical aspects and the bioinformatic tools used in this protocol.

2. Materials

1. 1% (w/v) sodium deoxycholate, 0.1M triethylammonium bicarbonate pH 8
2. Benzonase (Sigma Aldrich)
3. BCA assay (Thermo Fisher Scientific)
4. DTT
5. Iodoacetamide
6. Trypsin (Promega)
7. Formic acid
8. Acetonitrile
9. Trifluoroacetic acid
10. Glycolic acid
11. Titansphere TiO₂ beads 5µm (GL Sciences)
12. Ammonia
13. C18 disk (3M Empore)
14. Lobind microcentrifuge tubes (Eppendorf)
15. Q-Exactive mass spectrometer (Thermo Fisher Scientific).
16. MaxQuant software V1.5
17. Perseus software V1.5

3. Methods

Our group commonly conducts phosphopeptide enrichment from cancer cell lines and tissue from human and animal origin. Apart from the selection of a suitable lysis buffer depending on the nature of the sample (*see Note 1*), this methodology is standardised for human cancer cell lines. However, optimisation of this protocol might be necessary when other types of samples are analysed. A schematic representation of the main steps of this protocol is shown in Figure 1. Detailed description of each step is also given in this section. Principal component analysis, hierarchical clustering and volcano plot presented here are taken from a phosphopeptide enrichment performed on SW480 human colon carcinoma cell lines.

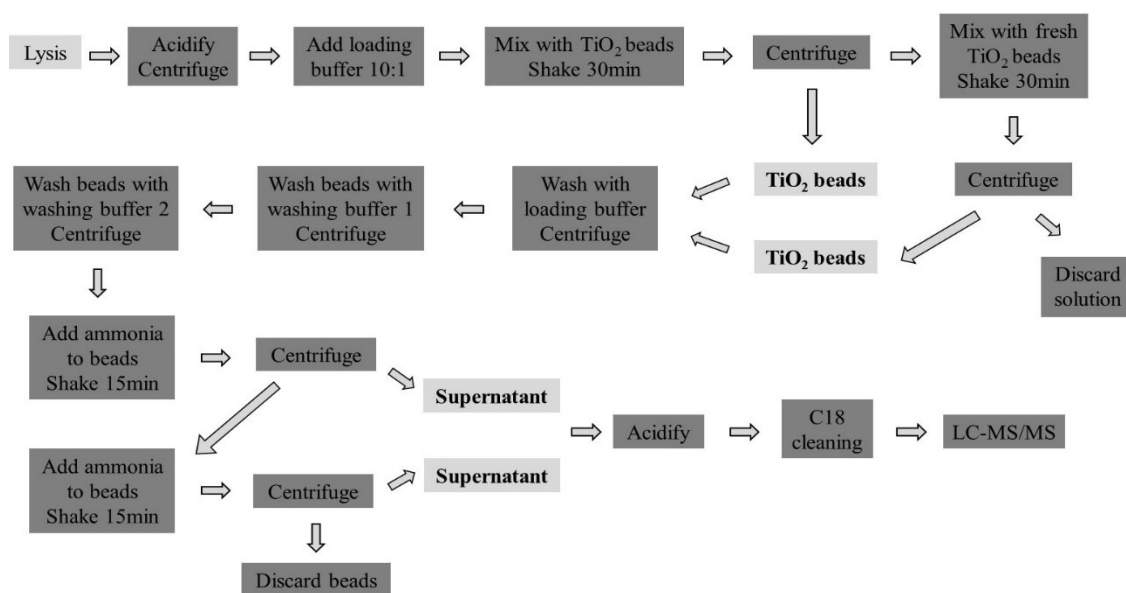


Figure 1. Workflow of phosphopeptide enrichment protocol

3.1 Protein lysis and sample preparation

1. Resuspend cell pellet or tissue in 1% (w/v) sodium deoxycholate, 0.1M triethylammonium bicarbonate pH 8 (*see Note 1*).

2. Heat lysate at 95°C for 1 minute (*see Note 2*).
3. Cool samples at room temperature on ice and sonicate. Add 2µL of benzonase (10,000 units) for complete DNA degradation.
4. Centrifuge at 10,000xg at 4°C for 10 minutes and collect supernatant.
5. Determine protein concentration using the BCA assay.
6. Aliquot 500µg of protein and reduce by adding DTT to a final concentration of 10mM followed by incubation at 60°C for 30 minutes.
7. Alkylate with iodoacetamide by adding at a final concentration of 25mM followed by incubation at room temperature for 20 minutes in the dark.
8. Digest sample with trypsin in a 1:50 enzyme: protein ratio (i.e. 10µg of trypsin). Incubate at 37°C overnight.

3.2 Phosphopeptide enrichment

1. Acidify with formic acid to a final concentration of 2% (v/v) (*see Note 3*). Centrifuge at 10,000xg for 10 minutes and collect supernatant.
2. Add loading buffer (80% (v/v) acetonitrile, 5% (v/v) trifluoroacetic acid (TFA), 76 mg/ml glycolic acid) to the sample in a 10:1 ratio (*see Notes 4 and 5*).
3. Wash 3mg of TiO₂ beads with 100µL of loading buffer. Mix for a few seconds and centrifuge (1,000xg for 10 seconds) to pellet down beads. Discard supernatant.
4. Add sample to the beads and incubate at room temperature with constant shaking for 30 minutes. Centrifuge (1,000xg for 10 seconds) to pellet down beads.
5. Wash a new batch of 3mg of TiO₂ beads as in step 3.
6. Add supernatant from step 4 to the new beads and incubate at room temperature with constant shaking for 30 minutes. Centrifuge (1,000xg for 10 seconds) to pellet down beads. Discard supernatant.

7. Combine the TiO₂ beads from the 2 incubations in a new low-binding tube and wash with 100µL of loading buffer. Mix for a few seconds and centrifuge (1,000xg for 10 seconds) to pellet down beads. Discard supernatant.
8. Wash beads with washing buffer 1 (80% (v/v) acetonitrile, 1% (v/v) TFA). Mix for a few seconds and centrifuge (1,000xg for 10 seconds) to pellet down beads. Discard supernatant.
9. Wash beads with washing buffer 2 (10% (v/v) acetonitrile, 0.1% (v/v) TFA). Mix for a few seconds and centrifuge (1,000xg for 10 seconds) to pellet down beads. Discard supernatant.
10. Remove any remnant of solvent by placing sample in the vacuum centrifuge for 5 minutes.
11. Elute phosphopeptides by adding 100µL of 1% (v/v) ammonia (*see Note 6*). Incubate for 15 minutes under constant shaking. Centrifuge (1,000xg for 10 seconds) to pellet down beads and collect supernatant in a new low binding tube.
12. Add for a second time 100µL of 1% (v/v) ammonia. Incubate for 15 minutes under constant shaking. Centrifuge (1,000xg for 10 seconds) to pellet down beads and pool the 2 supernatants. Acidify with 16µL of formic acid.

3.3 C18 cleaning

1. Cut 1cm above the end of a 200µL tip. With a needle tip cut 2 stack layers of C18 material and insert them into the tip. Place the stacked tip inside a 1.5ml tube.
2. Equilibrate by adding 100µL of methanol into the tip and centrifuge at 1,000xg for 2 minutes or until the complete volume passes through the C18 material. Discard flowthrough.
3. Wash with 100µL of 2% (v/v) acetonitrile, 0.1% (v/v) TFA, centrifuge (1,000xg for 2 minutes) and discard flowthrough.

4. Add phosphopeptide solution, centrifuge (1,000xg for 2 minutes) and discard supernatant.
5. Wash with 100µL of 2% (v/v) acetonitrile, 0.1% (v/v) TFA, centrifuge (1,000xg for 2 minutes) and discard flowthrough.
6. Elute with 70% (v/v) acetonitrile, 0.1% (v/v) TFA, centrifuge (1,000xg for 2 minutes) and collect flowthrough in a new low-binding tube.
7. Remove solvent by complete drying in a vacuum centrifuge.

3.4 Mass spectrometry (LC-MS/MS)

1. Reconstitute dried phosphopeptides in 20µL of 0.1% (v/v) formic acid.
2. Analyse samples on a Q-Exactive mass spectrometer coupled to an EASY nLC1000 (Thermo Fisher Scientific).
3. Reverse phase chromatography separation is achieved on a 75µm x 100mm C18 Halo, 2.7µm bead size, 160Å pore size column.
4. Elute phosphopeptides with an A buffer B (100% (v/v) acetonitrile, 0.1% (v/v) formic acid) gradient of 5-35% in a 100min run using electrospray ionization (*see Note 7*).
5. Data-dependent MS/MS acquisition mode consists of a full MS resolution of 70,000 scan acquisition, 350-1800 *m/z*. Peptide fragmentation requires 10 HCD and a MS² resolution of 17,500.

3.5 Data processing and analysis

1. Files (.raw) are processed using MaxQuant (15) with a 1% peptide and protein FDR.
2. Database search used the parameters: 2 missed cleavages, peptide mass tolerance of 4.5ppm, carbamidomethylation (C) as fixed modification and oxidation (M), acetylation (Protein N-term), and phosphorylation (STY) as variable modifications.
3. Label free quantitation mode and match between runs functions are activated.

3.6 Statistical analysis

1. Statistical analysis using Perseus (18) is performed on the 'phospho (STY) sites' files (.txt).
2. Intensity values are moved to the 'main columns' box.
3. Reverse and contaminant peptides are removed with the 'filter rows based on categorical column' function. Phosphopeptides with a localisation probability lower than 75% are also removed with the 'filter rows based on numerical/main column' function.
4. Intensities are $\log_2(x)$ transformed.
5. Using the 'filter rows based on valid values' proteins with high number of missing values are removed. Missing values are replaced by imputation (*see Note 8*).
6. Data is normalised by median subtraction.
7. Principal component analysis and volcano plots can be generated by using the corresponding functions (Figure 2).
8. 'Multiple-sample test' using the ANOVA test and the selection of an appropriate FDR cut-off permits the identification of phosphosites that their expression is significantly altered among all the conditions. 'Filter rows based on categorical column' enables the filtration of significant phosphosites in the matrix from non-significant phosphosites. After data filtration, 'Z-score' normalises the phosphosites expression values according to mean and standard deviation. These significant changes can then be visualised with the 'hierarchical clustering' function (Figure 3).
9. Significant regulated phosphosites between two conditions are determined by 'two-sample test' and the selection of an appropriate FDR cut-off. Fold change (located in the 'Student's t-test Difference' column) thresholds can help in the identification of statistical significant changes.

10. Enrichment analysis on significant regulated sites can be performed using the Fisher exact test. Data is first filtered using 2 criteria: Q-value and fold change with the objective of selecting statistical significant up-regulated and down-regulated values. Fisher exact test is applied using an appropriate FDR cut-off. At this point, Perseus calculates an enrichment factor for the overrepresented kinase motifs.

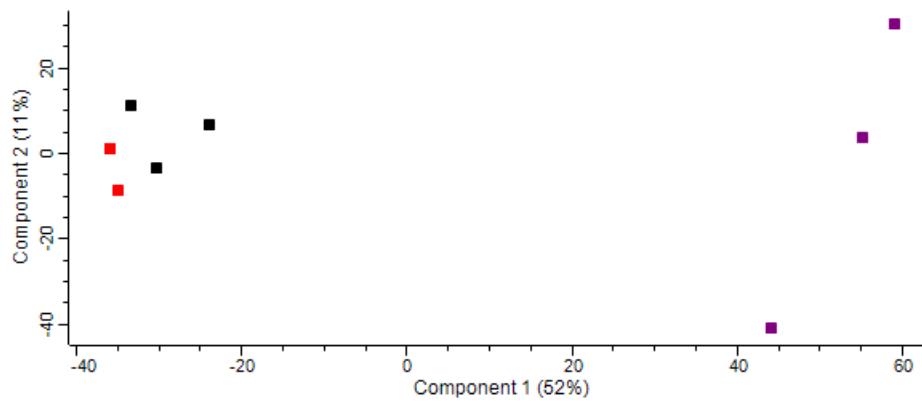


Figure 2. Principal component analysis representing overall phosphopeptide expression in response to lipopolysaccharides (red), and lipopolysaccharides + resveratrol (purple) SW480-treated cells; untreated cells in black.

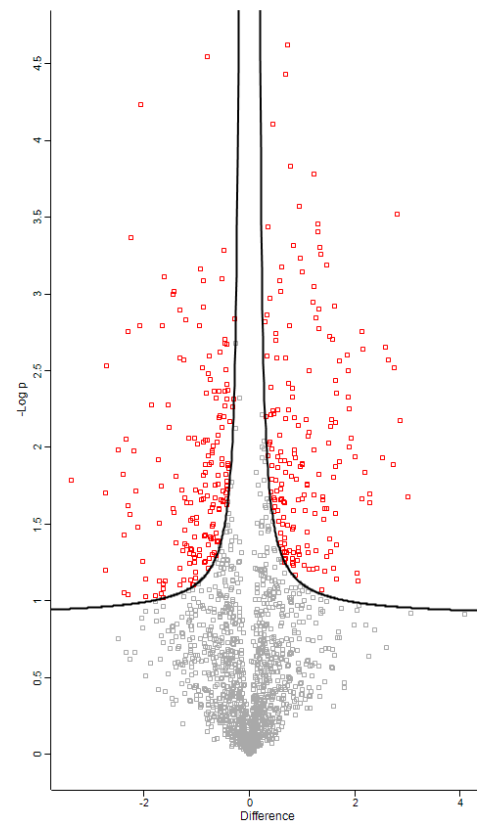


Figure 3. Volcano plot representing significantly regulated phosphopeptides in response to resveratrol compared to lipopolysaccharides SW480-treated cells (red). Two-sample t-test, FDR<0.05.

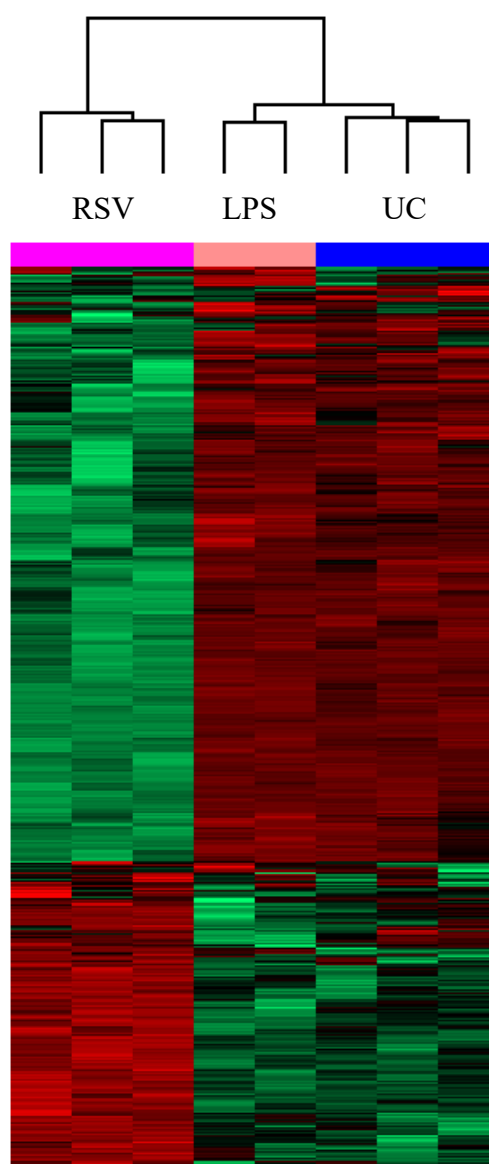


Figure 4. Hierarchical clustering representing significantly regulated phosphopeptides in response to resveratrol (RSV) and lipopolysaccharides (LPS) SW480-treated cells; untreated cells (UC). ANOVA multiple sample test, FDR<0.05.

4. Notes

1. Using 1% (w/v) sodium deoxycholate, 0.1M triethylammonium bicarbonate pH 8 as a lysis buffer provides compatibility with TiO₂ enrichment (19) and trypsin-mediated digestion (20). Selection of a suitable lysis buffer will depend on the nature of sample.

2. Excessive heating induces protein precipitation. Addition of protease or phosphatase inhibitors may not be necessary as heating decreases enzyme activity. Additionally, it is reported that phosphatases show great affinity for TiO_2 and therefore reduce phosphopeptide enrichment efficiency (19).
3. Addition of formic acid ensures complete salt precipitation when the lysis buffer used is 1% (w/v) sodium deoxycholate, 0.1M triethylammonium bicarbonate pH 8.
4. It is recommended to prepare loading buffer and washing buffers fresh in order to avoid any potential contamination.
5. Acidic conditions permit better recovery of phosphopeptides by reducing interference from acidic non-phosphorylated peptides (21).
6. Preparation of fresh ammonia is recommended given that high pH is critical for complete elution of phosphopeptides.
7. Phosphopeptides due to their hydrophilic nature tend to elute at low concentrations of the acetonitrile gradient.
8. Perseus offers multiple options for the imputation of missing values. Replacement of missing values from normal distribution permits their simulation from a typical abundance region if they had been measured and their random selection from a normal distribution (18).



References

1. Hunter T. Signaling—2000 and beyond. *Cell*. 2000;100(1):113-27.
2. Smith CC, Wang Q, Chin CS, Salerno S, Damon LE, Levis MJ, et al. Validation of ITD mutations in FLT3 as a therapeutic target in human acute myeloid leukaemia. *Nature*. 2012;485(7397):260-3.
3. Morin PJ, Sparks AB, Korinek V, Barker N, Clevers H, Vogelstein B, et al. Activation of beta-catenin-Tcf signaling in colon cancer by mutations in beta-catenin or APC. *Science*. 1997;275(5307):1787-90.
4. Reimand J, Wagih O, Bader GD. The mutational landscape of phosphorylation signaling in cancer. *Sci Rep*. 2013;3:2651.
5. Radivojac P, Baenziger PH, Kann MG, Mort ME, Hahn MW, Mooney SD. Gain and loss of phosphorylation sites in human cancer. *Bioinformatics*. 2008;24(16):i241-7.
6. Chapman PB, Hauschild A, Robert C, Haanen JB, Ascierto P, Larkin J, et al. Improved survival with vemurafenib in melanoma with BRAF V600E mutation. *N Engl J Med*. 2011;364(26):2507-16.
7. Tiacci E, Trifonov V, Schiavoni G, Holmes A, Kern W, Martelli MP, et al. BRAF mutations in hairy-cell leukemia. *N Engl J Med*. 2011;364(24):2305-15.
8. van Veelen W, Le NH, Helvensteijn W, Blonden L, Theeuwes M, Bakker ER, et al. beta-catenin tyrosine 654 phosphorylation increases Wnt signalling and intestinal tumorigenesis. *Gut*. 2011;60(9):1204-12.
9. Mann M, Hendrickson RC, Pandey A. Analysis of proteins and proteomes by mass spectrometry. *Annu Rev Biochem*. 2001;70:437-73.
10. Kuster B, Mortensen P, Andersen JS, Mann M. Mass spectrometry allows direct identification of proteins in large genomes. *Proteomics*. 2001;1(5):641-50.
11. Aebersold R, Mann M. Mass spectrometry-based proteomics. *Nature*. 2003;422(6928):198-207.
12. Ong SE, Blagoev B, Kratchmarova I, Kristensen DB, Steen H, Pandey A, et al. Stable isotope labeling by amino acids in cell culture, SILAC, as a simple and accurate approach to expression proteomics. *Mol Cell Proteomics*. 2002;1(5):376-86.
13. Mueller LN, Brusniak M-Y, Mani D, Aebersold R. An assessment of software solutions for the analysis of mass spectrometry based quantitative proteomics data. *Journal of proteome research*. 2008;7(01):51-61.
14. Eyrich B, Sickmann A, Zahedi RP. Catch me if you can: Mass spectrometry-based phosphoproteomics and quantification strategies. *Proteomics*. 2011;11(4):554-70.
15. Cox J, Hein MY, Luber CA, Paron I, Nagaraj N, Mann M. Accurate proteome-wide label-free quantification by delayed normalization and maximal peptide ratio extraction, termed MaxLFQ. *Molecular & Cellular Proteomics*. 2014;13(9):2513-26.
16. Parker R, Clifton-Bligh R, Molloy MP. Phosphoproteomics of MAPK inhibition in BRAF-mutated cells and a role for the lethal synergism of dual BRAF and CK2 inhibition. *Molecular cancer therapeutics*. 2014;13(7):1894-906.
17. Casado P, Hijazi M, Britton D, Cutillas PR. Impact of phosphoproteomics in the translation of kinase targeted therapies. *Proteomics*. 2016.
18. Tyanova S, Temu T, Sinitcyn P, Carlson A, Hein MY, Geiger T, et al. The Perseus computational platform for comprehensive analysis of (prote) omics data. *Nature methods*. 2016;13(9):731-40.
19. Rogers LD, Fang Y, Foster LJ. An integrated global strategy for cell lysis, fractionation, enrichment and mass spectrometric analysis of phosphorylated peptides. *Molecular BioSystems*. 2010;6(5):822-9.
20. Zhou J, Zhou T, Cao R, Liu Z, Shen J, Chen P, et al. Evaluation of the application of sodium deoxycholate to proteomic analysis of rat hippocampal plasma membrane. *Journal of proteome research*. 2006;5(10):2547-53.

21. Sugiyama N, Masuda T, Shinoda K, Nakamura A, Tomita M, Ishihama Y. Phosphopeptide enrichment by aliphatic hydroxy acid-modified metal oxide chromatography for nano-LC-MS/MS in proteomics applications. *Molecular & cellular proteomics*. 2007;6(6):1103-9.

Biosafety and Animal Ethics approvals

Biosafety approval

SECTION A		Biohazard Risk Assessment Form – NON GMO		Notification Number: MAM150115BHA
				
Department	Chemistry and Biomolecular Sciences	Date:	15/01/2015	
Chief investigator:	Mark Molloy			
Contact number/email:	x6218 mark.molloy@mq.edu.au			
Title of research/practical	Human cancer cell line cultures			
Is additional approval required?	Animal Ethics <input type="checkbox"/> Human Ethics <input type="checkbox"/> Fieldwork Manager <input type="checkbox"/> Other <input type="checkbox"/> (state) _____			
Exact location(s) of research:				
E8C rooms 323 and 326				
Control measures: Eliminate risk <input type="checkbox"/> Substitute the hazard <input type="checkbox"/> Isolate the hazard <input checked="" type="checkbox"/> Implement engineering controls <input type="checkbox"/> Administration <input type="checkbox"/> (e.g. Training) <input checked="" type="checkbox"/> PPE <input checked="" type="checkbox"/> E.g. Eliminate by irradiation prior to use, isolation by class II biological safety cabinets, administration by following SWP as below, PPE as listed below.				
Supporting documents which must be read in conjunction with this assessment. (e.g. Safe Working Procedures, Safety Data Sheets, Guidelines/Protocols)				
MQU - A guide to Biological Risk Management: http://staff.mq.edu.au/human_resources/health_and_safety/policies-procedures-guidelines_forms/				
What is the type of the biological material?				
Bacteria <input type="checkbox"/> Fungi <input type="checkbox"/> Virus <input type="checkbox"/> Cell Line <input checked="" type="checkbox"/> Tissue <input type="checkbox"/> Parasite <input type="checkbox"/> Animal <input type="checkbox"/> Plant <input type="checkbox"/> Soil <input type="checkbox"/> Toxin <input type="checkbox"/> Prions <input type="checkbox"/> Nucleic Acid <input type="checkbox"/> other <input type="checkbox"/> _____				
What is the name of the biological agent?				
Various human cancer cell lines – non GMO				
List the Personal Protective Equipment required:				
Gloves <input checked="" type="checkbox"/> (e.g. chemical resistant) Eye protection <input checked="" type="checkbox"/> (e.g. safety glasses/goggles) Clothing <input checked="" type="checkbox"/> (e.g. button up lab coat/coveralls/apron)				
Footwear <input checked="" type="checkbox"/> (e.g. Enclosed/Gumboots/overshoe covers) Respiratory Protection <input type="checkbox"/> (e.g. PF2 face mask) Other <input type="checkbox"/> _____				

Animal Ethics approval

Dear Dr Kautto

Your new application was considered and approved by the Animal Ethics Committee on 23/09/2015

RE: 5201500129 - Dr Kautto - (Collaborative) Effect of Nutrikane on immunosystem and gut microbiome in lean, obese and diabetic mice

Decision

The Committee agreed to approve the application and to issue an Animal Research Authority for work to commence.

Animal Research Authority (ARA) is attached to your online application. Please carefully note the approval dates and read the conditions of approval (if any) outlined in the ARA.

Grants:

If you have applied for funding for the above project, you will need to advise the Research Office Grants Team of your Ethics Reference Number: 5201500129

Please note the following standard conditions of approval (mandatory under The Animal Research Act 1985 NSW and Australian code for the care and use of animals for scientific purposes 8th edition (2013)) :

1. A Progress Report must be submitted before the end of each 12-month (or less) approval period while the project is still current. The date of expiry of approval is shown clearly on the ARA.

Progress reports must be submitted to the AEC Secretariat in time for review at an AEC meeting before the ARA expires. Any animal work carried out during the period after expiry of an ARA, and before issuance of a new ARA, is in breach of the NSW Animal Research Act. If reports are submitted after the required closing date and cannot be reviewed by the AEC before expiry of the ARA, researchers will be expected to cease their animal work until such time as the AEC issues approval for the work to continue.

The Progress Report form (along with instructions for submission of the form) is available at http://www.research.mq.edu.au/for/researchers/how_to_obtain_ethics_approval/animal_ethics/forms

Please note that although the Research Office may issue a report reminder notice, timely submission of reports remains the responsibility of the ARA holder.

2. A Final Report must be submitted within one month of expiration of the full duration of approval or within one month of completion or abandonment of the work, whichever occurs sooner. If the Final Report is not submitted within three months of expiry of the final ARA, no further AEC approvals will be issued until the report is submitted. The full duration of approval is shown clearly on the attached ARA. Researchers are highly encouraged to make contact with the Animal Ethics Secretariat regarding any difficulty with submitting reports on time.

The Final Report form (along with instructions for submission of the form) is available at website

3. An amendment request must be submitted to the AEC for approval should you wish to make any changes to the approved protocol, including the addition of new research personnel, prior to the changes occurring.

Amendment request forms (along with instructions for submission of the forms) are available from website.

4. Any unexpected adverse events, including illnesses of animal(s), unexpected animal deaths or any event that may affect animal welfare and/or the continued ethical acceptability of the project must be notified to the Animal Welfare Officer within 72 hours of occurrence. The Unexpected Adverse Events form is available

5. At all times you are responsible for the ethical conduct of your research in accordance with the guidelines established by Commonwealth and State bodies and the University. If you have any queries regarding such guidelines, they are accessible online, or you may direct your queries to the AEC Secretariat at animal.ethics@mq.edu.au

All forms available at: http://www.research.mq.edu.au/for/researchers/how_to_obtain_ethics_approval/animal_ethics/forms

Please retain a copy of this email and the attached ARA as proof of approval by the Animal Ethics Committee.

Regards,

Professor Mark Connor
Chair, Animal Ethics Committee



RESEARCH INTEGRITY
Animal Ethics Committee

Wednesday, 1 July 2015

Assoc Prof Anandwardhan Hardikar
School of Public Health: NH&MRC Clinical Trials Centre; Sydney Medical School
The University of Sydney

Email: anand.hardikar@sydney.edu.au

Dear Assoc Prof Hardikar

Project Title: Effects of changes in gut microbiota on development of obesity and diabetes.

Project Number: 2014/611

Your request to modify the above project submitted on **22 May 2015** was considered by the Animal Ethics Committee at its meeting on **18 June 2015**.

The Committee had no ethical objections to the modification(s) and has approved the project to proceed with change in protocol.

Details of the approval are as follows:

Authorised Personnel: Hardikar Anandwardhan; Joglekar Mugdha; Kristensen-Walker Holly; Satoor Sarang; Wong Wilson; Bucio-Noble Daniel; Chong Wei; Kautto Liisa; Gamage Hasinika;

Change to Study Procedures as outlined in the Modification to an Existing Approved Application Form in IRMA.

Documents Approved:

Date	Type	Document
22/05/2015	Other	Experimental plan

Animals Approved:

Please refer to the document at the end of this letter, which details your approved animal usage.

Conditions of Approval

Approval of this project is conditional upon your adherence to the conditions outlined in this letter and your continuing compliance with the Animal Research Act (1985 – Animal Research Regulation 2010) and the 8th Edition of the Australian code for the care and use of animals for scientific purposes (NHMRC 2013).

1. The Animal Ethics Committee (AEC) reviews and approves protocols for their compliance with the NSW Animal Research Act (and associated regulations) and the 8th Edition of the Australian code for the care and use of animals for scientific purposes (NHMRC, 2013).
2. This approval is in accordance with your original submission together with any additional information provided as part of the approval process.
3. Any changes to the protocol must be approved by the AEC before continuation of the study. This includes notifying the AEC of any changes to named personnel, source of animals, animal numbers, location of animals and experimental procedures.

Research Integrity
Research Portfolio
Level 2, Margaret Telfer
The University of Sydney
NSW 2006 Australia

T +61 2 8627 8174
F +61 2 8627 8177
E animal.ethics@sydney.edu.au
sydney.edu.au

ABN 15 211 513 484
CRICOS 00028A